‘GREEN’ FINISHING FOR CELLULOSE AND PROTEIN-BASED FIBERS AND FABRICS

A Dissertation

Presented to the Faculty of the Graduate School

of Cornell University

In Partial Fulfillment of the Requirements for the Degree of

Doctor of Philosophy

by

Namrata Vinay Patil

December 2019

‘GREEN’ FINISHING FOR CELLULOSE AND PROTEIN-BASED FIBERS AND FABRICS

Namrata Vinay Patil, Ph. D.

Cornell University 2019

Most apparel and textile products undergo various finishing treatments to attain aesthetic and functional properties. In many cases toxic chemicals are used in these finishing treatments. For example, formaldehyde-based chemical agents have been commonly used to treat cotton fabrics to attain ‘easy-care’ properties. Similarly, fluorine-based chemicals are used to attain self-cleaning or superhydrophobic fabrics. Formaldehyde and glutaraldehyde are used to crosslink keratin-based fibers such as wool and hair to improve their mechanical properties or to attain durable hair styling effects.

Environmental issues and consumer awareness about synthetics have promoted the use of natural fibers to manufacture products that have improved environmental profiles. Consumer awareness and concerns about the use of formaldehyde, perfluoroalkyl substances (PFAS), glutaraldehyde and glyoxal, commonly used finishing agents for natural fabrics such as cotton and wool have prompted manufacturers to find greener and sustainable solutions. These chemicals are not only toxic but are known to bioaccumulate in nature for long time and can find their way into human body through direct skin contact and water.

This research highlights the current textile chemistry that goes into finishing the fabrics. It also states some of the greener alternatives developed so far. The main

aims of this research, however, are to develop sustainable and ‘green’ chemistry-based solutions for creating wrinkle-free cotton fabrics, superhydrophobic cotton fabrics and for crosslinking of wool fibers to increase their strength as well as for stabilizing and shaping of human hair. The research was also focused on developing such finishing processes using inexpensive, readily available and renewable (mostly plant based) raw materials and in many cases, wastes or by-products generated in food processing.

Sucrose and cyclodextrin-based multifunctional carboxylic acid were synthesized as ‘green’ crosslinkers for crosslinking cellulose, separately, to create wrinkle-free cotton fabrics. A green process of covalently bonding multi-shaped silica particles synthesized from tetra ethyl ortho silicate (TEOS) and fatty acid grafting was developed to create superhydrophobic cotton fabrics. Sucrose and soy flour sugar based crosslinkers were developed to enhance the strength of the wool fibers to enhance its ability to be spun into finer yarns as well as to reduce breakage during spinning and weaving and, thus, reducing the defects in both yarns and fabrics. The effects and durability of these chemical treatments on the fabrics were characterized. Sugar-based crosslinker was developed to treat human hair for creating internal crosslinks for hair-styling and stability that was durable to high humidity environment as well as shampoo washings.

BIOGRAPHICAL SKETCH

Namrata Patil was born in Aurangabad and grew-up in Mumbai, India. Inspired by her father, she decided to learn more about polymers, materials and textiles and earned a Bachelor of Technology (B. Tech) degree in Fiber and Textile Processing Technology from Institute of Chemical Technology (formerly known as UDCT), Mumbai, India in 2013. She graduated with Master of Science (M. S.) from Cornell University, Ithaca NY in 2015 where she worked on developing cellulose and starch-based composites to replace petroleum-based products in packaging and structural applications in Dr. Netravali's lab. She further continued working in the same group to develop 'green' chemistry solutions for natural fibers and fabrics such as cotton, wool and hair for her Doctor of Philosophy (Ph.D.). She finished her doctoral experimental work in Summer 2019 and started working as a Materials R&D Intern at Bolt Threads, San Francisco Bay area, CA where is she working on developing mycelium-based leather which will be an alternative to cattle-based leather. Namrata is passionate about developing 'green chemistry' and 'sustainable' materials to be used in day-to-day life with the aim to reduce the dependence on petroleum-based products to save the environment.

Dedicated to my Family

ACKNOWLEDGMENTS

I would like to thank my supervisor, Prof. Anil N. Netravali for giving me the opportunity to work on exciting and important industrial projects. His constant support, invaluable advice, endless passion for developing ‘green’ technologies and strong encouragement were a great motivation to complete this work. I would like to thank Prof. Lara A. Estroff for the valuable courses on materials chemistry and biomineralization which helped me improve my chemistry and apply in my research. My special gratitude to Prof. Minglin Ma for introducing me to the field of biomaterials through the design and analysis of biomaterials course. The excellent design of his advanced topics in biomaterials course broadened my knowledge of biomaterials and improved my critical thinking and presentation skills.

I would like to acknowledge Cornell Center for Materials Research (CCMR) for the use of instruments and the Department of Fiber Science and Apparel Design for the financial support.

All the faculty members, staff and friends in the Department of Fiber Science, especially in the Netravali lab have been indispensable part of my research. I would like to thank my parents and friends for the infinite care and support. This work would not have been possible with the unconditional love and support from my husband.

Finally, I would like to extend my acknowledgment to Prof. Huiju Park for his valuable comments and suggestions during the A exam and Prof. Shefford P. Baker who kindly accepted to examine my work during A exam.

TABLE OF CONTENTS

LIST OF FIGURES

LIST OF TABLES

LIST OF ABBREVIATIONS

AATCC: American Association of Textile Chemists and Colorists.
ATR-FTIR: Attenuated total reflectance-Fourier transform infrared.
$BaCl_2$: Barium dichloride.
BC: Bacterial cellulose.
BTCA: 1,2,3,4-butanetetra-carboxylic acid.
CA: Citric acid.
C-CD: Carboxylated cyclodextrin.
CCMR: Cornell Center for Materials Research.
CD: Cyclodextrin.
DCFM: Dichlorodifluoromethane.
DI: Deionized.
DMDHEU: Dimethyloldihydroxyethyleneurea.
DP: Durable press.
DTMS: n-Dodecyltrimethoxysilane.
DWR: Durable water repellent.
epi: Ends per inch.
FA: Fatty acids.
FESEM: Field emission scanning electron microscope.
H_2O_2: Hydrogen peroxide.
HA: Heptanoic anhydride.
HCl: Hydro chloric acid.
HNT: Halloysite nanotubes.
MA: Malic acid.
MFC: Microfibrillated cellulose.
MR: Molar ratio.
MW: Molecular weights.
NCC: Nano crystalline cellulose.
NH_4OH: Ammonium hydroxide.
NMR: Nuclear magnetic resonance.
NYCSGA: New York Corn & Soybean Growers Association.
O-CD: Oxidized cyclodextrin.
OSFS: Oxidized soy flour sugar.
PCA: Polycarboxylic acid.
PDMS: Polydimethylsiloxane.
PFAs: Perfluoroalkyl substances.
PFOA: Perfluorooctanoic acid.
PFPAs: Perfluoroalkyl phosphate acrylates.
ppi: Picks per inch.
PVP: Polyvinyl pyrrolidone.
RH: Relative humidity.
RT: Room temperature.
SEM: Scanning electron microscopy.
SF: Soy flour.

SFS: Soy flour sugar.
SHP: Sodium hypophosphite monohydrate.
Si-HNT: HNT decorated with silica nanospheres.
SPC: Soy protein concentrate.
SPI: Soy protein isolate.
TEM: Transmission electron microscopy.
TEOS: Tetraethyl orthosilicate. ,
USEPA: United States Environmental Protection Agency.
WCA: Water contact angle.
WRA: Wrinkle recovery angle.

LIST OF SYMBOLS

α Alpha
β Beta
μ Micro

Chapter 1 Introduction

1.1 Natural fibers in textiles

In the past two decades there has been a significant increase in worldwide awareness in terms of sustainability which has pushed the use of natural and plant-based materials in every aspect of our lives.[1] This interest comes from an urge to minimize or stop, where possible, the use of synthetic or petroleum-based materials that are non-biodegradable.[2] They are also not sustainable because petroleum itself is non-sustainable. Consumers are aware of the environmental crisis associated with the use of petroleum-based materials that are commonly dumped in landfills and oceans, that linger in almost 'as is' condition for several centuries without degrading.[1]

Textile products are integral part of our daily life and with the latest trend of fast-fashion, significant amount of textile fabrics end up in landfill.[3-4] The fast-fashion ideology has created the 'today's treasure – tomorrow's trash' problem.[4] According to United States Environmental Protection Agency (USEPA) approximately 13 million tons of textile waste was generated in 2013.[3] This accounted for up to 9% of total municipal solid waste in the United States.[3] The demand for synthetic fibers has always been higher than that of the natural fibers during the past 2-3 decades primarily because of their lower cost and durability.[5] Sustainable development includes achieving a state at which humans are able to live and co-exist indefinitely with the natural world without harming or causing damage to either side.[4] The increase in the use of natural fibers, especially in textiles and clothing, is considered as a sustainable development towards good fashion.[6] World production of natural fibers in 2013 was

estimated to be 33 million tons with cotton being the largest (26 million tons), followed by jute (3.3 million tons) and wool (1.2 million tons).[7] Other natural fibers such as abaca, flax, hemp, kapok, ramie, sisal and silk accounted for 1.6 million tons and coir accounted for about 0.9 million tones.[7] The present dissertation mainly focuses on textile finishing for cellulose and keratin-based fibers and fabrics which are the two of the largest natural fibers used in the apparel industry. Sections 1.1.1 and 1.1.2 discuss more about chemistry, properties and applications of cotton and wool fibers, respectively. Section 1.2 focuses on wet-chemical processing associated with natural fibers and fabrics with an emphasis on cotton and wool.

1.1.1 Cotton

Cotton is made up of cellulose, which is one of the most abundant renewable polymer on earth.[8] Cellulose was first characterized in 1838 and has been used in variety of applications since then.[9] Cotton fibers are staple (short) fibers, 2 to 2 ½ inch long, and can be spun into yarns and then woven or knitted into fabrics to be used in apparel, upholstery and other products.[10] Cellulose fibers are also used on a large scale to make non-woven products used in personal care such as wipes, in medical textiles such as masks, and in other industrial applications such as microfluidic devices, lithium ion battery separators and filters.[11-13] Use of micro- and nano-cellulose in the form of nanocrystalline cellulose (NCC), microfibrillated cellulose (MFC) and bacterial cellulose (BC) has also been on the rise in many applications including fiber reinforced composites.[14-19] There are many more niche applications of cellulose as well. For example, cellulose is commonly used in the form of hydrogel for biomedical applications such as drug delivery and tissue engineering as it is biocompatible and

has been approved by the US FDA.[20-21] In general, cellulosic products are lightweight, moderately strong, eco-friendly, fully sustainable and biodegradable and can be found in many day-to-day products.[15, 19] However, around 48% of cotton fiber produced worldwide is consumed as clothing material worldwide.[10] Cotton fabrics form an integral part of the apparel industry due to their properties such as softness, high water and moisture absorbency which make them comfortable to wear.[22-23] The inherently hydrophilic nature of the cotton fibers is because of the chemical structure of cellulose. Figure 1.1 shows the chemical structure of the repeat unit (cellobiose) of cellulose that is formed by combining two D-glucose units. As seen from Figure 1.1, cellulose is a linear homopolymer consisting of β(1-4) linked D-glucose units. Each glucose unit consists of one primary hydroxyl group and two secondary hydroxyl groups giving the cellulose molecule its highly hydrophilic characteristic.[23] The hydrophilicity and the porous structure of the cotton yarns and fabrics enable them to absorb sweat from the side touching the body and efficiently wicking it to the other side for faster evaporation. This keeps the body dry and makes cotton fabrics comfortable to wear. As a result, cotton is the most preferred choice in clothing.

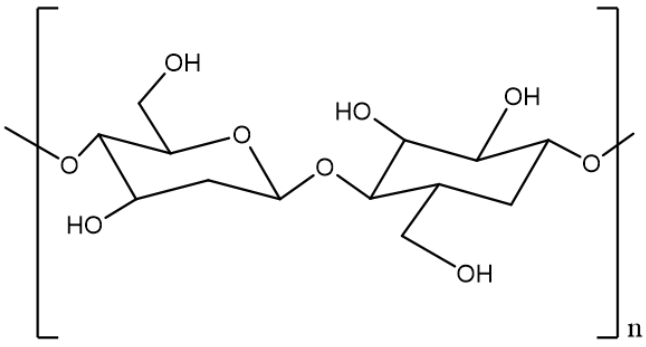

Figure 1.1 Chemical structure of the repeat unit (cellobiose) of cellulose.

1.1.2 Wool

Wool is the most important animal fiber used in textiles.[24] These fibers are hair of animals, most commonly sheep. However, hair from llamas, alpacas, camel and many different types of goats (e.g., angora, cashmere, etc.) are also considered as wool fibers. This natural fiber is a renewable resource. Wool fibers form an outer layer of covering for animals and protect them from the wide range of environmental conditions.[24] Wool is an α-keratin fiber made up of biological polymer of polypeptide chains consisting of 18 to 19 different amino acids.[24] Wool typically contains diamino acid residue, cystine in the peptide chains which contribute to the mechanical stability of the keratin structure through covalent S-S (disulfide) crosslinks.[24] Being of biological origin, wool fibers are not continuous like other synthetic fibers. Their length typically varies from 3 to 7 inches, depending on which animal and which part of the body they come from. They are made up of compact group of cells which originate at the bottom of hair follicle.[25] The structure of the wool fiber is made up of three distinct components namely cuticle, cortex and medulla.[25] Cuticle forms the outer surface of the wool fiber and exhibits a hydrophobic character and a scalar structure as seen in Figure 1.2.[25] The cortex is found beneath (inside) the cuticle and is the most important and major component of the wool fiber making up about 90% of the wool fiber. It is made up of two distinct regions called orthocortex and paracortex, both containing respective cortical cells. Paracortical cells consist of polypeptide cells that have covalent disulfide crosslinks whereas the orthocortical cells do not contain such disulfide crosslinks. This difference in the disulfide crosslinks results in varying degree of moisture absorption and related longitudinal expansion in these regions. The

absence of the covalent crosslinks in the orthocortical cells facilitates more moisture absorption, swelling and elongations compared to the paracortical cells.[24] This results in a natural crimp or waviness in the fiber with the paracortex that expands less, always on the inside of the crimp wave. Medulla is made up of special cells which are hollow and run through the axis of the fibers. Medullated wool fibers are avoided in the apparel sector due to their coarseness and irregular dye-uptake characteristics.[24] Wool fibers and fabrics are mainly used for providing warmth, such as in sweaters or blankets. Wool fibers and fabrics are good insulators because of the inherently crimpy nature of the fiber which allows trapping of air around the body and decreases heat transfer via convection and conduction.[26] Fabrics made from wool have natural warmth and hydrophobic characteristics which make them an ideal choice for use in winter outerwear garments.

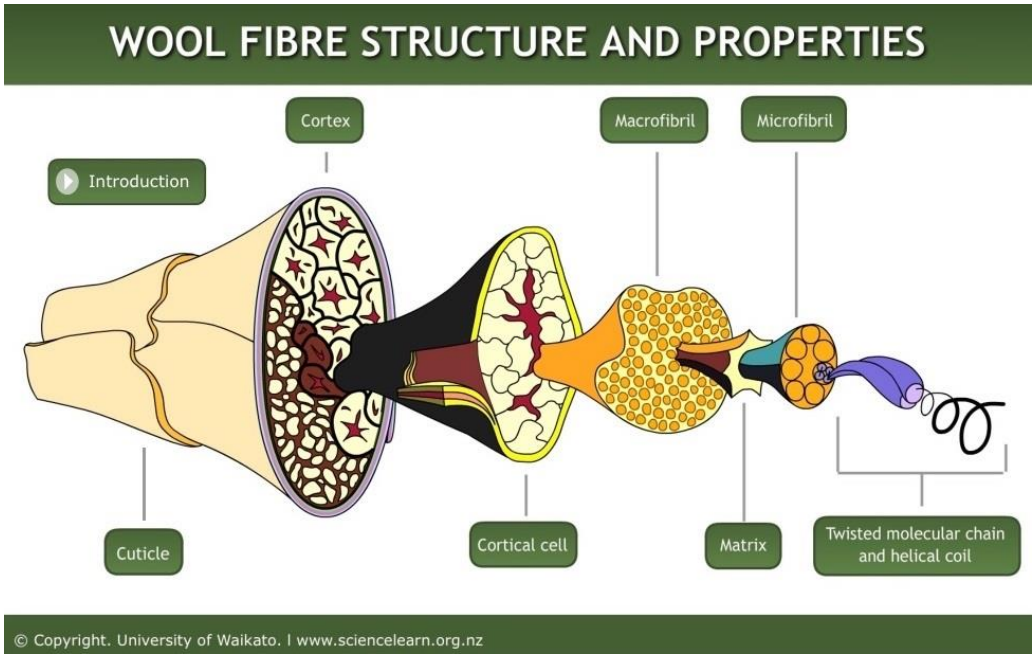

Figure 1.2 Structure of merino wool fiber.[25]

1.2 Wet-chemical processing of natural fibers and fabrics

Natural fibers are renewable, mostly yearly, and biodegradable.[27] They are considered to be the best choice of fibers for making environment friendly fabrics.[27] However, processing of natural fibers and obtaining the desired properties involve a lot of chemical processing right from the fiber stage such as removing impurities, to preparation for yarn spinning and fabric manufacturing. A broad array of chemicals are also used during dyeing, printing and finishing processes that cause severe water and land pollution.[28] As the textile sector has grown with the growing population, chemical consumption has also increased and has had a significant negative impact on the environment.[28] In addition, the concept of apparel has undergone a transformation and various functional finishes are now commonly applied onto the fabrics.[29] Such finishes that use toxic chemicals have added the urgency to develop environment friendly processes that do not harm the air, land or water.

Although natural fibers such as cotton and wool are very comfortable to wear, various chemical treatments are used to improve their performance and expand their applications. For example, as discussed earlier in section 1.1.1, cotton fabrics are lightweight, hydrophilic, breathable and makes an excellent fabric for apparel use. In hot and humid summer days, it can soak up the sweat, allow the heat to escape from the body and help to keep the wearer comfortable.[27] However, it certainly has some limitations. For example, in case of excess sweating, it can retain moisture or sweat and will not dry as quick as the synthetic fabrics and hence, is not an ideal fabric for active sportswear or hiking purposes. Cotton fabrics also wrinkle easily and require

certain amount of after-care such as ironing after washing. Ironing can be a tedious and time consuming chore, but wearing wrinkled shirts is not aesthetically pleasing.[29] To overcome, the undesired wrinkling of the fabrics, cotton fabrics are treated with easy-care finishes.[27] The history and chemistry that go into easy-care finishing of cotton fabrics is discussed later in section 1.2.1. Durable water repellent (DWR) finish which is generally applied to cotton fabrics for use in outerwear such a jackets, denims or bags to make them hydrophobic is discussed in section 1.2.2.

As discussed in 1.1.2, wool is a polypeptide obtained from hair of certain animals. The raw fleece contains impurities which are removed by scouring which involves washing with hot water and detergents to remove soil, grease and other impurities. The cleaned wool is carded and/or combed to form roving or sliver. The fibers in the roving are held together by the cohesive force resulting from the curliness of the fibers and the natural hooks (scales) present on the surface of the wool fibers.[30] The sliver is drawn to desired level (linear density) and twisted to form yarns. The yarns can then be woven or knitted into fabrics. Yarns need to undergo high tension and processing speeds during spinning, weaving and knitting and hence need to be twisted to appropriate level to attain necessary strength. In the fabric form, wool requires a great deal of attention in wash-care as it is a very delicate and prone to permanent shrinkage, known as felting, which occurs when moisture, heat and agitation are provided simultaneously.[30] Under those conditions, typically present in dryers, the scales on the fiber surface permanently lock with each other. Some chemical treatments associated with wool fibers and fabrics are discussed in section 1.2.3.

1.2.1 Easy-care finishes for cotton fabrics

Easy-care finishes for cotton fabrics have become very popular as they add smooth, aesthetic and flawless look to the fabrics. The primary goal of easy-care finishing is to be able to wash the clothing with minimal creasing so that it requires minimal to no ironing to restore its pristine appearance.[27] Easy-care finishes are generally applied to shirts and trousers to avoid wrinkled appearance while wearing or after washing. They are applied as functional finishes to suit the aspirational lifestyle to follow 'wash, dry and go' concept, saving time and energy spent on ironing clothes.

Fabrics made using cotton and other cellulose fibers such as lyocell and viscose easily wrinkle due to both, the chemical structure of cellulose and the fiber morphology.[27] As seen in Figure 1.1, cellulose contains large amount of hydroxyl groups and is highly hydrophilic. In addition, the cotton fiber contains both amorphous and crystalline regions due to its mostly fibrillar nature within which the molecules are highly oriented in a crystal form.[31] The hydroxyl groups in the amorphous region are held together by weaker forces, e.g., hydrogen bonds, and absorption of water can easily cause molecular slippage and fibril movement. During wear and washings of the apparel, hydrogen bonds in the amorphous region are broken and re-formed at new locations creating permanent wrinkles.[32] The primary method of creating wrinkle-resistant cotton fabrics is to use appropriate agents to crosslink the cellulose chains in the fiber. This prevents the relative displacement of the cellulose chains in cotton fibers when washed or worn. Fabrics may also be coated with resin or crosslinked via reaction with hydroxyl groups of cellulose to avoid the molecular movement to create wrinkle-resistant fabrics. This is achieved by passing the fabrics through a bath

containing crosslinker, catalyst and softener and then squeezed through a padding mangle to control the add-on or loading of the resin on the fabrics. The fabrics are further passed through a stenter (tenter) to accomplish curing to achieve the required easy-care finish and to obtain uniform width.

Earlier, phenol/formaldehyde or urea/formaldehyde resins were applied onto cotton fabrics to obtain wrinkle resistance.[33] They react together forming a small molecule, which could then penetrate inside the fibers or in between them and impart wrinkle-resistance to the fabrics.[33] However, these resins suffered from the disadvantage wherein the treated fabrics absorbed chlorine during hypochlorite bleaching or laundering causing tendering of fabrics which means degrading the cellulose fibers often leading to strength loss.[33-34] Methylolmelamines were also used in place of urea/formaldehyde-based resins to overcome the chlorine retention.[34] Fabrics treated with methylolmelamines could resist tendering. However, since chloramines of melamines are yellow in color, it led to the yellowing of the fabrics after bleaching.[33-34] N-H containing compounds have been shown to absorb chlorine causing tendering or yellowness.[33,34] As a result, crosslinking reactants that did not contain N-H groups were used to impart wrinkle resistance to the cotton fabrics.[33] Currently, Dimethyloldihydroxyethyleneurea (DMDHEU) is the most effective and low-cost crosslinking agent used to finish cotton fabrics to impart wrinkle-resistance.[32] However, DMDHEU treated fabrics have shown to release formaldehyde during finishing as well as during use.[32] The rate of formaldehyde release was shown to increase in water and sweat.[35] Environmental concerns have led to banning of formaldehyde-based or formaldehyde-releasing chemicals during processing of textile

materials as it poses a significant threat to human health and, thus, there is a need to replace DMDHEU-based finishing for cotton fabrics.[32, 35]

Since then, many non-formaldehyde based new crosslinking agents have been developed to impart wrinkle-resistance to cotton fabrics. Polycarboxylic acids (PCAs) such as citric acid (CA), maleic acid, 1,2,3,4-butanetetra-carboxylic acid (BTCA) have been studied extensively as non-formaldehyde based crosslinkers for cellulose since the early 1990s.[31] PCAs with three or more carboxylic acid groups adjacent to each other in the molecular backbone are effective crosslinking agents for cellulose.[36] The crosslinking using PCAs generally proceeds in two steps where the two adjacent carboxylic groups first form an anhydride and then react with the hydroxyl groups from cellulose leaving the second carboxylic acid group in the anhydride open for reaction.[36] The second carboxylic acid can then form an anhydride with the third adjacent carboxylic acid group and react with the hydroxyl group from the cellulose.[37] Since, at least two esters are formed with PCA contain three carboxylic acid groups, it successfully crosslinks the cellulose and imparts the desired wrinkle-free finish.[31] However, PCAs are expensive and also require a catalyst.[32, 36] Crosslinking using CA also causes significant yellowing of the fabrics.[34] Crosslinking with PCAs in general causes strength loss in fabrics because of the acidic nature of the PCAs which causes depolymerization of the cellulose backbone.[31, 34, 36] In summary, high cost, yellowing and strength reduction are major factors why PCAs are not being used at industrial scale.

Several other greener crosslinkers have been developed to crosslink cellulose.[29, 38, 39] Qi et al. reacted acryloyl chloride with malic acid, as seen in Figure

1.3(a), to create a crosslinker with double bond or vinyl group on one end and bifunctional carboxylic acid group on the other end.[38] While the bifunctional carboxylic acid can form one ester bond with the cellulose, the vinyl group on the other end can polymerize in the presence of catalyst, sodium hypophosphite (SHP), as seen in Figure 1.3(b).[38]

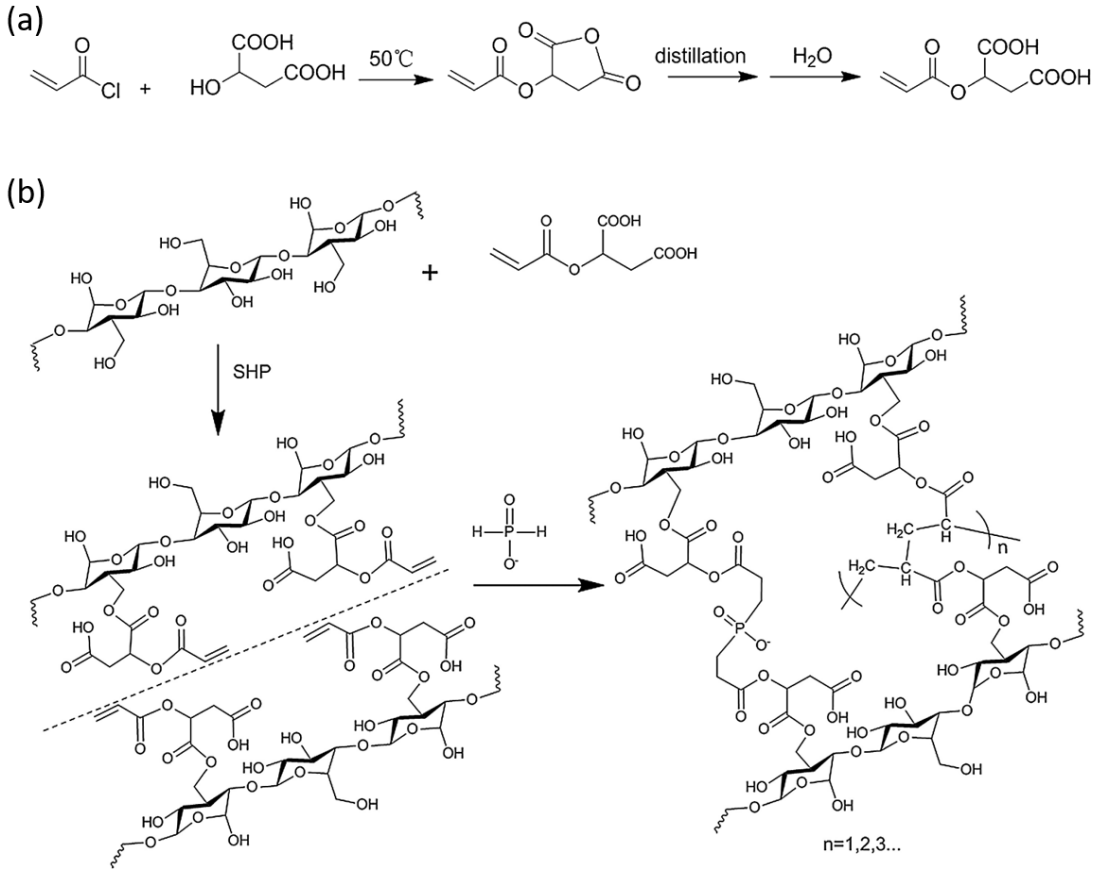

Figure 1.3 (a) synthesis of acryol malic acid crosslinker (b) crosslinking of cellulose using acryol malic acid.[38]

Dehabdi, Buschmann and Gutmann carried out carboxylation of polyvinyl amine by reacting polyvinyl amine and bromoacetic acid to form polyamino carboxylic acid.[39] The reaction product was used for crosslinking cellulose as seen in Figure 1.4.[39]

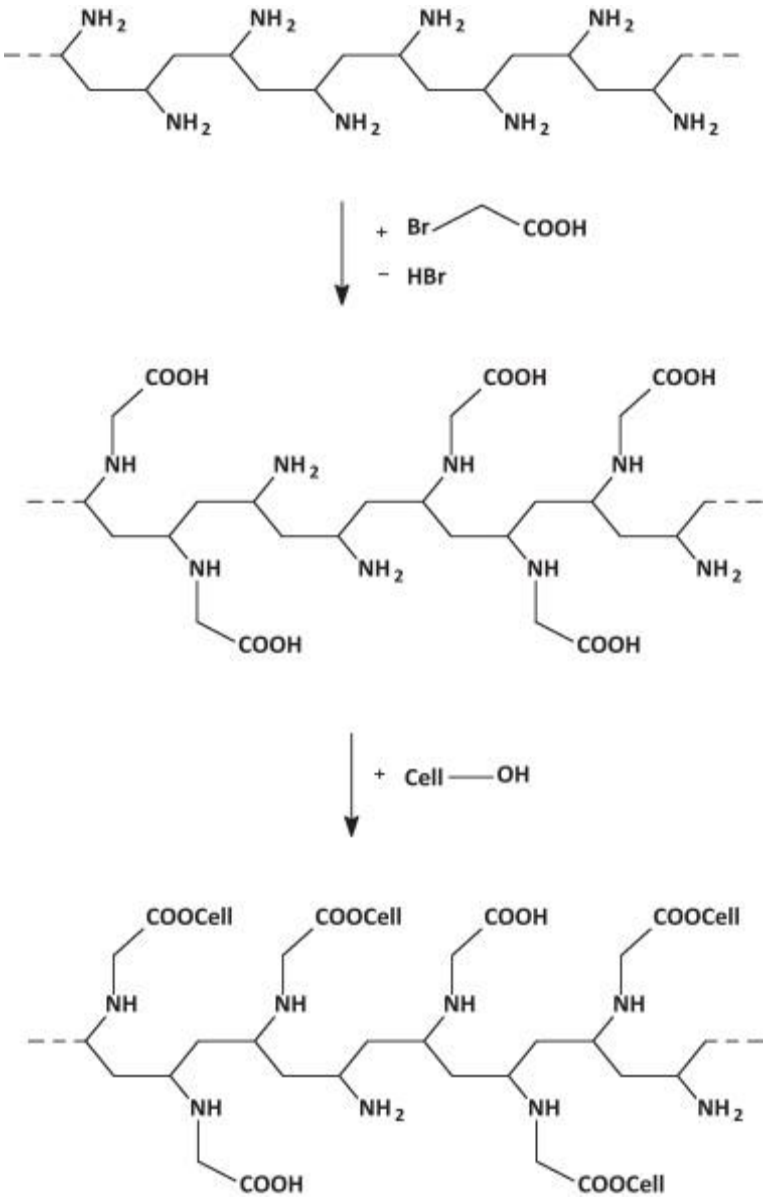

Figure 1.4 Proposed reaction for carboxylation of polyvinyl amine with bromoacetic acid and crosslinking of cellulose.[39]

Schramm and Amann synthesized a novel organic-inorganic hybrid crosslinker for crosslinking cellulose via sol-gel method. The hydrolyzed trialkoxysilane (3-triethoxysilylpropyl) succinic anhydride was reacted with 2,4,6-triamine-1,3,5-triazine melamine at elevated temperature until reflux and applied onto cotton fabrics at 160ºC

and 220ºC.[29] Their proposed reaction scheme for crosslinking cellulose is shown in Figure 1.5.

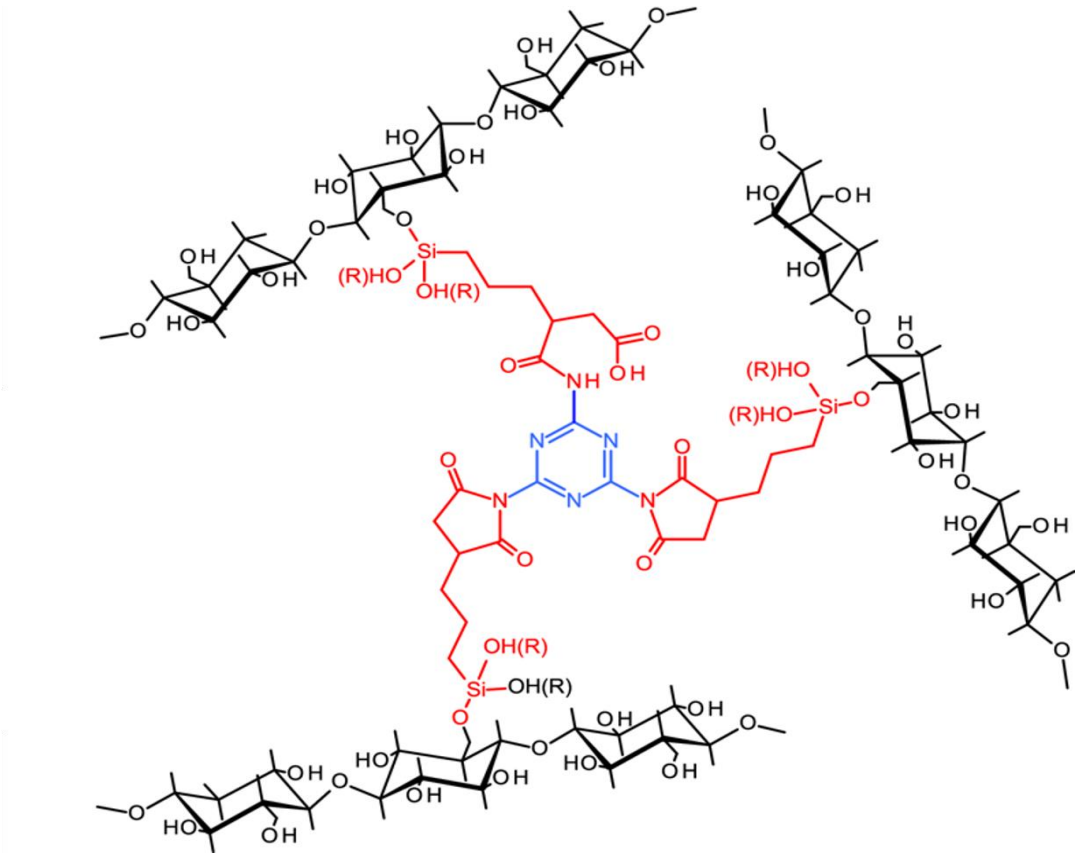

Figure 1.5 Proposed reaction for crosslinking of cellulose using hydrolyzed dicarboxylic acid based alkoxysilane/melamine.[29]

1.2.2 Durable water repellent (DWR) finishes for cotton fabrics

Although good wettability of the fabrics is important from the point of view of wet processing of cotton fabrics and wearing comfort, the ability of cotton fabrics to repel water after finishing is a desirable property in many applications. Some natural surfaces such as duck feather and lotus leaf which exhibit high level of water repellency and self-cleaning abilities, show multi-scale roughness of waxy texture on the surface.[40] The water repellency of a fabric depends upon the resistance to wetting

and penetration by water. Three main factors: chemical nature of the fiber surface, geometry or roughness and the inter-fiber and inter-yarn capillary spaces are considered to determine the resistance of fabrics to wetting.[41] The majority of the DWR finishes can be applied to woven and non-woven fabrics as they tend to have less inter-yarn capillary spaces as opposed to the knitted fabrics which can have large inter-yarn spaces that allow water to penetrate readily.[41] The use of water repellent finishes in sportswear, protective clothing, curtains, upholstery, table linens and others is a growing market sector. Based on the chemicals applied, the fabrics may also exhibit oil repellency and stain-release properties.[42] However, it is possible that DWR obtained with low surface energy surfaces can be oleophilic that can attract and retain oil.

Many DWR finishes have been developed for cotton fabrics. Fluorochemicals (also known as fluorocarbons) are commonly used for creating water repellent fabrics. They were first applied to textiles in 1960s.[42] Since 1990s there has been an increasing demand for fluorochemical-finished fabrics as they exhibit outstanding water and oil-repellency.[42] This imparts a unique level of protection for textile surfaces against most liquids and enhances stain and soil-repellent properties. Fluorochemicals are organic compounds containing a perfluoroalkyl residue in which all hydrogen atoms are replaced by fluorine as seen in Figure 1.6(a). They can be applied onto fabrics using regular pad-dry-cure method or via coating the fabrics with nanoparticles using audio frequency plasma of fluorocarbon derivative.[43] Creating surface roughness on fabric surfaces is another way to enhance the water repellency of the fabrics.[43] A combination of various SiO_2 particles along with water repellent agents has been

shown to impart hydrophobicity to the fabrics.[47] Perfluorooctyl quaternary ammonium silane coupling agents are commonly applied to achieve water repellency.[27] Polyfluoroalkyl substances (PFASs) can be divided into two categories based on perfluoroalkyl moiety chain lengths into long chain PFAS and short chain PFAS.[44-45] However, there are growing concerns in using PFAS in textiles as they bioaccumulate and show potential of increased risk of cancer and thyroid hormone disorders. C-6 chains have been proposed instead of C-8 as they are shorter in length and reduce the impact on the environment.[45] Never the less, intensified legislations and increased research on toxicity of PFAS compounds have necessitated developing and using non-fluorinated chemistry in textile products.[44-45]

Non-fluorinated chemistry for creating DWR finishes on cotton fabrics include the use of paraffin waxes and silicones (Figure 1.6(b)) along with nanoparticles.[41] Various finishes based on paraffin wax (melting point 52 -56 °C) itself or along with higher fatty acids have been used as non-fluorinated DWR finishes.[43] Fatty acids, biodiesel or plant oils can be excellent substitutes for creating hydrophobic fabrics.[46-47] Fatty acids are hydrocarbons and can react with cotton fabrics as seen in Figure 1.6(c) to lower the surface energy of the fabrics creating a hydrophobic surface.[47]

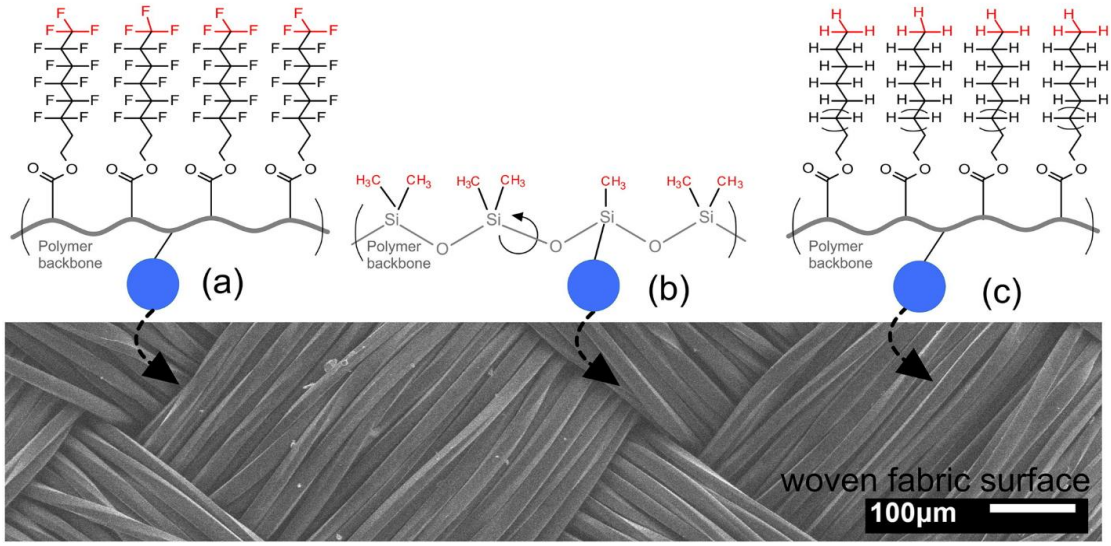

Figure 1.6 Grafting of (a) fluorinated polymer (b) silicone and (c) hydrocarbons on cotton fabrics.[42]

1.2.3 Chemical treatments for wool fibers and fabrics

As discussed earlier in section 1.1.2, woolen fabrics have excellent thermal regulative properties because of its natural crimp which maintains high amount of air embedded in the fabrics.[48] Woolen fabrics wrinkle less compared to cotton fabrics and they also have low flammability because of their polypeptide (keratin) chemistry. However, wool is an expensive fiber and it can be more expensive to maintain woolen fabrics. Machine washing wool fabrics can damage the fibers, so it is recommended to either dry clean them or hand wash them. Woolen fabrics and apparel are also prone to shrinkage or felting and moth-attacks and so require a great deal of after-care.[48]

Significant amount of chemical processing goes into the production of wool fabrics. The fleece or the raw wool sheared from the sheep needs to be cleaned (scoured) by washing in soap water to remove soil, grease and other impurities. The

cleaned fibers are then carded to from sliver or wool tops. These fibers are weak and do not have the strength required to withstand the spinning speeds and the high-tension cycles during the weaving process. As a result, many times they are treated with bifunctional crosslinkers to improve their strength.[49] Glyoxal, glutaraldehyde, diisocyanates and carbodiimides and other formaldehyde-based crosslinkers have been used to improve the strength of the fibers.[49] However, such crosslinkers are classified as toxic and some of them may be even carcinogenic.[50]

Hydrogen bonds present in wool can be broken in the presence of water and reconnect at another location while drying. This rearrangement of hydrogen bonds trigger wrinkling in a similar way as seen in cotton fabrics, but to a lesser extent.[48] Wool fabrics are generally finished to improve the existing properties and/or to add desired functional properties to meet the modern 'wash and go' requirements. For example, the fabrics can be crosslinked with the above mentioned crosslinkers to improve the dimensional stability, i.e., reduce felting, and the wrinkle-resistance of the fabrics. The scales on wool fibers get interlocked during washing, particularly in the dryer, where moisture, agitation and heat combine, to cause permanent shrinkage commonly known as felting.[51] Finishing the fibers/fabrics using crosslinking agents can improve the shrinkage to some extent. However, the most commonly used method to avoid shrinkage is to treat the scales with chlorine and apply thin polymer coating containing polyamide-epichlorohydrin. The smoother surface allows sliding of fibers instead of interlocking of the scales. The above process used to treat the scales of the fibers to reduce interlocking is called the chlorine-Hercosett process. Although this process can avoid wool felting, it comes at a great environmental cost.[51]

Epichlorohydrin is toxic in nature and can be a skin irritant.[51] In addition, the wastewater generated from this process shows a significant level of adsorbable organic halogens (AOX). These toxic substances created when chlorine reacts with available carbon-based compounds are generally not acceptable in wastewater treatment facilities.[51]

Due to environmental concerns, researchers have worked hard and successfully obtained better alternatives to the chlorine-based treatments. One such environment friendly treatment involves the use of enzymes. Enzyme such as protease can be used to treat the surface of the fabrics to remove outer protein layer from the scales and smoothen them.[52] However, it is very difficult to limit the action of the protease only to the surface. Penetration of protease inside the fiber causes enzymatic degradation of the fiber. The penetration and degradation of the inner cortical cells of the fibers reduces their strength and can be avoided by increasing the molecular size of the enzyme by reacting it with another polymer.[53] However, enzymatic modifications or treatments are very expensive and still could fail to achieve the commercial standard for machine washable wool fabrics. Keratin extracted from the chicken feathers used to crosslink wool fibers with diepoxy crosslinker, glycerol diglycidyl ether have also shown to reduce the felting of wool fabrics.[51] This can be an inexpensive alternative to the enzyme treatment.[51]

1.3 Objectives and layout of the present research

Textile industry has a huge market and variety of applications as seen above. A large number of chemical processes are used in manufacturing and maintaining of

textiles. Natural fibers are yearly renewable as well as biodegradable. However, products made using natural fibers do not always qualify as environmentally sound materials. As described above, various chemical processing that go into the manufacturing and functionalizing the natural fibers and fabrics for different finishing processes can have a negative impact on human health as well as the environment. The main objective of the present research was to find 'green' alternatives and chemistry solutions to replace the existing toxic chemical processing for finishing cellulosic and protein-based fibers and fabrics. This research mainly discusses cleaner and greener alternatives for creating wrinkle-free and superhydrophobic cotton fabrics and also includes a green crosslinking process for wool fibers to improve its strength. The 'green' chemistry developed for wool fibers was also extended to human hair, a keratin-based fiber similar to wool for styling and stabilizing.

Chapter 2 and chapter 3 present sugar-based 'crosslinkers' for creating wrinkle-free cotton fabrics. Chapter 2 focuses on sucrose-based crosslinker while chapter 3 describes cyclodextrin-based crosslinker for obtaining wrinkle-resistant cotton fabrics. Sucrose and cyclodextrin (CD) were chemically modified, separately, to create multiple carboxylic acid groups and then used to crosslink the cotton fabrics via esterification. The chemical modifications of sucrose and CD were fully characterized. The wrinkle-resistance of the fabrics was measured as wrinkle recovery angle. The effect of crosslinking on tensile properties and its durability to laundry washings were also studied.

Chapter 4 and chapter 5 present a non-fluorinated process to create durable superhydrophobic cotton fabrics. Different shapes of silica nanoparticles were

synthesized and covalently bonded to the cotton fabrics. The silica nanoparticles created desired surface roughness on the fabrics and their covalent bonding ensured laundry durability. The fabrics were further grafted with fatty acid via esterification to lower their surface energy. Superhydrophobicity was measured in terms of water contact angle. The effect of treatment on tensile properties and durability to washings was studied.

Chapter 6 presents the synthesis of a unique sugar-based crosslinker derived from soy flour. The soy flour sugar based crosslinker was used to enhance the tensile strength and modulus of wool slivers. Stronger wool fibers can enhance the spinning and weaving efficiency of the yarn and fabrics and reduce fiber wastage as well as defects.

Chapter 7 presents the applications of sucrose-based crosslinker of hair stabilization process. The applications of crosslinker is beneficial for obtaining durable hair-styling effects.

Chapter 8 presents the conclusions and future direction and suggestions for further research.

1.4 References

1. Netravali, A. N.; Chabba, S., Composites get greener. *Materials today* **2003,** *4* (6), 22-29.

2. Patil, N., Polysacharide Based Hybrid 'Green'Composites. Cornell Univeristy, Ithaca NY **2016**.

3. Lewis, T. L.; Park, H.; Netravali, A. N.; Trejo, H. X., Closing the loop: a scalable zero-waste model for apparel reuse and recycling. *International Journal of Fashion Design, Technology and Education* **2017,** *10* (3), 353-362.

4. Joy, A.; Sherry Jr, J. F.; Venkatesh, A.; Wang, J.; Chan, R., Fast fashion, sustainability, and the ethical appeal of luxury brands. *Fashion theory* **2012,** *16* (3), 273-295.

5. https://www.textileworld.com/textile-world/fiber-world/2015/02/man-made-fibers-continue-to-grow/.

6. Yasin, S.; Sun, D., Propelling Textile Waste to Ascend the Ladder of Sustainability: EOL Study on Probing Environmental Parity in Technical Textiles. *Journal of Cleaner Production* **2019**.

7. Townsend, T.; Sette, J., Natural fibres and the world economy. In *Natural fibres: advances in science and technology towards industrial applications*, Springer: 2016; pp 381-390.

8. Patil, N. V.; Netravali, A. N., Microfibrillated cellulose-reinforced nonedible starch-based thermoset biocomposites. *Journal of Applied Polymer Science* **2016,** *133* (45).

9. Roy, D.; Semsarilar, M.; Guthrie, J. T.; Perrier, S., Cellulose modification by polymer grafting: a review. *Chemical Society Reviews* **2009,** *38* (7), 2046-2064.

10. Bashar, M. M.; Khan, M. A., An overview on surface modification of cotton fiber for apparel use. *Journal of Polymers and the Environment* **2013,** *21* (1), 181-190.

11. Zhang, J.; Liu, Z.; Kong, Q.; Zhang, C.; Pang, S.; Yue, L.; Wang, X.; Yao, J.; Cui, G., Renewable and superior thermal-resistant cellulose-based composite nonwoven as lithium-ion battery separator. *ACS applied materials & interfaces* **2012,** *5* (1), 128-134.

12. Kim, C.-W.; Kim, D.-S.; Kang, S.-Y.; Marquez, M.; Joo, Y. L., Structural studies of electrospun cellulose nanofibers. *Polymer* **2006,** *47* (14), 5097-5107.

13. Hoenich, N. A., Cellulose for medical applications: past, present, and future. *BioResources* **2006,** *1* (2), 270-280.

14. Nishino, T.; Matsuda, I.; Hirao, K., All-cellulose composite. *Macromolecules* **2004,** *37* (20), 7683-7687.

15. Lee, K.-Y.; Aitomäki, Y.; Berglund, L. A.; Oksman, K.; Bismarck, A., On the use of nanocellulose as reinforcement in polymer matrix composites. *Composites Science and Technology* **2014,** *105*, 15-27.

16. Khalil, H. A.; Bhat, A.; Yusra, A. I., Green composites from sustainable cellulose nanofibrils: A review. *Carbohydrate polymers* **2012,** *87* (2), 963-979.

17. Nakagaito, A.; Iwamoto, S.; Yano, H., Bacterial cellulose: the ultimate nano-scalar cellulose morphology for the production of high-strength composites. *Applied Physics A* **2005,** *80* (1), 93-97.

18. Qiu, K.; Netravali, A. N., A review of fabrication and applications of bacterial cellulose based nanocomposites. *Polymer Reviews* **2014,** *54* (4), 598-626.

19. Rahman, M. M.; Netravali, A. N., Oriented bacterial cellulose-soy protein based fully 'green'nanocomposites. *Composites Science and Technology* **2016,** *136*, 85-93.

20. Edgar, K. J., Cellulose esters in drug delivery. *Cellulose* **2007,** *14* (1), 49-64.

21. Petersen, N.; Gatenholm, P., Bacterial cellulose-based materials and medical devices: current state and perspectives. *Applied microbiology and biotechnology* **2011,** *91* (5), 1277.

22. Patil, N. V.; Netravali, A. N., Direct Assembly of Silica Nanospheres on Halloysite Nanotubes for "Green" Ultrahydrophobic Cotton Fabrics. *Advanced Sustainable Systems* **2019**, 1900009.

23. Netravali, A. N.; Zhong, Y.; Patil, N. V., Modified cellulosic compositions having increased hydrophobicity and processes for their production. Google Patents: 2018.

24. Hearle, J., A critical review of the structural mechanics of wool and hair fibres. *International Journal of Biological Macromolecules* **2000,** *27* (2), 123-138.

25. https://www.sciencelearn.org.nz/resources/875-wool-fibre-properties

26. Wilson, C. A.; Laing, R. M., The effect of wool fiber variables on tactile characteristics of homogeneous woven fabrics. *Clothing and Textiles Research Journal* **1995,** *13* (3), 208-212.

27. Yetisen, A. K.; Qu, H.; Manbachi, A.; Butt, H.; Dokmeci, M. R.; Hinestroza, J. P.; Skorobogatiy, M.; Khademhosseini, A.; Yun, S. H., Nanotechnology in textiles. *ACS nano* **2016,** *10* (3), 3042-3068.

28. De Smet, D.; Weydts, D.; Vanneste, M., Environmentally friendly fabric finishes. In *Sustainable Apparel*, Elsevier: 2015; pp 3-33.

29. Schramm, C.; Amann, A., Formaldehyde-free, crease-resistant functionalization of cellulosic material modified by a hydrolyzed dicarboxylic acid based alkoxysilane/melamine finishing system. *Cellulose* **2019,** *26* (7), 4641-4654.

30. Kaur, A.; Chakraborty, J., Controlled eco-friendly shrink-resist finishing of wool using bromelain. *Journal of Cleaner Production* **2015,** *108*, 503-513.

31. Ji, B.; Zhao, C.; Yan, K.; Sun, G., Effects of acid diffusibility and affinity to cellulose on strength loss of polycarboxylic acid crosslinked fabrics. *Carbohydrate polymers* **2016,** *144*, 282-288.

32. Hashem, M.; Ibrahim, N. A.; El-Shafei, A.; Refaie, R.; Hauser, P., An eco-friendly–novel approach for attaining wrinkle–free/soft-hand cotton fabric. *Carbohydrate Polymers* **2009,** *78* (4), 690-703.

33. Harifi, T.; Montazer, M., Past, present and future prospects of cotton cross-linking: New insight into nano particles. *Carbohydrate polymers* **2012,** *88* (4), 1125-1140.

34. Lu, Y.; Yang, C. Q., Fabric yellowing caused by citric acid as a crosslinking agent for cotton. *Textile research journal* **1999,** *69* (9), 685-690.

35. Li, B.; Dong, Y.; Wang, P.; Cui, G., Release behavior and kinetic evaluation of formaldehyde from cotton clothing fabrics finished with DMDHEU-based durable press agents in water and synthetic sweat solution. *Textile Research Journal* **2016,** *86* (16), 1738-1749.

36. Ji, B.; Tang, P.; Yan, K.; Sun, G., Catalytic actions of alkaline salts in reactions between 1, 2, 3, 4-butanetetracarboxylic acid and cellulose: II. Esterification. *Carbohydrate polymers* **2015,** *132*, 228-236.

37. Šauperl, O.; Stana-Kleinschek, K.; Ribitsch, V., Cotton Cellulose 1, 2, 3, 4 Buthanetetracarboxylic Acid (BTCA) Crosslinking Monitored by some Physical—chemical Methods. *Textile Research Journal* **2009,** *79* (9), 780-791.

38. Qi, H.; Huang, Y.; Ji, B.; Sun, G.; Qing, F.-l.; Hu, C.; Yan, K., Anti-crease finishing of cotton fabrics based on crosslinking of cellulose with acryloyl malic acid. *Carbohydrate polymers* **2016,** *135*, 86-93.

39. Dehabadi, V. A.; Buschmann, H.-J.; Gutmann, J. S., Durable press finishing of cotton fabrics with polyamino carboxylic acids. *Carbohydrate polymers* **2012,** *89* (2), 558-563.

40. Liu, Y.; Chen, X.; Xin, J., Hydrophobic duck feathers and their simulation on textile substrates for water repellent treatment. *Bioinspiration & biomimetics* **2008,** *3* (4), 046007.

41. Roach, P.; Shirtcliffe, N. J.; Newton, M. I., Progess in superhydrophobic surface development. *Soft matter* **2008,** *4* (2), 224-240.

42. Holmquist, H.; Schellenberger, S.; van Der Veen, I.; Peters, G.; Leonards, P.; Cousins, I. T., Properties, performance and associated hazards of state-of-the-art durable water repellent (DWR) chemistry for textile finishing. *Environment international* **2016,** *91*, 251-264.

43. Kissa, E., Repellent finishes. In *Handbook of Fiber Science and Technology Volume 2*, Routledge: 2018; pp 143-210.

44. Schellenberger, S.; Gillgard, P.; Stare, A.; Hanning, A.; Levenstam, O.; Roos, S.; Cousins, I. T., Facing the rain after the phase out: Performance evaluation of alternative fluorinated and non-fluorinated durable water repellents for outdoor fabrics. *Chemosphere* **2018,** *193*, 675-684.

45. Hill, P. J.; Taylor, M.; Goswami, P.; Blackburn, R. S., Substitution of PFAS chemistry in outdoor apparel and the impact on repellency performance. *Chemosphere* **2017,** *181*, 500-507.

46. Yoo, Y.; Youngblood, J. P., Green one-pot synthesis of surface hydrophobized cellulose nanocrystals in aqueous medium. *ACS Sustainable Chemistry & Engineering* **2016,** *4* (7), 3927-3938.

47. Zhong, Y.; Netravali, A. N., 'Green'surface treatment for water-repellent cotton fabrics. *Surface Innovations* **2016,** *4* (1), 3-13.

48. Kuzuhara, A.; Hori, T., Reducing wrinkle formation in wool with 2-Iminothiorane Hydrochloride. *Textile research journal* **2002,** *72* (4), 285-289.

49. Di Modica, G.; Marzona, M., Cross-linking of wool keratin by bifunctional aldehydes. *Textile Research Journal* **1971,** *41* (8), 701-705.

50. Mohsin, M.; Farooq, U.; Raza, Z. A.; Ahsan, M.; Afzal, A.; Nazir, A., Performance enhancement of wool fabric with environmentally-friendly bio-cross-linker. *Journal of cleaner production* **2014,** *68*, 130-134.

51. Eslahi, N.; Moshggoo, S.; Azar, S. K.; Dadashian, F.; Nejad, N. H., Application of extracted feather protein to improve the shrink resistance of wool fabric. *Journal of Industrial Textiles* **2015,** *44* (6), 835-848.

52. Cortez, J.; Bonner, P. L.; Griffin, M., Transglutaminase treatment of wool fabrics leads to resistance to detergent damage. *Journal of Biotechnology* **2005,** *116* (4), 379-386.

53. Heine, E.; Höcker, H., Enzyme treatments for wool and cotton. *Review of progress in coloration and related Topics* **1995,** *25* (1), 57-70.

Chapter 2 Multifunctional sucrose acid as a 'green' crosslinker for wrinkle-resistant cotton fabrics

Namrata V. Patil and Anil N. Netravali*

Department of Fiber Science & Apparel Design,

Cornell University, 37 Forest Home Dr., Ithaca, NY 14853, USA

Submitted to:
Springer Cellulose

2.1 Abstract

In this study, a ‘green’ crosslinker was developed using sucrose, an inexpensive natural resource, as replacement for conventional durable-press finishing agents for cotton fabrics. Sucrose was oxidized using a benign oxidizing agent, hydrogen peroxide (H_2O_2), and carboxylated using malic acid (MA) to form multifunctional sucrose acid (MSA). The structural chemical changes and presence of multiple carboxylic acid groups after oxidation and carboxylation were confirmed using ATR-FTIR and 13C NMR. Cotton fabrics treated with MSA showed a maximum wrinkle recovery angle (WRA) of 202º, over 77% improvement compared to 114º for untreated fabrics. More importantly, the chemical crosslinks introduced in the fabrics after MSA treatment as confirmed by ATR-FTIR were found durable to multiple laundry washings. MSA treated fabrics showed only 18% loss in tensile strength in the warp direction and SEM images of the treated fibers do not show surface change. This suggested that MSA could be used to replace currently used dimethylol dihydroxyethyleneurea (DMDHEU) or 1,2,3,4-butanetetracarboxylic acid (BTCA) based finishing agents which are toxic and expensive, respectively. The crosslinking mechanism using MSA and the changes in the physical properties of the fabrics such as WRA, color and tensile strength and strain are discussed.

2.2 Introduction

Wrinkle-free cotton garments, the latest fashion trend, entail the benefit of easy care and low maintenance after washing them while retaining their comfort characteristic (Wang et al. 2017). While the garments made from untreated cotton

fabrics show wrinkled surface after washing and requires time-consuming ironing to restore its pristine look, garments made from wrinkle-free treated fabrics require no ironing. They retain their aesthetic look wash after wash. Wrinkle-free or easy-care finish is therefore applied to many cotton fabrics (Kim et al. 2000; Schramm and Rinderer 2015). The first group of easy-care finishes introduced in 1920s consisted of N-methylol compounds, namely urea-formaldehyde or melamine-formaldehyde (Dehabadi et al. 2013). After various iterations of the formaldehyde-based compounds to achieve maximum wrinkle-resistance, dimethylolethylene urea compounds were developed and have been predominantly used in easy-care finishes since 1947. The main product of this group was dimethyloldihydroxyethyleneurea (DMDHEU) which was the final product of the reaction between urea, glyoxal and formaldehyde (Dehabadi et al. 2013). Even today, DMDHEU remains the most effective and low-cost easy-care finishing agent for cotton fabrics to impart wrinkle-resistance (Dehabadi et al. 2013; Ibrahim et al. 2018; Lao et al. 2017).

To obtain desired wrinkle-free characteristics, cotton fabrics are generally coated with resin or crosslinked via reaction with the hydroxyl groups of cellulose (Qi et al. 2016). The hydroxyl groups present in the cellulose chains are hydrogen bonded by weak secondary forces, especially in the amorphous region and can be easily distorted during laundry or other external forces during wear causing wrinkles on the fabrics (Lao et al. 2017). The wrinkle-free finishes thereby act by creating crosslinks or ‘bridges’ between the cellulose molecular chains, by reacting with hydroxyl groups (Qi et al. 2016). Crosslinking eliminates hydroxyl groups and, as a result, inhibits the easy movement of the cellulose chains and prevents the wrinkles from forming on the

cotton fabrics (Qi et al. 2016). Environmental concerns and the potential risks associated with formaldehyde-based easy-care finishes have led to the introduction of some formaldehyde-free finishes (Hashem et al. 2009; Schramm and Rinderer 2015). Polycarboxylic acids (PCAs) such as 1,2,3,4-butanetetracarboxylic acid and citric acid have been the most promising formaldehyde-free chemicals to have imparted wrinkle-resistance to cotton fabrics (Lam et al. 2011; Xu and Li 2000). However, high cost associated with the PCAs and the catalysts have hampered the use of such PCAs on an industrial scale. Unacceptable loss in strength and yellowing of the fabrics are other drawbacks in addition to the cost that impedes the use of PCAs for practical applications and in spite of being toxic, the use of DMDHEU still prevails in the industry (Liu et al. 2016; Yao et al. 2013). This has called for moving towards a cleaner and inexpensive alternative to the DMDHEU and PCA-based easy-care finishes.

Sucrose is non-toxic, inexpensive and derived from abundantly available renewable source in nature. Sucrose has been oxidized using sodium periodate, 2,2,6,6-tetramethyl-1-piperidine oxoammonium salt (TEMPO) or through electrocatalytic oxidation to introduce aldehyde or carboxylic acid groups on it (Jalaja and James 2015; Lemoine et al. 2000; Parpot et al. 1997; Xu et al. 2015; Zhang et al. 2014). These involve either complex oxidation processes or expensive oxidizers and toxic metal catalysts (Edye et al. 1994; Mallat and Baiker 1994). None of the studies have reported the oxidation and carboxylation using a benign and inexpensive agents such as H_2O_2 and malic acid (MA) to introduce multiple bifunctional carboxylic acid

groups to form multifunctional sucrose acid (MSA) that can be used as a crosslinking agent for easy-care finishes of the cotton fabrics.

This study presents the preparation and application method of MSA as a non-toxic, inexpensive crosslinker to be used as an easy-care finishing agent for industrial application. The main focus of the study was to use a natural renewable source, sucrose and modify it to create reactive functional groups that could be used to crosslink cellulose to create wrinkle-free cotton fabrics. The preparation of MSA was a two-step process. The first step involved oxidation of sucrose using H_2O_2 to introduce carboxylic acid groups onto sucrose forming sucrose acid (SA) as shown in the reaction scheme in Figure 2.1. Fabrics treated with SA showed only a slight improvement in wrinkle recovery angle (WRA) of the fabrics, probably because the lack of adjacent carboxylic acid groups required for successful crosslinking of cellulose which in turn increases the WRA (Patil and Netravali 2019a). A second step involving carboxylation of SA using MA which introduced multiple bifunctional acid groups onto sucrose as shown in the reaction scheme in Figure 2.1 was important to increase the WRA of fabrics. The resultant multifunctional sucrose acid, MSA can be used to replace currently used toxic and expensive crosslinking agents such as DMDHEU and BTCA to impart wrinkle-resistance to the fabrics.

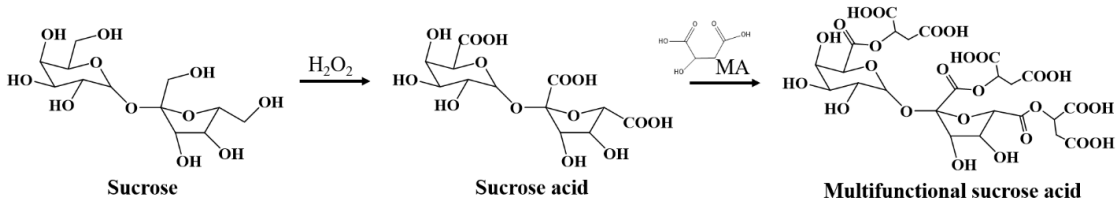

Figure 2.1. Proposed reaction scheme for oxidation and carboxylation of sucrose to form multifunctional sucrose acid (MSA).

2.3 Materials and Methods

2.3.1 Materials

A plain weave cotton fabric with 80 ends (warp) per inch (epi) and 70 picks (weft) per inch (ppi) was provided by TAL Apparel (Hong Kong). Sucrose and 30% Hydrogen peroxide (H_2O_2) were purchased from Fisher Scientific (Pittsburgh, PA). Catalase GC118 was provided by DuPont (Wuxi, China). Malic acid (MA) and sodium hypophosphite monohydrate (SHP) were purchased from VWR (Philadelphia, PA).

2.3.2 Preparation of MSA

In the 1st step a 10% solution of sucrose was oxidized using 30 mL of H_2O_2 at 60°C for 12 h with magnetic stirring at 300 rpm. At the end of 12 h, reactant sucrose solution was cooled down to room temperature and 1 µL of catalase was added to decompose the oxidizing agent, H_2O_2. The effervescence observed after addition of catalase due to decomposition of H_2O_2 to H_2O and the O_2 generated was allowed to subside by stirring the solution at low speed (100 rpm) for an additional 4 h. This resultant product was called sucrose acid (SA). In the 2nd step 2.5 g SHP was added to SA and the temperature was raised to 70°C to deprotonate the carboxylic acid groups created due to oxidation of sucrose. Three moles of MA was added to the deprotonated SA and the mixture was placed in a boiling bath (100°C) for 10 min to react the hydroxyl groups from MA with the deprotonated carboxylic acid groups from SA. As seen from the reaction scheme in Figure 2.1, SA has at least 3 carboxylic acid groups from oxidation of primary hydroxyl groups on sucrose. MA is a dicarboxylic acid with one hydroxyl group. Thus, each MA attached to the sucrose introduces 2 acid groups

on sucrose by consuming the one created by the oxidation process. Overall, if 3 moles of MA react with sucrose, we get six carboxylic acid groups on the sucrose. This solution containing at least 6 carboxylic acid groups was termed as multifunctional sucrose acid (MSA). The prepared MSA solution was stored at room temperature (RT) until used for fabric treatment.

2.3.3 Crosslinking of cotton fabrics using MSA

For treating cotton fabrics, 2.5 g of SHP was added to the prepared MSA solution as a catalyst. Cotton fabric specimens (20 cm x 20 cm) were immersed in the MSA mixture and laid flat on the glass plate and squeezed to remove the excess solution. They were dipped in the MSA solution for a 2nd time to increase the add-on % on fabrics and squeezed again and cured at 130°C, 140°C or 150°C, separately, for 30 min in an air circulating oven. After curing, the fabrics were thoroughly rinsed with DI water 2-3 times to make sure the excess unreacted chemicals were washed off and dried at RT. All fabrics were conditioned at 65 ± 2% relative humidity (RH) and 21 ± 1°C for 24 h prior to any characterization. The add-on % on the fabrics was calculated using the following equation:

$$\text{Add} - \text{on } \% = \frac{Wt - Wc}{Wc} \times 100$$

Where Wt is the weight of the treated fabrics after conditioning and Wc is the weight of the control fabrics after conditioning.

2.3.4 Attenuated total reflectance Fourier-transform infrared (ATR-FTIR)

ATR-FTIR analysis was used to study the effect of oxidation and carboxylation of sucrose. This technique was also used to study the effect of MSA treatment on cotton fabrics. ATR-FTIR spectra were collected using Thermo Nicolet Magna-IR 560 spectrometer (Madison, WI) with a split pea accessory. Each scan was an average of 300 scans from 4000 cm^{-1} to 500 cm^{-1} wavenumbers.

2.3.5 Nuclear magnetic resonance spectroscopy (NMR)

^{13}C NMR spectra were recorded using a Bruker Biospin AVIII HD 500 MHz spectrometer (France) to illustrate the chemical structural changes in sucrose after oxidizing with H_2O_2 as well as carboxylation with MA using D_2O as the solvent.

2.3.6 Evaluation of fabric wrinkle recovery angle (WRA)

AATCC test method 66-2008 was used to evaluate WRA of the control as well as treated fabrics. Six specimens of 40 mm × 15 mm dimensions were cut from randomly located parts of the control and treated fabrics. Three specimens were cut with their long dimensions parallel to the warp direction of the fabric while the other 3 had their long dimensions parallel to the weft (filling) direction. For the WRA test, each specimen was folded at the center and a dead load of 500 g was kept on it for 5 min. After removing the load, one end of the specimen was mounted in the circular scale of the WRA test instrument and the specimen was allowed to recover for 5 min before the recovery angle was measured. Three different fabric samples were treated with the prepared MSA solution made at 3 different times and specimens were tested from each of the fabric samples to ensure reproducibility of the results. The sum of

average of 9 specimens in warp direction and the 9 specimens in weft direction from 3 different fabrics treated is reported as the WRA value for each treatment condition.

2.3.7 Color evaluation of fabrics

The color coordinates L*, a* and b* of the control and treated fabrics were measured at five different spots using Macbeth Color-eye spectrophotometer, Model M2020PT, (Newburgh, NY). The b* value stands for -b* (blueness) to +b* (yellowness) and average of five b* values for each fabric is reported.

2.3.8 Laundry durability of WRA

Laundry durability of the treated fabrics was characterized using modified version of AATCC test method 61-2003. Specimens having dimensions of 10 cm × 10 cm were cut from the treated fabrics and washed in a flask containing 150 mL of aqueous solution of 0.15% (w/w) Tide® laundry detergent and 50 stainless steel balls (diameter 6 mm) at 49°C for 45 min with a constant stirring speed of 45 rpm and then rinsed with water. Each laundry cycle in this study is considered to be equivalent to 5 home laundering.

2.3.9 Evaluation of tensile properties

Tensile strength of the fabrics was determined according to ASTM D5035 strip method. Fabrics having dimensions of 25 mm × 150 mm were cut and tested on Instron universal testing machine (model 5566, Canton, MA) at a gage length of 75 mm and crosshead speed of 300 mm/min (strain rate of 4 min^{-1}). Averages of 10 specimens each in warp and weft directions, treated at different times, are reported.

2.4 Results and discussion

Figure 2.2 shows ATR-FTIR spectra of pure sucrose, SA, MA and MSA. As seen in Figure 2.2(a), the spectrum of sucrose shows two absorption zones: between 3700 cm^{-1} and 2800 cm^{-1} and between 1500 cm^{-1} and 500 cm^{-1}. The absorption peaks at 3338 cm^{-1} and 3385 cm^{-1} are due to the O-H stretching vibrations from water as well as hydroxyl groups on sucrose (Patil and Netravali 2019b). The absorption peaks between 1500 cm^{-1} and 500 cm^{-1} are characteristic peaks of the saccharide configuration. For example, the peak at 918 cm^{-1} corresponds to C−H bending in sucrose. The peak at 997 cm^{-1} is the characteristic peak of sucrose associated with the disaccharide linkage α-D-glucopyranosyl and β-D-fructofuranosyl groups. The peaks at 1043 cm^{-1} and 1255 cm^{-1} correspond to the C−O stretch in C−OH groups as well as C-C stretch in sucrose, whereas the peak at 1110 cm^{-1} corresponds to the stretching of C-O band in the C-O-C linkage (Patil and Netravali 2019). The peaks at 1321 cm^{-1} and 1411 cm^{-1} correspond to the combination of O-H bending of C-OH (Patil and Netravali 2019b). The ATR-FTIR spectrum of SA shows similar peaks similar to sucrose in 3700 cm^{-1} to 2800 cm^{-1} and 1500 cm^{-1} to 500 cm^{-1} absorption zones. In addition to these peaks, the spectrum of SA shows a sharp peak at 1710 cm^{-1} which lies in the carbonyl region (Jalaja and James 2015). This additional peak at 1710 cm^{-1} confirms that the oxidation of sucrose using H_2O_2 produces carboxylic acid groups on sucrose (Dastidar and Netravali 2013). Sucrose contains 3 primary hydroxyl groups and 5 secondary hydroxyl groups. The primary hydroxyl groups on sucrose are readily available for reaction due to less steric hindrance as compared to the secondary hydroxyl groups and can be easily oxidized to carboxylic acid groups to obtain SA. As

seen from the structure of SA, at least three carboxylic acid groups are present on SA due to oxidation of primary hydroxyl groups. The formation of carboxylic acid groups onto sucrose after reaction is also confirmed from the drastic drop in pH from 6 to 2.5 after 12 h of oxidation. The sharp peaks at 1680 cm^{-1} and 3437 cm^{-1} in the spectrum of MA is due to the C=O from the carboxyl groups and OH stretch absorption from the hydroxyl group on MA (Max and Chapados 2002). The spectrum of MSA shows all the peaks from sucrose and MA in the 1500 cm^{-1} to 500 cm^{-1} absorption zone. The carbonyl absorption region of MSA shows multiple peaks and thus an enlarged image of the region from 1600 cm^{-1} to 1900 cm^{-1} is presented in Figure 2.2(b). As seen in Figure 2.2(b), MSA shows four peaks in the carbonyl region at 1737 cm^{-1}, 1722 cm^{-1} and 1710 cm^{-1} and 1680 cm^{-1}. The additional peak in the MSA spectrum at 1722 cm^{-1} is due to the ester bond formed as a result from reaction between the carboxylic acid group of SA and hydroxyl group of MA. The addition of SHP facilitates the deprotonation of the carboxylic acid groups from SA and after MA is added to the deprotonated SA, the hydroxyl groups from MA react with deprotonated carboxylic acid groups from SA via esterification to form MSA as shown in Figure 2.1.

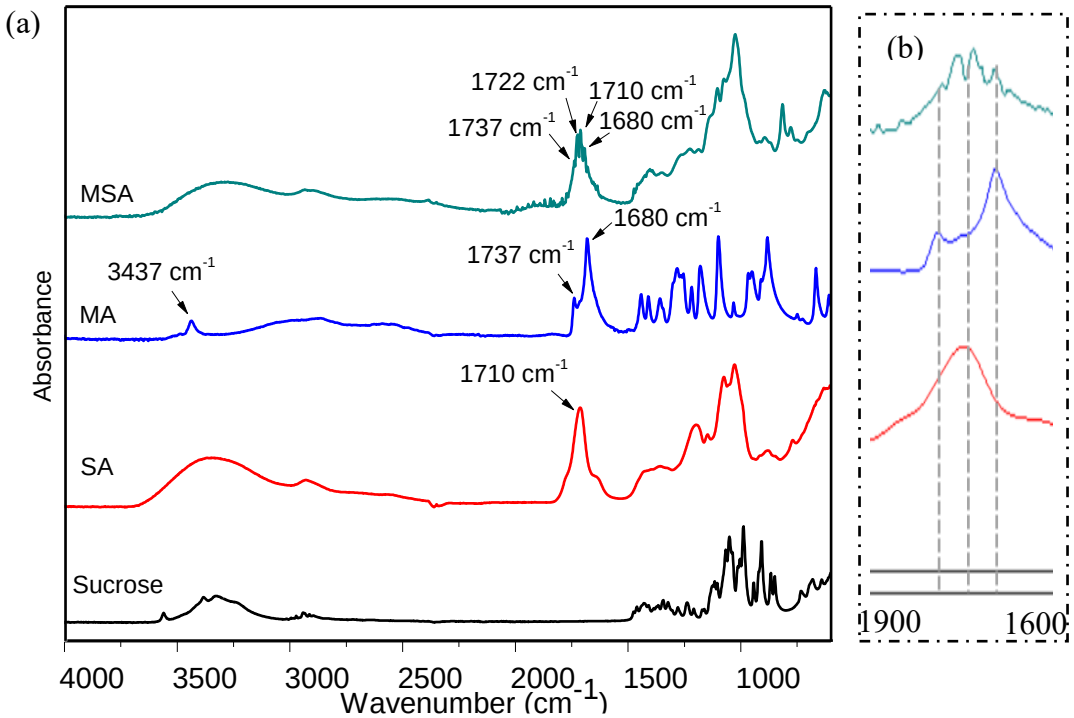

Figure 2.2. ATR-FTIR spectra of sucrose, sucrose acid (SA), malic acid (MA) and multifunctional sucrose acid (MSA) from (a) 600 – 4000 cm^{-1} and (b) magnified carboxyl region from 1600 – 1900 cm^{-1}.

^{13}C-NMR can elucidate more on the changes in the chemical structure of sucrose upon oxidation and carboxylation. Figure 2.3 shows ^{13}C-NMR spectra of sucrose, SA, MA and MSA along with the chemical structures of the respective products labelled with the corresponding carbons in the spectra and structure. The 12 carbons present on the sucrose have been clearly marked on the chemical structure and the peaks associated with them are also numbered in the ^{13}C-NMR spectrum of sucrose. The ^{13}C-NMR spectrum of sucrose shows the presence of 12 carbons between 110 ppm and 60 ppm. The ^{13}C-NMR spectrum of SA shows multiple peaks between the 115 ppm and 60 ppm and some additional peaks between 160 ppm and 180 ppm. The intensity of the 3 peaks between 62 ppm and 65 ppm in sucrose were found to reduce in the ^{13}C-NMR spectrum of SA. The peaks between 62 ppm and 65 ppm

correspond to the primary hydroxyl groups (C-10, C-11 and C-12). The reduction of these peaks and the appearance of the new peaks at 173 ppm and 175 ppm (which correspond to C-13, C-14 and C-15 as marked in the chemical structure of SA from the carboxylic acid groups) clearly indicates that the primary groups of sucrose have been converted to carboxylic acid groups in SA (Zhang et al. 2009). The drastically reduced intensity of the C-11 and C-12 implies that most of the primary hydroxyl groups on sucrose were oxidized to carboxylic acid groups. The peaks associated with the C-5, C-6, C-7, C-8 and C-9 carbons in sucrose remained unaffected after oxidation in SA which imply that the oxidation of secondary hydroxyl groups was rather insignificant as compared to the primary hydroxyl groups. The oxidation of primary hydroxyl groups on sucrose introduces at least three carboxyl groups onto sucrose as seen in the chemical structure (Figures 2.1 and 2.3) as well as seen before from the ATR-FTIR spectra. The two carboxylic acid groups present on MA are marked in the structure as C-16 and C-17 and are present at 174 ppm and 176 ppm, respectively, in the spectrum of MA. The ^{13}C-NMR spectrum of MSA shows the peaks corresponding to SA and MA. The additional peaks between 171 ppm and 176 ppm indicate the formation of ester bonds from the reaction of hydroxyl groups from MA and carboxyl groups from SA (Qi et al. 2016). Addition of SHP to SA facilitates the deprotonation and nucleophilic substitution of the hydroxyl group from the carboxylic acid group on the primary carbon and addition of MA to SA favors the reaction between the hydroxyl group from MA and carboxylic acid groups from SA as opposed to the reaction between the secondary hydroxyl group of SA and carboxylic acid group of

MA. However, as MA has both, carboxylic acid and hydroxyl groups, it is possible it can undergo self-polymerization to form dimer or trimer.

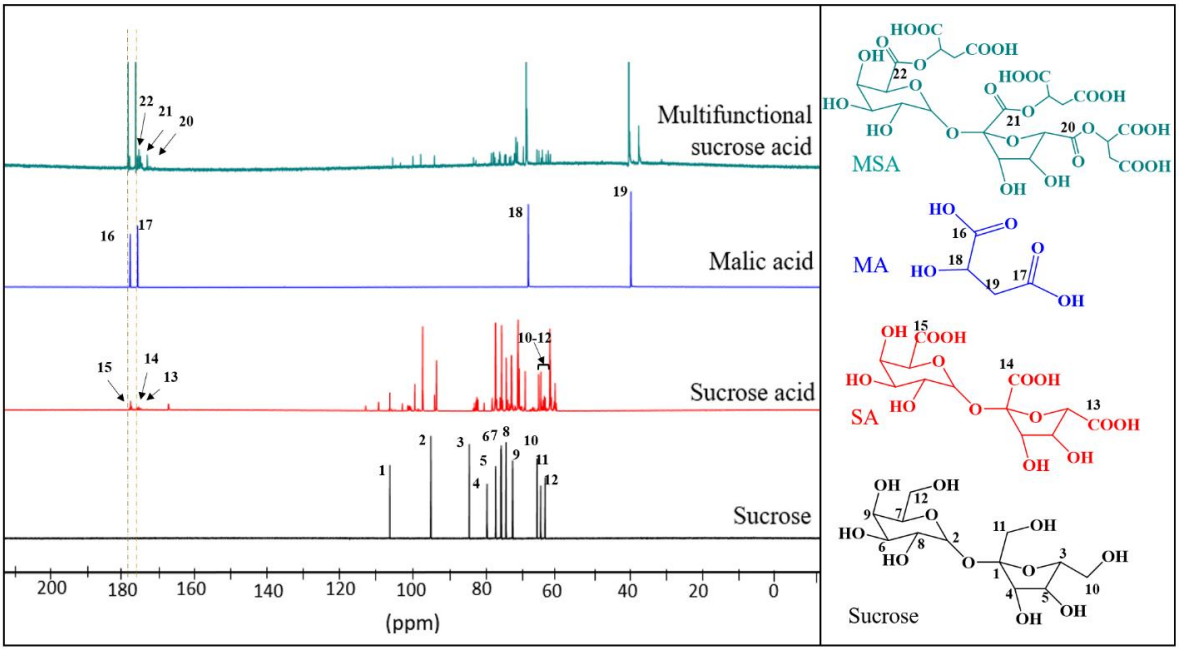

Figure 2.3. ^{13}C-NMR spectra of sucrose, sucrose acid (SA), malic acid (MA) and multifunctional sucrose acid (MSA).

Figure 2.4 shows ATR-FTIR spectra of control and MSA treated cotton fabrics. The broad peak seen between 3200 cm^{-1} and 3400 cm^{-1} in spectrum for control cotton fabric is due to the OH stretch while the peak at 1635 cm^{-1} is due to the adsorbed water. The intensity of both these peaks reduced after treating the fabric with MSA due to crosslinking of the cellulose. A new peak seen at 1730 cm^{-1} in the spectrum for treated fabric confirms the esterification of cotton through the reaction between carboxyl groups from MSA and hydroxyl groups from cellulose forming a covalent ester bond (Dehabadi et al. 2012). Several other researchers have observed similar peak that resulted from esterification reaction through various PCAs such as citric acid and BTCA at 1730 cm^{-1} (Yang 1991; Yang and Wang 1997; Yang et al.

1997). It is well-known that the esterification of hydroxyl groups is a two-step reaction which proceeds via formation of a 5 membered cyclic anhydride (Patil and Netravali 2016). Two adjacent carboxylic acid groups react to form a cyclic anhydride which then reacts with the hydroxyl group on cellulose (Schramm and Rinderer 2015). Since, MSA has at least 6 carboxylic acid groups, the two adjacent carboxylic groups can easily form an anhydride group, which in turn can react with the hydroxyl groups on cotton. Three such anhydride groups can be formed on each molecule of MSA, each of which can react with one hydroxyl group from cellulose to form three ester bonds. The multiple ester bonds per MSA molecule formed with the different cellulose chains introduces crosslinked bridges between the cellulose chains and forms a dense 3D network in cellulose.

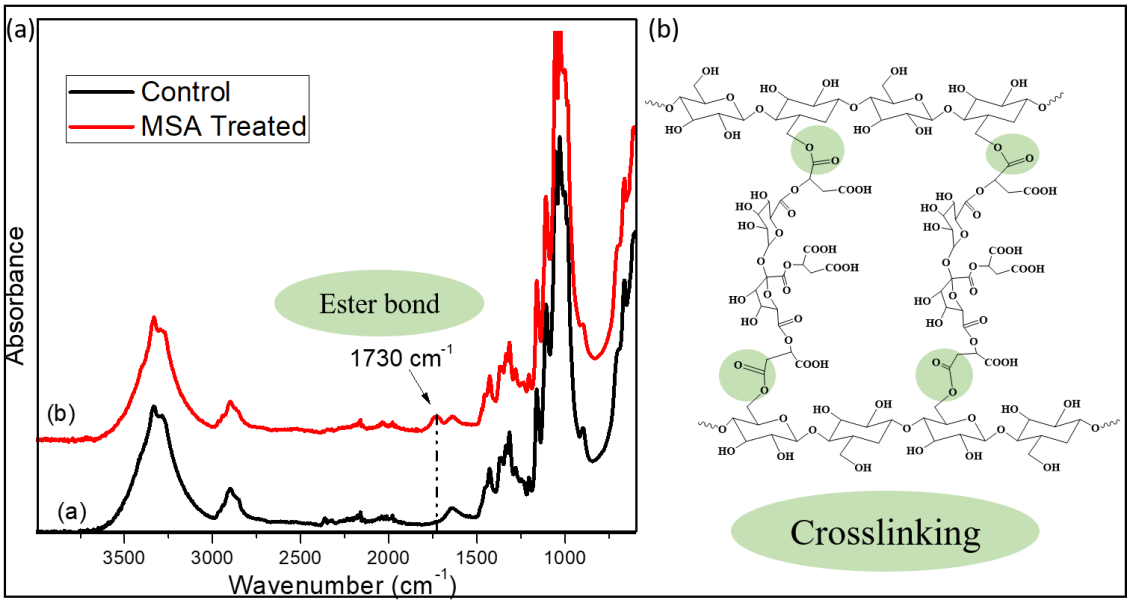

Figure 2.4. (a) ATR-FTIR spectra of control and treated fabrics and (b) proposed reaction for crosslinking of cellulose using MSA.

Figure 2.4(b) shows the proposed crosslinking reaction between MSA and cellulose. As shown in Figure 2.4(b), MSA can form intermolecular bridges between the cellulosic chains and crosslink them. As discussed above, each MSA can react with three hydroxyl groups in cellulose and crosslink them. The crosslinking of cellulose restricts the molecular movement of the cellulose chains and increases the WRA (Luo et al. 2019). The WRA of control fabric was 114º. Figure 2.5(a) shows the effect of curing temperature on WRA of the fabrics treated for 30 min. As seen in Figure 2.5(a), the WRA increased with increase in the curing temperature. WRA of the fabrics cured at 130 ºC for 30 min was found to be 170º which increased to 193º and 202º as the curing temperature was increased to 140 ºC and 150 ºC, respectively. Curing of fabrics promotes crosslinking reaction and, as a result, the extent of crosslinking increases with the increase in temperature, ultimately increasing the WRA (Patil and Netravali 2016). The add-on % of fabrics crosslinked with MSA at 150ºC for 30 min was found to be 12%. It should be noted that the carboxyl groups present on SA and MA, individually, are capable of reacting with the hydroxyl groups of cellulose to form an ester. Thus, SA and MA were used, separately, to treat the cotton fabrics and cured for 30 min at 150 ºC. Figure 2.5(b) shows the effect of different crosslinkers on WRA of the fabrics. As seen from Figure 2.5(b), the WRA of control fabric increased from 114º to 130º after treating with SA for 30 min. The slight increase in WRA of the fabrics can be due to esterification of small number of hydroxyl groups from cellulose (cotton). Esterification can result in reduction in the hydroxyl groups on cellulose as it is consumed by SA and increase the WRA. However, since SA has only 3 carboxylic acid groups, it can form only 1 anhydride

group (probably on the fructose part of SA), which can react with 1 hydroxyl group on cellulose. The single anhydride group on SA leaves one carboxylic acid group open for reaction after forming an ester with cellulose. However, since these carboxylic acid groups on SA are at least 5 carbons away and not in the vicinity of each other to readily form an anhydride group, it is difficult to form the second anhydride group. The lack of forming a second anhydride group in SA only results in formation of one ester bond with cellulose and fails to crosslink the cellulose chains (Kim et al. 2000). Curing of fabrics at higher temperature resulted in browning of the fabrics with no apparent improvement in WRA and thus the curing was restricted to 150 ºC. The browning of fabrics cured above 150 ºC could be a result of caramelization of sucrose which occurs at higher temperatures. Figure 2.5(b) shows that the WRA of control fabrics increased to 170º from 114º after treating with MA. In this case the amount of MA required to form MSA was used to treat cotton fabrics, but without SA. The increase in WRA of the fabrics treated with just MA is the result of crosslinking of cellulose chains. As seen from the chemical structure of MA in Figure 2.3, it has 2 carboxylic acid groups and 1 hydroxyl group. The two carboxylic acid groups are in the vicinity of each other and, hence, form an anhydride which can react with the hydroxyl group on cellulose to form an ester bond. However, MA is also known to self-polymerize into dimer, trimer and other oligomers while curing and is capable of crosslinking the cellulose chains (Kim et al. 2000). The increase in WRA with MA was not as significant as the one treated with MSA simply because MSA has a greater number of functional groups (carboxylic acid) that can easily form anhydride groups that can react with the cellulose chains to crosslink them as discussed earlier. MA has

been used in combination of other PCAs such as BTCA which improved the WRA of cotton fabrics from 198º to 275º, an increase of about 39% (Welch and Peters 1997). However, as mentioned earlier BTCA is quite expensive. Kim et al. formed trimeric α, β-malic acid and reacted with cotton fabrics along with polyurethane resin and found that the WRA fabrics increased from 164º to 294º, 79% improvement (Kim et al. 2000). Dehabadi et al. treated cotton fabrics with carboxylated polyvinyl amine with SHP as the catalyst and obtained a 60% increase in WRA of cotton fabrics from 101° in control to 161° (Dehabadi et al. 2012). Plasma treatment of cotton fabrics combined with acrylic acid and dodecanoic acid was found to improve the WRA by 42% from 165° in control to 235° after treatment (Panda et al. 2016). Yang et al. observed that the combination of citric acid and polymers of maleic acid along with SHP, resulted in 54% increase in the WRA from 189° for control fabrics to 292° (54% increase) for treated fabrics which were comparable to the BTCA and DMDHEU treatment with WRA 299º and 295º respectively (Yang et al. 1998). The MSA treated cotton in this study showed 77% improvement in the WRA from 114º in control to 202º after the treatment. These results are comparable or better than most of the results using different crosslinkers mentioned above. Thus, MSA can be a good alternative to DMDHEU or PCA-based crosslinkers.

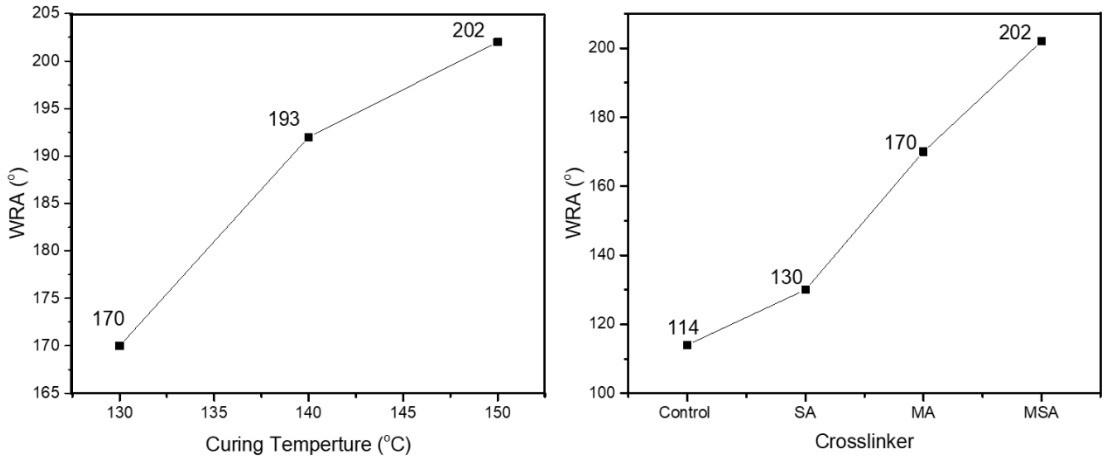

Figure 2.5. (a) Effect of curing temperature on WRA treated for 30 min (b) WRA of fabrics crosslinked with different acids at 150°C for 30 min.

Fabrics were washed repeatedly to see the effect of washing, especially the detergent on the durability of the treatment and the change in color. Table 2.1 presents the results of laundry cycle study on WRA as well as yellowness of the fabrics (b*). Each laboratory laundry cycle is considered equivalent to 5 home launderings and higher b* value indicates more yellowness of the fabrics. As seen from Table 2.1, the WRA of MSA treated fabrics reduced from 202° to 196° after the first laundry cycle and b* value changed from 2.5 to 2.22. The WRA further reduced to 191° and b* value reduced to 0.79 after the second laundry cycle. It is possible that some of the crosslinks on the surface of the fabrics get hydrolyzed due to the detergent during laundering which causes a slight reduction in WRA. The reduction in the b* value, though small, is beneficial as it indicates improved whiteness of the fabrics after washing. Some amount of yellowing observed in the MSA treated fabrics could be due to presence of unreacted MA which can form unsaturated compounds due to dehydration of the hydroxyl groups (Luo et al. 2019). The presence of unsaturated

compounds is considered to be responsible for yellowing of the cotton fabrics. The significant reduction in b* value after two washes suggests that the washing can remove most of the unreacted by-product of MA. No more reduction or change in WRA and b* was observed after third laundry cycle suggesting the durability of the MSA treated cotton fabrics. It was found that the WRA remained stable around 170º and the b* around 0.2 up to 5 laundry cycles which corresponds to 25 home laundry washings. While some cellulase enzymes in detergent can act on the surface of the fabric which results in reduction in WRA and b*, MSA being a small molecule, can penetrate well inside the cotton fibers in the fabric and crosslink them internally to give durable wrinkle-resistant cotton fabrics.

Table 2.1. Effect of laundry cycles on WRA and yellowness of the fabrics.

Sample	**Control**	**MSA Treated**	**Laundry Cycle 1**	**Laundry Cycle 2**	**Laundry Cycle 3**	**Laundry Cycle 4**	**Laundry Cycle 5**
WRA (°)	114	202	196	191	167	169	171
b*	-5.80 (0.06)	2.5 (0.23)	2.22 (0.23)	0.79 (0.12)	0.31 (0.18)	0.24 (0.11)	0.21 (0.22)

Figure 2.6 shows the effect of crosslinking on tensile properties of control and treated fabrics such as tensile stress and tensile strain in both warp and weft directions. As seen from Figure 2.6(a) the tensile stress of the control fabrics was observed to be 102 MPa and 41 MPa in the warp and weft direction respectively. After treating the fabrics with MSA, the tensile stress of the fabrics was observed to be 84 MPa in the warp direction and 29 MPa in the weft direction. This shows about 18% and 28% reduction the tensile stress in the warp and weft direction, respectively. As seen in Figure 2.6(b), the tensile strain of the control fabrics was 10.6% and 11.4% in warp

and weft directions, respectively. After treating the fabrics with MSA, the tensile strain of the fabrics was found to be 6.0% and 8.6% in warp and weft directions, respectively. This shows about 44% and 25% reduction in the tensile strain in warp and weft directions, respectively. The MSA treatment alters the chemical structure of the cellulose by introducing crosslinks within the cellulosic chains. The new crosslinks restrict the mobility of the molecules and, thus, hydroxyl groups, making it more resistant to wrinkle formation. However, the restricted molecular mobility of the cellulose chains causes the fabric to be brittle, reducing the tensile strain of the fabrics (Wang et al. 2017). Tensile strength and strain reduction has been commonly observed in cotton fabrics after chemical crosslinking (Wang et al. 2017). For example, crosslinking of cellulose with BTCA, CA and DMDHEU has shown about 43%, 40%, and 66% reduction in the tensile strength, respectively (Yao et al. 2013). Besides crosslinking, acid degradation of the cellulosic chains have been shown to cause depolymerization or molecular weight reduction which results in reduced tensile stress and strain of the fabrics (Ji et al. 2016a; Ji et al. 2016b). Crosslinking of cotton fabrics with the combination of BTCA and MA showed about 42% strength loss (Welch and Peters 1997). The tensile strength loss due to MSA treatment is much lower than DMDHEU and some PCAs treated fabrics mentioned above which makes it suitable for an industrial scale-up to replace toxic chemicals from the textile industry. A common industrial practice is to use softeners after crosslinking of the fabrics to reduce their brittleness and the amount of strength loss (Bao and Yun-Jun 2018).

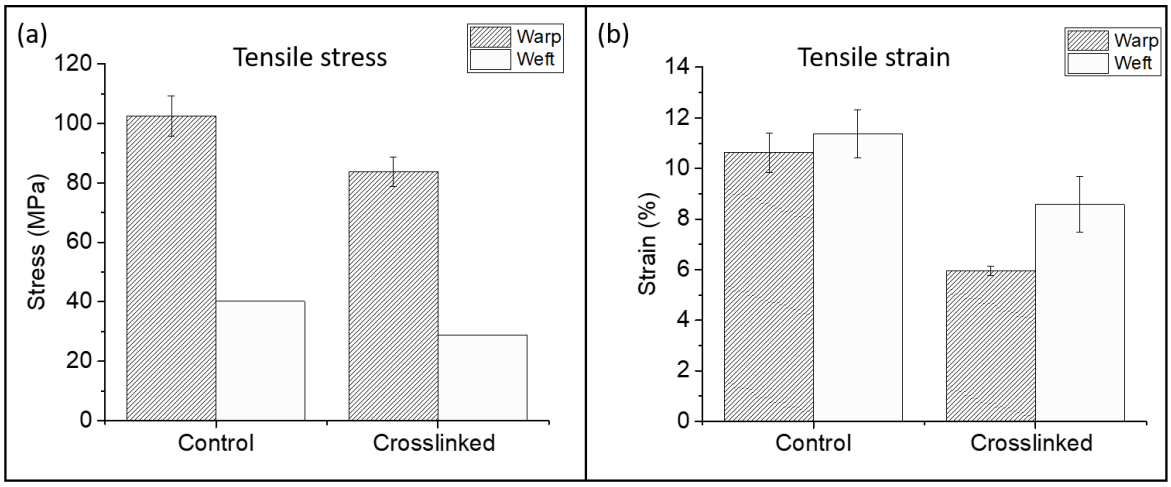

Figure 2.6. Tensile (a) stress and (b) strain of the control and MSA treated fabrics.

Figure 2.7 shows the SEM images of the control and MSA treated fabrics at different magnifications. As seen from Figure 2.7(a), the surface of the fibers from the control cotton fabric is smooth and flat with average diameter of 20 µm. The magnified image of the control fiber as seen in image 7b shows that the smooth flat surface of the fibers have some convolutions and natural creases along the length of the fiber. Figure 2.7(c) shows the SEM image of the fibers taken from the MSA treated fabrics. The surface of the MSA treated fiber looks quite similar to that of the control fibers (Figure 2.7(a)). It also shows the presence of smooth and flat surface. The average diameter of the MSA treated fibers was also found to be 20 µm showing no swelling or contraction of the fibers after crosslinking. The magnified image of the MSA treated fibers shown in Figure 2.7(d) also shows the surface to be similar to that of control fibers. Overall, no surface damage, swelling or contraction of fibers was observed after treating the fabrics with MSA. Most of the crosslinking occurs internally within the fiber, especially in the amorphous region leaving the surface of the fibers unaffected as seen from images in Figure 2.7(c) and Figure 2.7(d).

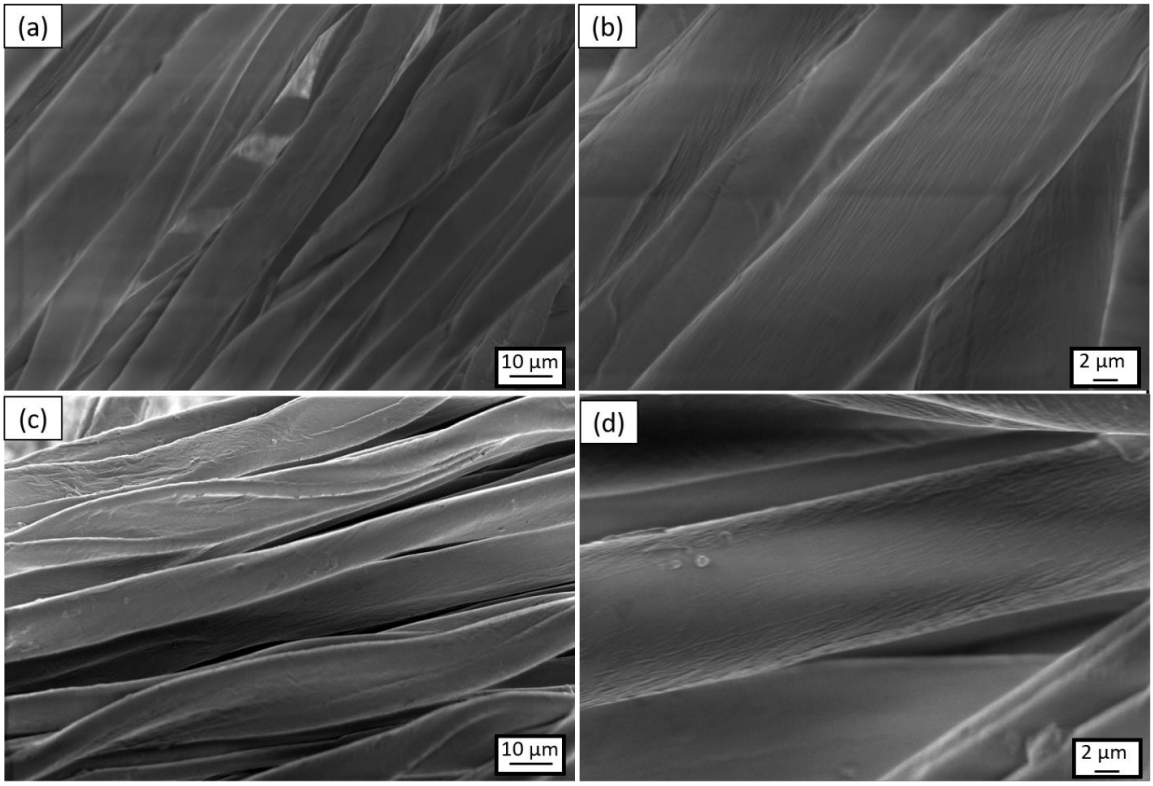

Figure 2.7. SEM images of (a, b) control and (c, d) MSA treated fibers are different magnifications.

2.5 Conclusions

A green crosslinker was developed using a naturally available inexpensive source, sucrose. Sucrose was oxidized using hydrogen peroxide (H_2O_2) and then carboxylated using malic acid (MA) to form multifunctional sucrose acid (MSA). The multiple carboxylic acid groups on MSA were allowed to react with the hydroxyl groups of cellulose via esterification. This resulted in crosslinked cellulosic structure that was responsible for imparting durable wrinkle resistance to cotton fabrics. WRA of the fabrics increased from 114º for control to 202º after MSA treatment. The chemical crosslinking using MSA was not limited to the surface of the cotton fabrics but occurred well inside the fibers as MSA is a small molecule and can penetrate the

amorphous regions of the cotton fibers and crosslink it. The internal crosslinking makes the treatment durable against laundry washings. In addition to the excellent laundry durability, MSA treated fabrics showed more strength retention as compared to many of the commonly used durable-press finishing agents. Surface analysis of the MSA treated fibers showed no signs of surface change or damage. These promising results show that the process developed in this study can be easily used to replace some of the expensive and toxic chemicals currently used to treat cotton fabrics.

Acknowledgments

This work made use of the Cornell University NMR Facility, which is supported, in part, by the NSF through MRI award CHE-1531632.

2.6 References

Bao L-h, Yun-Jun L (2018) Silicone Softener for Stain Repellent Stain Release and Wrinkle Resistance Fabric Finishing Journal of Engineered Fibers and Fabrics 13:155892501801300301

Dastidar TG, Netravali AN (2013) A soy flour based thermoset resin without the use of any external crosslinker Green Chemistry 15:3243-3251

Dehabadi VA, Buschmann H-J, Gutmann JS (2012) Durable press finishing of cotton fabrics with polyamino carboxylic acids Carbohydrate polymers 89:558-563

Dehabadi VA, Buschmann H-J, Gutmann JS (2013) Durable press finishing of cotton fabrics: An overview Textile Research Journal 83:1974-1995

Edye LA, Meehan GV, Richards GN (1994) Influence of temperature and pH on the platinum catalysed oxidation of sucrose Journal of carbohydrate chemistry 13:273-283

Hashem M, Ibrahim NA, El-Shafei A, Refaie R, Hauser P (2009) An eco-friendly–novel approach for attaining wrinkle–free/soft-hand cotton fabric Carbohydrate Polymers 78:690-703

Ibrahim NA, Aly AA, Eid BM, Fahmy HM (2018) Green Approach for Multifunctionalization of Cellulose-Containing Fabrics Fibers and Polymers 19:2298-2306

Jalaja K, James NR (2015) Electrospun gelatin nanofibers: A facile cross-linking approach using oxidized sucrose International journal of biological macromolecules 73:270-278

Ji B, Yan K, Sun G (2016a) Investigation on functional properties of 1, 2, 3, 4-butanetetracarboxylic acid cross-linked fabrics impacted by molecular structures and chemical affinity of catalysts Industrial & Engineering Chemistry Research 55:5216-5222

Ji B, Zhao C, Yan K, Sun G (2016b) Effects of acid diffusibility and affinity to cellulose on strength loss of polycarboxylic acid crosslinked fabrics Carbohydrate polymers 144:282-288

Kim B-H, Jang J, Ko S-W (2000) Durable press finish of cotton fabric using malic acid as a crosslinker Fibers and Polymers 1:116-121

Lam Y, Kan C, Yuen C (2011) Physical and chemical analysis of plasma-treated cotton fabric subjected to wrinkle-resistant finishing Cellulose 18:493-503

Lao L, Fu L, Qi G, Giannelis EP, Fan J (2017) Superhydrophilic wrinkle-free cotton fabrics via plasma and nanofluid treatment ACS applied materials & interfaces 9:38109-38116

Lemoine S, Thomazeau C, Joannard D, Trombotto S, Descotes G, Bouchu A, Queneau Y (2000) Sucrose tricarboxylate by sonocatalysed TEMPO-mediated oxidation Carbohydrate research 326:176-184

Liu J, Wang B, Xu X, Chen J, Chen L, Yang Y (2016) Green finishing of cotton fabrics using a xylitol-extended citric acid cross-linking system on a pilot scale ACS Sustainable Chemistry & Engineering 4:1131-1138

Luo X, Shao D, Xu C, Wang Q, Gao W (2019) An eco-friendly way to whiten yellowish anti-wrinkle cotton fabrics using TBCC-activated peroxide low-temperature post-bleaching Cellulose 26:3575-3588

Mallat T, Baiker A (1994) Oxidation of alcohols with molecular oxygen on platinum metal catalysts in aqueous solutions Catalysis Today 19:247-283

Max J-J, Chapados C (2002) Infrared spectroscopy of aqueous carboxylic acids: Malic acid The Journal of Physical Chemistry A 106:6452-6461

Panda PK, Jassal M, Agrawal AK (2016) In situ atmospheric pressure plasma treatment of cotton with monocarboxylic acids to impart crease-resistant functionality Cellulose 23:993-1002

Parpot P, Kokoh K, Belgsir E, LE J-M, Beden B, Lamy C (1997) Electrocatalytic oxidation of sucrose: analysis of the reaction products Journal of applied electrochemistry 27:25-33

Patil NV, Netravali AN (2019a) Cyclodextrin-based “green” wrinkle-free finishing of cotton fabrics. Ind Eng Chem Res. doi:10.1021/acs.iecr.9b04092

Patil NV, Netravali AN (2016) Microfibrillated cellulose-reinforced nonedible starch-based thermoset biocomposites Journal of Applied Polymer Science 133

Patil NV, Netravali AN (2019b) Enhancing Strength of Wool Fiber Using a Soy Flour Sugar-Based “Green” Cross-linker ACS Omega 4:5392-5401

Qi H, Huang Y, Ji B, Sun G, Qing F-l, Hu C, Yan K (2016) Anti-crease finishing of cotton fabrics based on crosslinking of cellulose with acryloyl malic acid Carbohydrate polymers 135:86-93

Schramm C, Rinderer B (2015) Non-formaldehyde, crease-resistant modification of cellulosic material by means of an organotrialkoxysilane and metal alkoxides Cellulose 22:2811-2824

Wang Y et al. (2017) Effect of anti-creasing component on properties of two-ply cotton yarn Cellulose 24:3073-3082

Welch CM, Peters JG (1997) Malic Acid as a Nonformaldehyde DP Finishing Agent Activated by BTCA and Polymer Additives Textile Chemist & Colorist 29

Xu H, Liu P, Mi X, Xu L, Yang Y (2015) Potent and regularizable crosslinking of ultrafine fibrous protein scaffolds for tissue engineering using a cytocompatible disaccharide derivative Journal of Materials Chemistry B 3:3609-3616

Xu W, Li Y (2000) Cotton fabric strength loss from treatment with polycarboxylic acids for durable press performance Textile research journal 70:957-961

Yang CQ (1991) FT-IR spectroscopy study of the ester crosslinking mechanism of cotton cellulose Textile Research Journal 61:433-440

Yang CQ, Wang X (1997) Infrared spectroscopy studies of the cyclic anhydride as the intermediate for the ester crosslinking of cotton cellulose by polycarboxylic acids. III. Molecular weight of a crosslinking agent Journal of Polymer Science Part A: Polymer Chemistry 35:557-564

Yang CQ, Wang X, Kang I-S (1997) Ester crosslinking of cotton fabric by polymeric carboxylic acids and citric acid Textile Research Journal 67:334-342

Yang CQ, Xu L, Li S, Jiang Y (1998) Nonformaldehyde durable press finishing of cotton fabrics by combining citric acid with polymers of maleic acid Textile Research Journal 68:457-464

Yao W, Wang B, Ye T, Yang Y (2013) Durable press finishing of cotton fabrics with citric acid: enhancement of whiteness and wrinkle recovery by polyol extenders Industrial & Engineering Chemistry Research 52:16118-16127

Zhang SD, Zhang YR, Wang XL, Wang YZ (2009) High carbonyl content oxidized starch prepared by hydrogen peroxide and its thermoplastic application Starch-Stärke 61:646-655

Zhang X, Yang Y, Yao J, Shao Z, Chen X (2014) Strong collagen hydrogels by oxidized dextran modification ACS Sustainable Chemistry & Engineering 2:1318-1324

Chapter 3 Cyclodextrin-based 'green' wrinkle-free finishing of cotton fabrics

Namrata V. Patil and Anil N. Netravali
Department of Fiber Science & Apparel Design,
Cornell University, 37 Forest Home Dr., Ithaca, NY 14853, USA

Graphical abstract

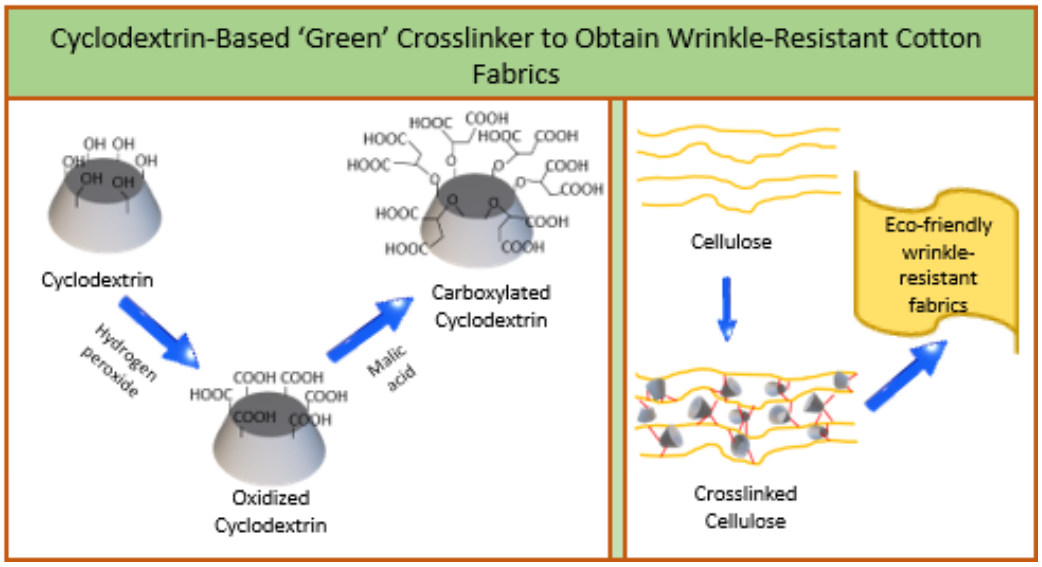

Published as:

Patil, N. V. and A. N. Netravali (2019). "Cyclodextrin-based 'Green' Wrinkle-Free Finishing of Cotton Fabrics." Industrial & Engineering Chemistry Research.

3.1 Abstract

This study presents a cyclodextrin-based inexpensive, green crosslinker to enhance the wrinkle-recovery angle (WRA) of cotton fabrics. Cyclodextrin (CD) was oxidized using hydrogen peroxide (H_2O_2) and further carboxylated with malic acid (MA) to introduce multiple carboxylic acid groups onto CD. The structural chemical changes and presence of multiple carboxylic acid groups on CD after oxidation and carboxylation were confirmed using ATR-FTIR and ^{13}C NMR. The resultant carboxylated product (C-CD) was used to crosslink cotton fibers via multiple ester bond formation. Inter-molecular and inter-fibrillar crosslinking was confirmed using ATR-FTIR and increase in WRA. The impact of crosslinking on the color change and, mechanical properties such as tensile strength, strain, breaking load and tear strength of the fabrics were characterized. Crosslinking of the treated fabrics was found to be durable for up to 25 home laundry washings. The present method would be an excellent substitute for the currently used toxic, expensive treatments.

3.2 Introduction

Cotton fabrics have become an integral part of the apparel industry because of their beneficial properties such as softness and high moisture absorbency which make them comfortable to wear.[1] Cotton is the second highest consumed fiber after polyester.[2] The total consumption of cotton fibers was reported to be 26.1 million metric tons in 2017-2018.[2] This large amount of cotton fiber utilization is because of the advantageous properties such as feel and breathability it offers.[3] Cotton fibers are made of parallel stacks of cellulose fibrils which are held together by hydrogen bonds.

Individual fibrils themselves are made of many linear homopolymers consisting of β(1-4) linked D-glucose units forming cellulose molecules. While the fibrils are highly crystalline, some variations in the alignment of the cellulose molecules divides the fibers into crystalline and amorphous regions.[4] The cellulose molecules are highly aligned and compactly packed within the crystalline region forming cellulose-I crystals while the amorphous regions consist of molecules that are less aligned or organized and held together by weak secondary forces such as hydrogen bonds. Each glucose unit on the cellulose molecule has three hydroxyl groups, which makes the cotton fabric hydrophilic. While the hydrophilic nature of cotton makes it very comfortable to wear, it leads to absorption of moisture, especially in the amorphous region which disrupts the inter- and the intra-molecular hydrogen bonds causing the molecular slippage and the fibril movements.[5] On drying or removal of the moisture, hydrogen bonds reform in the newly deformed position and since there are no recovery forces to bring back the deformed fibrils to their original position, the fabric stays wrinkled.[6]

Crosslinking agents have been often used as durable press (DP) finishing agents in chemical processing of cellulosic textiles to make them wrinkle-free or wrinkle-resistant. Dimethyloldihydroxyethyleneurea (DMDHEU), an equilibrating mixture of formaldehyde, glyoxal and urea, and other N-methylol compounds are currently the dominant products used for DP finishing.[7-10] Environmental concerns have led to banning products that emit formaldehyde during processing, production or storage from textile materials as it poses a significant threat to human health.[11] This has resulted in several efforts in developing benign crosslinking agents to crosslink cotton

fibers. For example, several polycarboxylic acids (PCAs) such as citric acid (CA), maleic acid, 1,2,3,4-butanetetra-carboxylic acid (BTCA) have been studied extensively for crosslinking cellulose since the early 1990s.[6-7, 9] However, some of these PCAs are expensive making it difficult to scale-up for industrial applications.[7, 9, 12] This has generated a great interest in developing inexpensive and non-toxic crosslinking agents for cotton fabrics to obtain wrinkle-free fabrics for apparel.[13]

α-Cyclodextrin (CD), a cyclic oligosaccharide with six glucose units is non-toxic, inexpensive and derived from abundantly available renewable source, starch. CD molecules can form inclusion complexes with a large number of organic molecules, which enable them to be used to impart different functional properties in fabrics.[14] CD has been crosslinked onto cotton fabrics using PCAs such as BTCA to impart antimicrobial, antistatic, aroma and various other finishes.[15-21] However, none of the research has mentioned the use of CD as a crosslinking agent for wrinkle-free finishing of cotton fabrics. Each glucopyranose unit in CD contains three free hydroxyl groups, which differ in their availability and reactivity. In total, six primary and twelve secondary hydroxyl groups in CDs are located on the shorter and longer ridges of the toroidal-shaped structure, respectively. None of these hydroxyl groups can react with the hydroxyl groups present in cellulose, directly. However, they can be oxidized to create reactive functional groups which can be used to crosslink cellulose.

The main aims of this research were to prepare a non-toxic crosslinker that is also inexpensive, to crosslink cotton fibers using it and to characterize effect of crosslinking on the wrinkle resistance of the fabrics. The 1st step in preparing the crosslinker involved oxidizing CD using hydrogen peroxide (H_2O_2) to create multiple

carboxylic acid groups on its surface. The resultant oxidized CD (O-CD) was used to treat cotton fabrics. The O-CD, however, was unable to impart wrinkle-resistance to the fabrics. This was perhaps because only the primary hydroxyl groups would be oxidized to carboxylic acid groups as can be seen in the reaction scheme presented in Figure 3.1. It is likely that the created carboxylic acid groups cannot form an anhydride intermediate, required for reacting with the hydroxyl groups from cellulose to crosslink them and hence does not increase the wrinkle recovery angle (WRA). In the 2nd step the carboxylic acid groups in O-CD were further reacted with the hydroxyl groups from malic acid (MA) to form carboxylated CD (C-CD) as shown in Figure 3.1. C-CD when used to treat the cotton fabrics increased the WRA of the cotton fabrics significantly. This treatment can be extended to various other cellulosic fabrics such as viscose, linen, etc. to impart wrinkle resistance and can be easily scaled-up to an industrial level.

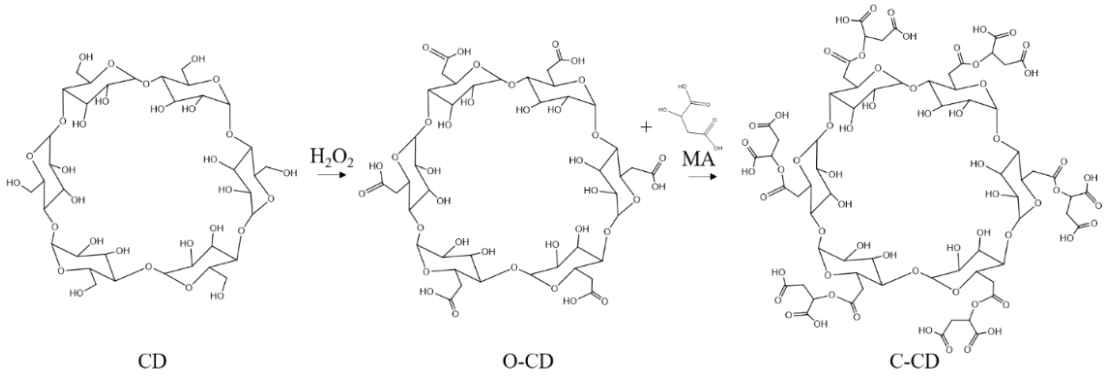

Figure 3.1 Proposed reaction scheme for oxidation and carboxylation of CD.

3.3 Material and methods

3.3.1 Materials

A plain weave cotton fabric with ends per inch (epi) 80 and picks per inch (ppi) 70 was provided by TAL Apparel (Hong Kong), α-cyclodextrin (CD) was provided by Wacker (Eddyville, IA), 30% Hydrogen peroxide (H_2O_2) was purchased from Fisher Scientific (Pittsburgh, PA). Catalase GC118 was provided by DuPont (Wuxi, China). Malic acid (MA) and sodium hypophosphite monohydrate (SHP) were purchased from VWR (Philadelphia, PA).

3.3.2 Carboxylation of α-cyclodextrin

In the 1st step a 5% solution of CD was oxidized for 15 h using 10 ml H_2O_2 at 60°C. At the end of 15 h, CD reaction mixture was cooled down to room temperature and 50 µl of catalase was added to decompose the oxidizing agent, H_2O_2. The effervescence observed after addition of catalase due to decomposition of H_2O_2 to H_2O and O_2 was allowed to subside. The pH of the oxidized cyclodextrin was found to be 3. Oxidized CD was termed as O-CD. In the 2nd step 2.5 g SHP was added to O-CD and the temperature was raised to 70°C to deprotonate the carboxylic acid groups created due to oxidation of CD. Required amount of MA (molar ratio CD:MA of 0.034 and 0.046) was added to deprotonated O-CD and placed in a boiling water bath for 15 min to allow the hydroxyl groups from MA to react with the deprotonated carboxylic acid groups from O-CD. The carboxylated mixture was termed as C-CD.

3.3.3 Fabric treatment

For treating cotton fabrics, 8 g of SHP was added to the prepared C-CD mixture mentioned in section 3.3.2. Cotton fabric specimens (20 cm x 20 cm) were immersed in the C-CD mixture and laid flat on the glass plate and squeezed to remove the excess solution. They were dipped in the C-CD mixture for a 2nd time and

squeezed again and cured at 180°C for predetermined lengths of time (5 min and 10 min) in an air circulating oven. After curing, the fabrics were thoroughly rinsed with DI water 2-3 times to make sure the excess unreacted chemicals are washed off and dried at room temperature (RT). All fabrics were conditioned at 65 ± 2% relative humidity (RH) and 21 ± 1°C for 24 h prior to any characterization.

3.3.4 Attenuated total reflectance Fourier-transform infrared (ATR-FTIR)

ATR-FTIR analysis was used to study the effect of oxidation and carboxylation on CD. This technique was also used to study the effect of C-CD treatment on cotton fabrics. The ATR-FTIR spectra were collected using Thermo Nicolet Magna-IR 560 spectrometer (Madison, WI) with a split pea accessory. Each scan was an average of 300 scans from 4000 cm^{-1} to 500 cm^{-1} wavenumbers.

3.3.5 Nuclear magnetic resonance spectroscopy (NMR)

^{13}C NMR spectra were recorded using a Bruker Biospin AVIII HD 500 MHz spectrometer (France) to illustrate the chemical structural changes upon oxidizing CD using H_2O_2 and carboxylation using MA using D_2O as a solvent.

3.3.6 Evaluation of wrinkle recovery angle (WRA)

AATCC test method 66-2008 was used to evaluate WRA of the control as well as treated fabrics. Six specimens of 40 mm × 15 mm dimensions were cut from randomly located parts of the control and treated fabrics. Three specimens were cut with their long dimension parallel to the warp direction of the fabric while the other 3 had their long dimension parallel to the weft (filling) direction. For the WRA test each specimen was folded at the center and a load of 500 g was applied on it for 5 min. After removing the load, one end of the specimen was mounted in the circular scale of

the WRA test instrument and the specimen was allowed to recover for 5 min before the recovery angle was measured. Three different fabric samples were treated with the C-CD solution made at 3 different times and specimens were tested from each of the fabric samples to ensure reproducibility of results. The sum of average of 9 specimens in warp direction and the 9 specimens in weft direction from 3 different fabrics is reported as the WRA value for each sample.

3.3.7 Color evaluation of fabrics

The color coordinates L*, a* and b* of the control and treated fabrics were measured at five different spots using Macbeth Color-eye spectrophotometer, Model M2020PT, (Newburgh, NY). The L*, a*, b* values stand for L* = 0 (black) to L* =100 (white), -a* (greenness) to +a* (redness), and -b* (blueness) to +b* (yellowness).

3.3.8 Laundry durability of WRA

Laundry durability of the treated fabrics was characterized using modified version of AATCC test method 61-2003. Specimens with dimensions of 10 cm × 10 cm were cut from the treated fabrics and washed in a flask containing 150 ml of aqueous solution of 0.15% (w/w) Tide® laundry detergent and 50 stainless steel balls (diameter 6 mm) at 49°C for 45 min with a constant stirring speed of 45 rpm and then rinsed with water. Each laundry cycle in this study is considered to be equivalent to 5 home laundering.

3.3.9 Evaluation of tensile and tear properties

Tensile strength of the fabrics was determined according to ASTM D5035 strip method. Fabrics having dimensions of 25 mm × 150 mm were cut and tested on

Instron universal testing machine (model 5566, Canton, MA) at a gage length of 75 mm and crosshead speed of 300 mm/min (strain rate of 4 min^{-1}). Averages of 10 specimens in both warp and weft direction each treated at 2 different times are reported. Tear strength of the fabrics was measured according to ASTM D1424-09 standard using a falling-pendulum Elmendorf tearing tester (Thwing-Albert Instrument Company, Philadelphia, PA). Average of 4 different specimens in both warp and weft direction each is reported

3.4 Results and discussion

3.4.1 Characterizations of CS, O-CD, MA and C-CD

Figure 3.2 shows the ATR-FTIR and ^{13}C NMR spectra of CD, O-CD, MA and C-CD. CD is a cyclic α(1-4) linked oligosaccharide consisting of 6 glucose units. As seen in Figure 3.2(a), the ATR-FTIR spectra of CD showed absorption peaks between 3200 cm^{-1} and 3400 cm^{-1}, at 2927 cm^{-1} and 1641 cm^{-1} corresponding to the O-H stretching vibrations, saturated C-H stretching vibration in glucose units and H-O-H bending, respectively. The absorption peaks at 1153 cm^{-1} and 1023 cm^{-1} correspond to the C-O stretching vibration and C-O-C stretching vibrations, respectively. As seen in Figure 3.2(a), the ATR-FTIR spectrum of O-CD shows an additional peak at 1730 cm^{-1}. This peak is assigned to the C=O bond from the carboxylic acid groups created as a result of the oxidation of the hydroxyl groups from CD as seen in the reaction in Figure 3.1. Figure 3.2(b) shows the ^{13}C NMR spectra of CD, O-CD, MA and C-CD. The six peaks seen in the ^{13}C NMR spectrum of CD correspond to the six carbons in the glucose unit of CD. Two additional peaks are seen at 176 ppm and 174 ppm in O-

CD. These peaks correspond to the carboxylic acid peaks from O-CD confirming that the oxidization of CD using H_2O_2 creates carboxylic acid groups as seen in the reaction in Figure 3.1. MA has one hydroxyl group and 2 carboxylic acid groups. The intense peak at 1681 cm^{-1} in Figure 3.2(a) in the ATR-FTIR spectrum of MA and the peaks at 176 ppm and 174 ppm in Figure 3.2(b) in the ^{13}C NMR spectrum of MA correspond to the carboxylic acid peaks from MA.[22] The hydroxyl group on MA can react with the carboxylic acid peak from O-CD. Addition of SHP results in the deprotonation of the carboxylic acid groups from the O-CD. When MA is added to the deprotonated O-CD, the hydroxyl groups react with the deprotonated carboxylate. Reaction between carboxylic acid groups from O-CD and the hydroxyl group from MA results in the formation of ester groups as seen in the reaction in Figure 3.1. It was found that the sharp peak from carboxylic acid from MA shifted from 1681 cm^{-1} to 1709 cm^{-1} after the reaction with O-CD. This peak lies in the carbonyl region and can be due to the presence of carboxylic acid in C-CD. The ester bond formation by reacting hydroxyl groups from MA and the carboxylic acid group from O-CD can be confirmed from the additional peaks observed between 171 ppm to 174 ppm in the ^{13}C NMR spectrum of C-CD in Figure 3.2(b).[23] In addition to the peak at 1709 cm^{-1}, the ATR-FTIR spectrum of C-CD shows vibration peaks from the C-O-C, C-O and C-H stretching vibration from O-CD at 1023 cm^{-1}, 1153 cm^{-1} and 2927 cm^{-1} respectively and the 1098 cm^{-1} from C-OH in MA. Similar characteristic peaks were observed by Telegdi et al. after reacting MA with CD.[22]

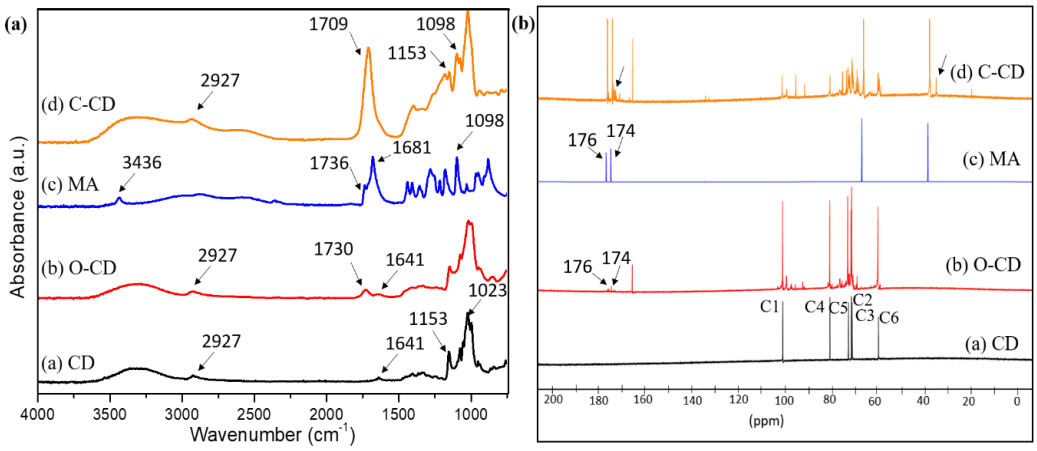

Figure 3.2 (a) ATR-FTIR and (b) ^{13}C NMR spectra of CD, O-CD, MA and C-CD.

3.4.2 Characterization of the control and treated fabrics

Figure 3.3 shows the ATR-FTIR spectra of control and crosslinked cotton fabrics. The broad absorption peak seen between 3200 cm^{-1} and 3400 cm^{-1} in the spectrum for control cotton fabric comes from the OH stretching vibration while the peak at 1635 cm^{-1} is due to the adsorbed water in the cellulose.[24] The intensity of both these peaks was found to reduce as seen in the spectrum of the crosslinked fabrics after treating the fabric with C-CD. This is due to the decrease in the number of hydroxyl groups in the cotton fabrics after crosslinking and also because crosslinking of cellulose reduces the moisture absorption of the fabrics.[25] The spectrum of the crosslinked fabrics showed a new peak at 1725 cm^{-1} which corresponds to the carbonyl groups from the ester bonds.[23] Several other researchers have observed similar peak around 1725 cm^{-1} resulting from esterification reactions between cellulose and various PCAs such as CA and BTCA.[25-27]

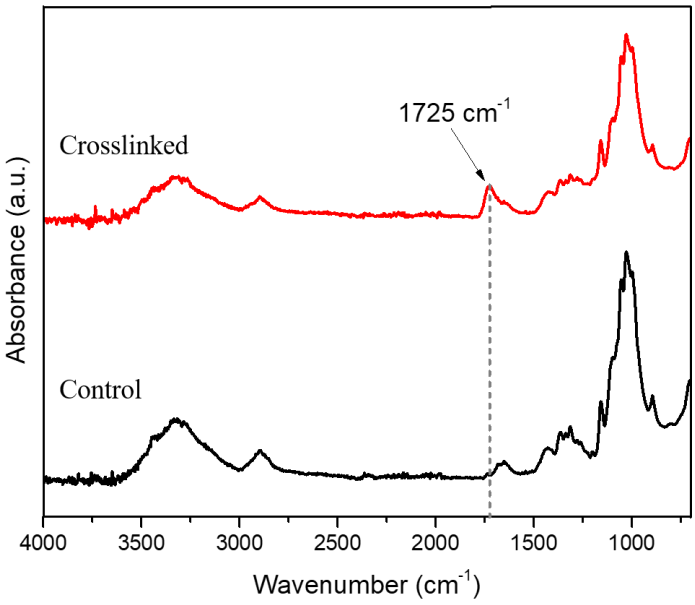

Figure 3.3 ATR-FTIR spectra of control and crosslinked cotton fabrics.

Table 3.1 presents the WRA and color values of the control and treated fabrics. Crosslinking of cellulose forms a rigid network of cellulose chains within the fibers and increases the WRA of the fabrics.[28-29] As seen in Table 3.1, the WRA of the control fabrics is 114° which increased to 130° after crosslinking with O-CD at 180°C for 10 min. Further increasing the curing time to 15 and 20 min did not increase the WRA of the fabrics beyond 130°. It has been shown that the two carboxylic acid groups should be utmost 2 carbons away from each other to form one cyclic anhydride which, in turn, can form one ester bond with the hydroxyl group from the cellulose.[9, 30] The second carboxylic acid group cannot efficiently esterify the hydroxyl group in cellulose (as it cannot form an anhydride) and so the bifunctional carboxylic acids are not very efficient crosslinkers.[31-32] As seen from the structure of O-CD in Figure 3.1, it consists of many carboxylic acid groups. However, the crosslinking with O-CD is not

efficient as the carboxylic acid groups are not in the vicinity of each other to form an anhydride, even after using a catalyst, SHP.[9] It was observed that the WRA increased from 114° for untreated (control) fabrics to 220° after treating the cotton fabrics with C-CD at 180°C for 10 min (93% improvement in WRA). This is due to the fact that C-CD consists of multiple bifunctional carboxylic acid groups on each of the O-CD as seen from the chemical structure in Figure 3.1. The bifunctional carboxylic acid groups can readily form anhydride because of their close vicinity and then react with the hydroxyl groups from cellulose at elevated temperature of 180°C during curing of the fabrics. Since, multiple bifunctional carboxylic acid groups are present on C-CD to form anhydrides, it can efficiently crosslink the cellulose. As the efficiency of crosslinking of the cellulose increases, the number of hydroxyl groups and mobility of the cellulose chains decreases. The molar ratio of CD:MA was optimized to obtain highest WRA using C-CD. Molar ratio CD:MA 0.046 cured at 180°C for 10 min gave the highest WRA of 220°. C-CD, being a small molecule can be expected to diffuse easily in between the cellulose fibrils as well as in the amorphous regions and react with the hydroxyl groups to from crosslinks between the cellulose chains in the fiber. This replaces the earlier hydrogen bonded cellulose network in the amorphous region with the stronger covalently bonded crosslinked structure which restricts the mobility of the chains. Cotton and other cellulosic fabrics generally wrinkle after washing and drying due to the presence of abundant hydroxyl groups in cellulose chains which allow significant water to be absorbed. Absorbed water acts as a lubricant allowing the cellulose chains or microfibrils to move with respect to each other and form hydrogen bonds at new positions after drying, creating the undesired wrinkles. During

crosslinking, many OH groups are consumed leaving a lesser number of sites for water to attach. Crosslinking also brings cellulose molecules closer, leaving less space for the water to reside. The restricted molecular movement of the cellulose chains and the decreasing water absorption due to crosslinking are the main reasons responsible for the increase in the WRA seen in Table 3.1.

Table 3.1 WRA and color values.

Sample Treatment	Temperature (°C)	Time (min)	WRA (°)	l*	a*	b*
Control	-	-	114	88.32	1.16	-5.80
O-CD	180	10	130	88.06	0.10	-2.66
C-CD (CD:MA 0.034)	180	10	208	86.09	-0.65	-0.15
C-CD (CD:MA 0.046)	180	05	211	87.95	-0.99	-0.36
C-CD (CD:MA 0.046)	180	10	220	88.09	-0.92	-0.57
15% MA	180	10	194	87.86	-0.97	1.02
20% MA	180	10	186	87.92	-1.21	1.33

Figure 3.4 shows the proposed side reactions that occur while curing the fabrics. Since MA has both hydroxyl and carboxylic acid groups, it is possible that MA molecules can react with other MA molecules to form dimers, trimers or oligomers as shown in Figure 3.4(a). These oligomers are capable of forming multiple ester bonds with cellulose and, thus crosslinking it. To confirm that the increase in WRA using C-CD is the result of the multiple bifunctional carboxylic acid groups on C-CD and not just the oligomers formed due to MA, fabrics were treated with just MA

and the catalyst (SHP) at the same concentrations present in C-CD. In this case the WRA increased from 114° in control fabrics to 194° at 15% MA concentration and to 186° at 20% MA concentration. An improvement of just over 70% in WRA was observed by using 15% MA. Kim et al. observed similar results using 16% MA and SHP to get 79% improvement in the WRA from 164° for control to 294° after crosslinking with MA and SHP at 180°C.[33] The WRA of the fabrics treated with MA is lower than the WRA of fabrics treated with C-CD at same temperature and time. Although MA crosslinks the fabrics to increase the WRA, the WRA is not as high as the one treated with C-CD. Another significant advantage of C-CD over MA is that the b* value of the fabrics treated with C-CD is lower than that of the fabrics treated with MA. The b* value indicates the yellowness of the fabrics. As seen from data presented in Table 3.1, the b* value for the fabrics treated with MA increased with the concentration of MA. The b* value increased to 1.02 and 1.33 after treating with 15% and 20% MA, respectively. The yellowing observed for the fabrics treated with MA is due to the dehydration of the hydroxyl group from MA forming a double bond as shown in Figure 3.4(b). As most of the hydroxyl groups are reacted with the carboxylic acid groups while forming C-CD, the extent of dehydration is less in C-CD as compared to MA and so the fabrics treated with C-CD shows much less yellowing as compared to the fabrics treated with MA alone. The b* value of the fabrics treated with C-CD at 180°C for 10 min is -0.57 which shows very little yellowing as compared to the control fabrics (b* of -5.8). Dehydration of the hydroxyl groups from the unreacted MA which form the C=C conjugated compound can be seen from the peak at 134 and 132 ppm in Figure 3.2(b) which causes yellowing.[23, 34]

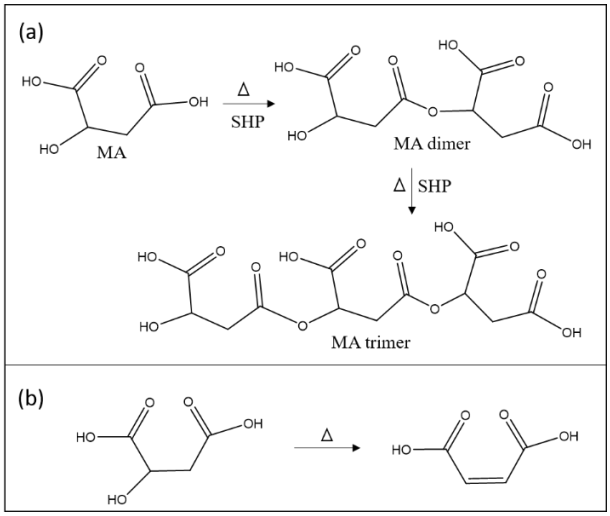

Figure 3.4 Proposed side reactions (a) self-polymerization of MA (b) dehydration of MA.

Overall, the highest WRA (220°), a 93% increase, was obtained by treating the fabrics using C-CD prepared using CD:MA molar ratio 0.046 at 180°C for 10 min. Dehabadi et al. observed a 60% increase in the WRA from 101° in control to 161° after treating the cotton fabrics with carboxylated polyvinyl amine with SHP as the catalyst.[35] Hashim et al. carried out dual treatment of esterification and ionic crosslinking by cationization of cotton fabric and then crosslinking with ammonium citrate with SHP as the catalyst.[8] This dual treatment led to an increase of 70% in WRA from 122° for control fabrics to 209° in the treated fabrics.[8] Plasma treatment of cotton fabrics combined with acrylic acid and dodecanoic acid was found to improve the WRA by 42% from 165° in control to 235° after treatment.[6] In another study, succinic acid treated cotton fabric in presence of TiO_2 nanocatalyst and UV irradiation showed an increase of only 4% in the WRA from 169° to 176°.[36] Yang et al. showed that the combination of citric acid and polymers of maleic acid along with SHP,

resulted in 54% increase in the WRA from 189° for control fabrics to 292° (54% increase) for treated fabrics which were comparable to the BTCA and DMDHEU treatment with WRA 299 and 295 respectively.[37] Crosslinking of cotton with C-CD in this study showed comparable or better WRA as compared to several other methods mentioned above by using inexpensive and sustainable process and chemicals, making it easy to upscale on an industrial level.

3.4.3 Laundry durability of the treated fabrics

Table 3.2 presents the results of the laundry cycles of the crosslinked fabrics on WRA and b* values. It was observed that the WRA of C-CD treated fabrics reduced from 220° to 210° after the first laundry cycle. As mentioned earlier, each AATCC laboratory laundry cycle is considered equivalent to 5 home launderings. It is possible that the crosslinks on the surface of the fabrics are hydrolyzed due to the detergent during laundering. The WRA further reduced to 198° after the second laundry cycle after which it remained stable at around 200° after 5 laundry cycles. Figure 3.5 shows the ATR-FTIR spectra of C-CD treated and laundry cycle 5 washed cotton fabrics. The ATR-FTIR spectra of the crosslinked and washed fabrics do not show any change in the spectra after five laundry cycles. For example, no change in the ester peak at 1725 cm^{-1} was observed showing that the detergent wash does not completely hydrolyze the crosslinks created due to C-CD treatment. C-CD is a small molecule and can readily diffuse inside the cotton fibers and react with the molecules. Only 9% loss of WRA was observed after 5 laundry cycles which correspond to 25 home washes. Since the crosslinking in the present case is not limited to the surface of cotton fabrics or fibers but occurs well inside the amorphous regions of the cotton

fibers as well as between the fibrils, the treatment results in durable anti-wrinkle finishing of the cotton fabrics. As seen in Table 3.2, the b* value i.e. the yellowness of the fabrics did not show a significant change after 5 laundry cycles.

Table 3.2 Laundry durability of the wrinkle resistance of crosslinked fabrics.

Sample	**Treated**	**Laundry Cycle 1**	**Laundry Cycle 2**	**Laundry Cycle 3**	**Laundry Cycle 4**	**Laundry Cycle 5**
WRA (°)	220 ± 1.3	210 ± 1.5	198 ± 2.6	199 ± 1.4	203 ± 1.2	200 ± 1.8
b*	-0.57	-0.18	-0.30	-0.27	-0.50	-0.49

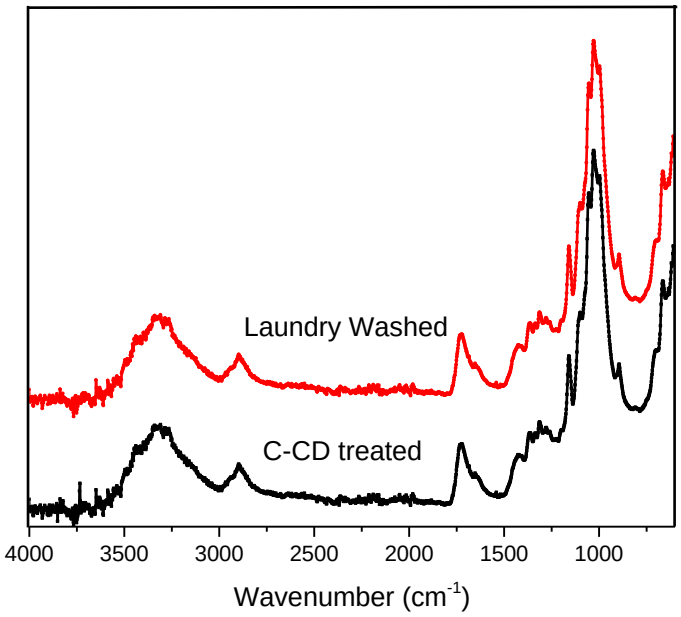

Figure 3.5. ATR-FTIR spectra of C-CD treated and laundry cycle 5 washed cotton fabrics.

3.4.4 Tensile properties of the control and treated fabrics

Table 3.3 shows the tensile properties of the control and treated fabrics such as tensile stress, tensile strain, breaking load, modulus and the tear strength. As seen from Table 3.3, the tensile stress of the fabrics reduced from 102 MPa in control to 57 MPa in the warp direction after crosslinking with C-CD at 180°C for 10 min. This shows about 44% strength loss in the warp direction after crosslinking. A similar strength loss of 48.8% was observed in the weft direction after crosslinking. As seen in Table 3.3, the breaking load was found to reduce by 38% in the warp direction from 487 N in control to 300 N after crosslinking and 42% in the weft direction from 196 N to 114 N after crosslinking. Crosslinking of cellulose using various acids such as BTCA, CA and even DMDHEU have shown about 43%, 40%, 66% reduction in the tensile strength of the fabrics.[38] Crosslinking and depolymerization of cellulose due to acid degradation have been shown to reduce the tensile strength of the cotton fabrics after treatment.[24, 39-40] Tensile strain of the crosslinked fabrics reduced from 10.6% in control to 7.3% in the warp direction after crosslinking. This is primarily because of the crosslinking which restricts the relative mobility of the cellulose and makes the fiber brittle.[38-39] Crosslinking, while it increases the WRA, it also decreases the tear strength of the fabrics, after C-CD treatment. It was found that the tear strength reduced from 10 cN to 4.5 cN and from 12 cN to 6.2 cN in the warp and weft direction, respectively. The tear strength retention of the C-CD treated was 45% and 53% in warp and weft direction respectively, is higher as compared to citric acid treated fabrics.[7] The tear strength retention of citric treated fabric was found to reduce

from 34.3 N to 10 N after treatment with about 29% tear strength retention.[7] However, the process can be optimized to increase the tear strength retention.

Table 3.3 Tensile properties of the control and treated fabrics.

Sample	Tensile stress (MPa)	Tensile strain (%)	Breaking load (N)	Modulus (Mpa)	Tear strength (cN)
Control warp	102.49 ± 6.45	10.62 ± 0.69	486.84 ± 32.03	1294.29 ± 14.00	9.92 ± 1.98
Treated warp	57.02 ± 9.10	7.25 ± 0.88	300.00 ± 50.22	1065.59 ± 78.39	4.48 ± 0
Control weft	41.31 ± 3.52	10.49 ± 1.33	196.21 ± 16.73	677.84 ± 21.36	11.68 ± 1.68
Treated weft	21.15 ± 4.52	10.33 ± 0.76	114.46 ± 24.12	446.84 ± 108.95	6.24 ± 1.32

3.4.5 Shelf-Life of the Prepared C-CD.

The shelf-life stability of the prepared C-CD was evaluated to check its efficiency as a function of days. The prepared C-CD was stored at room temperature and used to treat the fabrics every 7 days. The WRA of the fabrics treated after 1 week of C-CD preparation was found to be 215°. Further treating the fabrics after 2 and 3 weeks showed WRA of 215° and 228° respectively. It was found that the WRA remained constant at 219° after treating the fabrics after 4, 5 and 6 weeks of the preparation of C-CD. Overall, the shelf-life of the C-CD was found to be stable. This promising results show that the inexpensive raw material, CD can be modified using a benign oxidizer H2O2 and further with MA which is considered edible to crosslink cotton fabrics and avoid the use of toxic chemicals.

3.4.6 XRD analysis of Control and Treated Fabrics.

Figure 3.6 shows the XRD pattern of control, MA and C-CD treated fabrics. The strong peaks at 2θ of 14.8º , 16.5º , 22.6º , and 34.3º seen in the control fabrics are the characteristic peaks of cellulose I crystalline form. The XRD pattern of the MA treated and the C-CD treated cotton fabrics do not show any change in the characteristic peaks showing that the crosslinking using MA and C-CD does not alter the ordered crystalline structure of the cellulose as seen in the control fabrics. MA and C-CD are both small molecules and can penetrate and crosslink the amorphous region in the cellulose leaving the crystalline region unaffected as seen from the XRD patterns in Figure 3.6.

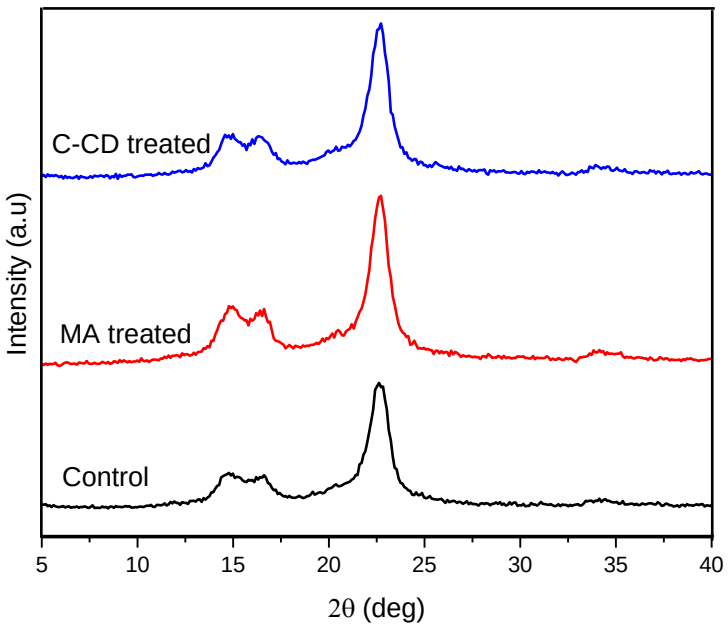

Figure 3.6. XRD pattern of control, MA and C-CD treated fabrics.

3.4.7 Surface Analysis of the Control and Treated Fabrics.

Figure 3.7 shows the SEM images of control, MA and C-CD treated fibers at different magnifications. As seen from Figure 3.7(a), the surface of the fibers from the control cotton fabric is smooth and flat with average diameter of 20 µm. Figure 3.7(b) shows the magnified image of the control fibers which show the presence of some convolutions and natural creases along the length of the fiber. Figures 3.6(c) and 3.6(d) show the SEM images of MA treated fibers. The MA treated fibers show the presence of some particulate matter on the surface. Figure 3.7(e) and 3.7(f) show the SEM images of C-CD treated fibers. As seen from the images in Figure 3.7(e) and 3.7(f), the surface of the fibers show a presence of particulate matter and some flakes confirming the grafting of C-CD onto the fibers. Although, most of the crosslinking using C-CD occurs within the fibers, the presence of some particulate matter on the surface of the fibers confirms the grafting of C-CD onto the fibers.

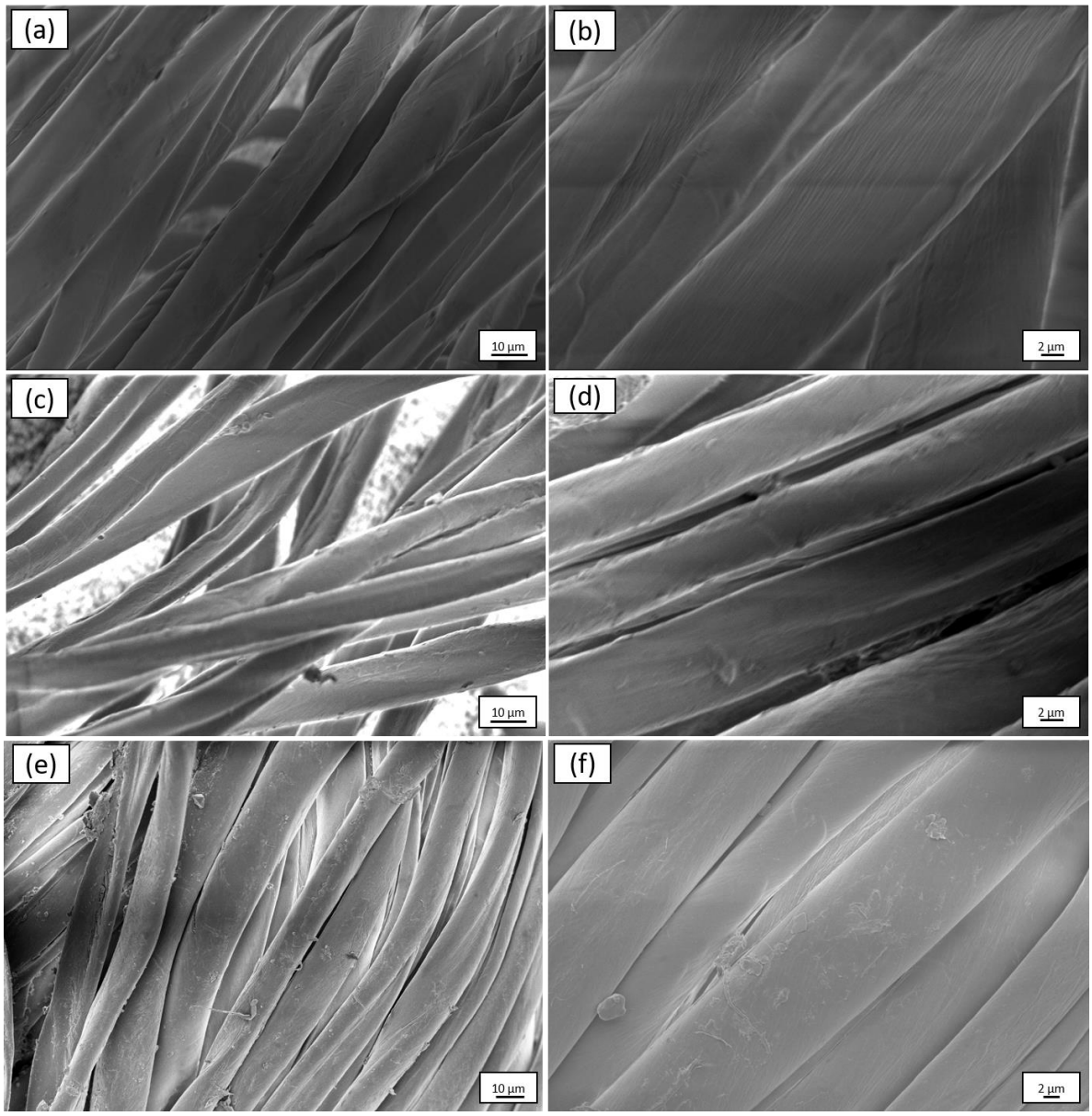

Figure 3.7. SEM images of (a, b) control, (c, d) MA treated and (e, f) C-CD treated fibers at different magnifications.

3.5 Conclusions

α-Cyclodextrin (CD) was used as a 'green' and inexpensive crosslinker for cotton fabrics. Since CD does not have any reactive groups that can crosslink cellulose

directly, it was oxidized using a benign oxidizer H_2O_2 and further carboxylated with malic acid to form C-CD. The chemical structural changes characterized after oxidation and carboxylation, using ATR-FTIR and ^{13}C NMR, confirmed the presence of multiple carboxylic acid groups on CD, as desired. C-CD was allowed to diffuse inside the cotton fibers and the carboxylic acid groups on C-CD were made to react with the hydroxyl groups creating multiple crosslinks between cellulose molecules/fibrils through the formation of ester bonds. The crosslinked network formed inside the cotton fibers, especially in the amorphous region, resulted in restricted molecular motion which in turn resulted in increased WRA of 220°, significantly higher compared to 114° obtained for control fabrics. The wrinkle resistance of the treated fabrics was also found to be durable for up to 25 home laundry washing. The C-CD method presented here would be an inexpensive and 'green' substitute for the currently used formaldehyde-based or other expensive DP finishing agents.

Acknowledgments

This work made use of the Cornell University NMR Facility, which is supported, in part, by the NSF through MRI award CHE-1531632.

3.6 References

1. Yetisen, A. K.; Qu, H.; Manbachi, A.; Butt, H.; Dokmeci, M. R.; Hinestroza, J. P.; Skorobogatiy, M.; Khademhosseini, A.; Yun, S. H., Nanotechnology in Textiles. *ACS nano* **2016,** *10* (3), 3042-3068.

2. https://www.usda.gov/oce/forum/2018/commodities/Cotton.pdf.

3. Hashem, M.; Ibrahim, N. A.; El-Shafei, A.; Refaie, R.; Hauser, P., An eco-friendly–novel approach for attaining wrinkle–free/soft-hand cotton fabric. *Carbohydrate Polymers* **2009,** *78* (4), 690-703.

4. Ibrahim, N.; El-Zairy, E.; Eid, B.; Emam, E.; Barkat, S., A new approach for imparting durable multifunctional properties to linen-containing fabrics. *Carbohydrate Polymers* **2017,** *157*, 1085-1093.

5. Harifi, T.; Montazer, M., Past, present and future prospects of cotton cross-linking: New insight into nano particles. *Carbohydrate polymers* **2012,** *88* (4), 1125-1140.

6. Panda, P. K.; Jassal, M.; Agrawal, A. K., In situ atmospheric pressure plasma treatment of cotton with monocarboxylic acids to impart crease-resistant functionality. *Cellulose* **2016,** *23* (1), 993-1002.

7. Liu, J.; Wang, B.; Xu, X.; Chen, J.; Chen, L.; Yang, Y., Green finishing of cotton fabrics using a xylitol-extended citric acid cross-linking system on a pilot scale. *ACS Sustainable Chemistry & Engineering* **2016,** *4* (3), 1131-1138.

8. Hashem, M.; Elshakankery, M.; El-Aziz, S. A.; Fouda, M. M.; Fahmy, H., Improving easy care properties of cotton fabric via dual effect of ester and ionic crosslinking. *Carbohydrate polymers* **2011,** *86* (4), 1692-1698.

9. Yang, C. Q.; Chen, D.; Guan, J.; He, Q., Cross-linking cotton cellulose by the combination of maleic acid and sodium hypophosphite. 1. Fabric wrinkle resistance. *Industrial & engineering chemistry research* **2010,** *49* (18), 8325-8332.

10. Jang, T.-R.; Sheu, T.-C.; Sheu, J.-J.; Chen, C.-C., Crosslinking of cotton fabrics premercerized with different alkalis part III: crosslinking and physical

properties of DMDHEU-treated fabrics. *Textile research journal* **1993,** *63* (11), 679-686.

11. Haule, L. V.; Michael Carr, C.; Rigout, M., Investigation into the removal of a formaldehyde-free easy care cross-linking agent from cotton and the potential for subsequent regeneration of lyocell-type fibres. *The Journal of The Textile Institute* **2016,** *107* (1), 23-33.

12. Lee, E. S.; Kim, H. J., Durable press finish of cotton/polyester fabrics with 1, 2, 3, 4-butanetetracarboxylic acid and sodium propionate. *Journal of applied polymer science* **2001,** *81* (3), 654-661.

13. Xu, H.; Canisag, H.; Mu, B.; Yang, Y., Robust and Flexible Films from 100% Starch Cross-Linked by Biobased Disaccharide Derivative. *ACS Sustainable Chemistry & Engineering* **2015,** *3* (11), 2631-2639.

14. Bajpai, M.; Gupta, P.; Bajpai, S., Silver (I) ions loaded cyclodextrin-grafted-cotton fabric with excellent antimicrobial property. *Fibers and Polymers* **2010,** *11* (1), 8-13.

15. Voncina, B.; Le Marechal, A. M., Grafting of cotton with β-cyclodextrin via poly (carboxylic acid). *Journal of applied polymer science* **2005,** *96* (4), 1323-1328.

16. Lee, M. H.; Yoon, K. J.; Ko, S. W., Grafting onto cotton fiber with acrylamidomethylated β-cyclodextrin and its application. *Journal of Applied polymer science* **2000,** *78* (11), 1986-1991.

17. Selvam, S.; Gandhi, R. R.; Suresh, J.; Gowri, S.; Ravikumar, S.; Sundrarajan, M., Antibacterial effect of novel synthesized sulfated β-cyclodextrin crosslinked cotton fabric and its improved antibacterial activities with ZnO, TiO2 and Ag nanoparticles coating. *International journal of pharmaceutics* **2012,** *434* (1-2), 366-374.

18. Sricharussin, W.; Sopajaree, C.; Maneerung, T.; Sangsuriya, N., Modification of cotton fabrics with β-cyclodextrin derivative for aroma finishing. *The journal of the Textile Institute* **2009,** *100* (8), 682-687.

19. Abdel-Halim, E.; Abdel-Mohdy, F.; Al-Deyab, S. S.; El-Newehy, M. H., Chitosan and monochlorotriazinyl-β-cyclodextrin finishes improve antistatic

properties of cotton/polyester blend and polyester fabrics. *Carbohydrate Polymers* **2010,** *82* (1), 202-208.

20. Nazi, M.; Malek, R. M. A.; Kotek, R., Modification of β-cyclodextrin with itaconic acid and application of the new derivative to cotton fabrics. *Carbohydrate polymers* **2012,** *88* (3), 950-958.

21. Abdel-Halim, E.; Al-Deyab, S. S.; Alfaifi, A. Y., Cotton fabric finished with β-cyclodextrin: Inclusion ability toward antimicrobial agent. *Carbohydrate polymers* **2014,** *102*, 550-556.

22. Telegdi, J.; Trif, L.; Mihály, J.; Nagy, E.; Nyikos, L., Controlled synthesis and characterization of biodegradable, stereomer co-polycondensates of L-malic acid. *Journal of Thermal Analysis and Calorimetry* **2015,** *121* (2), 663-673.

23. Qi, H.; Huang, Y.; Ji, B.; Sun, G.; Qing, F.-l.; Hu, C.; Yan, K., Anti-crease finishing of cotton fabrics based on crosslinking of cellulose with acryloyl malic acid. *Carbohydrate polymers* **2016,** *135*, 86-93.

24. Qi, H.; Pan, J.; Qing, F.-l.; Yan, K.; Sun, G., Anti-wrinkle and UV protective performance of cotton fabrics finished with 5-(carbonyloxy succinic)-benzene-1, 2, 4-tricarboxylic acid. *Carbohydrate polymers* **2016,** *154*, 313-319.

25. Montazer, M.; Alimohammadi, F.; Shamei, A.; Rahimi, M. K., Durable antibacterial and cross-linking cotton with colloidal silver nanoparticles and butane tetracarboxylic acid without yellowing. *Colloids and Surfaces B: Biointerfaces* **2012,** *89*, 196-202.

26. Zhao, H.; Liang, Q.; Lu, Y., Microstructure and properties of copper plating on citric acid modified cotton fabric. *Fibers and Polymers* **2015,** *16* (3), 593-598.

27. Yang, C. Q.; Wang, X.; Kang, I.-S., Ester crosslinking of cotton fabric by polymeric carboxylic acids and citric acid. *Textile Research Journal* **1997,** *67* (5), 334-342.

28. Hou, A.; Sun, G., Multifunctional finishing of cotton fabrics with 3, 3′, 4, 4′-benzophenone tetracarboxylic dianhydride: reaction mechanism. *Carbohydrate polymers* **2013,** *95* (2), 768-772.

29. Ji, B.; Tang, P.; Yan, K.; Sun, G., Catalytic actions of alkaline salts in reactions between 1, 2, 3, 4-butanetetracarboxylic acid and cellulose: II. Esterification. *Carbohydrate polymers* **2015,** *132*, 228-236.

30. Ji, B.; Qi, H.; Yan, K.; Sun, G., Catalytic actions of alkaline salts in reactions between 1, 2, 3, 4-butanetetracarboxylic acid and cellulose: I. Anhydride formation. *Cellulose* **2016,** *23* (1), 259-267.

31. Yang, C. Q.; Wang, X., Formation of cyclic anhydride intermediates and esterification of cotton cellulose by multifunctional carboxylic acids: An infrared spectroscopy study. *Textile Research Journal* **1996,** *66* (9), 595-603.

32. Xiaohong, G.; Yang, C. Q., FTIR spectroscopy study of the formation of cyclic anhydride intermediates of polycarboxylic acids catalyzed by sodium hypophosphite. *Textile Research Journal* **2000,** *70* (1), 64-70.

33. Kim, B.-H.; Jang, J.; Ko, S.-W., Durable press finish of cotton fabric using malic acid as a crosslinker. *Fibers and Polymers* **2000,** *1* (2), 116-121.

34. Lu, Y.; Yang, C. Q., Fabric yellowing caused by citric acid as a crosslinking agent for cotton. *Textile research journal* **1999,** *69* (9), 685-690.

35. Dehabadi, V. A.; Buschmann, H.-J.; Gutmann, J. S., Durable press finishing of cotton fabrics with polyamino carboxylic acids. *Carbohydrate polymers* **2012,** *89* (2), 558-563.

36. Chen, C.-C.; Wang, C.-C., Crosslinking of cotton cellulose with succinic acid in the presence of titanium dioxide nano-catalyst under UV irradiation. *Journal of sol-gel science and technology* **2006,** *40* (1), 31-38.

37. Yang, C. Q.; Xu, L.; Li, S.; Jiang, Y., Nonformaldehyde durable press finishing of cotton fabrics by combining citric acid with polymers of maleic acid. *Textile Research Journal* **1998,** *68* (6), 457-464.

38. Yao, W.; Wang, B.; Ye, T.; Yang, Y., Durable press finishing of cotton fabrics with citric acid: enhancement of whiteness and wrinkle recovery by polyol extenders. *Industrial & Engineering Chemistry Research* **2013,** *52* (46), 16118-16127.

39. Ji, B.; Zhao, C.; Yan, K.; Sun, G., Effects of acid diffusibility and affinity to cellulose on strength loss of polycarboxylic acid crosslinked fabrics. *Carbohydrate polymers* **2016,** *144*, 282-288.

40. Ji, B.; Yan, K.; Sun, G., Investigation on functional properties of 1, 2, 3, 4-butanetetracarboxylic acid cross-linked fabrics impacted by molecular structures and chemical affinity of catalysts. *Industrial & Engineering Chemistry Research* **2016,** *55* (18), 5216-5222.

Chapter 4 Direct assembly of silica nanospheres on halloysite nanotubes for 'green' ultrahydrophobic cotton fabrics

Namrata V. Patil and Anil N. Netravali

Department of Fiber Science & Apparel Design,

Cornell University, 37 Forest Home Dr., Ithaca, NY 14853, USA

Graphical abstract

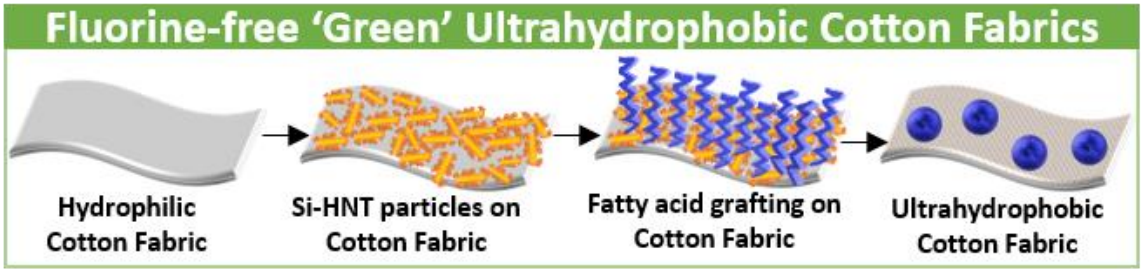

Published as:

Patil, N. V.; Netravali, A. N., Direct Assembly of Silica Nanospheres on Halloysite Nanotubes for "Green" Ultrahydrophobic Cotton Fabrics. Advanced Sustainable Systems 2019, 1900009.

And

Netravali, A. N.; Zhong, Y.; Patil, N. V., Modified cellulosic compositions having increased hydrophobicity and processes for their production - US20180119334/ US15/832,725.

4.1 Abstract

This paper presents a sustainable biomimetic approach to create ultrahydrophobic cotton fabrics. Cotton fabrics were modified using biobased raw materials to create multiple scale roughness and low surface energy on their surfaces. Naturally occurring halloysite nanotubes (HNT) were modified by silanization and direct assembly of silica (SiO_2) nanospheres on surface of HNT. HNT 'decorated' with SiO_2 nanospheres were covalently bonded onto the surface of cotton fabrics creating a durable multiple scale surface roughness. Surface modified cotton fabrics were further grafted with fatty acid without using any solvent, via esterification. The combination of hierarchical roughness pattern created on the surface through modified HNT and fatty acid treatment resulted in ultrahydrophobic fabrics with water contact angles (WCAs) above 150°. Surface topographies of modified HNT particles and chemical changes were fully characterized. ATR-FTIR and WCA studies were used to confirm the grafting of modified HNT particles and aliphatic fatty chains on surface of fabrics. The ultrahydrophobic cotton fabrics washed for 5 standard laundry cycles (25 home washings) showed that ultrahydrophobicity was durable. Moreover, the ultrahydrophobic fabrics were oleophilic, making them suitable for use in oil-water separation, anti-biofouling and packaging and other applications apart from water repellent clothing.

4.2 Introduction

Cotton fabrics are widely used in apparel because of their soft feel and comfortable characteristic.[1, 2] The main constituent of cotton fibers is cellulose, a linear polymer made up of β(1-4) linked glucose units. Each glucose unit contains three hydroxyl groups: one primary and two secondary. These hydroxyl groups make cotton fibers inherently hydrophilic. There is great interest in making cotton fabrics ultrahydrophobic and significantly expand their potential applications.[3] For example, they can be used in apparel to make water repellent outdoor gear, rainwear, and self-cleaning apparel while retaining their breathability and soft feel.[4] Cellulose is also the most abundant polymer on earth and has innumerable applications because it is renewable, biodegradable, plant-derived and fully sustainable. Some of the other applications of ultrahydrophobic cellulose include anti-biofouling, separating oil from water for cleaning oil spills in offshore oil fields or tanker vessels, cellulose films used in packaging and improving interfacial bonding of cellulosic fibers or micro- and nano-fibrils for use in non-polar resins for fabricating fiber reinforced composites or simply obtaining high strength resins.[5-7]

Ultrahydrophobic surfaces found in nature such as lotus leaves, cicada wings and many others show a unique combination of the hierarchical rough structure with a hydrophobic waxy layer present on the surface.[8] Detailed earlier studies of such unique structures have shown that ultrahydrophobic surfaces can be created by a combination of structured rough surfaces and low surface energy using fluorocarbon compounds and have led to developing many 'bioinspired' materials.[9-13] Various techniques such as chemical etching, lithography, atomic layer deposition, radio

frequency plasma, dichlorodifluoromethane (DCFM) plasma, vapor phase deposition have been used to deposit fluorocarbon nanoparticulate hydrophobic film, or fluorinated alkyl silane compounds onto cotton fabrics to obtain ultrahydrophobic surfaces.[14-18] Several researchers have shown the successful 2-step ultrahydrophobic modification of cotton fabrics through fabrication of rough surface using nanoparticles such as SiO_2, ZnO and TiO_2 followed by low surface energy chemical treatment using fluoroalkylsilane.[19, 20]

Lithographic or plasma etching techniques require expensive instruments and chemicals and are only capable of fabricating ultrahydrophobic surfaces on a small scale. These techniques are limited to the use of only certain types of chemicals which makes it difficult to scale-up the process to an industrial level. In addition, while perfluoroalkyl compounds (PFAs) have worked well to make cotton hydrophobic, they have been recognized as emerging environmental pollutants as they are toxic and carcinogenic.[21] Perfluorooctanoic acid (PFOA) also known as C8 belongs to PFAS is highly stable with long half-life and, thus, a potential health hazard as it stays in the environment and in humans and animals for a long time. Ironically it is still widely used in consumer products from paints, stain and water repellent carpets and fabrics to food packaging.[22, 23] Long term exposure to PFOA has been shown to result in high bioaccumulation in human and animal bodies through direct contact and water and soil contamination posing a risk of cancer and thyroid disorders.[24, 25] Such identified hazards and ban by United States Environmental Protection Agency (USEPA) has called for cleaner alternatives to PFOA compounds to create ultrahydrophobic surfaces.[26] In spite of numerous efforts to make ultrahydrophobic cotton fabrics, very

few attempts that have focused on using sustainable materials and non-toxic processes. Dankovich and Hseih used various plant triglycerides to modify the surfaces of cellulose to achieve sustainable hydrophobic treatment.[27] Their attempt of using olive oil resulted in increased water contact angle (WCA) from 27° to over 72°.[27] Samyn et al. improved the surface hydrophobicity of paper by increasing WCA from 84° to 112° using different vegetable oils along with hybrid organic nanoparticle coatings.[28] Another sustainable green chemistry hydrophobic modification of cellulose involved grafting naturally occurring, biocompatible and biodegradable fatty acids.[29] Garcia et al. carried out the esterification of cellulose with saturated fatty acids, n-octanoic to n-octadecanoic with acetic anhydride co-reactant in lithium chloride/N,N-dimethylacetamide (LiCl/DMAc) medium which improved the WCA from 70°to 115°.[30] Zhong and Netravali grafted various fatty acids onto cellulose to get a WCA of 137°, making it significantly more hydrophobic.[29] Completely green and durable ultrahydrophobic modification of cotton has not been reported up to date.

The main aim of the present research was to develop a 'green' process to obtain ultrahydrophobic cotton fabrics using naturally available raw materials. Amine functionalized silica nanospheres were assembled on the surfaces of halloysite nanotubes (HNT) which were then covalently bonded onto the cotton fabrics. HNT a natural clay that exists in a tube form is known for its biocompatibility and worldwide availability at low cost. SiO_2 nanospheres were assembled on HNT surfaces to create a tailored roughness at multiple scales. The amine functionalization allowed covalent bonding of the HNT decorated with silica nanospheres (Si-HNT) and ensured long-term durability of the modified cotton fabrics during wear and washing. The rough

surface topography of the Si-HNT allowed significant air entrapment at the fabric surface and reduced the contact area of water. The covalent bonding of Si-HNT also eliminated environmental concerns about the particles being washed away during laundering. After obtaining the surface topography of the fibers with desired roughness, fatty acid was grafted onto the fabric. Fatty acids are biocompatible and biodegradable with a long aliphatic hydrocarbon chain. While the carboxyl (acid) group can covalently react with the hydroxyl group on the cellulose forming an ester bond, the aliphatic hydrocarbon chain creates a fabric surface with low surface energy. The effect of surface roughness resulting from Si-HNT particles and grafting of fatty acid on the hydrophobicity of the fabrics was fully characterized.

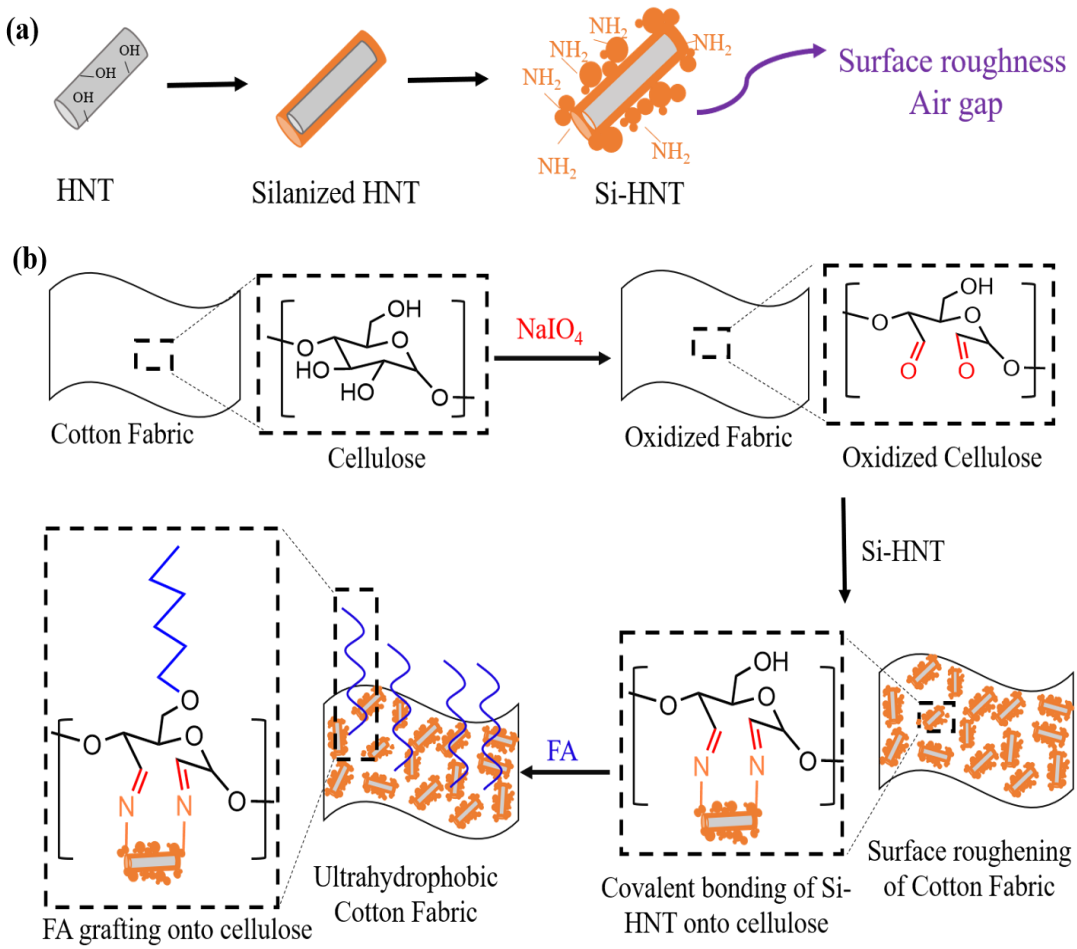

Figure 4.1 Schematic illustration of (a) One-step synthesis of Si-HNT (b) Preparation of ultrahydrophobic cotton fabrics using Si-HNT.

4.3 Materials and methods

4.4.1 Materials

Desized and bleached plain weave cotton fabric (#400) was purchased from Testfabrics, Inc, PA. Sodium periodate ($NaIO_4$), ≥ 99% purity, was purchased from Acros Organics, Bound Brook, NJ. Heptanoic anhydride was purchased from TCI America, Philadelphia, PA. Ethanol (≥99.5% purity, absolute) and ammonium hydroxide (~28% NH_4OH) were purchased from Sigma-Aldrich Chemical, Allentown, PA. Halloysite nanotube, Kaolin clay (HNT), tetraethyl orthosilicate

(TEOS), (3-Aminopropyl) triethoxysilane (APTES) were also purchased from Sigma-Aldrich Chemical. Milli-Q deionized (DI) water (resistivity, 18.2 MΩ.cm, Millipore RiOs and Elix water purification systems, Millipore Corporation, MA) was used for hydrolysis of TEOS.

4.4.2 Preparation of amine functionalized HNT decorated with silica nanospheres (Si-HNT)

HNT (1 g) was dispersed in 50 ml ethanol using sonicator for 20 min. Water (1 ml), NH_4OH (2 ml) and TEOS (2 ml) were added to the HNT dispersion and stirred at 1200 rpm at room temperature (RT). This triggered the hydrolysis, silanization and condensation of TEOS in the form of silica nanospheres on the surface of HNT. After 30 min, 2 ml (3-Aminopropyl) triethoxysilane (APTES) was added to the dispersion to functionalize the particles with amine groups and further stirred overnight at RT. It was then purified by centrifuging at 10,000 rpm for 20 min and washing with ethanol. The centrifuge and washing steps were repeated two more times to get rid of all the residual chemicals.

4.4.3 Covalently bonding Si-HNT particles onto cotton fabrics

The secondary hydroxyl groups on the cotton fibers in the fabrics were oxidized to aldehyde groups using $NaIO_4$ by immersing the fabrics (15 cm × 15 cm) in 0.5% solution of $NaIO_4$ solution at 60°C for 20 min.[31] The fabrics were further washed with DI water and dried in an air circulation oven at 80°C for 1 h. These fabrics are henceforth termed as oxidized cotton fabrics. Si-HNT dispersion of required concentrations 0.1%, 0.3% and 0.5% (w/v) were made by dispersing Si-HNT in

ethanol using an ultrasonicator for 15 min. Oxidized cotton fabrics were placed in the Si-HNT dispersions in the shaker bath for 1 h and then placed in an air circulating oven at 130°C for 20 min to allow covalent bonding between amine groups from Si-HNT and aldehyde groups from cellulose as shown in the schematic illustration in Figure 4.1(b). These fabrics are termed as cotton-Si-HNT.

4.4.4 Preparation of ultrahydrophobic cotton fabrics

The cotton-Si-HNT fabrics were further treated to graft fatty acid having low surface energy onto the fabrics. Many fatty acids (FA) such as heptanoic acid, octanoic acid, dodecanoic acid, stearic acid and others can be selected.[29] For the present research, heptanoic anhydride was selected as a candidate as anhydrides react faster as compared to carboxylic acids with the hydroxyl group on cellulose. Cotton-Si-HNT fabrics were dipped in the heptanoic anhydride solution placed flat on the glass plate and cured in an air-circulating oven at 130°C for 30 min. While the Si-HNT particles can be covalently bonded (grafted) onto the cotton fabrics using secondary hydroxyl groups converted to aldehyde groups through oxidation, the primary hydroxyl groups on the cellulose can be used to graft long chain hydrocarbon fatty acid. The treated fabrics were then washed using ethanol to remove the residual fatty acid. The fabrics were then dried at 50°C for 3 h to get rid of any fatty acid odor. These fabrics were termed cotton-Si-HNT-FA. These fabrics were conditioned at 21°C and 65% RH for 24 h prior to their characterization.

4.4.5 Characterization of Si-HNT and treated fabrics

The surface morphology of pure HNT and Si-HNT particles was characterized using a LEO 1550 field emission scanning electron microscope (FESEM, Germany) at

5 kV accelerating voltage. An average value obtained from six different SEM images of the Si-HNT particles synthesized at two different times was reported for the nanosphere size. SEM was also used to characterize the change in the surface topography of the fibers before and after the treatment. Thermo Fisher Scientific, FEI Tecnai T12 Transmission electron microscope (TEM, Hillsboro, OR), was used to characterize the Si-HNT particles.

Attenuated total reflectance Fourier-transform infrared (ATR-FTIR) analysis was used to study the chemical modification of HNT. The ATR-FTIR spectra were collected using Thermo Nicolet Magna-IR 560 spectrometer (Madison, WI) having a split pea accessory. Each scan was an average of 300 scans from 4000 cm^{-1} to 500 cm^{-1} wavenumbers. ATR-FTIR was also used to confirm the covalent bonding of Si-HNT and grafting of FA onto the cotton fabrics.

Contact angle analyzer (CAA2, Imass Inc., Accord, MA) was used to measure the WCAs of the treated cotton fabrics. A water droplet of 5 μL volume was gently placed onto the specimen using a syringe. Average of ten different drops at different locations for each of the three specimens prepared at different times were recorded.

Tensile strength of the fabrics was determined according to ASTM D5035 strip method. Fabrics having dimensions of 25 mm x 150 mm were cut and tested on Instron 5566 universal testing machine (Canton, MA) at a gage length of 75 mm and crosshead speed of 300 mm/min. Five different specimens in both warp and weft directions were tested to obtain average values.

The color coordinates L*, a* and b* of the control and treated fabrics were measured at five different spots using Macbeth Color-eye spectrophotometer, Model

M2020PT, (Newburgh, NY). The L*, a*, b* values stand for L* = 0 (black) to L* =100 (white), -a* (greenness) to +a* (redness), and -b* (blueness) to +b* (yellowness). Values reported are averages of 5 different tests.

Laundry durability evaluation was carried out using a modified version of American Association of Textile Chemists and Colorists (AATCC) Test Method 61–2003.[29] The test was performed using a 500 mL flask containing 150 mL aqueous solution of Tide® laundry detergent (0.15%, w/w) and 50 stainless steel balls (diameter = 6 mm), the test was performed at 49°C, 40 rpm for 45 min. The size of the fabric specimens was 5 cm × 5 cm for the test. Each laundry test in this study is equivalent to five home launderings.

4.4 Results and discussion

4.4.1 Characterization of Si-HNT

Figure 4.1(a) shows the schematic illustration of the one-step synthesis of Si-HNT particles and Figure 4.1(b) shows the process developed in this study for preparing ultrahydrophobic cotton fabrics. The SEM images of pure HNT and the synthesized Si-HNT particles are shown in Figure 4.2. As seen in Figure 4.2(a) pure HNT particles show a smooth surface and tubular structure with diameters less than 100 nm and lengths varying from 500 nm to 800 nm. The arrows in Figure 4.2(a) show the hollow structure of HNT. Figure 4.2(b) show SEM images of the Si-HNT particles where the surfaces of the HNT particles are fully covered with SiO_2 layer as well as nanospheres. The external surfaces of HNT are composed of siloxane (Si-O-Si) groups.[32-36] The chemical similarity between the outer layer of HNT and the

hydrolyzed tetraethyl orthosilicate (TEOS) together with the catalytic condensation due to ammonium hydroxide (NH_4OH) allow easy formation of a layer on the HNT surface (silanization) and SiO_2 nanospheres on the silanized HNT by Stöber process.[37] While the chemical structure of the outer surface of HNT is similar to SiO_2, the inner cylinder core surface is similar to Al_2O_3 with many hydroxyl groups on the internal structure as compared to the outer.[36, 37] As a result, pure HNT is hydrophilic and can readily absorb water.[37] Thus, it is necessary to modify the surface of the HNT particles to enhance their hydrophobicity. As seen in Figure 4.2(b), the modification of HNT shows the presence of a SiO_2 layer around the HNT that covers the inner core and the nanospheres attached to the surface enhance the roughness of the particles. It is critical that the silanization layer fully encapsulates the HNT, specially covering the sides and, thus, sealing the ends of the hollow tube. Since the HNT particles are small, it is possible that the silanization covers some clusters of HNT particles. A few of such clusters are visible in Figure 4.2(b). The average diameter of the SiO_2 nanospheres assembled on the silanized HNT was found to be 83 nm. The arrows in Figure 4.2(b) show nanospheres assembled on silanized HNT particles which create rough surfaces, a characteristic critical to enhancing the hydrophobicity. These nanospheres create the needed air gaps that reduce the solid-liquid interaction.[38] The highly irregular shapes of Si-HNT particles is helpful in creating surface roughness on the cotton fibers which increases the WCA.[39]

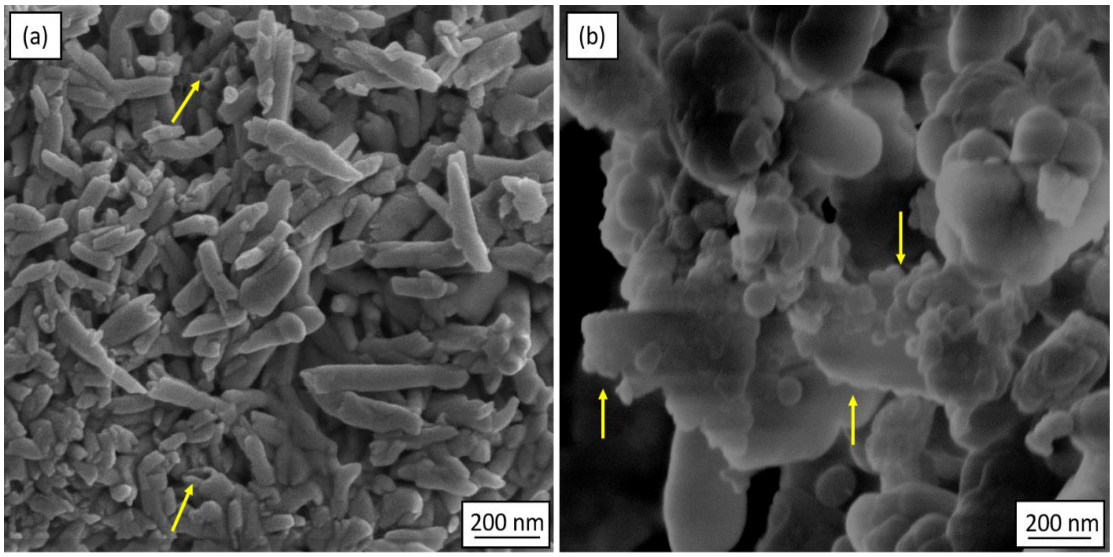

Figure 4.2 SEM images of (a) Pure HNT and (b) Si-HNT particles.

Figure 4.3 shows TEM images of Si-HNT particles at different magnifications. The Si-HNT particles show the silanized layer as well as the nanospheres assembled on the surface. Feng et al. have demonstrated that the silanization forms a thin layer encompassing the HNT as well as fill the core partly.[37]

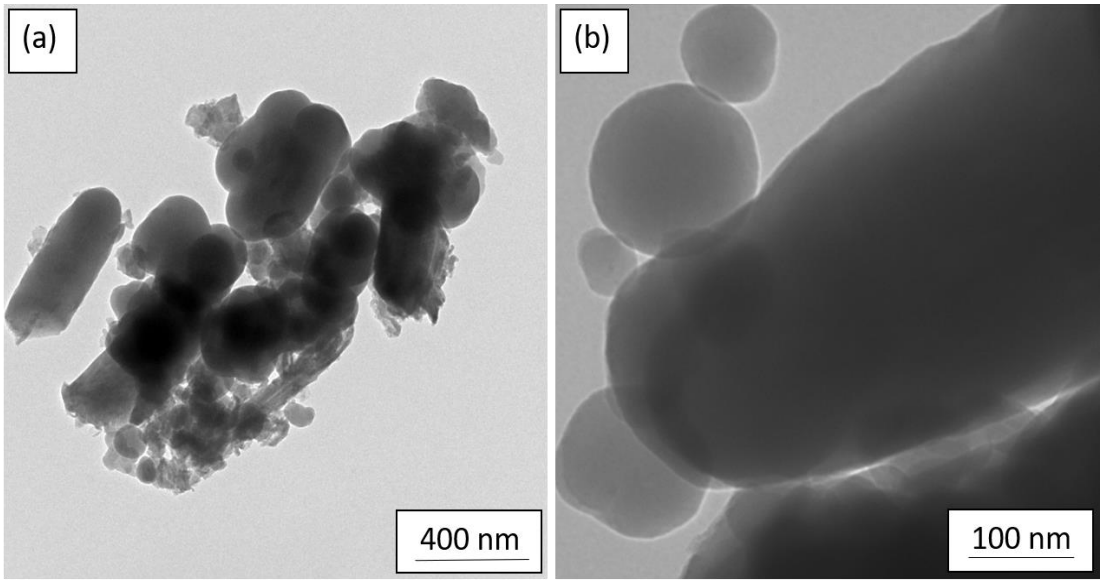

Figure 4.3 TEM images of Si-HNT particles at different magnifications.

Figure 4.4 shows the ATR-FTIR spectra of pure HNT and Si-HNT particles. As can be seen in Figure 4.4, the spectrum of pure HNT has two characteristic peaks at 3690 cm^{-1} and 3621 cm^{-1}. They are assigned to the O-H stretching vibration of the inner surface having Al-OH groups and the O-H stretching vibration of the interface between Si-O tetrahedron and Al-O octahedron, respectively.[40] The peaks at 1120 cm^{-1} and 1001 cm^{-1} are due to the perpendicular and in-plane Si-O stretching, respectively.[33] The peak at 907 cm^{-1} is due to the O-H vibration of the inner hydroxyl groups.[33] Compared to pure HNT, the Si-HNT spectrum shows three new peaks at 2930 cm^{-1}, 1552 cm^{-1} and 1330 cm^{-1} assigned to the symmetric stretching of C-H_2, deformation of N-H_2 and Si-CH, respectively, due to silanization using TEOS and amine functionalization using (3-Aminopropyl) triethoxysilane (APTES).[33] The peaks for hydroxyl groups seen at 3690 cm^{-1} and 3621 cm^{-1} in spectrum of pure HNT reduced significantly due to the formation of SiO_2 layer and nanospheres on the surface of HNT. The Si-O-Si peak shifted from 1001 cm^{-1} in pure HNT to 1031 cm^{-1} in Si-HNT particles due to silanization. As mentioned earlier, surface modification of HNT is necessary to cover the exposed hydroxyl groups and to create surface roughness required for creating ultrahydrophobic surfaces, somewhat mimicking the ultrahydrophobic lotus leaf surface. The amine functionalization allows the covalent bonding of the Si-HNT particles to the fabrics.

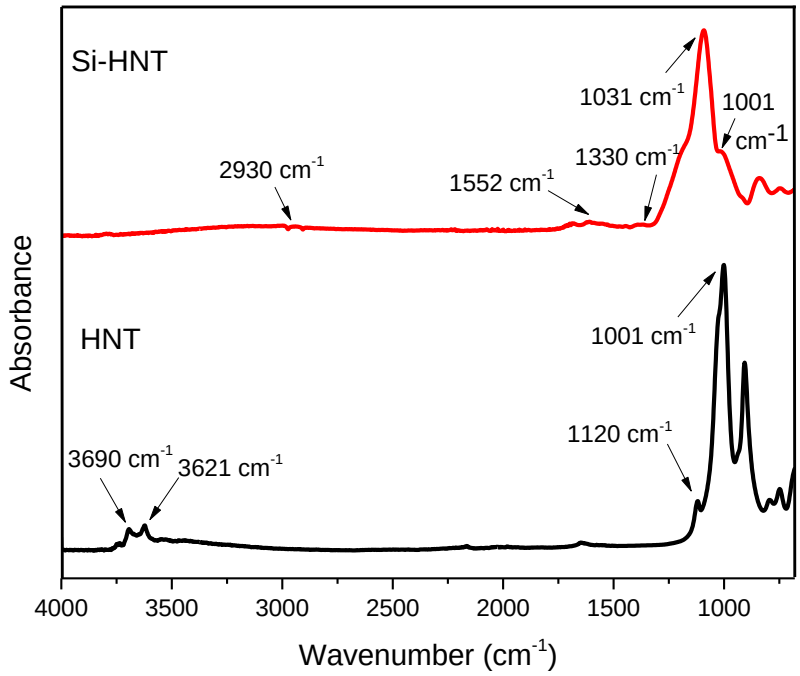

Figure 4.4 ATR-FTIR spectra of pure HNT and Si-HNT.

4.4.2 Characterization of treated fabrics

Figure 4.5(a) shows the ATR-FTIR spectra of control and oxidized cotton. The ATR-FTIR spectrum of pure cotton shows a broad peak between 3400 cm^{-1} and 3200 cm^{-1} which is assigned to the stretching of hydrogen-bonded hydroxyl groups in cellulose as well as the absorbed moisture while the intense absorbance at 2902 cm^{-1} is due to the symmetric C-H and C-H_2 stretching vibrations.[41, 42] The peak at 1635 cm^{-1} is due to the adsorbed/absorbed moisture. The peaks between 1056 cm^{-1} and 1250 cm^{-1} are characteristic cellulose peaks due to the C-O-C antisymmetric stretch. Oxidization of cellulose using periodate has been known to cleave the vicinal hydroxyl groups (secondary hydroxyl) to form aldehyde groups as shown in the schematic in Figure 4.1(b) .[41] The additional peak at 1728 cm^{-1} as seen in Figure 4.5(a) corresponds to the

aldehyde groups generated through oxidation.[28, 43] The intensity of the peak is low because mild oxidation process was used in this study. Strong oxidation of cellulose can disrupt the structure and crystallinity of cellulose and decrease the mechanical properties of cotton fabrics.[43] The amine functionalized Si-HNT can react with aldehyde groups on the cellulose fibers to form covalent bonds. As seen in Figure 4.5(b) for cotton-Si-HNT, the aldehyde peak at 1728 cm^{-1} disappears and a small peak at 1560 cm^{-1} appears which corresponds to the amine region. This confirms the grafting of Si-HNT particles on to the surface of oxidized cotton fabrics. A small peak seen at 800 cm^{-1} in cotton-Si-HNT fabric corresponds to Si-C bending vibration from Si-HNT particles.[44] While grafting of Si-HNT particles on the cotton fabrics create the desired surface roughness, the fabric still needs to undergo hydrophobic treatment. This can be achieved by lowering the surface energy of the fabric by attaching long chain hydrocarbons or fatty acids. Figure 4.6 shows the chemical reaction between cellulose and heptanoic anhydride. As seen in Figure 4.6, heptanoic anhydride can react with the hydroxyl groups of cellulose to form an ester bond resulting in grafting of seven-carbon aliphatic chain on the surface of fabrics.[29] Figure 4.5(b) shows the ATR-FTIR spectrum of cotton fabric grafted with Si-HNT and heptanoic anhydride (cotton-Si-HNT-FA). The additional peak at 1730 cm^{-1} seen in cotton-Si-HNT-FA corresponds to the ester group formed because of the grafting of fatty acid. The intensity of the peak at 2850 cm^{-1} increased as compared to control cotton fabric (Figure 4.5(a)) due to the $C\text{-}H_2$ symmetric stretching from the long chain hydrocarbons. This confirms the grafting of both, Si-HNT and fatty acid, onto the surface of cotton fabrics.

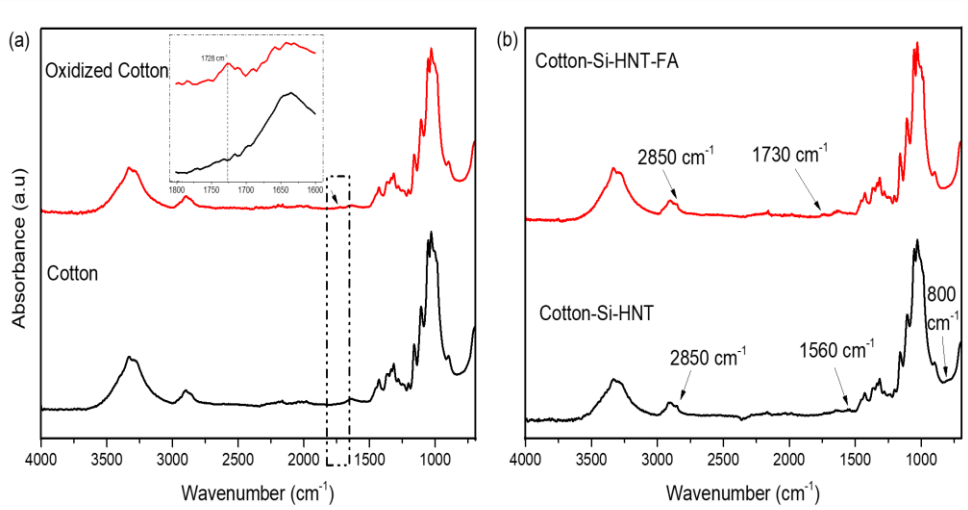

Figure 4.5 ATR-FTIR spectra of (a) cotton and oxidized cotton (b) cotton-Si-HNT and cotton-Si-HNT-Fatty acid.

As mentioned earlier, optimum combination of surface roughness and low surface energy molecules is critical to obtain ultrahydrophobic cotton fabrics. Table 4.1 shows the effect of Si-HNT particle concentration on WCA of the treated fabrics. The fatty acid treatment on fabrics without any particles results in hydrophobic surface with a WCA of 127° compared to almost zero for the control cotton fabric, which readily absorbs the water drop making it difficult to measure the WCA. As seen in Table 4.1 the WCA increases with increase in concentration of Si-HNT particles on the cotton fabric. It is necessary to create surface roughness on the fabric to create ultrahydrophobic surfaces.[45] The WCA increases from 127° to 143° by grafting just 0.1% Si-HNT particles and fatty acid on the fabric. The WCA further increases to 149° and 153° after grafting 0.3% and 0.5% Si-HNT particles, respectively, onto cotton fabrics and after the fatty acid treatment. These increases in WCA are primarily due to the increase in the surface roughness created by the Si-HNT particles. The increased surface roughness is clearly evident from the SEM images shown in Figure

4.7 of control and treated fabrics with different concentrations of Si-HNT and fatty acid. As can be seen in Figure 4.7(a), the surface of the control cotton fiber is mostly flat with some convolutions and shows the presence of natural folds running parallel along the cotton fiber axis.[46] This may be described as smooth fiber surface. Figures 4.7(b), 4.7(c) and 4.7(d) show SEM images of 0.1%, 0.3% and 0.5% Si-HNT particles and fatty acid grafted fibers, respectively. It is evident that as the concentration of Si-HNT particle increases, the particle loading on the fiber surface increases. Fabrics treated with 0.1% and 0.3% Si-HNT particle concentration show that much of the cotton fiber surface is bare and does not contain many Si-HNT particles, while fabric treated with 0.5% Si-HNT particle concentration shows most of cotton fiber surface covered with particles. As mentioned earlier, pure HNT particle is hydrophilic and readily absorbs water. Whereas fabric treated with pure HNT particles and fatty anhydride results in ultrahydrophobic fabric at first, but the water drop gets absorbed in just a few seconds. Since the HNT particle inner surface contains OH groups it is necessary to cap the HNT particle ends when their surface is modified via silanization. In an earlier study on cotton fabrics a hydrophobic coating based on spherical silica nanoparticles and perfluoroactylated quaternary ammonium silane coupling agent (PFSC) resulted in WCA of 145°.[47] In another study by Miao et al. perfluoroalkyl phosphate acrylates (PFPAs) grafted onto a cotton fabric via γ-ray irradiation showed WCA of over 150°.[48] In yet another publication, SiO_2 nanoparticle and ZnO nanorod arrays with subsequent n-dodecyltrimethoxysilane (DTMS) modification on cotton fabrics were shown to result in WCAs of 159° and 153°, respectively.[49] The present study shows that similar or higher WCA can be achieved by combining Si-HNT and

fatty acid treatments making it a 'greener' as well as an inexpensive alternative to toxic fluorine-based treatments. Such ultrahydrophobic fabrics can find many applications including water repellent clothing, packaging liners, and filtration. Because of the hydrophobicity (lower surface energy) of the surface created by the hydrocarbon fatty acid layer, these surfaces tend to be highly oleophilic as well. This property can be useful in developing oil absorbing cellulosic materials for oil-water separation. Oil pollution caused by the petrochemical, food industries as well as the frequent oil spills due to accidents during offshore oil production or transportation is a major problem.[50, 51]

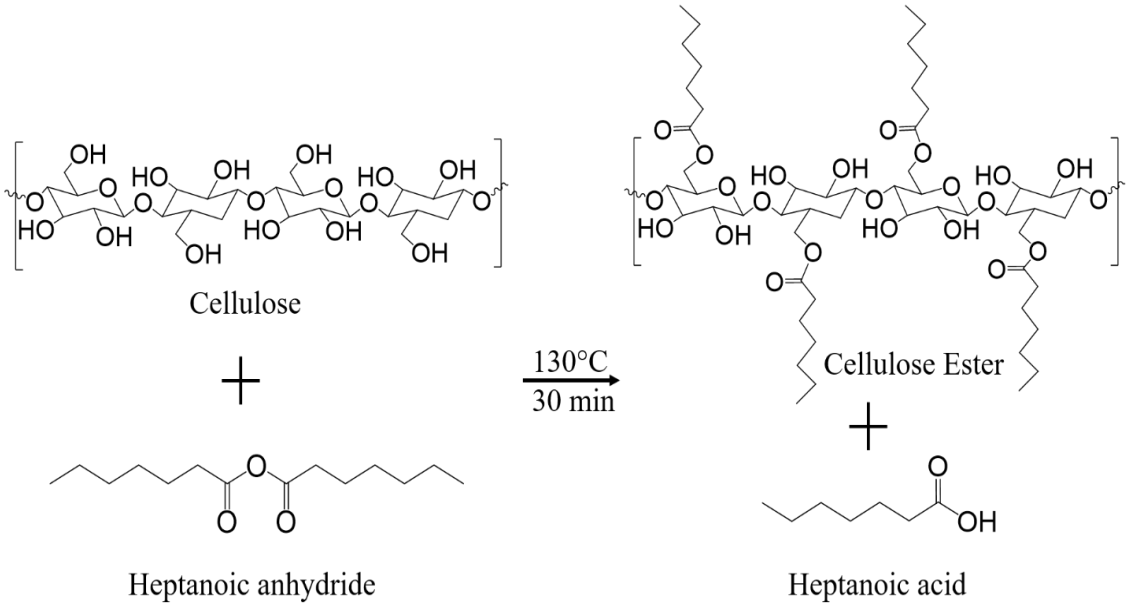

Figure 4.6 Chemical reaction between cellulose and heptanoic anhydride.

Table 4.1 Effect of Si-HNT particle concentration on WCA.

Treatment	**WCA**	**Std. Dev.**
Control-FA	127	2.1
Cotton-0.1% Si-HNT-FA	143	1.2

Cotton-0.3% Si-HNT-FA	149	2.0
Cotton-0.5% Si-HNT-FA	153	1.9

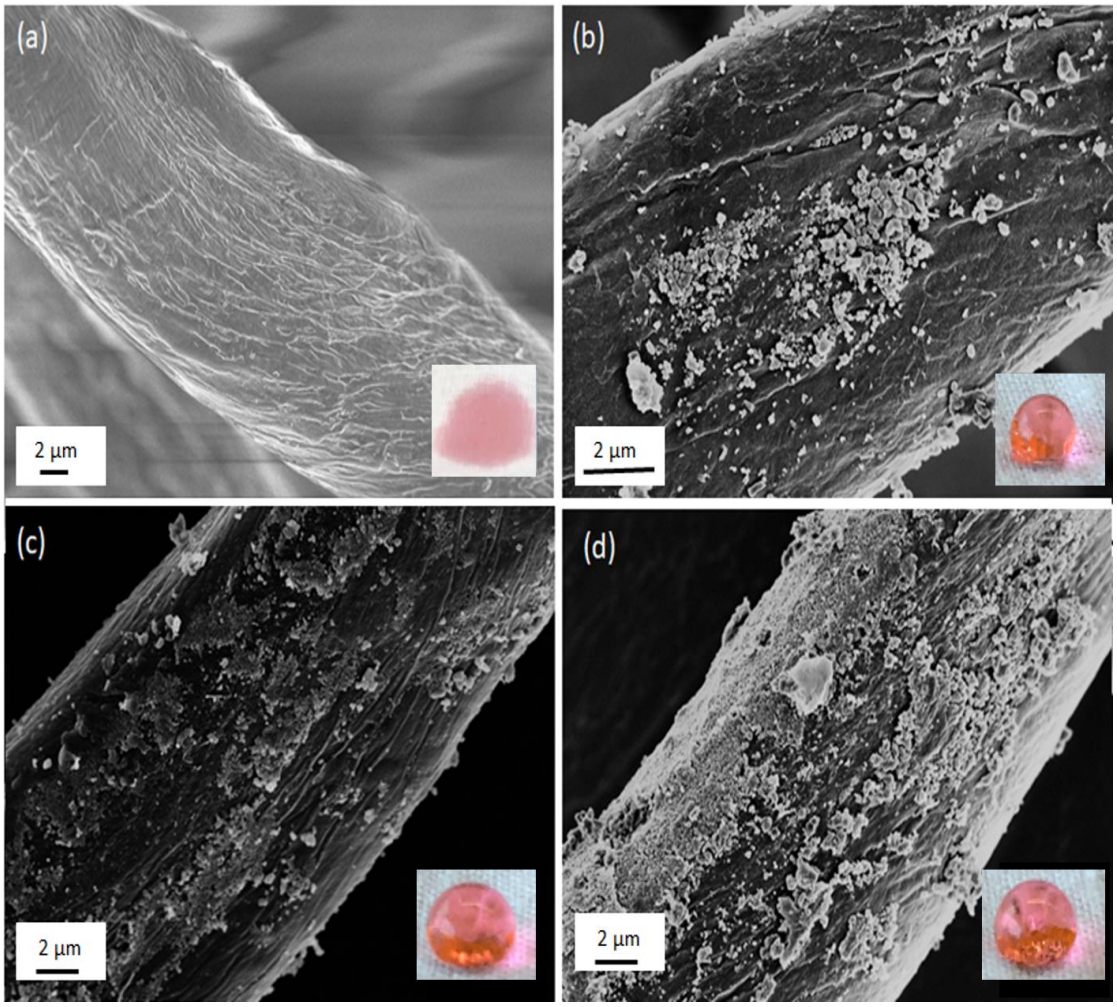

Figure 4.7 SEM images of (a) control (b) 0.1% (c) 0.3% and (d) 0.5% Si-HNT particles and fatty acid treated fabrics with the pictures of water droplets in the inset.

Figure 4.8 shows the effect of various treatments on the tensile properties such as tensile stress and strain of the fabrics. As seen in Figure 4.8(a), tensile stress (strength) of the fabrics oxidized using sodium periodate reduced to 46 MPa from 56.8 MPa for untreated (control) fabrics in the warp direction and to 29.3 MPa from 35.4

MPa in the weft direction. The oxidation by sodium periodate is known to break the crystalline structure of the cellulose in the cotton fabric.[52] These results indicate loss of tensile stress of about 19% in the warp direction and 17% in the weft direction. Figure 4.8(b) presents the tensile strains of the fabrics. It is clear that the oxidation process of fabrics increases the tensile strain from 6% to 8.3% in the warp direction and from 13.3% to 15% in the weft direction. The increase in the tensile strain can be expected due to the partial breaking of the crystalline structure of the cellulose after oxidation. The other reason for higher tensile strain could be due to relaxation of the built-up stress in the fabric, caused by high tension experienced by the fabrics during weaving and finishing such as tentering.[5] The tensile data presented in Figures 4.8(a) and 4.8(b) indicate that the covalent bonding of the Si-HNT through the amine and aldehyde reaction (cotton-Si-HNT) and the subsequent fatty acid treatment (cotton-Si-HNT-FA) does not have any significant effect on the tensile stress and strain of the treated fabrics. Cotton-Si-HNT-FA fabrics showed a tensile stress of 46.8 MPa and 30 MPa in warp and weft directions, respectively. The strength of cotton-SiO_2-FA fabrics is similar to the strength of the oxidized cotton fabrics. This confirms that the strength loss observed in the cotton-SiO_2-FA fabrics is during the oxidation process only. The covalent bonding of particles and/or the fatty acid grafting do not contribute to any strength loss. This can be expected since both these activities are only surface related and do not attack the fibrils or the crystalline part in the cotton fiber. Cotton fabrics treated with only the fatty acid (cotton-FA), without oxidizing the fabrics and covalently bonding of the Si-HNT particles, showed tensile stress of 55.5 MPa and 36 MPa in the warp and weft directions, respectively. These values are statistically same

as the tensile stress of the control fabrics (56.8 MPa and 35.4 MPa in warp and weft direction respectively) using the statistical t-test analysis. While the results of an earlier study had indicated that the fatty acid grafting on cotton fabrics using microwave causes 47% and 50% strength loss in the warp and weft directions, respectively, due to the high temperature caused by microwave treatment, no such strength loss was found in this study.[29]

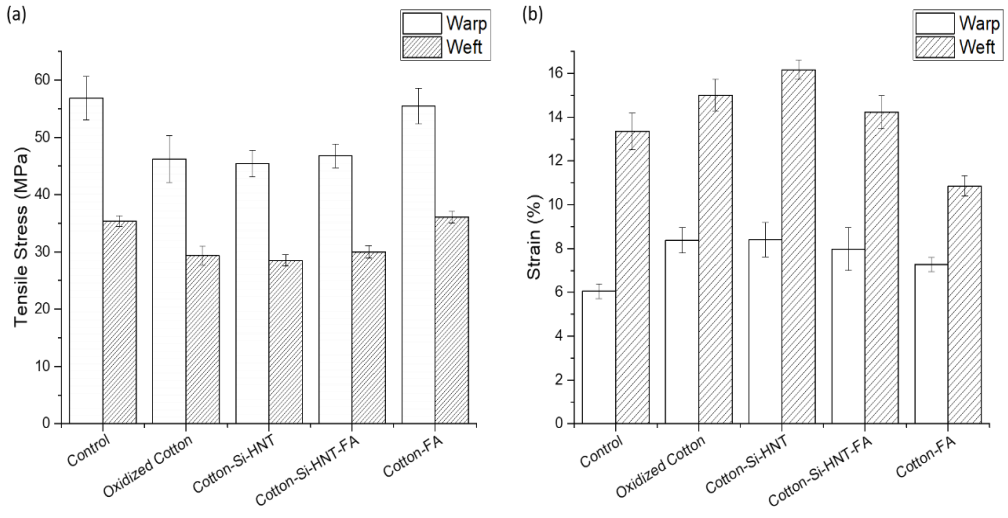

Figure 4.8 Effect of various treatments on the (a) tensile stress and (b) tensile strain of the fabrics.

The effect of ultrahydrophobic treatment on the color change of the fabrics was evaluated using Macbeth Color-eye spectrophotometer. The L* which indicates the lightness of the fabric remained unchanged after the treatment. It was found to be 85.8 for control and 85.5, essentially unchanged, for the cotton-Si-HNT-FA fabrics. The a* which indicates the color value from green to red remained unchanged from -0.41 in control to -0.52 after treatment. The b* which indicates the color value from blue to

yellow changed slightly from 0.45 in control to 1.11 after treatment. The b* value of the standard white calibration tile is 1. While the spectrophotometer b* values suggest slight yellowness of the fabric, no visible difference in the color or yellowing or a change in the feel/softness of the fabrics was observed after the ultrahydrophobic treatment.

Table 4.2 shows the effect of laundry durability (up to 5 laboratory laundry cycles) on the durability of the ultrahydrophobic treatment. The washing treatments were carried out according to the modified AATCC Test Method 61–2003. Each laboratory laundry cycle, as mentioned earlier, corresponds to 5 home laundry washes. As can be seen from data in Table 4.2, WCA decreased slightly with the number of laundry cycles. The WCA decreased from 127° to 120° after 5 laundry cycles for the fatty acid grafted fabrics (cotton-FA). The WCA decreased from 153° to 150° after 3 laundry cycles for the 0.5% Si-HNT and fatty acid grafted fabrics (cotton-Si-HNT-FA). The WCA further decreased to 149° after 5 laundry cycles. It was observed that 0.5% Si-HNT and fatty acid grafted fabric retained its ultrahydrophobic characteristic after 3 cycles (15 home laundry washes) after which it is still found to be hydrophobic. Even though the contact angle decreased slightly, all the fabrics maintained their hydrophobic characteristics after 5 laundry cycles which correspond to 25 home laundry washes. Excellent durability of the ultrahydrophobic characteristics to laundry washing obtained in this study is primarily due to the covalent bonding of Si-HNT particles to cotton fibers (cellulose). The fatty acid treatment after the grafting of Si-HNT particles ensures that all fiber surface is covered with the low surface energy hydrocarbon. Apart from reacting with the primary hydroxyl groups on the cellulose,

it is also possible that the fatty acid reacts with the surface silanol -OH groups from Si-HNT to form ester bonds overall improving the ultrahydrophobicity of the cotton fabrics. The slight decrease in the WCA is believed to be due to the presence of cellulase enzyme in the detergent, which can degrade the top surface layer of the cotton fabrics.[29]

Table 4.2 Effect of ultrahydrophobic treatment on laundry durability.

Specimen	**CA_0***	**CA_1**	**CA_3**	**CA_5**
Control-FA	127± 2.1	126±2.7	119±1.3	120±3.3
Cotton-0.1% Si-HNT-FA	143±1.2	142±2.1	140±1.2	136±1.7
Cotton-0.3% Si-HNT-FA	149±2.0	148±3.1	144±2.3	143±1.3
Cotton-0.5% Si-HNT-FA	153±1.9	153±2.3	150±1.4	149±1.6

* The subscripts indicate number of laundry washings.

4.5 Conclusions

This study has clearly demonstrated that the hydrophilic cotton fabrics can be converted to ultrahydrophobic fabrics using a sustainable yet cost-effective method. HNT, an inexpensive natural clay, was modified by silanization and silica nanosphere assembly to cover its hydrophilic lumen. This also created desired surface roughness on the smooth tubular HNT. Cotton fabrics were treated with $NaIO_4$ to oxidize the secondary hydroxyl groups to aldehyde groups. Modified HNT particles were then covalently bonded onto the surface of the cotton fibers by reacting the amine groups from Si-HNT particles with the aldehyde groups on the cotton fibers. It was observed that the optimum concentration of the Si-HNT particles was required to coat the fiber surface with the particles to a desired level. Fatty acid treatment of the cotton fabric was then carried out to obtain hydrophobic surface (low surface energy). Combination

of fabric surface roughness due to Si-HNT and low surface energy resulting from the fatty acid treatment resulted in an ultrahydrophobic cotton fabric with a durable WCA of 153°. Such ultrahydrophobic cellulosic materials can find applications in performance outdoor clothing, packaging, water repellent materials, oil-water separation devices and others.

Acknowledgments

This research made use of Cornell Center for Materials Research (CCMR) shared facilities supported through the NSF MRSEC program (DMR-1719875).

4.6 References

1. Wu, M.; Ma, B.; Pan, T.; Chen, S.; Sun, J., Silver-nanoparticle-colored cotton fabrics with tunable colors and durable antibacterial and self-healing superhydrophobic properties. *Advanced Functional Materials* **2016,** *26* (4), 569-576.

2. Yetisen, A. K.; Qu, H.; Manbachi, A.; Butt, H.; Dokmeci, M. R.; Hinestroza, J. P.; Skorobogatiy, M.; Khademhosseini, A.; Yun, S. H., Nanotechnology in textiles. *ACS nano* **2016,** *10* (3), 3042-3068.

3. Liu, Y.; Tang, J.; Wang, R.; Lu, H.; Li, L.; Kong, Y.; Qi, K.; Xin, J., Artificial lotus leaf structures from assembling carbon nanotubes and their applications in hydrophobic textiles. *Journal of Materials chemistry* **2007,** *17* (11), 1071-1078.

4. Gu, S.; Yang, L.; Huang, W.; Bu, Y.; Chen, D.; Huang, J.; Zhou, Y.; Xu, W., Fabrication of hydrophobic cotton fabrics inspired by polyphenol chemistry. *Cellulose* **2017,** *24* (6), 2635-2646.

5. Rana, M.; Chen, J. T.; Yang, S.; Ma, P. C., Biomimetic Superoleophobicity of Cotton Fabrics for Efficient Oil–Water Separation. *Advanced Materials Interfaces* **2016,** *3* (16).

6. Kollarigowda, R. H.; Abraham, S.; Montemagno, C. D., Antifouling Cellulose Hybrid Biomembrane for Effective Oil/Water Separation. *ACS Applied Materials & Interfaces* **2017,** *9* (35), 29812-29819.

7. Teisala, H.; Tuominen, M.; Kuusipalo, J., Superhydrophobic Coatings on Cellulose-Based Materials: Fabrication, Properties, and Applications. *Advanced Materials Interfaces* **2014,** *1* (1).

8. Liu, M.; Wang, S.; Jiang, L., Nature-inspired superwettability systems. *Nature Reviews Materials* **2017,** *2* (7), natrevmats201736.

9. Ma, M.; Gupta, M.; Li, Z.; Zhai, L.; Gleason, K. K.; Cohen, R. E.; Rubner, M. F.; Rutledge, G. C., Decorated electrospun fibers exhibiting superhydrophobicity. *Advanced Materials* **2007,** *19* (2), 255-259.

10. Wang, S.; Jiang, L., Definition of superhydrophobic states. *Advanced Materials* **2007,** *19* (21), 3423-3424.

11. Marmur, A., The lotus effect: superhydrophobicity and metastability. *Langmuir* **2004,** *20* (9), 3517-3519.

12. Li, B.; Zhang, J., Durable and self-healing superamphiphobic coatings repellent even to hot liquids. *Chemical Communications* **2016,** *52* (13), 2744-2747.

13. Fan, L.; Li, B.; Wang, Q.; Wang, A.; Zhang, J., Superhydrophobic gated polyorganosilanes/halloysite nanocontainers for sustained drug release. *Advanced Materials Interfaces* **2014,** *1* (5), 1300136.

14. Wang, C.; Yao, T.; Wu, J.; Ma, C.; Fan, Z.; Wang, Z.; Cheng, Y.; Lin, Q.; Yang, B., Facile approach in fabricating superhydrophobic and superoleophilic surface for water and oil mixture separation. *ACS applied materials & interfaces* **2009,** *1* (11), 2613-2617.

15. Zhang, J.; France, P.; Radomyselskiy, A.; Datta, S.; Zhao, J.; van Ooij, W., Hydrophobic cotton fabric coated by a thin nanoparticulate plasma film. *Journal of Applied Polymer Science* **2003,** *88* (6), 1473-1481.

16. Bhat, N.; Netravali, A.; Gore, A.; Sathianarayanan, M.; Arolkar, G.; Deshmukh, R., Surface modification of cotton fabrics using plasma technology. *Textile Research Journal* **2011,** *81* (10), 1014-1026.

17. Cunha, A. G.; Gandini, A., Turning polysaccharides into hydrophobic materials: a critical review. Part 1. Cellulose. *Cellulose* **2010,** *17* (5), 875-889.

18. Korhonen, J. T.; Kettunen, M.; Ras, R. H.; Ikkala, O., Hydrophobic nanocellulose aerogels as floating, sustainable, reusable, and recyclable oil absorbents. *ACS applied materials & interfaces* **2011,** *3* (6), 1813-1816.

19. Athauda, T. J.; Hari, P.; Ozer, R. R., Tuning physical and optical properties of ZnO nanowire arrays grown on cotton fibers. *ACS applied materials & interfaces* **2013,** *5* (13), 6237-6246.

20. Li, S.; Huang, J.; Ge, M.; Cao, C.; Deng, S.; Zhang, S.; Chen, G.; Zhang, K.; Al-Deyab, S. S.; Lai, Y., Robust Flower-Like TiO2@ Cotton Fabrics with Special Wettability for Effective Self-Cleaning and Versatile Oil/Water Separation. *Advanced Materials Interfaces* **2015,** *2* (14).

21. Hekster, F. M.; Laane, R. W.; de Voogt, P., Environmental and toxicity effects of perfluoroalkylated substances. In *Reviews of Environmental Contamination and Toxicology*, Springer: 2003; pp 99-121.

22. Lv, G.; Wang, L.; Liu, S.; Li, S., Determination of perfluorinated compounds in packaging materials and textiles using pressurized liquid extraction with gas chromatography-mass spectrometry. *Analytical Sciences* **2009,** *25* (3), 425-429.

23. Xie, S.; Wang, T.; Liu, S.; Jones, K. C.; Sweetman, A. J.; Lu, Y., Industrial source identification and emission estimation of perfluorooctane sulfonate in China. *Environment international* **2013,** *52*, 1-8.

24. Melzer, D.; Rice, N.; Depledge, M. H.; Henley, W. E.; Galloway, T. S., Association between serum perfluorooctanoic acid (PFOA) and thyroid disease in the

US National Health and Nutrition Examination Survey. *Environmental health perspectives* **2010,** *118* (5), 686.

25. Post, G. B.; Louis, J. B.; Cooper, K. R.; Boros-Russo, B. J.; Lippincott, R. L., Occurrence and potential significance of perfluorooctanoic acid (PFOA) detected in New Jersey public drinking water systems. *Environmental science & technology* **2009,** *43* (12), 4547-4554.

26. Posner, S., Perfluorinated compounds: occurrence and uses in products. In *Polyfluorinated chemicals and transformation products*, Springer: 2012; pp 25-39.

27. Dankovich, T. A.; Hsieh, Y.-L., Surface modification of cellulose with plant triglycerides for hydrophobicity. *Cellulose* **2007,** *14* (5), 469-480.

28. Samyn, P.; Schoukens, G.; Stanssens, D.; Vonck, L.; Van den Abbeele, H., Hydrophobic waterborne coating for cellulose containing hybrid organic nanoparticle pigments with vegetable oils. *Cellulose* **2013,** *20* (5), 2625-2646.

29. Zhong, Y.; Netravali, A. N., 'Green'surface treatment for water-repellent cotton fabrics. *Surface Innovations* **2016,** *4* (1), 3-13.

30. Vaca-Garcia, C.; Thiebaud, S.; Borredon, M.; Gozzelino, G., Cellulose esterification with fatty acids and acetic anhydride in lithium chloride/N, N-dimethylacetamide medium. *Journal of the American Oil Chemists' Society* **1998,** *75* (2), 315-319.

31. Zhang, D.; Chen, L.; Zang, C.; Chen, Y.; Lin, H., Antibacterial cotton fabric grafted with silver nanoparticles and its excellent laundering durability. *Carbohydrate polymers* **2013,** *92* (2), 2088-2094.

32. Lvov, Y.; Wang, W.; Zhang, L.; Fakhrullin, R., Halloysite clay nanotubes for loading and sustained release of functional compounds. *Advanced Materials* **2016,** *28* (6), 1227-1250.

33. Yuan, P.; Southon, P. D.; Liu, Z.; Green, M. E.; Hook, J. M.; Antill, S. J.; Kepert, C. J., Functionalization of halloysite clay nanotubes by grafting with γ-aminopropyltriethoxysilane. *The Journal of Physical Chemistry C* **2008,** *112* (40), 15742-15751.

34. Liu, M.; Guo, B.; Du, M.; Lei, Y.; Jia, D., Natural inorganic nanotubes reinforced epoxy resin nanocomposites. *Journal of Polymer Research* **2008,** *15* (3), 205-212.

35. Yang, J.; Wu, Y.; Shen, Y.; Zhou, C.; Li, Y.-F.; He, R.-R.; Liu, M., Enhanced therapeutic efficacy of doxorubicin for breast cancer using chitosan oligosaccharide-modified halloysite nanotubes. *ACS applied materials & interfaces* **2016,** *8* (40), 26578-26590.

36. Wu, Y.-P.; Yang, J.; Gao, H.-Y.; Shen, Y.; Jiang, L.; Zhou, C.; Li, Y.-F.; He, R.-R.; Liu, M., Folate-conjugated halloysite nanotubes, an efficient drug carrier, deliver doxorubicin for targeted therapy of breast cancer. *ACS Applied Nano Materials* **2018,** *1* (2), 595-608.

37. Feng, K.; Hung, G.-Y.; Liu, J.; Li, M.; Zhou, C.; Liu, M., Fabrication of high performance superhydrophobic coatings by spray-coating of polysiloxane modified halloysite nanotubes. *Chemical Engineering Journal* **2018,** *331*, 744-754.

38. Ali, A.; Haidar, A.; Polonskyi, O.; Faupel, F.; Abdul-Khaliq, H.; Veith, M.; Aktas, O., Extreme tuning of wetting on 1D nanostructures: from a superhydrophilic to a perfect hydrophobic surface. *Nanoscale* **2017,** *9* (39), 14814-14819.

39. Ren, S.; Yang, S.; Zhao, Y.; Yu, T.; Xiao, X., Preparation and characterization of an ultrahydrophobic surface based on a stearic acid self-assembled monolayer over polyethyleneimine thin films. *Surface science* **2003,** *546* (2-3), 64-74.

40. Zhang, Y.; He, X.; Ouyang, J.; Yang, H., Palladium nanoparticles deposited on silanized halloysite nanotubes: synthesis, characterization and enhanced catalytic property. *Scientific reports* **2013,** *3*, 2948.

41. Sun, B.; Hou, Q.; Liu, Z.; Ni, Y., Sodium periodate oxidation of cellulose nanocrystal and its application as a paper wet strength additive. *Cellulose* **2015,** *22* (2), 1135-1146.

42. Siller, M.; Amer, H.; Bacher, M.; Roggenstein, W.; Rosenau, T.; Potthast, A., Effects of periodate oxidation on cellulose polymorphs. *Cellulose* **2015,** *22* (4), 2245-2261.

43. Xu, Q.; Xie, L.; Diao, H.; Li, F.; Zhang, Y.; Fu, F.; Liu, X., Antibacterial cotton fabric with enhanced durability prepared using silver nanoparticles and carboxymethyl chitosan. *Carbohydrate polymers* **2017,** *177*, 187-193.

44. Zhang, D.; Williams, B. L.; Shrestha, S. B.; Nasir, Z.; Becher, E. M.; Lofink, B. J.; Santos, V. H.; Patel, H.; Peng, X.; Sun, L., Flame retardant and hydrophobic coatings on cotton fabrics via sol-gel and self-assembly techniques. *Journal of colloid and interface science* **2017,** *505*, 892-899.

45. Zhou, H.; Wang, H.; Niu, H.; Zhao, Y.; Xu, Z.; Lin, T., A Waterborne Coating System for Preparing Robust, Self-healing, Superamphiphobic Surfaces. *Advanced Functional Materials* **2017,** *27* (14), 1604261.

46. Hung, O.-n.; Chan, C.-k.; Kan, C.-w.; Yuen, C.-w. M., Microscopic study of the surface morphology of CO2 laser-treated cotton and cotton/polyester blended fabric. *Textile Research Journal* **2017,** *87* (9), 1107-1120.

47. Yu, M.; Gu, G.; Meng, W.-D.; Qing, F.-L., Superhydrophobic cotton fabric coating based on a complex layer of silica nanoparticles and perfluorooctylated quaternary ammonium silane coupling agent. *Applied surface science* **2007,** *253* (7), 3669-3673.

48. Miao, H.; Bao, F.; Cheng, L.; Shi, W., Cotton fabric modification for imparting high water and oil repellency using perfluoroalkyl phosphate acrylate via γ-ray-induced grafting. *Radiation Physics and Chemistry* **2010,** *79* (7), 786-790.

49. Xu, B.; Cai, Z.; Wang, W.; Ge, F., Preparation of superhydrophobic cotton fabrics based on SiO 2 nanoparticles and ZnO nanorod arrays with subsequent hydrophobic modification. *Surface and Coatings Technology* **2010,** *204* (9), 1556-1561.

50. Chu, Z.; Feng, Y.; Seeger, S., Oil/water separation with selective superantiwetting/superwetting surface materials. *Angewandte Chemie International Edition* **2015,** *54* (8), 2328-2338.

51. Li, S.; Huang, J.; Ge, M.; Cao, C.; Deng, S.; Zhang, S.; Chen, G.; Zhang, K.; Al-Deyab, S. S.; Lai, Y., Robust flower-like TiO2@ cotton fabrics with special wettability for effective self-cleaning and versatile oil/water separation. *Advanced Materials Interfaces* **2015,** *2* (14), 1500220.

52. Zhang, F.; Chen, Y.; Lin, H.; Wang, H.; Zhao, B., HBP-NH2 grafted cotton fiber: Preparation and salt-free dyeing properties. *Carbohydrate polymers* **2008,** *74* (2), 250-256.

Chapter 5 Bioinspired 'green' process using anisotropic silica particles and fatty acid for superhydrophobic cotton fabrics

Namrata V. Patil and Anil N. Netravali

Department of Fiber Science & Apparel Design,

Cornell University, 37 Forest Home Dr., Ithaca, NY 14853, USA

Graphical abstract

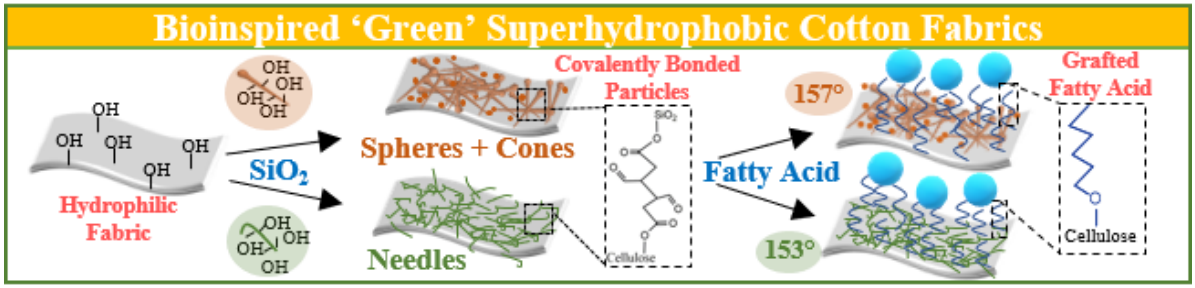

Published as:

Patil, N. V. and A. N. Netravali "Bioinspired process using anisotropic silica particles and fatty acid for superhydrophobic cotton fabrics." Cellulose: 1-15.

5.1 Abstract

Cotton fabrics with superhydrophobic surfaces were prepared via 2-step 'green' process using fully sustainable bio-based raw-materials. In the 1st step, silica particles with different shapes were synthesized using water-in-alcohol emulsion and different molecular weights (MW) of polyvinyl pyrrolidone (PVP). Low MW PVP resulted in a combination of spherical and cone-shaped particles while high MW PVP resulted in needle-shaped particles. Particles were covalently bonded to the fabrics to create desired permanent surface roughness. In the 2nd step, fabrics with altered surfaces were grafted with fatty acid to lower the surface energy of fabrics. Covalent bonding of particles and grafting of fatty acids onto the fabrics was confirmed using ATR-FTIR. The combination of surface roughness obtained through silica particles and low surface energy of the fatty acid resulted in superhydrophobic cotton fabrics. Fabrics grafted with spherical and cone-shaped particles, mimicking lotus leaf, showed water contact angle (WCA) of 157° whereas needle-shaped particles gave WCA of 153°. The durability of the superhydrophobic treatment was confirmed by repeated washing of the fabrics. The 'green' process developed in this study can be scaled-up for other cellulosic materials such as viscose rayon, paper, etc., to expand their applications in self-cleaning surfaces, water repellent protective coatings, packaging and others.

5.2 Introduction

Cotton fibers are made-up of cellulose, the most abundantly used natural polymer on earth. With worldwide efforts to curb the use of non-biodegradable petroleum-based products and replacing them with fully sustainable natural products, both

government and industry have put increased emphasis on promoting the use of cellulosic products. As a result, the use of cellulose in the form of fabrics, non-woven mats, paper, micro- and nano-fibrillated cellulose, nano-crystalline cellulose, bacterial cellulose, etc., has been on the rise.[1] Apart from the conventional uses as apparel, footwear, bags, upholstery, automotive materials, food packaging, and filters, cellulose can now be found in many novel applications such as hydrogels, oil-water separation membranes, microfluidic devices and composite materials.[2] Some common characteristics of the products made using cellulose are light weight, flexible, portable and sustainable.[3-12] However, as a result of the enormous amount of hydroxyl groups present in cellulose the products made with it are inherently hydrophilic. They absorb moisture causing them to swell and lose their strength and stiffness, a very undesirable characteristic in many applications. With significant increase in the use of cellulose over the past decade, engineering of superhydrophobic cellulosic surfaces has gained significant attention in the industrial arena as water-repellency can increase potential applications and durability of the cellulosic materials.[13-16]

Superhydrophobic surfaces which exhibit water contact angles (WCAs) greater than 150° is a natural phenomenon found in many plant leaves, the most prominent example being the lotus leaf, and some insects such as the water strider legs.[17] Decades of study of such naturally occurring surfaces have revealed that micro- and nano-scaled hierarchical structures along with the presence of low surface energy compounds make these surfaces inherently superhydrophobic.[17] Numerous strategies for mimicking nature's superhydrophobic surfaces on cotton fibers/fabrics have been put forward which are based on the principle of creating surface roughness using

inorganic particles such as SiO_2, ZnO, TiO_2, Ag, Au, CeO_2, CuO, followed by chemical treatments to create hydrophobic surfaces using low surface energy fluorinated compounds such as Perfluorooctanoic acid (PFOA), fluoroalkylsilane and other fluorochemicals.[14, 18-23] Electrochemical deposition, layer-by-layer assembly, chemical vapor deposition, etching, templated nanopatterning, plasma, lithography and other such techniques have been used for creating superhydrophobic fabrics.[16, 19]

Most of the techniques mentioned above do need expensive instrumentation or hazardous solvents such as tetrahydrofuran and N,N-dimethylformamide.[24] In recent years the use of fluorinated polymers has been restricted due to their bio-accumulative potential and toxicity to both humans and the environment.[24, 25] A major challenge in using inorganic particles in practical applications is their poor bonding to the fabrics. As most of them are physically deposited and use hydrogen bonding or ionic interactions as the primary mechanisms to stay on the fabric, these particles can easily leach out from the fabrics during washing or during use giving rise to significant environmental concerns. All these issues have hampered the scaling up of such techniques to create superhydrophobic cotton fabrics for commercial applications. At the same time, these issues have also generated calls for developing greener processes to obtain superhydrophobic cotton fabrics.

The main aim of the present research was to create superhydrophobic cotton fabrics using non-toxic and inexpensive methods and materials that are industrially scalable for practical applications. Colloidal syntheses of different shapes (spheres + cones and needles) of silica (SiO_2) particles were carried out using two different molecular weights (MWs) of the emulsion stabilizer, polyvinyl pyrrolidone (PVP) as

shown in the schematic representation in Figure 5.1. The synthesized sphere + cone and needle-shaped silica particles were covalently bonded onto the cotton fabrics, separately, using a simple dip-cure method. The covalent bonding of the particles permanently altered the surface topography of the fabrics and increased the durability of the treatment. Seven-carbon aliphatic chains were then grafted on to the surface-altered fabrics using a simple dip-cure method via esterification as shown in the chemical reaction in Figure 5.2. The presence of SiO_2 particles on the surface creates micro-structured pockets that act as air-gaps at the interface between the fabric and the water droplet, enhancing the WCA of the fabrics. The combined effects of surface roughness created by two different types of SiO_2 particles and the low surface energy caused by the aliphatic chains on the hydrophobicity of the fabrics were studied.

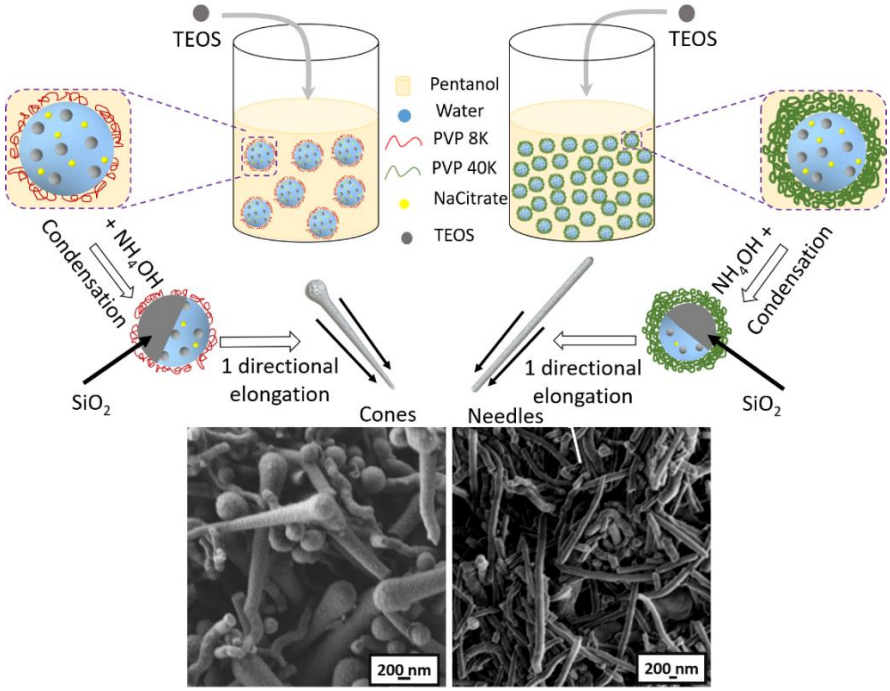

Figure 5.1 Schematic representation of the colloidal synthesis of anisotropic SiO2 particles using two different molecular weights of PVP.

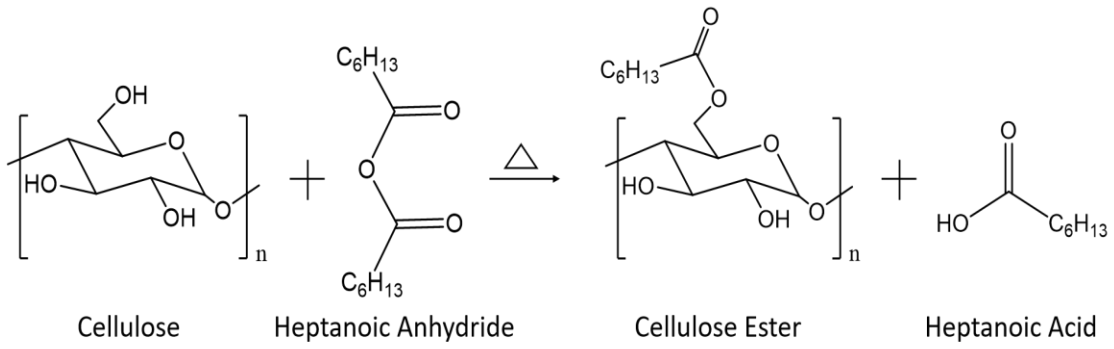

Figure 5.2 Chemical reaction between cellulose and heptanoic anhydride via esterification.

5.3 Materials and methods

5.3.1 Materials

Desized and bleached plain weave cotton fabric (#400) was purchased from Testfabrics, Inc, PA. Tetraethyl orthosilicate, 98% (TEOS), PVP (MW 8000 and 40,000) were purchased from Sigma Aldrich, Allentown, PA. 1-pentanol was purchased from Krackeler Scientific, Inc. Albany, NY. Heptanoic anhydride (HA) was purchased from TCI America, Philadelphia, PA. Ethanol (≥99.5% purity, absolute), sodium citrate, ammonium hydroxide (~28% NH_4OH), and butane tetra carboxylic acid (BTCA) were purchased from Sigma-Aldrich Chemical, Allentown, PA. Sodium hypophosphite monohydrate (SHP) was purchased from VWR international. Milli-Q deionized water (resistivity, 18.2 MΩ.cm, Millipore RiOs and Elix water purification systems, Millipore Corporation, MA) was used for hydrolysis of TEOS and deionized (DI) water was used for the measurement of WCA.

5.3.2 Synthesis of anisotropic SiO_2 particles

Two g of PVP, both 8K and 40K were dissolved, separately, in 30 ml of 1-pentanol. The solutions were stirred continuously using magnetic stirrer at 300 rpm. Ethanol (3 ml) and 840 µl ultrapure water were added to the PVP solutions. Two hundred µl of 0.17 M sodium citrate was added to the water in oil (pentanol) emulsion. Both PVP and sodium citrate act as stabilizers for the water-in-pentanol emulsion. TEOS and NH_4OH, 300 µl and 500 µl, respectively, were added to the emulsions and left stirring at 300 rpm at room temperature for 18 h. At the end of 18 h, the emulsion was centrifuged at 20,000 rpm for 20 min and the supernatant was discarded. The precipitate was dissolved in ethanol using vortex meter and centrifuged again at 20,000 rpm for 20 min. This process was repeated thrice to remove the surplus reactants.

5.3.3 Physical deposition vs. covalent bonding of anisotropic SiO_2 particles on to cotton fabrics

The SiO_2 particles were dispersed in ethanol by stirring at 1000 rpm for 30 min. Cotton fabric specimens (15 cm × 15 cm) were then dipped in 0.1% SiO_2 particle dispersion for 10 min and dried in an air-circulating oven at 130°C for 20 min to get SiO_2 particles immobilized on the fabrics based on hydrogen bonding. These physically deposited SiO_2 fabrics are termed as PD-SiO_2. SiO_2 particles were covalently bonded to cotton fabric surface using BTCA. To obtain covalent bonding, cotton fabrics were immersed in 0.1% SiO_2 particle dispersion containing 3% BTCA and 1.5% SHP for 10 min and cured at 140°C for 20 min. These fabrics are termed as Xlink-SiO_2.

5.3.4 Grafting of fatty acid onto cotton fabrics

Control fabrics as well as PD-SiO_2 and Xlink-SiO_2 fabrics were grafted with low surface energy molecules, on the surface. Cotton fabrics were dipped in HA and squeezed by hand to remove excess HA. They were further dipped and squeezed again and cured at 130°C in an air-circulating oven for required time. The fabrics were then rinsed with ethanol to remove the by-product, heptanoic acid and unreacted HA, if any. The fabrics were then dried at 50°C in an air-circulating oven to get rid of the treatment odor. The cotton fabrics with physically deposited sphere + cone-shaped and needle-shaped SiO_2 particles and treated with HA are termed as PD-SiO_2(cones)-HA fabrics and PD-SiO_2(needles)-HA fabrics, respectively. The covalently bonded sphere + cone-shaped and needle-shaped SiO_2 particles on cotton fabrics and further treated with HA are termed as Xlink-SiO_2(cones)-HA fabrics and Xlink-SiO_2(needles)-HA fabrics, respectively.

5.3.5 Scanning electron microscopy (SEM)

The surface morphologies of synthesized SiO_2 particles and the treated fibers were observed using a Zeiss Gemini 500 SEM (Germany) at 1 kV accelerating voltage. Image J software was used to analyze diameters and lengths of the particles. An average of 50 particles from 5 different images were reported. Images were taken from particles synthesized at two different times to ensure reproducibility of the results.

5.3.6 Transmission electron microscopy (TEM).

Cross-sections of the sphere + cone and needle-shaped particles were observed under FEI Tecnai T12 TEM (Thermo Fisher Scientific, Hillsboro, OR). The particles were dispersed in epoxy and cured. A thin slice of 70 nm thickness was cut using an ultramicrotome fitted with a diamond knife to observe the cross-sections of the particles.

5.3.7 Attenuated total reflectance Fourier-transform infrared spectroscopy (ATR-FTIR)

The ATR-FTIR spectra collected using Thermo Nicolet Magna-IR 560 spectrometer (Madison, WI) with a split pea accessory was used to confirm the grafting of both SiO_2 particles as well the aliphatic fatty chains onto the cotton fabrics. Each scan was an average of 300 scans from 4000 cm^{-1} to 500 cm^{-1} wavenumbers.

5.3.8 Water contact angle (WCA)

Contact angle analyzer CAA2, Imass Inc., (Accord, MA) was used to measure the contact angles of control and treated cotton fabrics. A DI water droplet (5 μL) was gently placed onto the specimen using a syringe and reading was taken after 30 s. Average of ten drops at different locations for each of the three specimens prepared at different times were recorded.

5.3.9 Laundering durability

Laundry durability evaluation was carried out using a slightly modified version according to the American Association of Textile Chemists and Colorists (AATCC) Test Method 61–2003. The test was performed using a 500 mL flask containing 150 mL aqueous solution of Tide® laundry detergent (0.15%, w/w) and 50 stainless steel

balls (diameter = 6 mm), the test was performed at 49°C, 40 rpm for 45 min. The size of the fabric specimens used in this test was 5 cm × 5 cm. Each laundry cycle in this study is considered to be equivalent to five home launderings.

5.3.10 Tensile properties

Tensile strength of the fabrics was determined according to ASTM D5035 strip method. Fabric specimens having dimensions of 25 mm × 150 mm were cut and tested on Instron universal testing machine (model 5566, Canton, MA) at a gage length of 75 mm and crosshead speed of 300 mm/min (strain rate of $4min^{-1}$). Six specimens each from different areas of the fabrics in both warp and weft directions were tested to obtain average values.

5.4 Results and discussion

5.4.1 Mechanistic insight into synthesis of anisotropic SiO_2 particles

Stöber process has been widely used since 1968 to create sphere-shaped silica particles.[26] However, apart from the conventional spherical particles, it has been possible to create anisotropic silica particles from an emulsion containing alcohol and water.[27] The biggest advantage of silica particles is the ease of chemical modifications of the particle surfaces due to presence of reactive terminal Si-OH bonds.[28] Anisotropic colloidal silica particles exhibit many advantages such as high surface area, biocompatibility, low toxicity, optical transparency and others.[29] Due to such advantages, anisotropic silica particles have found applications in diverse fields that include catalysis, biomedical, photonic crystals, imaging sensors, coatings, electronics and many others.[30-32] However, the use of anisotropic particles has been limited in the field of textiles. In this study, two distinct anisotropic morphological silica particles

(spheres + cones and needles), were obtained by using different molecular weights of PVP. For this, 8K and 40K PVP were dissolved in equal amount of pentanol, separately. Equal amounts of ethanol and water were added to the two different PVP solutions. PVP has both polar and non-polar binding sites and can act as an emulsion stabilizer by prohibiting the droplets from coalescing.[33, 34] When water is added to the high concentrated PVP solution (in pentanol), the water molecules bind to the PVP and water no longer acts only as a site for hydrolysis of TEOS, but also acts as a structure-directing agent due to bound PVP as shown earlier.[35] The ionic species induced after addition of sodium citrate creates inverse emulsion due to phase separation causing aqueous droplets to be dispersed in the pentanol-rich continuous phase.[36] The silica precursor, TEOS, when added to the emulsion, goes to the water phase and gets hydrolyzed.[27] Ethanol facilitates the hydrolysis of TEOS. Addition of NH_4OH at this stage causes condensation of TEOS and SiO_2 nucleation occurs at the interface of water droplet as shown in the schematic representation in Figure 5.1. While condensation due to addition of NH_4OH causes nucleation, which attaches the head of the particles at the water-pentanol droplet interface, the reactive moieties in PVP cause growth in one direction leading to cone and needle shaped particles.[27] Figure 5.3 shows the SEM images of the particles made using 8K and 40K PVP at different reaction times. It was observed that 8K PVP resulted in cone-shaped SiO_2 particles along with some nanospheres whereas 40K PVP resulted in needle-shaped SiO_2 particles. As stated, 8K PVP resulted in a mixture of nanospheres and cones, as not all the spheres could elongate to form cones. It was observed that the shape and morphology of the cones did not change with the reaction time from 2 h to 18 h.

However, it was observed that the particle yield increased with time and, as a result, the suspension got cloudier. The average diameter of the head of the cone was found to be 240 nm and the average length of the cones after 18 h of reaction time was 2.2 µm. The average diameter of the needle-shaped particles was found to be 189 nm and the average length to be 3.8 µm after 18 h of reaction. It was observed that the diameter of the particles decreased, and the length increased when higher MW PVP was used. The 40K PVP has longer chain lengths and higher molecular entanglements as compared to 8K PVP. This may be a factor why 40K PVP resulted in smaller droplet size in the emulsion as shown the Figure 5.1. As a result, the diameter of the needle-shaped particles was much lower as compared to that of cone shaped particles.

Some earlier studies have shown that the use of gold, silver or magnesium particles or precursors are the essential templates along with PVP for water-in-pentanol emulsions to create non-centrosymmetric or anisotropic SiO_2 particles such as rods, tubes or cones.[28, 34, 35] The present study, however, clearly shows that the formation of anisotropic SiO_2 is independent of presence of such particles and the morphology of the SiO_2 particles is tunable using different MWs of PVP.[28, 34, 35] Overall, it was observed that keeping all other emulsion parameters (reactant ratios and stirring speed) constant and varying the MWs of PVP gave different shapes and sizes of SiO_2 particles. This suggests that factors such as initial droplet size, terminal droplet stability and the subsequent nucleation and growth of the SiO_2 particles are influenced by the molecular chain length and the resultant entanglements of PVP.[37]

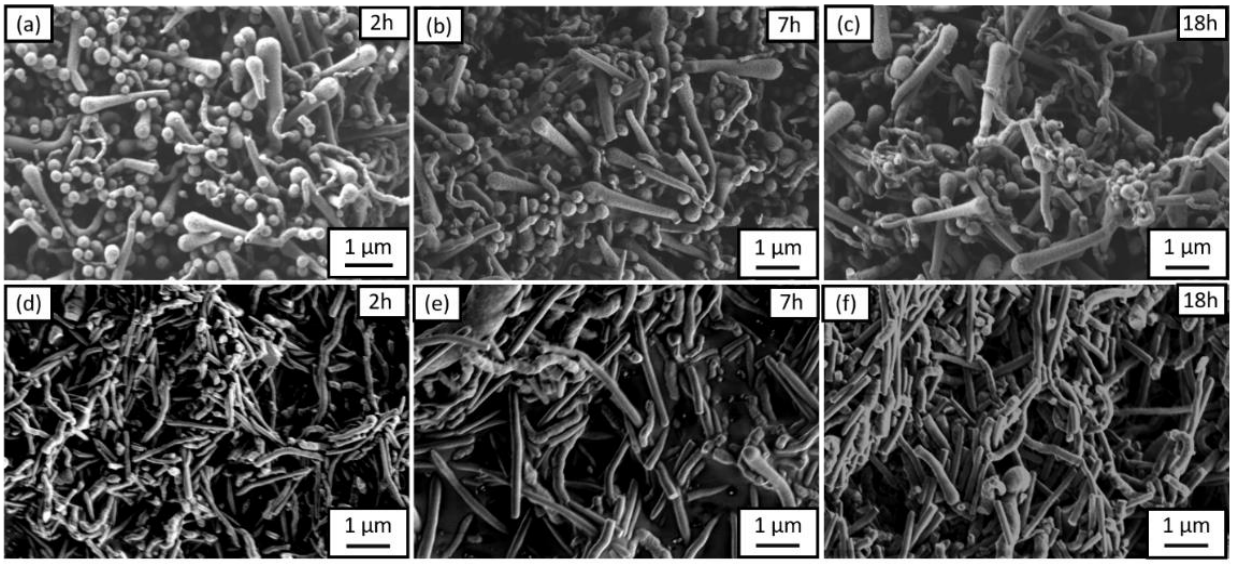

Figure 5.3 SEM images of (a-c) sphere + cone and (d-f) needle-shaped particles at different reaction times (2h, 7h, and 18h).

Figure 5.4 shows TEM images of the cross sections of the sphere + cone and needle-shaped particles at different magnifications. From their cross-sectional views seen in these images it can be concluded that the synthesized particles are solid and not hollow, and no core-shell structure exists.

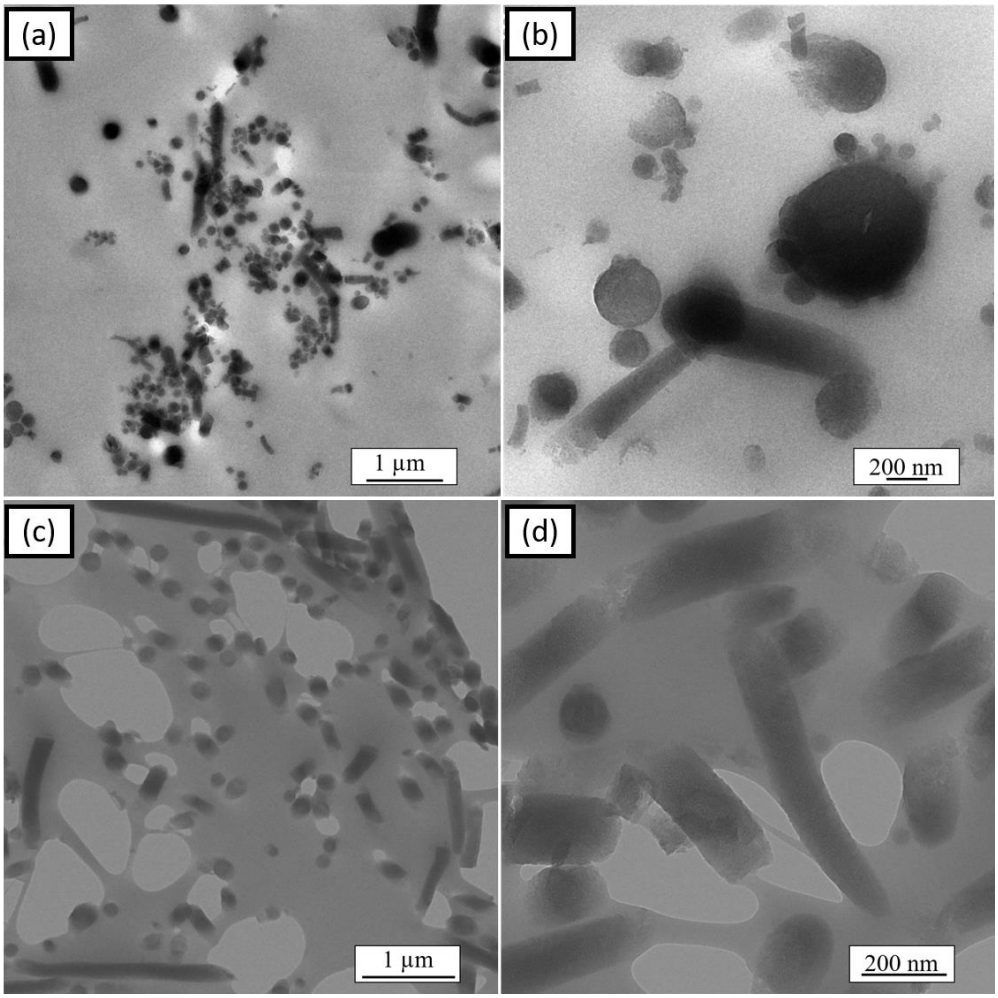

Figure 5.4 Cross-sectional TEM images of (a, b) sphere + cone and (c, d) needle-shaped particles at different magnifications.

5.4.2 Effect of heptanoic anhydride treatment on cotton fabrics

Figure 5.5 shows ATR-FTIR spectra of control and treated cotton fabrics. Figure 5.5(a) shows ATR-FTIR spectra of the cotton fabric and the cotton fabrics treated with HA for 10, 20, and 30 min at 130°C. Control cotton fabrics show a broad peak between 3400 cm^{-1} and 3200 cm^{-1} which is due to the stretching of hydroxyl groups in cellulose as well as the absorbed moisture.[38] The peak at 2902 cm^{-1} is due to the symmetric C-H and C-H_2 stretching vibrations and the peak around 1053 cm^{-1} and

1030 cm^{-1} is due to the C-O-C stretching absorption. These peaks are consistent with all the cellulosic materials.[39] As seen in Figure 5.5(a), a new peak at 1730 cm^{-1} was observed in the HA treated fabrics which was found to grow stronger with the treatment time. This peak corresponds to the ester group formed due to the reaction between the hydroxyl groups on the cellulose and the anhydride groups from HA as shown in the chemical reaction in Figure 5.2.[40, 41] The degree of substitution of the hydroxyl groups from cellulose increases with increase in treatment time as seen from the increasing intensity of the peak at 1730 cm^{-1} in Figure 5.5(a). While the control fabrics can be quickly and completely wetted by water, WCAs of the fabrics treated with HA were found to be 112°, 120° and 127° after 10, 20, and 30 min of treatment time, respectively. The esterification results in the covalent attachment of the flexible seven-carbon planar zigzag aliphatic chains of HA which form a layer on the surface of the fibers in the fabric making it hydrophobic. The surface polarity of the fabrics decreases as the hydroxyl groups from the cellulose are substituted by long aliphatic chains which have low surface energy. This lowers the surface energy of the fabrics without changing the surface topography of the fibers in the fabrics. Dankovich and Hsieh grafted eighteen-carbon aliphatic chains onto cotton fabrics using stearic acid dissolved in ethanol to get a WCA of only 40°.[41] This is because fatty acids have extremely low reactivity towards the hydroxyl groups of the cellulose.[41, 42] On the other hand, anhydride groups are acylating agents known for their high reactivity as compared to carboxylic acids and thus, the use of heptanoic anhydride resulted in a significantly higher WCA of 127° in this research.

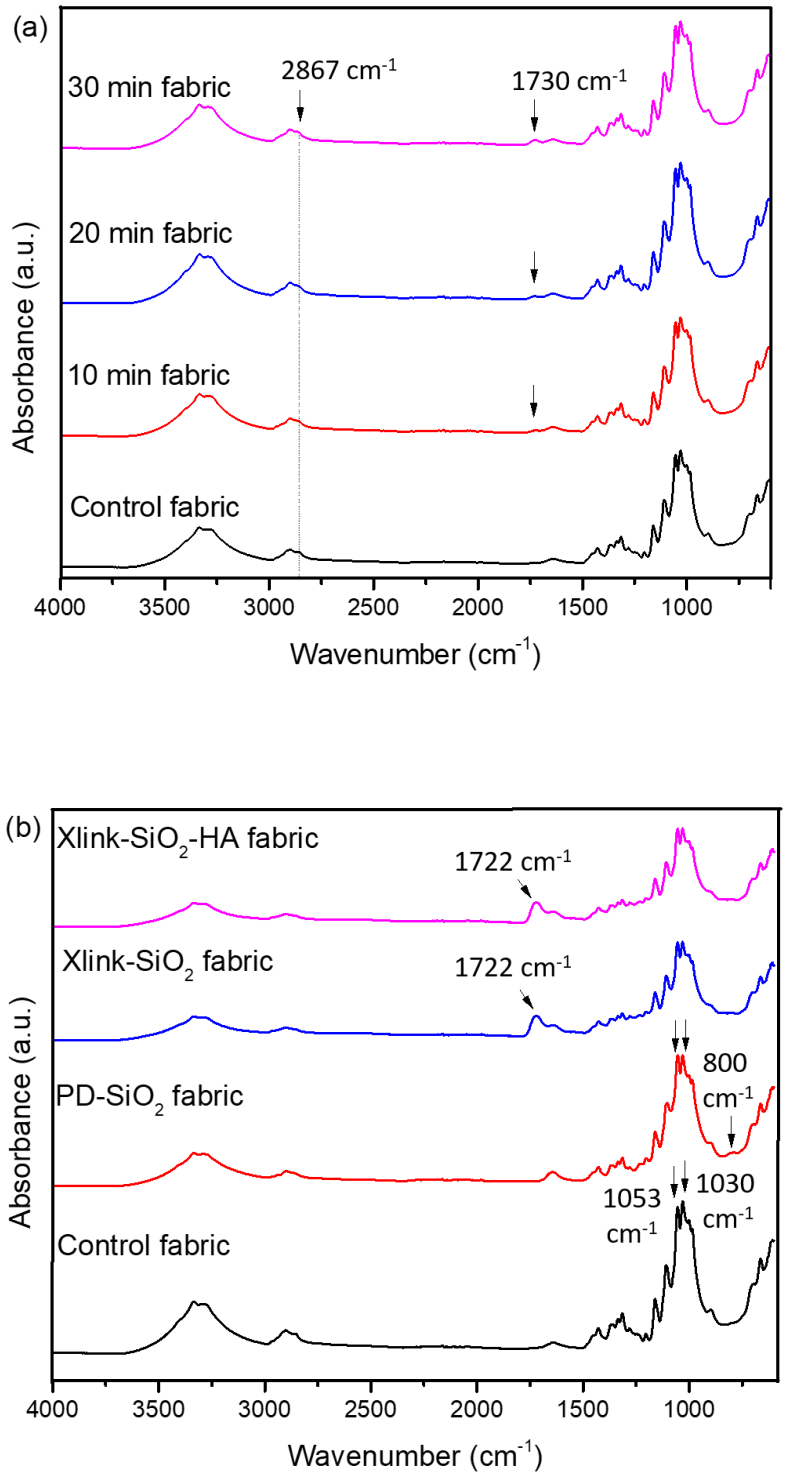

Figure 5.5 ATR-FTIR spectra of cotton fabrics treated with (a) HA for 10, 20 and 30 min (b) Control, PD-SiO2, Xlink-SiO2 and Xlink-SiO2-HA fabrics treated for 30 min.

5.4.3 Effect of SiO_2 particles and HA treatment on cotton fabrics

A combination of surface roughness along with low surface energy is critical to create superhydrophobic surfaces (WCA above 150°).[43] Two different shapes, cones + spheres and needles, of SiO_2 particles were physically deposited and covalently bonded, in separate processes, onto the cotton fabrics to change the surface topography. Figure 5.5(b) shows ATR-FTIR spectra of PD-SiO_2 fabrics and Xlink-SiO_2 fabrics. As seen in Figure 5.5(b), an additional small peak is observed in both physically deposited and covalently bonded SiO_2 cotton fabrics at 800 cm^{-1}. This peak is the characteristic stretching vibration peak for Si-C from the SiO_2 particles.[44, 45] The intensity of the peak at 1053 cm^{-1} is lower than the intensity of the peak at 1030 cm^{-1} for the control cotton fabrics. The peak between 1015 cm^{-1} and 1060 cm^{-1} corresponds to C-O stretch in cellulose. The Si-O-Si asymmetric stretch overlaps with the C-O stretch in cellulose.[38] However, after the SiO_2 treatment, the intensity of peak at 1053 cm^{-1} increases (Figure 5.5(b)). This is due to the presence of Si-O-Si from the SiO_2 particles. An additional peak at 1722 cm^{-1} is observed in the Xlink-SiO_2 fabrics. This peak is the result of the ester bonds formed by the co-condensation of Si-OH from the particles and the -COOH from BTCA as well as the reaction between -OH from cellulose and the -COOH from BTCA. Polycarboxylic acids such as BTCA are often used as heterogenous crosslinkers to improve the bonding between the inorganic-organic interfaces, especially between silica particles and cellulose.[46-49] BTCA has four carboxyl groups which can react with both, the SiO_2 particles as well as the cellulose from the fabric and act as a crosslink (bridge) between the two. This covalent

bonding between SiO_2 particles and fabrics prevent these particles from leaving fabric during use and laundering and, thus, increases the washing durability. Physical deposition of the SiO_2 particles as well as covalent bonding of SiO_2 particles on the fabrics are able to create new surface topography of the fabrics. However, the fabrics still remain hydrophilic. The HA treatment is necessary to lower the surface energy of the fabrics and increase the hydrophobicity to the desired level.

The WCA for Xlink-SiO_2(cones)-HA (8K PVP) fabrics was found to be 157° and Xlink-SiO_2(needles)-HA (40K PVP) fabrics was found to be 153°. Figure 5.6 shows the SEM images of the fibers taken from control and treated fabrics along with the digital photographs of the WCA test. The surface of the control cotton fibers (Figure 5.6(a)) is mostly smooth and flat with some convolutions and natural creases and does not change after the HA treatment (Figure 5.6(b)). The Xlink-SiO_2(cones)-HA and Xlink-SiO_2(needles)-HA fibers (Figures 5.6(c) and 5.6(d)) show that the surface of the fibers is coated with SiO_2 cones and needles, respectively. This changes the surface topography of the fabrics and creates a desired surface roughness. The combination of surface roughness created by the SiO_2 particles along with the low surface energy created by the grafting of HA results in a fabric surface that is superhydrophobic with significantly enhanced WCA, above 150°. Higher WCA was observed for the Xlink-SiO_2(cones)-HA as compared to Xlink-SiO_2(needles)-HA. This is because of the presence of nanospheres that are mixed with the micrometer size cone shaped SiO_2 particles that together create a dual surface roughness on the fabrics, creating a “petal effect” explained by many researchers.[50, 51] The dual size roughness creates numerous air-pockets that can entrap a layer of air between SiO_2 particles and

water droplet further enhancing the WCA.[52-54] The concentration of the SiO_2 particles used to treat the cotton fabrics was varied from 0.05% to 0.5%. Table 5.1 in the supplementary material shows the effect of SiO_2 concentration on WCA of the fabrics. It was observed that the WCA increased from 152° to 157° as the concentration of the sphere + cone shaped particles increased from 0.05% to 0.1%. However, further increasing the concentration of sphere + cone shaped particles to 0.3% or even 0.5% did not increase the WCA of the fabrics. Similar behavior was observed for the fabrics treated with needle shaped particles. Figure 5.7 shows the SEM images of Xlink-0.5% SiO_2(cones)-HA and Xlink-0.5% SiO_2(needles)-HA. Some particle clusters can be observed at 0.5% SiO_2 concentration in fabrics treated with both sphere + cone and needle-shaped particles.

Lin et al. used O_2 plasma to activate cotton fabrics and then deposited irregular shaped ammonium polyphosphate particles via hydrogen bonding and further coated the fabrics with TEOS and polydimethylsiloxane (PDMS) to achieve WCA 162°.[45] Bae et al. physically deposited spherical shaped SiO_2 particles of two different diameters (143 and 378 nm) to create dual size roughness followed by treatment with perfluoroacrylate-based commercial water repellent agent to get WCA 130°.[55] Wen et al. deposited iron stearate, copper stearate and zinc stearate onto paper to get yellow, blue and white colored superhydrophobic paper with WCA of 153°, 154° and 151° respectively.[56] The process developed in this study obtains comparable WCAs using fully sustainable and ‘green’ raw materials.

Table 5.1 Effect of SiO_2 concentration on WCA.

Sphere + cone SiO_2particle concentration	**WCA (°)**	**Needle SiO_2 particle concentration**	**WCA (°)**
0.05 %	152 ± 1.2	**0.05 %**	149 ± 1.1
0.10 %	157 ± 1.2	**0.10%**	153 ± 2.4
0.30 %	154 ± 3.1	**0.30%**	152 ± 3.2
0.50 %	156 ± 2.2	**0.50%**	152 ± 2.6

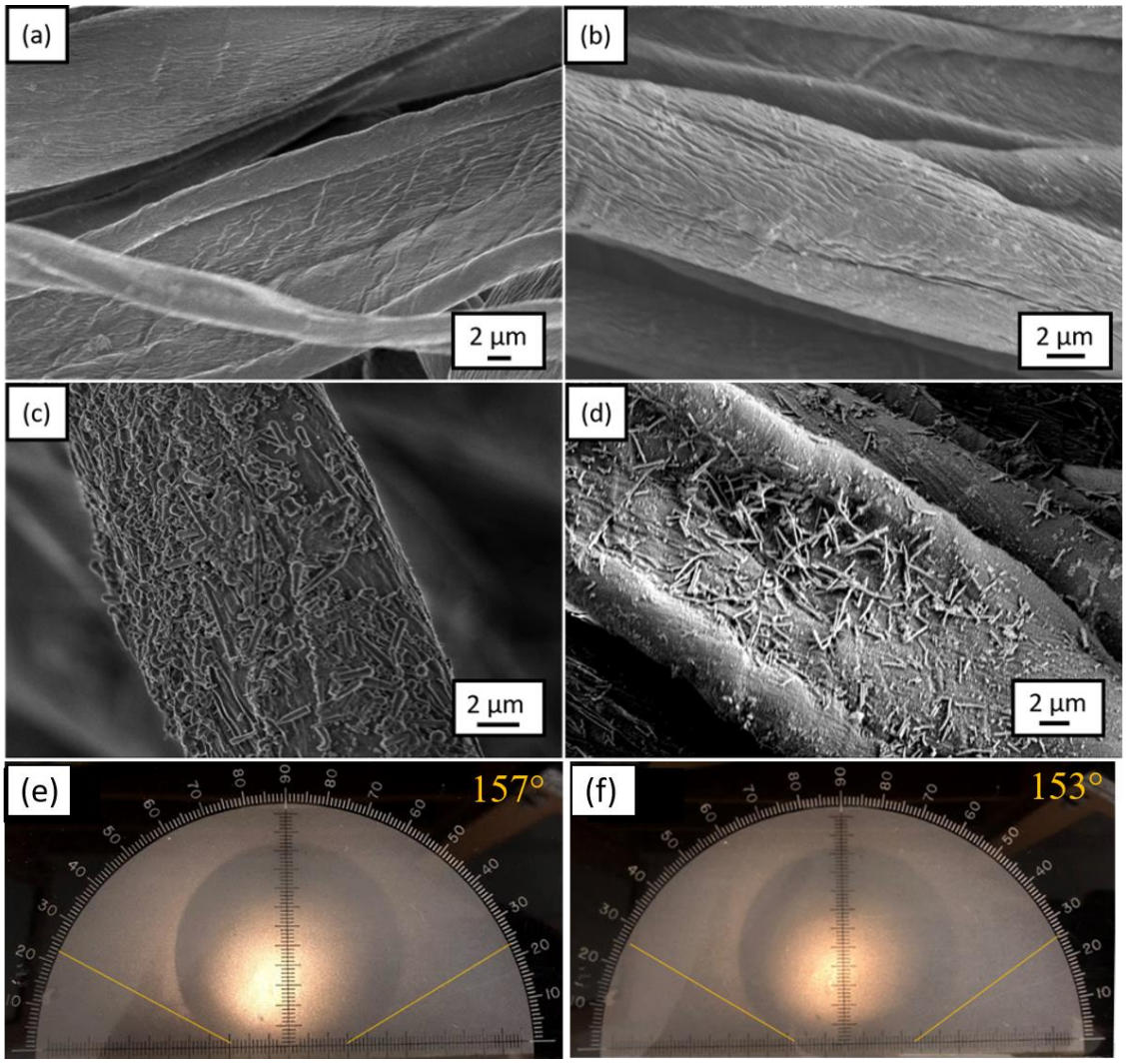

Figure 5.6 SEM images of (a) control (b) HA (c) Xlink-SiO2(cones)-HA (d) Xlink-SiO2(needles)-HA fibers and digital photographs of the WCA for (e) Xlink-SiO2(cones)-HA (f) Xlink-SiO2(needles)-HA fabrics.

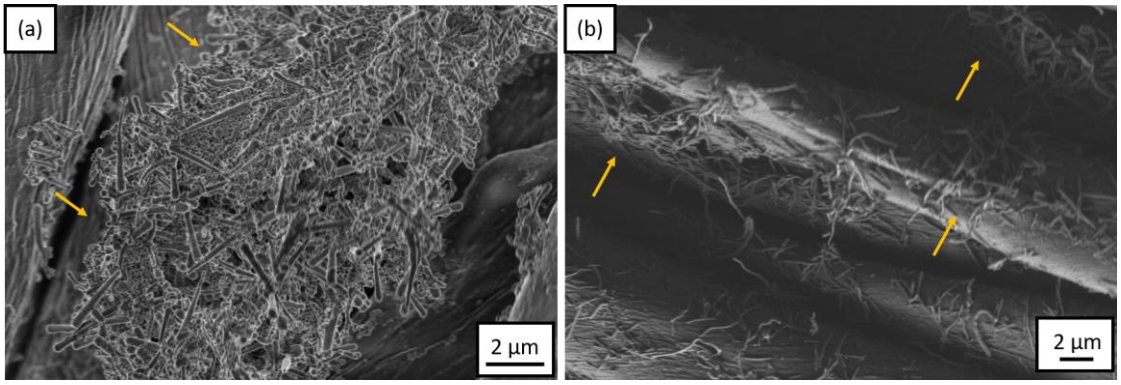

Figure 5.7 SEM image of (a) Xlink- 0.5% SiO2(cones)-HA and (b) Xlink- 0.5% SiO2(needles)-HA.

5.4.4 Laundry durability of the superhydrophobic fabrics

Table 5.2 shows the effect of laundering (up to 7 laboratory laundry cycles) on the durability of the superhydrophobic treatment. The washings were carried out according to the modified AATCC Test Method 61–2003. Each laboratory laundry cycle, as mentioned earlier, corresponds to 5 home laundry washes. As can be seen from data in Table 5.2, WCA decreased slightly with the number of laundry cycles. The decrease in the WCA was higher for the physically deposited particles as compared to the crosslinked particles as could be expected. The WCA decreased from 157° to 148° for the PD-SiO_2(cones)-HA samples after 7 laundry cycles (35 home washings) which was found to be statistically significant using unpaired t-test at a significance level of 0.05. The WCA decreased from 157° to 153° for the Xlink-SiO_2(cones)-HA samples which was statistically insignificant using unpaired t-test at a

significance level of 0.05. Figure 5.8 shows the SEM images of fibers after 7 laundry cycles. As seen in Figure 5.8(a), the surface of the physically deposited fibers is only partially covered with cone-shaped particles as some of the particles are detached from the surface of the fibers during washing. Washing can remove physically deposited (PD) and loosely bonded particles from the surface of the fabrics. Earlier studies have shown that SiO_2 particles can be immobilized in the cotton fabrics by heat treatment .[55] However, crosslinking creates a covalent bond between fabrics and particles and can be expected to increase the durability of the treatment. This can be confirmed from the image in Figure 5.8(b) which shows that majority of the fiber is still covered with the SiO_2 particles after 7 laundry cycles. Similar effect was observed for the fabrics treated with needle-shaped particles as can be seen in Figure 5.8(c) and 5.8(d). Both, Xlink-SiO_2(cones)-HA and Xlink-SiO_2(needles)-HA fabrics maintained their superhydrophobicity, WCAs above 150°, after 7 laundry cycles which correspond to 35 home washings. The slight decrease in the WCA for the crosslinked fabrics could be due to the presence of cellulase enzyme in the detergent which can degrade and remove the top layer of the fibers during washing.

Table 5.2 Effect of laundry cycles on the WCA* of the fabrics.

Specimen	**WCA (°)**	**WCA_1 (°)**	**WCA_3 (°)**	**WCA_5 (°)**	**WCA_7 (°)**
HA	127 ± 2.1	126 ± 2.7	119 ± 1.3	120 ± 3.3	118 ± 3.3
PD-SiO_2(cones)-HA	157 ± 1.4	154 ± 2.2	150 ± 1.3	149 ± 2.1	148 ± 2.7
Xlink-SiO_2(cones)-HA	157 ± 1.2	156 ± 1.1	154 ± 3.2	153 ± 2.1	153 ± 1.3
PD-SiO_2(needles)-HA	152 ± 2.2	150 ± 2.2	147 ± 1.5	146 ± 2.9	147 ± 1.1
Xlink-SiO_2(needles)-HA	153 ± 2.4	154 ± 1.2	152 ± 2.4	150 ± 3.1	150 ± 1.3

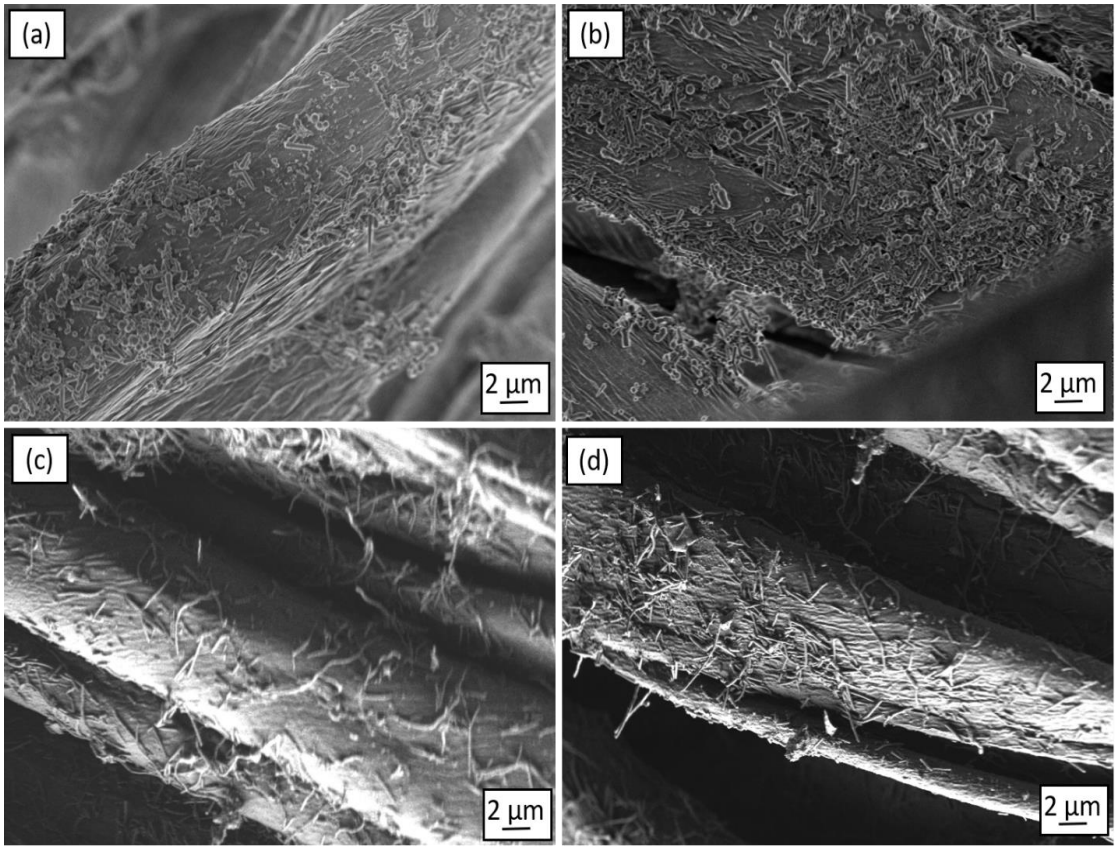

Figure 5.8 SEM images of (a) PD-SiO2(cones)-HA, (b) Xlink-SiO2(cones)-HA, (c) PD-SiO2(needles)-HA, and (d) Xlink-SiO2(needles)-HA fibers after 7 laundry cycles.

5.4.5 Tensile properties of the superhydrophobic fabrics

Figure 5.9 shows the effect of superhydrophobic treatment on the fracture (tensile) stress and strain of the fabrics in both warp and weft directions. As seen in Figure 5.9(a), the tensile stress values for control and the HA treated fabrics in the warp direction are 56.8 MPa and 55.5 MPa, respectively. No change in the tensile stress was observed after grafting HA onto the fabrics as it is simply a surface treatment and has no effect on the fiber morphology. Figure 5.9(b) shows the effect superhydrophobic treatment on the tensile strain of the fabrics in both warp and weft directions. It was observed that the tensile strain of the HA treated fabrics increased slightly from 6% for control to 7.1% for the HA treated fabrics in the warp direction. The increase in the strain in the warp direction could be primarily due the relaxation of the built-up stress while weaving and finishing of the fabrics. It was observed that the tensile stress values of the PD-SiO_2-HA and Xlink-SiO_2-HA fabrics reduced to 50.2 MPa and 29 MPa, respectively. The slight reduction in the tensile stress of the PD-SiO_2-HA fabric could be due to the heat treatment. The reduction in tensile stress in the Xlink-SiO_2-HA fabrics as seen in Figure 5.9(a) is a result of the crosslinking using BTCA which restricts the molecular movement causing a reduction in the stress as well the strain from 6% to 4.8% as seen in Figure 5.9(b). The acidic degradation of the cellulose chains due to BTCA is another reason for the loss in strength of the Xlink-SiO_2-HA fabrics.[57] Similar behavior was observed in the weft direction as can be seen in Figure 5.9.

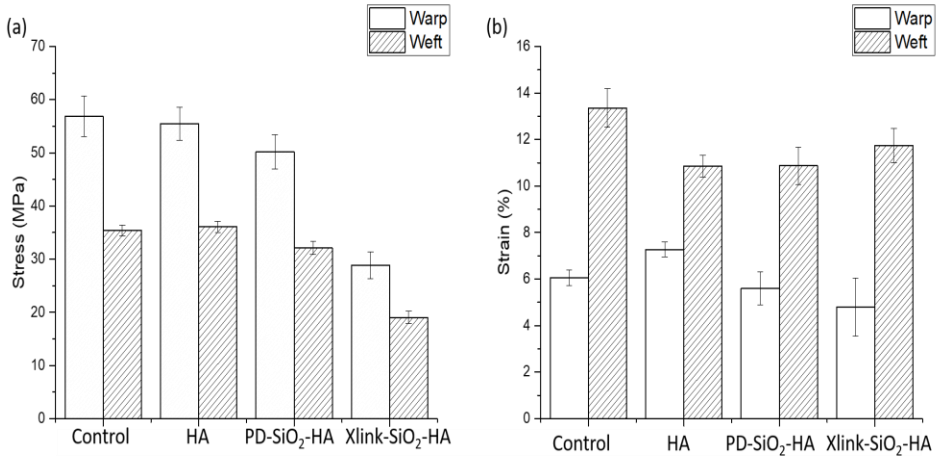

Figure 5.9 Effect of Superhydrophobic treatment on (a) stress and (b) strain of the fabrics.

5.5 Conclusions

This study has shown that anisotropic SiO_2 particles with distinct cone + sphere and needle shapes can be obtained using different molecular weights of PVP. The cone + sphere shaped particles when covalently bonded onto the surface of the cotton fabrics created a permanent dual size roughness on the fabrics, similar to lotus leaf, in concept. Further grafting of fatty acid onto the fabric surface lowered their surface energy. The combination of dual surface roughness and low surface energy resulted in creating durable superhydrophobic fabrics with WCA of 157°.

Anisotropic SiO_2 particles are crucial for creating desired complex surface roughness or textures on the fabrics which enhance their WCA as compared to spherical shaped particles commonly used to create surface roughness.[52, 55, 58, 59] Many researchers have used expensive nanoparticles such as Au, metal oxides such as iron oxide or manganese oxide or chemical etching to form anisotropic silica particles.[28, 35, 60, 61] However, the facile approach for synthesizing anisotropic SiO_2 particles used in

this study is not only ‘green’ but easily scalable to large scale commercial production. In addition, grafting of nontoxic fatty acid to lower the surface energy of the fabrics used in this study, compared to the current use of expensive fluoropolymers which are toxic in nature, creates a fully ‘green’ process to obtain superhydrophobic cotton fabrics.[55] The ‘green’ process developed here can be easily applied to other cellulosic materials such as viscose rayon, paper and others to expand their applications including self-cleaning surfaces, water repellent protective coatings, medical apparel, packaging and many others.

Acknowledgments

The authors would like to acknowledge the use of Cornell Center for Materials Research (CCMR) shared facilities supported through the NSF MRSEC program (DMR-1719875).

5.6 References

1. Yasim-Anuar, T. A. T.; Ariffin, H.; Norrrahim, M. N. F.; Hassan, M. A.; Tsukegi, T.; Nishida, H., Sustainable one-pot process for the production of cellulose nanofiber and polyethylene/cellulose nanofiber composites. *Journal of Cleaner Production* **2019,** *207*, 590-599.

2. Onur, A.; Ng, A.; Garnier, G.; Batchelor, W., The use of cellulose nanofibres to reduce the wet strength polymer quantity for development of cleaner filters. *Journal of Cleaner Production* **2019,** *215*, 226-231.

3. Li, Y.; Yu, Q.; Yin, X.; Xu, J.; Cai, Y.; Han, L.; Huang, H.; Zhou, Y.; Tan, Y.; Wang, L., Fabrication of superhydrophobic and superoleophilic polybenzoxazine-based cotton fabric for oil–water separation. *Cellulose* **2018,** *25* (11), 6691-6704.

4. Mulyadi, A.; Zhang, Z.; Deng, Y., Fluorine-free oil absorbents made from cellulose nanofibril aerogels. *ACS applied materials & interfaces* **2016,** *8* (4), 2732-2740.

5. Korhonen, J. T.; Kettunen, M.; Ras, R. H.; Ikkala, O., Hydrophobic nanocellulose aerogels as floating, sustainable, reusable, and recyclable oil absorbents. *ACS applied materials & interfaces* **2011,** *3* (6), 1813-1816.

6. Sehaqui, H.; Zimmermann, T.; Tingaut, P., Hydrophobic cellulose nanopaper through a mild esterification procedure. *Cellulose* **2014,** *21* (1), 367-382.

7. Rodionova, G.; Lenes, M.; Eriksen, Ø.; Gregersen, Ø., Surface chemical modification of microfibrillated cellulose: improvement of barrier properties for packaging applications. *Cellulose* **2011,** *18* (1), 127-134.

8. Song, Z.; Xiao, H.; Zhao, Y., Hydrophobic-modified nano-cellulose fiber/PLA biodegradable composites for lowering water vapor transmission rate (WVTR) of paper. *Carbohydrate polymers* **2014,** *111*, 442-448.

9. Li, F.; Biagioni, P.; Bollani, M.; Maccagnan, A.; Piergiovanni, L., Multi-functional coating of cellulose nanocrystals for flexible packaging applications. *Cellulose* **2013,** *20* (5), 2491-2504.

10. Shimizu, M.; Saito, T.; Fukuzumi, H.; Isogai, A., Hydrophobic, ductile, and transparent nanocellulose films with quaternary alkylammonium carboxylates on nanofibril surfaces. *Biomacromolecules* **2014,** *15* (11), 4320-4325.

11. Jonoobi, M.; Harun, J.; Mathew, A. P.; Hussein, M. Z. B.; Oksman, K., Preparation of cellulose nanofibers with hydrophobic surface characteristics. *Cellulose* **2010,** *17* (2), 299-307.

12. Sai, H.; Fu, R.; Xing, L.; Xiang, J.; Li, Z.; Li, F.; Zhang, T., Surface modification of bacterial cellulose aerogels' web-like skeleton for oil/water separation. *ACS applied materials & interfaces* **2015,** *7* (13), 7373-7381.

13. Afzal, S.; Daoud, W. A.; Langford, S. J., Superhydrophobic and photocatalytic self-cleaning cotton. *Journal of Materials Chemistry A* **2014,** *2* (42), 18005-18011.

14. Chen, T.; Hong, J.; Peng, C.; Chen, G.; Yuan, C.; Xu, Y.; Zeng, B.; Dai, L., Superhydrophobic and flame retardant cotton modified with DOPO and fluorine-silicon-containing crosslinked polymer. *Carbohydrate polymers* **2019,** *208*, 14-21.

15. Maity, J.; Kothary, P.; O'Rear, E. A.; Jacob, C., Preparation and comparison of hydrophobic cotton fabric obtained by direct fluorination and admicellar polymerization of fluoromonomers. *Industrial & Engineering Chemistry Research* **2010,** *49* (13), 6075-6079.

16. Zhao, Y.; Xu, Z.; Wang, X.; Lin, T., Photoreactive azido-containing silica nanoparticle/polycation multilayers: durable superhydrophobic coating on cotton fabrics. *Langmuir* **2012,** *28* (15), 6328-6335.

17. Zimmermann, J.; Reifler, F. A.; Fortunato, G.; Gerhardt, L. C.; Seeger, S., A simple, one-step approach to durable and robust superhydrophobic textiles. *Advanced Functional Materials* **2008,** *18* (22), 3662-3669.

18. Yang, M.; Liu, W.; Jiang, C.; Liu, C.; He, S.; Xie, Y.; Wang, Z., Facile preparation of robust superhydrophobic cotton textile for self-cleaning and oil-water separation. *Industrial & Engineering Chemistry Research* **2018**.

19. Molina, R.; Teixidó, J. M.; Kan, C.-W.; Jovančić, P., Hydrophobic coatings on cotton obtained by in situ plasma polymerization of a fluorinated monomer in ethanol solutions. *ACS applied materials & interfaces* **2017,** *9* (6), 5513-5521.

20. Deng, B.; Cai, R.; Yu, Y.; Jiang, H.; Wang, C.; Li, J.; Li, L.; Yu, M.; Li, J.; Xie, L., Laundering durability of superhydrophobic cotton fabric. *Advanced Materials* **2010,** *22* (48), 5473-5477.

21. Wang, L.; Zhang, X.; Li, B.; Sun, P.; Yang, J.; Xu, H.; Liu, Y., Superhydrophobic and ultraviolet-blocking cotton textiles. *ACS applied materials & interfaces* **2011,** *3* (4), 1277-1281.

22. Duan, W.; Xie, A.; Shen, Y.; Wang, X.; Wang, F.; Zhang, Y.; Li, J., Fabrication of superhydrophobic cotton fabrics with UV protection based on CeO2 particles. *Industrial & Engineering Chemistry Research* **2011,** *50* (8), 4441-4445.

23. Khalil-Abad, M. S.; Yazdanshenas, M. E., Superhydrophobic antibacterial cotton textiles. *Journal of colloid and interface science* **2010,** *351* (1), 293-298.

24. Jiang, C.; Liu, W.; Yang, M.; Liu, C.; He, S.; Xie, Y.; Wang, Z., Facile fabrication of robust fluorine-free self-cleaning cotton textiles with superhydrophobicity, photocatalytic activity, and UV durability. *Colloids and Surfaces A: Physicochemical and Engineering Aspects* **2018,** *559*, 235-242.

25. Yang, M.; Liu, W.; Jiang, C.; He, S.; Xie, Y.; Wang, Z., Fabrication of superhydrophobic cotton fabric with fluorinated TiO 2 sol by a green and one-step sol-gel process. *Carbohydrate Polymers* **2018**.

26. Wang, X.-D.; Shen, Z.-X.; Sang, T.; Cheng, X.-B.; Li, M.-F.; Chen, L.-Y.; Wang, Z.-S., Preparation of spherical silica particles by Stöber process with high concentration of tetra-ethyl-orthosilicate. *Journal of colloid and interface science* **2010,** *341* (1), 23-29.

27. Brijitta, J.; Ramachandran, D.; Rabel, A.; Raj, N. N.; Viswanathan, K.; Prasath, S. S., Evolution of shape isotropy in silica microparticles induced by the base. *Colloid and Polymer Science* **2017,** *295* (9), 1485-1490.

28. Longbottom, B. W.; Rochford, L. A.; Beanland, R.; Bon, S. A., Mechanistic insight into the synthesis of silica-based "matchstick" colloids. *Langmuir* **2015,** *31* (33), 9017-9025.

29. Chen, K.; Yu, G.; He, F.; Zhou, Q.; Xiao, D.; Li, J.; Feng, Y., A pH-responsive emulsion stabilized by alginate-grafted anisotropic silica and its application in the controlled release of λ-cyhalothrin. *Carbohydrate polymers* **2017,** *176*, 203-213.

30. Yi, D.; Zhang, Q.; Liu, Y.; Song, J.; Tang, Y.; Caruso, F.; Wang, Y., Synthesis of chemically asymmetric silica nanobottles and their application for cargo loading and as nanoreactors and nanomotors. *Angewandte Chemie International Edition* **2016,** *55* (47), 14733-14737.

31. Li, X.; Zhou, L.; Wei, Y.; El-Toni, A. M.; Zhang, F.; Zhao, D., Anisotropic growth-induced synthesis of dual-compartment Janus mesoporous silica nanoparticles for bimodal triggered drugs delivery. *Journal of the American Chemical Society* **2014,** *136* (42), 15086-15092.

32. Guerrero-Martínez, A.; Pérez-Juste, J.; Liz-Marzán, L. M., Recent progress on silica coating of nanoparticles and related nanomaterials. *Advanced materials* **2010,** *22* (11), 1182-1195.

33. Maruthamuthu, M.; Sobhana, M., Hydrophobic interactions in the binding of polyvinylpyrrolidone. *Journal of Polymer Science: Polymer Chemistry Edition* **1979,** *17* (10), 3159-3167.

34. Kyrychenko, A.; Korsun, O. M.; Gubin, I. I.; Kovalenko, S. M.; Kalugin, O. N., Atomistic simulations of coating of silver nanoparticles with poly (vinylpyrrolidone) oligomers: Effect of oligomer chain length. *The Journal of Physical Chemistry C* **2015,** *119* (14), 7888-7899.

35. Zhang, J.; Liu, H.; Wang, Z.; Ming, N., Au-Induced Polyvinylpyrrolidone Aggregates with Bound Water for the Highly Shape-Selective Synthesis of Silica Nanostructures. *Chemistry–A European Journal* **2008,** *14* (14), 4374-4380.

36. Wang, J.; Lu, Y., Facile synthesis of asymmetrical flower-like silica. *Materials & Design* **2016,** *111*, 206-212.

37. Murphy, R. P.; Hong, K.; Wagner, N. J., Synthetic control of the size, shape, and polydispersity of anisotropic silica colloids. *Journal of colloid and interface science* **2017,** *501*, 45-53.

38. Zhao, Y.; Tang, Y.; Wang, X.; Lin, T., Superhydrophobic cotton fabric fabricated by electrostatic assembly of silica nanoparticles and its remarkable buoyancy. *Applied Surface Science* **2010,** *256* (22), 6736-6742.

39. Xue, C.-H.; Jia, S.-T.; Zhang, J.; Tian, L.-Q.; Chen, H.-Z.; Wang, M., Preparation of superhydrophobic surfaces on cotton textiles. *Science and technology of advanced materials* **2008,** *9* (3), 035008.

40. Zhong, Y.; Netravali, A. N., 'Green'surface treatment for water-repellent cotton fabrics. *Surface Innovations* **2016,** *4* (1), 3-13.

41. Dankovich, T. A.; Hsieh, Y.-L., Surface modification of cellulose with plant triglycerides for hydrophobicity. *Cellulose* **2007,** *14* (5), 469-480.

42. Samyn, P.; Schoukens, G.; Stanssens, D.; Vonck, L.; Van den Abbeele, H., Hydrophobic waterborne coating for cellulose containing hybrid organic nanoparticle pigments with vegetable oils. *Cellulose* **2013,** *20* (5), 2625-2646.

43. Zhang, X.; Shi, F.; Niu, J.; Jiang, Y.; Wang, Z., Superhydrophobic surfaces: from structural control to functional application. *Journal of Materials Chemistry* **2008,** *18* (6), 621-633.

44. Singh, A. K.; Singh, J. K., Fabrication of durable superhydrophobic coatings on cotton fabrics with photocatalytic activity by fluorine-free chemical modification for dual-functional water purification. *New Journal of Chemistry* **2017,** *41* (11), 4618-4628.

45. Lin, D.; Zeng, X.; Li, H.; Lai, X.; Wu, T., One-pot fabrication of superhydrophobic and flame-retardant coatings on cotton fabrics via sol-gel reaction. *Journal of colloid and interface science* **2019,** *533*, 198-206.

46. Huang, W.; Song, Y.; Xing, Y.; Dai, J., Durable hydrophobic cellulose fabric prepared with polycarboxylic acid catalyzed silica sol. *Industrial & Engineering Chemistry Research* **2010,** *49* (19), 9135-9142.

47. Menaa, B.; Mizuno, M.; Takahashi, M.; Tokuda, Y.; Yoko, T., Polycarboxylic acids as network modifiers for water durability improvement of inorganic–organic hybrid tin-silico-phosphate low-melting glasses. *Journal of Solid State Chemistry* **2006,** *179* (2), 492-499.

48. Gashti, M. P.; Alimohammadi, F.; Shamei, A., Preparation of water-repellent cellulose fibers using a polycarboxylic acid/hydrophobic silica nanocomposite coating. *Surface and Coatings Technology* **2012,** *206* (14), 3208-3215.

49. Huang, W.; Xing, Y.; Yu, Y.; Shang, S.; Dai, J., Enhanced washing durability of hydrophobic coating on cellulose fabric using polycarboxylic acids. *Applied Surface Science* **2011,** *257* (9), 4443-4448.

50. Feng, L.; Zhang, Y.; Xi, J.; Zhu, Y.; Wang, N.; Xia, F.; Jiang, L., Petal effect: a superhydrophobic state with high adhesive force. *Langmuir* **2008,** *24* (8), 4114-4119.

51. Ebert, D.; Bhushan, B., Wear-resistant rose petal-effect surfaces with superhydrophobicity and high droplet adhesion using hydrophobic and hydrophilic nanoparticles. *Journal of colloid and interface science* **2012,** *384* (1), 182-188.

52. Hoefnagels, H.; Wu, D.; De With, G.; Ming, W., Biomimetic superhydrophobic and highly oleophobic cotton textiles. *Langmuir* **2007,** *23* (26), 13158-13163.

53. Athauda, T. J.; Ozer, R. R., Investigation of the effect of dual-size coatings on the hydrophobicity of cotton surface. *Cellulose* **2012,** *19* (3), 1031-1040.

54. Patil, N. V.; Netravali, A. N., Direct Assembly of Silica Nanospheres on Halloysite Nanotubes for "Green" Ultrahydrophobic Cotton Fabrics. *Advanced Sustainable Systems* **2019**, 1900009.

55. Bae, G. Y.; Min, B. G.; Jeong, Y. G.; Lee, S. C.; Jang, J. H.; Koo, G. H., Superhydrophobicity of cotton fabrics treated with silica nanoparticles and water-repellent agent. *Journal of colloid and interface science* **2009,** *337* (1), 170-175.

56. Wen, Q.; Guo, F.; Yang, F.; Guo, Z., Green fabrication of coloured superhydrophobic paper from native cotton cellulose. *Journal of colloid and interface science* **2017,** *497*, 284-289.

57. Ji, B.; Zhao, C.; Yan, K.; Sun, G., Effects of acid diffusibility and affinity to cellulose on strength loss of polycarboxylic acid crosslinked fabrics. *Carbohydrate polymers* **2016,** *144*, 282-288.

58. Yu, M.; Gu, G.; Meng, W.-D.; Qing, F.-L., Superhydrophobic cotton fabric coating based on a complex layer of silica nanoparticles and perfluorooctylated quaternary ammonium silane coupling agent. *Applied surface science* **2007,** *253* (7), 3669-3673.

59. Xue, C.-H.; Jia, S.-T.; Zhang, J.; Tian, L.-Q., Superhydrophobic surfaces on cotton textiles by complex coating of silica nanoparticles and hydrophobization. *Thin Solid Films* **2009,** *517* (16), 4593-4598.

60. Panwar, K.; Jassal, M.; Agrawal, A. K., In situ synthesis of Ag–SiO2 Janus particles with epoxy functionality for textile applications. *Particuology* **2015,** *19*, 107-112.

61. Hagemans, F.; van der Wee, E. B.; van Blaaderen, A.; Imhof, A., Synthesis of cone-shaped colloids from rod-like silica colloids with a gradient in the etching rate. *Langmuir* **2016,** *32* (16), 3970-3976.

Chapter 6 Enhancing strength of wool fiber using soy flour sugar-based 'green' crosslinker

Namrata V. Patil and Anil N. Netravali

Department of Fiber Science & Apparel Design,

Cornell University, 37 Forest Home Dr., Ithaca, NY 14853, USA

Graphical abstract

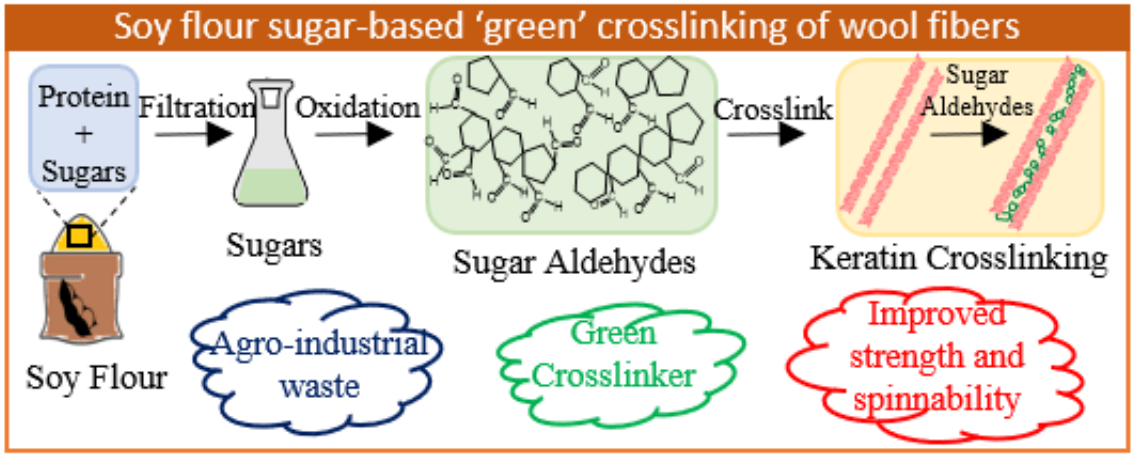

Published as:

Patil, N. V.; Netravali, A. N., Enhancing Strength of Wool Fiber Using a Soy Flour Sugar-Based "Green" Cross-linker. ACS Omega **2019,** *4* (3), 5392-5401.

6.1 Abstract

This study presents the preparation and use of a 'green' crosslinker derived from waste soy flour sugar mixture (SFS) to crosslink keratin in wool fibers to increase its tensile properties. Earlier studies of keratin crosslinking involved chemicals such as glyoxal and glutaraldehyde that are toxic to humans. In addition, their effectiveness in improving tensile properties has been significantly lower than obtained in this study using modified SFS. Characterization of SFS using ^{13}C NMR revealed the presence of 5 sugars having different molecular lengths. Oxidation of SFS using sodium periodate resulted in multiple aldehyde groups as confirmed by ^{1}H NMR and ATR-FTIR. The oxidized SFS (OSFS) when used to crosslink the amine groups from the wool keratin resulted in 36% and 56% increase in the tensile strength and Young's modulus of the fibers, respectively. These significant increases in strength and Young's modulus were a result of having multiple aldehyde groups on each sugar molecule as well as different molecular lengths of sugars which favored crosslinks of multiple lengths within the cortical cell matrix of wool fibers. The crosslinking between the aldehyde groups in OSFS and amine groups in wool fibers was confirmed using ATR-FTIR and from the color change resulting from the Maillard reaction as well as decrease in moisture absorption by the fibers. Stronger wool fibers can not only increase the efficiencies of wool fiber spinning and weaving and reduce yarn and fabric defects but can also allow spinning finer yarns from the same fibers. Oxidized sugars with optimum molecular lengths can be used to crosslink other biological proteins as well, replacing the currently used toxic crosslinkers.

6.2 Introduction

Wool is the most important animal fiber used in textiles and many other applications. It is a fully renewable but expensive fiber that is known for its comfort, warmth retention, moisture absorption and elasticity.[1-2] While wool is most commonly obtained from sheep, hair from other animals such as goats, llamas and alpacas are also used. The fleece (raw wool) obtained from the animals contains 30-70% impurities such as sand, dirt, grease, dried sweat, etc., most of which are removed through the scouring process.[3] The cleaned dry wool is commonly processed through a carding machine and comber to produce a continuous web or sliver (wool top) with individual fibers parallel to each other.[4] The length of fibers in the sliver can vary from 2 to 6 inches depending on the wool variety and the processes used. Sliver is drawn to the desired linear density and twisted during spinning to form continuous yarn.[4] Since wool fibers are inherently weak, fiber breakage during spinning and weaving processes, which are commonly carried out under tension, is a significant problem. Fiber breakages reduce the production efficiency, create fabric defects and generate significant amounts of fiber and fabric wastes.[4] Increasing the strength of the fibers can not only solve these issues but also allow spinning finer yarns from the same fibers, significantly increasing its value.

There have been many improvements in the genetic modifications of wool by selective breeding of sheep as well as by providing better nutrition to increase the length, fineness, yield, and strength of the fiber.[3] Plasma treatment of wool fibers has also been shown to reduce fiber breakage during the spinning process.[5] Genetic modifications and plasma treatments, however, can be expensive. Chemical

crosslinking can be much less expensive and an easier way to enhance the tensile properties of the fiber. The chemical composition of wool has shown the presence of many polar and non-polar amino acids. Amino acids with polar groups, e.g., in soy proteins, have shown excellent possibilities for chemical modifications through crosslinking.[6] While the exact content of polar amino acids varies based on the source, high contents of amino acids such as arginine (19.1%), serine (8.7%), glutamic acid (8.5%) and cystine (7.3%) have been found in merino wool.[7] Amino acids with acidic side chains such as glutamic acid, aspartic acid, asparagine, glutamine account for about 10% of the total amino acids. Amino acids with basic side chains such as lysine, histidine, tryptophan account for 3.5%. Threonine and tyrosine are amino acids with hydroxyl groups in the side chain and account for 9% of the total amino acids.[7] Glycine, leucine, proline, valine, alanine, isoleucine and phenylalanine, amino acids without reactive groups on their side chains, account for about 30% of amino acids.[7] In most crosslinking cases involving proteins, bifunctional crosslinkers such as glyoxal, glutaraldehyde, diisocyanates and carbodiimides have been used.[8-10] Some formaldehyde-based crosslinkers have also been reported.[11] These crosslinkers are skin irritant and toxic, not only to cells and biological systems but also to the environment.[9, 12] As a result, they pose a great danger to the health of the users. Formaldehyde has been classified as a carcinogen and is being banned in many places.

Soybean, a legume species, is an important agricultural and industrial crop. It is one of the major oilseeds produced in the US and worldwide. Soybean makes up over half of all the oilseeds in the world market. There has been an increase in the use of soybean oil to produce biodiesel in the last few years.[13] Apart from oil, soybeans

are also a major source of edible plant-based protein. Defatted soy flour (SF) is obtained as a by-product after extracting oil from soybeans. It consists of 50-54% protein, 30-32% carbohydrate, 2-3% dietary fibers and other minor components such as minerals, ash and moisture.[14] SF is purified to obtain soy protein concentrate (SPC) and further purified to get soy protein isolate (SPI). The purification process involves removing the 30-32% carbohydrates present in SF. The carbohydrate mixture, a by-product of SPC and SPI production is generally discarded as waste.[15] It consists of five different sugars: monosaccharides (fructose and glucose), disaccharide (sucrose), trisaccharide (raffinose) and tetrasaccharide (stachyose).[14] Raffinose and stachyose are not digestible by humans or animals. These sugars, as a mixture, can be modified and utilized for non-edible purposes.[15]

The main goal of this research was to crosslink protein (keratin) in wool fiber using a natural 'green' crosslinker formulated using soy flour sugars (SFS) and enhance the tensile properties. SFS, extracted from SF, was characterized, chemically modified and used as an inexpensive and non-toxic crosslinker for keratin, the protein in wool. The sugars in SFS were oxidized (OSFS) using sodium periodate ($NaIO_4$) to obtain aldehyde groups on them, as shown in Figure 6.1. Oxidation of the sugar mixture in SFS produces multiple lengths of oxidized sugars containing aldehyde groups. While the high number of functional (aldehyde) groups obtained can provide chemical reaction with the majority of the amine groups in keratin, the presence of different sugars, i.e., different molecular lengths, improves the possibility of reaching all reactive sites in keratin. These reactions lead to formation of both inter-molecular as well as intra-molecular linkages in the proteins forming a crosslinked system. The

effect of chemical crosslinking on the performance properties of the wool fibers such as tensile properties were studied.

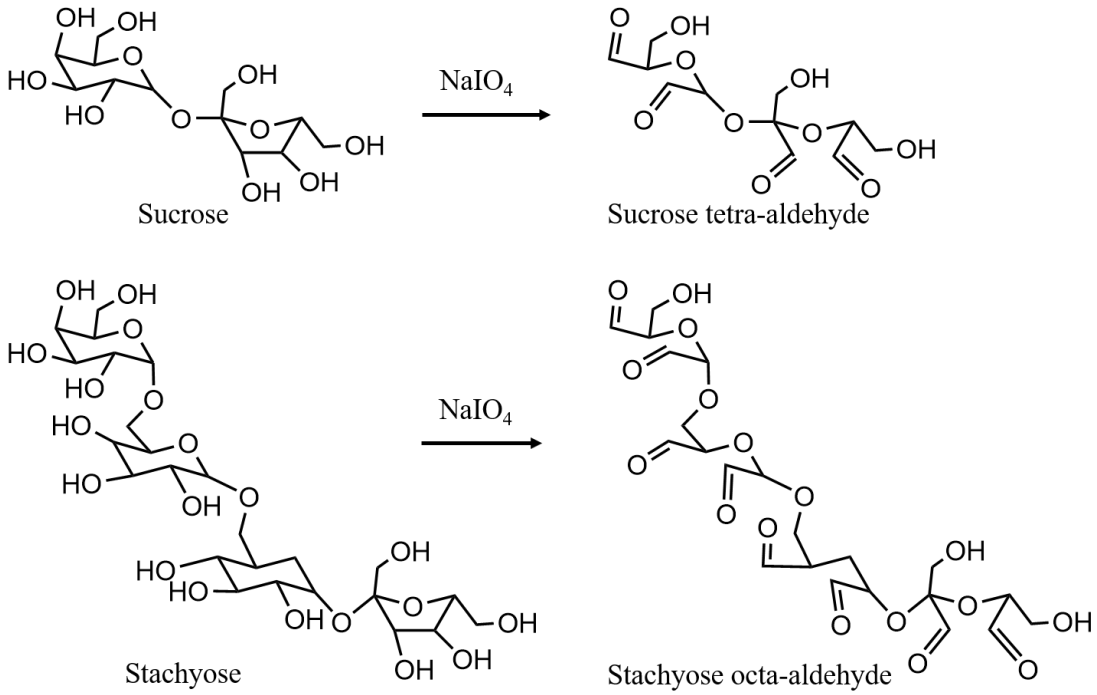

Figure 6.1 Proposed reactions for oxidation of sucrose and stachyose.

6.3 Materials and methods

6.3.1 Materials

Wool fibers in sliver form and defatted soy flour (SF) were provided by Raymond Woolen Mills, India and Archer Daniels Midland Co., Decatur, IL, respectively. Sodium periodate ≥ 99% and stachyose were purchased from Acros Organics, Bound Brook, NJ. Barium dichloride ($BaCl_2$) was purchased from VWR, Rochester, NY. Glucose, fructose, sucrose and raffinose were purchased from Sigma-Aldrich. Analytical grade sodium hydroxide (NaOH) pellets and hydrochloric acid

37% reagent grade (HCl) were also purchased from Sigma-Aldrich Chemical Co., Allentown, PA.

6.3.2 Extraction of sugars from SF

SF (65g) was added slowly to 400 ml of DI water and stirred at 300 rpm at room temperature (RT) until a homogeneous SF mixture was obtained. The pH of the mixture was adjusted to 4.5 using HCl. At 4.5 pH, most of the amino acids present in the proteins from SF are at their isoelectric point and remain insoluble in water. The mixture was stirred overnight at 300 rpm at RT to dissolve all the sugars present in SF into water. The sugars were then filtered using a microfiber polyester fabric to remove the insolubilized protein from SF. The pH of the filtered solution containing the sugars was then adjusted to 5.5 using NaOH, stirred for 6 h at RT and filtered again to remove the small amount of remaining protein having amino acids with isoelectric points close to 5.5. The filtered solution containing soy flour sugars is termed SFS. 250 ml of SFS was obtained after filtering twice. Assuming that we extract 30% residual sugars from the SF, the final concentration of sugars after filtration in SFS was close to 5%.

6.3.3 Oxidation of SFS.

Oxidation of SFS was carried out using $NaIO_4$. Different molar ratios (MR), 0.5 to 2.5 MR, of $NaIO_4$ to sugars were used to optimize the oxidizing reaction. The oxidation reaction was carried out in the dark for 22 h at RT with gentle stirring at 200 rpm. At the end of the reaction, the required amount of $BaCl_2$ was added to the solution to stop sugars from further oxidation (Figure 6.3). The solution was stirred for 5 min after addition of $BaCl_2$ and then placed at 4°C for 1 h to allow complete

precipitation of barium iodate $Ba(IO_3)_2$. It was then filtered to obtain the supernatant solution containing the mixture of oxidized SFS (OSFS). The pH of the prepared OSFS was found to be 3.

6.3.4 Optimization of $NaIO_4$:SFS molar ratio

Addition of oxidized soy flour sugars (OSFS) to soy flour (SF) shows an instantaneous color change due to Maillard reaction. Figure 6.2 shows the effect of addition of OSFS with different molar ratios of $NaIO_4$:SFS from 0.5 to 2.5 on the color of SF. As seen in Figure 6.2, the color of the SF changes from off-white to yellow-brown with the increase in the oxidation of soy flour sugars (SFS) from 0.5 to 2 after which it remains constant. $NaIO_4$:SF MR 2.5 showed maximum color change and thus was used to crosslink wool fibers. For the molar calculations, the molecular weight of SFS was assumed to be 342, which is the molecular weight of sucrose.

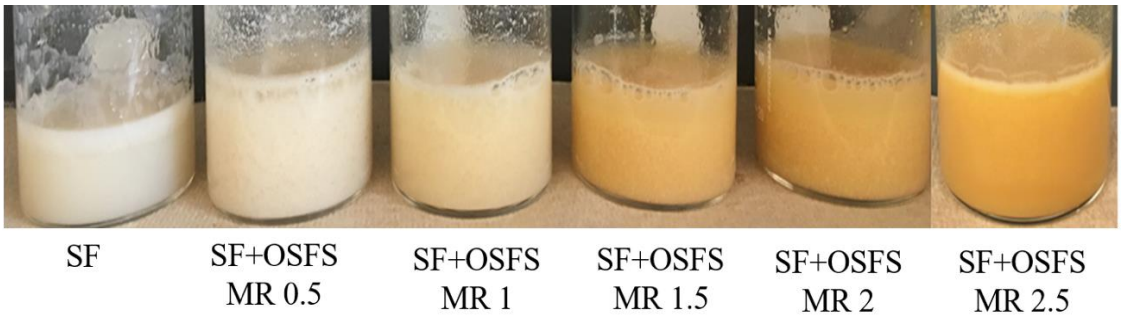

Figure 6.2 Effect of addition of OSFS with different molar ratios of NaIO4:SFS from 0.5 to 2.5 on the color of SF.

6.3.5 Optimization of $BaCl_2$:$NaIO_4$ molar ratio

At the end of the oxidation of SFS, optimum amount of $BaCl_2$ was added to curb the oxidation reaction. When $BaCl_2$ is added to $NaIO_3$, they react to form barium iodate $Ba(IO_3)_2$ which is insoluble in water at lower temperatures. The reaction

mixture was refrigerated to precipitate $Ba(IO_3)_2$. Different molar ratios of $BaCl_2$:$NaIO_4$ (0, 0.5, 1 and 1.5) were added to the reaction mixture and placed in the refrigerator for 1 h. As seen in Figure 6.3, the parafilm on the beaker without $BaCl_2$ turns purple possibly due to the presence of free iodine fumes. With increase in the amount of $BaCl_2$ and the time in refrigerator, the purple color on the parafilm reduced. At MR 1.5, no purple color (no free iodine fumes) was observed and OSFS turned clear, indicating formation of $Ba(IO_3)_2$. The OSFS was then filtered to obtain OSFS. Thus, $BaCl_2$:$NaIO_4$ MR 1.5 was used to remove $NaIO_3$ from the reaction mixture.

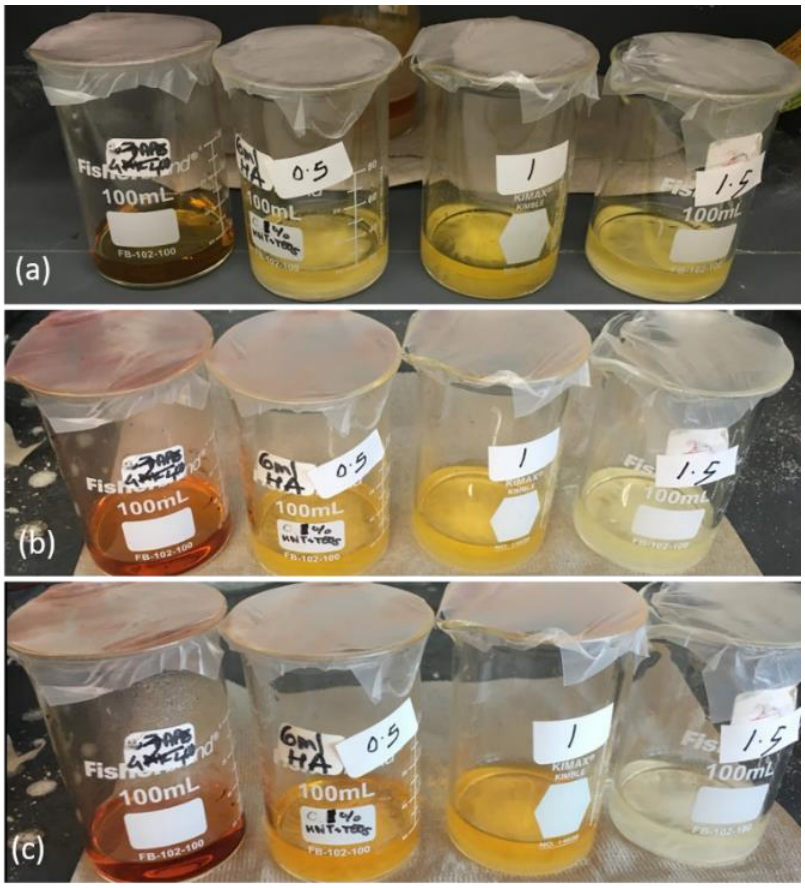

Figure 6.3 $BaCl_2$:$NaIO_4$ molar ratios of 0, 0.5, 1 and 1.5 (across a, b and c) added to OSFS (a) 15 min refrigerated (b) 30 min refrigerated (c) 1 h refrigerated.

6.3.6 Wool fiber crosslinking

Wool sliver, 7.5 inch long, was cut and immersed in flat form in the prepared OSFS solution for 10 min at RT in a rectangular Pyrex® box. After 10 min of immersion in OSFS, the sliver was taken out and gently squeezed to remove excess solution. The wet sliver was immersed flat again in the OSFS solution for 1 min at RT, taken out and gently squeezed again to ensure uniform wet pick-up by all fibers in the sliver with OSFS. The wet sliver was placed flat on a glass plate and cured in an air-circulation oven at 140°C and 150°C for 20 min to allow the crosslinking between aldehyde groups from OSFS and amine groups in wool keratin as shown in Figure 6.4.

The sliver was flipped upside down after the half curing time (10 min) in the oven to ensure uniform treatment to all fibers. The sliver was taken out and placed flat in a Pyrex® box containing DI water for washing. The crosslinked sliver was washed 2-3 times with water to remove all the unreacted sugars from the fiber surface. The crosslinked fibers in the sliver were dried and conditioned at ASTM conditions of 65 ± 3% RH and 21 ± 1°C for 24 h prior to any testing.

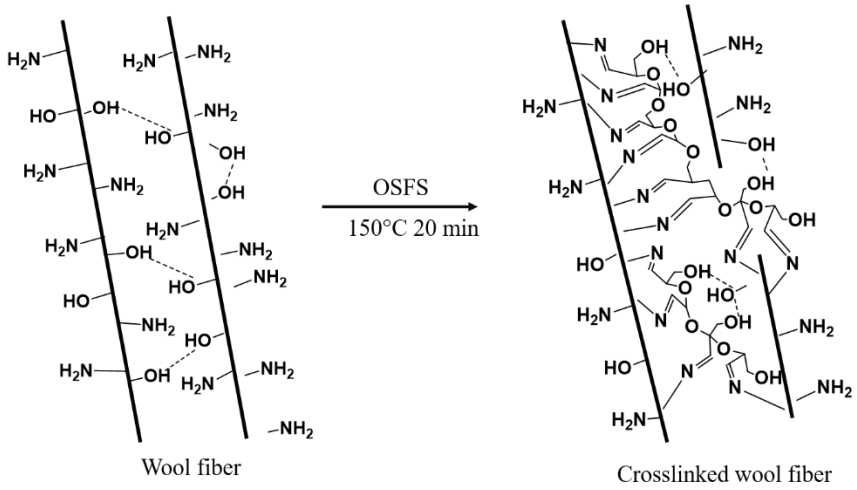

Figure 6.4 Crosslinking of wool fibers using OSFS by Schiff's base (imine)formation.

6.3.7 Characterization of SFS, OSFS, control and crosslinked wool.

A complete ^{13}C Nuclear Magnetic Resonance (NMR) analysis was performed to characterize SFS and various sugars present in SFS. The structural/chemical differences in SFS upon oxidizing were studied using ^{1}H NMR. ^{13}C and ^{1}H NMR spectra were recorded on an INOVA 400 spectrometer (Varian Inc., Palo Alto, CA, USA) using D_2O as the solvent for both.

Attenuated total reflectance Fourier-transform infrared (ATR-FTIR) analysis was done to characterize the effect of oxidation on SFS. ATR-FTIR was also used to study the crosslinking of wool. The ATR-FTIR spectra were collected using Thermo

Nicolet Magna-IR 560 spectrometer (Madison, WI) having a split pea accessory. Each scan was an average of 300 scans from 4000 cm^{-1} to 500 cm^{-1} wavenumbers.

CIELAB color parameters of control and crosslinked wool fibers were measured using a Macbeth Color-eye spectrophotometer, Model M2020PT, (Newburgh, NY). The L*, a*, b* values stand for L* = 0 (black) to L* =100 (white), -a* (greenness) to +a* (redness), and -b* (blueness) to +b* (yellowness). A standard value for the white calibration tile (L*= 95.91 a*= -0.43 b* = 1.01) was used to calibrate the spectrophotometer.

Tensile properties of single fibers were characterized using an Instron universal testing machine, model 5566 (Instron Corp., Canton, MA). Single wool fibers were individually mounted on rectangular paper tabs and the two ends were secured using self-adhesive tape. The diameters of every single fiber was measured using a calibrated optical microscope, Olympus, model BX51 (Melville, NY), at three different locations and the average was used to calculate the tensile properties of each fiber. The fibers were conditioned and tested at 65 ± 3% RH and 21 ± 1°C at a gauge length of 20 mm and strain rate of 0.6 min^{-1}. Thirty single fibers were randomly chosen from different parts of the wool sliver of each type (control and crosslinked) for testing and statistical analysis. For the crosslinked fibers, ten fibers were chosen from each of the three different slivers treated at different times using OSFS solutions prepared at different times to ensure reproducibility of the results. Savitzky-Golay fitting was used to smooth the tensile stress-strain plots.[48] Linear regression was performed on the smoothed plots to get accurate modulus values of the fibers. The

unpaired t-test was used to test if the control and crosslinked fiber properties were statistically significant from each other.

To study the effect of crosslinking on the surface of the fibers and the fracture behavior of the control and crosslinked wool fibers, the surface and the fractured ends of the fibers fractured during the tensile tests were carefully mounted on standard aluminum stubs with double sided electrically conductive carbon tapes and characterized using a Zeiss Gemini 500 scanning electron microscope, Germany, at 0.25 kV.

6.4 Results and discussion

6.4.1 Characteristics of SFS.

^{13}C NMR has been an important tool for the structural elucidation of carbohydrates.[16-17] Figure 6.5 shows the ^{13}C NMR spectra of various sugars such as fructose, glucose, sucrose, raffinose, stachyose and the SFS obtained in this study. As seen in Figure 6.5, all pure sugars showed chemical shifts between 60 ppm and 110 ppm.[17-19] Fructose and glucose are reducing monosaccharides consisting of six carbons each. The aqueous solutions of these monosaccharides consist of equilibrium mixtures of their tautomers.[20] In solution, fructose exists as an equilibrium of fructopyranose, fructofuranose, and other forms including acyclic structures.[20] Glucose exists in α and β pyranose together with their open chain forms.[19] The ^{13}C NMR spectra of fructose (Figure 6.5(a)) and glucose (Figure 6.5(b)) show more than six carbons because it shows tautomeric structures as they are present in aqueous solution.[20] Sucrose is a non-reducing disaccharide made up of fructose and glucose. ^{13}C NMR spectrum of

sucrose is shown in Figure 6.5(c). The twelve carbons from sucrose are seen between 60 ppm to 110 ppm.[21] Raffinose is a non-reducing trisaccharide composed of galactose, glucose and fructose consisting of eighteen carbons as seen in its spectrum shown in Figure 6.5(d). Stachyose is also a non-reducing tetrasaccharide but consists of two galactose units, one glucose and one fructose unit with a total of twenty four carbons as seen in its spectrum shown in Figure 6.5(e). The spectrum of SFS (Figure 6.5(f)) shows chemical shifts between 60 ppm and 110 ppm as seen in all other sugars mentioned above, confirming the presence of different sugars in the SFS. Obendorf et al. have shown that the embryos of soybean seed accumulate sucrose, raffinose and stachyose during seed development and maturation.[22] Qiu and Netravali showed that SFS extracted from the same SF as in the present case, consisted of 21.21 g/L sucrose, 11.92 g/L stachyose, 1.92 g/L fructose and glucose (combined), 1.59 g/L raffinose, water and other compounds such as water soluble proteins using HPLC analysis.[14] Their data indicate that sucrose and stachyose are present in large amounts amongst all the sugars in SFS.[14] The ^{13}C NMR spectrum of SFS (Figure 6.5(f)) shows all the chemical shifts present on sucrose and stachyose spectra (Figure 6.5(c) and 6.5(e)) confirming their presence in SFS.

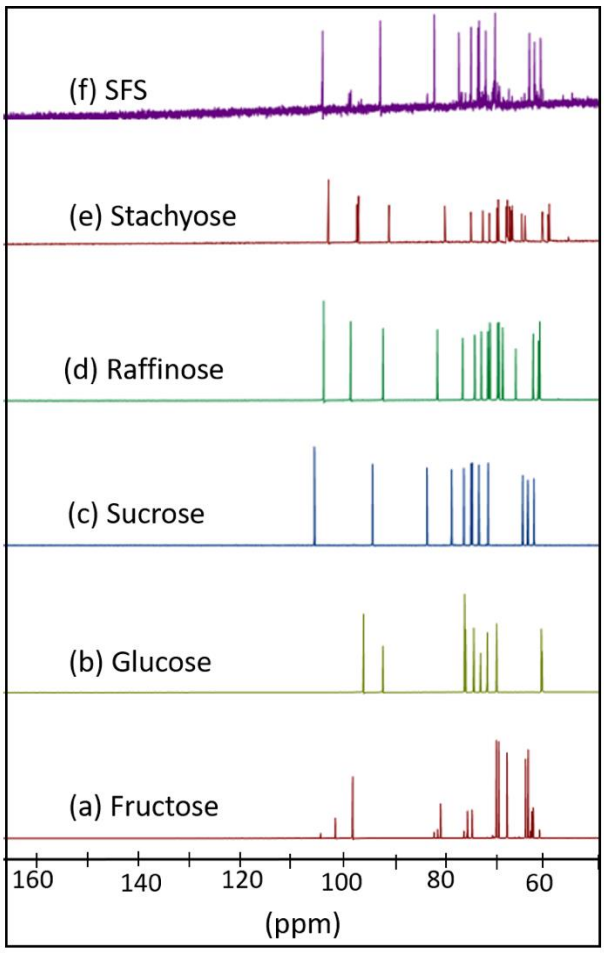

Figure 6.5 ^{13}C NMR spectra of (a) Fructose (b) Glucose (c) Sucrose (d) Raffinose (e) Stachyose and (f) SFS.

6.4.2 Characteristics of SFS and OSFS.

Figure 6.6 presents ATR-FTIR and NMR spectra of SFS and OSFS. Figure 6.6(a) shows ATR-FTIR spectra of SFS and OSFS. The ATR-FTIR spectrum of SFS shows absorption peaks between 3700 cm^{-1} to 2800 cm^{-1} and 1700 cm^{-1} to 900 cm^{-1}. The peaks between 1500 cm^{-1} and 500 cm^{-1} are characteristic peaks of the saccharide configurations as seen in sugars such as glucose, fructose, sucrose and others.[23] For example, the peak at 918 cm^{-1} corresponds to C-H bending in the saccharides.[23] The

peak at 997 cm^{-1} is the characteristic peak of sucrose associated with the disaccharide linkage α-D-glucopyranosyl and β-D-fructofuranosyl groups.[24] The peaks at 1043 cm^{-1} and 1250 cm^{-1} correspond to the C-O stretch in the C-OH group of the saccharides while the peak at 1411 cm^{-1} corresponds to the combination of OH bending of COH group and C-H bending of alkenes.[23, 25] The peak at 3270 cm^{-1} corresponds to the OH stretch from water.[25] The ATR-FTIR spectrum of SFS shows all the characteristic peaks present in saccharides confirming the presence of different sugars in it. The exact percentages of different sugars in SFS determined earlier by Qiu and Netravali using HPLC are presented in Table 6.1.[14] As seen from Table 6.1, sucrose and stachyose are present in considerable amounts in SFS, 58% and 32.5%, respectively, making over 90% of the total sugars. Fructose and glucose are reducing sugars and can exist in open-chain form in equilibrium forming aldehyde or ketone groups. Unlike monosaccharides such as fructose and glucose, sucrose, raffinose and stachyose are non-reducing sugars and do not exist in open-chain form, and, importantly, none of them have aldehyde groups. However, they can be oxidized to convert the hydroxyl groups to aldehyde groups. Figure 6.1 presented earlier showed the proposed oxidation reaction of sucrose and stachyose. As seen in Figure 6.1, $NaIO_4$ cleaves the vicinal diols and oxidizes the hydroxyl groups to aldehyde groups.[26] Sucrose and stachyose have five and eleven secondary hydroxyl groups, respectively, which form the vicinal diols that can be broken and oxidized to four and eight aldehyde groups, respectively (Figure 6.1). Thus, oxidation of sucrose and stachyose forms polyaldehyde (tetra-aldehyde sucrose and octa-aldehyde stachyose) derivatives (Figure 6.1). These aldehyde groups were confirmed through the ATR-FTIR spectrum of OSFS as shown

in Figure 6.6(a) through the absorption peak at 1720 cm^{-1}. A similar peak at 1718 cm^{-1} was seen by Jalaja and James after oxidizing sucrose using $NaIO_4$.[27] The peak intensities of both 1250 cm^{-1} and 1411 cm^{-1}, which correspond to the C-OH bending in sugars are seen to reduce as a result of oxidation of hydroxyls to aldehyde groups.[23] Similarly, glucose, fructose and raffinose in SFS get oxidized to form aldehyde groups as well. Since these three sugars account for less than 10% of total sugars in the SFS solution, Figure 6.1 presents only the sucrose and stachyose reactions.

The formation of polyaldehyde was also confirmed from the ^1H NMR spectra. Figure 6.6(b) shows the ^1H NMR spectra of SFS and OSFS. The spectrum of SFS shows characteristic sugar proton shifts at 5.4 ppm and between 4.2 ppm and 3.2 ppm.[28] The proton shift at 4.7 ppm is the solvent peak from D_2O. The proton shifts between 3 ppm and 4 ppm represent -CH and $-CH_2$ in the sugars.[29] The proton shifts at 4 ppm and 4.2 ppm represent the protons from the vicinal diols of the sugars. The additional peak in OSFS at 8.3 ppm shows the formation of aldehyde groups upon oxidation of SFS. Liu et al. observed the free aldehyde peak upon oxidation of sucrose using $NaIO_4$ between 8 ppm and 8.5 ppm.[29] The additional small proton shifts seen between 5 ppm and 5.6 ppm show the formation of hemiacetals because of the intermolecular reaction between aldehyde and hydroxyl groups. Similar proton shifts were observed by Xu et al. and Liu et al. after oxidizing sucrose using $NaIO_4$.[26, 29] The change in pH of SFS from 5.5 to 3 after oxidation also confirms the presence of aldehyde groups in OSFS.

Table 6.1 Percent content of different sugars in SFS.14

Fructose + Glucose	Sucrose	Raffinose	Stachyose
5.24 %	57.90%	4.33%	32.53%

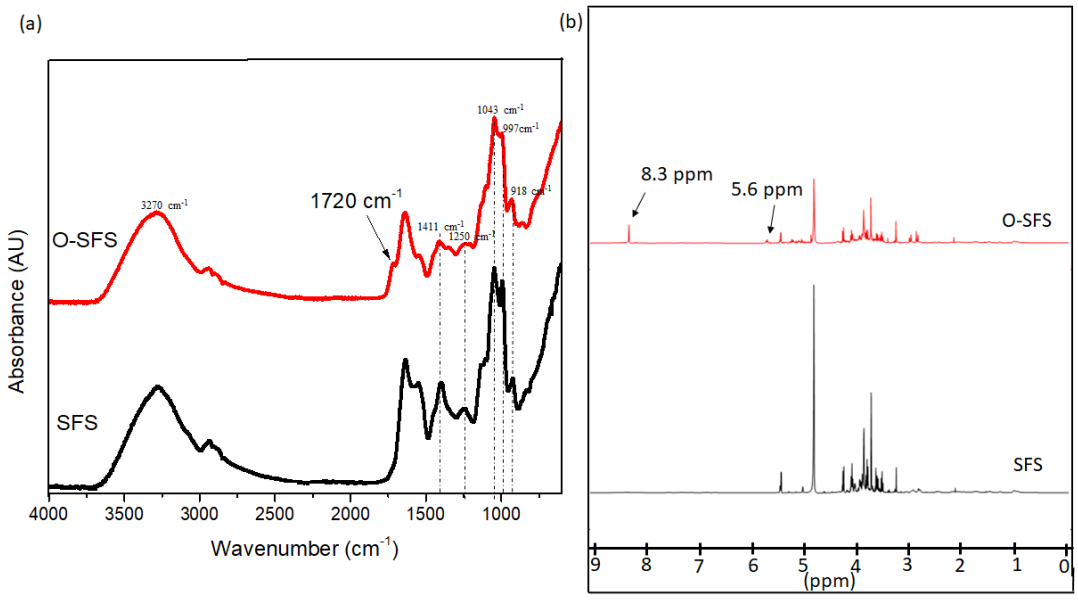

Figure 6.6 (a) ATR-FTIR spectra and (b) ^{1}H NMR spectra of SFS and OSFS.

6.4.3 Characteristics of Control and Crosslinked Wool Fibers.

Figure 6.7 presents the ATR-FTIR spectra of wool fibers. While Figure 6.7(a) shows the ATR-FTIR spectra of control and crosslinked wool fibers from 4000 cm^{-1} to 500 cm^{-1}, Figure 6.7(b) shows the spectra from 1800 cm^{-1} to 1000 cm^{-1}. The spectrum for untreated (control) wool fiber shows a broad peak around 3268 cm^{-1}. This peak is assigned to O-H stretching from adsorbed water and N-H bending vibrations from the amide A linkages.[30] The peak at 2923 cm^{-1} is due to CH_2 and CH_3 stretching vibrations

while the peak at 1447 cm^{-1} is due to C-H bending in protein. The spectrum for control wool fiber also shows three main characteristic peaks between 1700 cm^{-1} and 1200 cm^{-1}. For example, the strong absorbance peak at 1628 cm^{-1} is associated with the C=O stretch from the amide I linkages.[31] The medium strong absorbance peak at 1515 cm^{-1} is assigned to N-H in-plane bending in amide II linkages.[31] The peak at 1233 cm^{-1} is assigned to the C-N stretch of the amide III linkages.[30-31] The aldehyde groups of OSFS can react with the amine groups from keratin to form imine linkages as shown in Figure 6.4. Oxidized sucrose present in OSFS has four aldehyde groups while stachyose, the longer molecule, has eight aldehyde groups and, in theory, all aldehyde groups can react with the amine groups present in keratin to form crosslinks. This crosslinking leads to the formation of imine linkages. It is, however, very difficult to see formation of new imine linkages in the crosslinked fibers due to spectral complexity of the proteins.[15, 32-34] Figure 6.7(b) presents ATR-FTIR spectra of control and crosslinked wool fibers from 1800 cm^{-1} to 1000 cm^{-1}. As can be seen in Figure 6.6(b), the spectrum of crosslinked wool fibers shows an additional small peak at 1040 cm^{-1} which corresponds to the C-O stretch in C-OH as well as C-C stretch in the sugars.[23] This confirms the incorporation of OSFS within wool fibers. Similar additional peak at 1049 cm^{-1} was observed after crosslinking soy proteins with oxidized sugars.[15] Jalaja and James observed a peak at 1030 cm^{-1} corresponding to the C-O-C stretch of sugar moiety after crosslinking gelatin with oxidized sucrose.[27] The spectrum of crosslinked wool fibers in Figure 6.7(b) also shows a small peak at 1341 cm^{-1} which is not present in the spectrum of control wool fibers. This peak corresponds to the OH bending of the C-OH group and is present in sugars from SFS

and confirms the presence of sugars after crosslinking.[23] The shift in the amide I peak at 1628 cm^{-1} shows that the secondary structure of wool has changed after crosslinking.[35] It was observed that the amide II peak changed from the sharp and narrow peak to broad peak between 1510 cm^{-1} to 1540 cm^{-1} after crosslinking. Similar change in the amide II peak was observed when gelatin was crosslinked using glutaraldehyde.[36] The crosslinking reaction between primary amine groups in wool keratin with aldehydes from OSFS is through the formation of Schiff's base.[27, 37] The crosslinking of wool fibers can also be confirmed by the change in color and mechanical testing of the fibers. These results are discussed later.

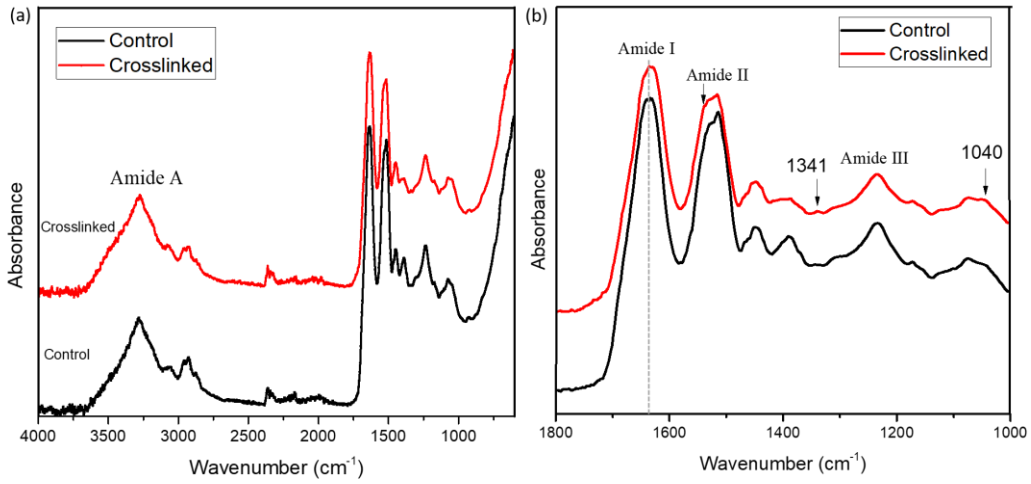

Figure 6.7 ATR-FTIR spectra of control and crosslinked wool fibers from (a) 4000 cm^{-1} to 500 cm^{-1} and (b) 1800 cm^{-1} to 1000 cm^{-1}.

Table 6.2 shows the L*, a*, b* values of control and crosslinked wool fibers. The change in color after Maillard reaction can be used to confirm crosslinking of proteins.[15, 32, 38] As shown in Table 6.2, the control fibers showed L*, a*, b* values of 78.02, -0.96, 3.80, respectively. Wool fibers crosslinked using OSFS (wool-OSFS) showed significant increase in the b* (yellowness) values. The b* value increased

from 3.80 for control fibers to 5.31 and 8.64 after crosslinking with OSFS at 140°C and 150°C for 20 min, respectively. The increase in b* after treating with OSFS is another evidence of crosslinking reaction between the oxidized sugars and the amino acids from wool keratin. Higher b* value for wool-OSFS 150°C (8.64) as compared to wool-OSFS 140°C (5.31) is due to the increased extent of crosslinking with the increase in the temperature. Similar change in color was observed when dialdehyde starch was used to crosslink soy protein isolate.[38] Other dialdehyde sugars and aldehydes such as glutaraldehyde and glyoxal have also resulted in yellow/brown coloration after crosslinking the proteins present in wool, zein, gelatin, soy protein isolate, soy flour, collagen and other proteins, typical of the Maillard reaction.[15, 36, 38-42] Two types of browning have been observed after heating of sugars. First one is caramelization, caused by heating of sugars, which breaks down the molecules giving the yellow/brown color. The second is Maillard reaction, in which the browning is caused by heating reducing sugars in the presence of protein (amino groups). Reducing sugars in OSFS such as fructose and glucose contain aldehyde groups in the open chain form while non-reducing sugars such as sucrose, stachyose and raffinose contain aldehyde groups due to oxidation. The Maillard reaction between aldehyde groups in OSFS and amino groups in keratin causes the increase in the b* value. To confirm the change in color was due to Maillard reaction (and not caramelization), wool sliver was treated with pure SFS solution at 150°C for 20 min. The pictures of the treated wool slivers are shown in Figure 6.8. As can be seen from the Figure 6.8 and in Table 6.2, the b* value of SFS treated wool (wool-SFS) sample is close to the pure wool sample, showing no evidence of caramelization. Thus, the increase in b*

value for OSFS treated samples prove that the browning is due to Maillard reaction.[15, 38, 42] Crosslinking of wool using OSFS was restricted to 140°C and 150°C because caramelization of sugars and subsequent pyrolysis is prominent at temperatures above 160°C.[43]

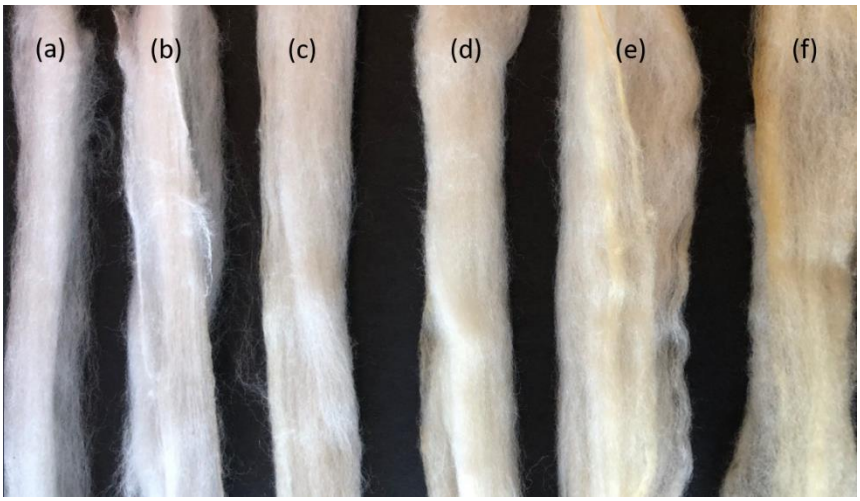

Figure 6.8 Pictures of control and treated wool slivers (a) control (b) wool-SFS (c) wool-OSFS MR 1, (d) wool-OSFS MR 1.5, (e) wool-OSFS MR 2, (f) wool-OSFS MR 2.5. All treatments carried out at 150°C for 20 min.

Table 6.2 L*, a*, b* hunter color values of control and crosslinked fibers.

Specimen	**L***	**a***	**b***
Control	78.02 ± 1.8	-0.96 ± 0.02	3.80 ± 0.60
Wool-SFS	78.07 ± 2.1	-0.98 ± 0.07	3.92 ± 0.98
Wool-OSFS 140	72.82 ± 2.4	-1.01 ± 0.03	5.31 ± 1.49
Wool-OSFS 150	72.95 ± 2.3	-1.02 ± 0.03	8.64 ± 3.01

Figure 6.9 shows typical stress-strain plots of control and crosslinked wool fibers. As seen in Figure 6.9, the stress-strain plots can be divided into three distinct regions: the initial Hookean region, yield region and the post yield (strain hardening) region. Tensile properties of control and crosslinked fibers are summarized in Table 6.3. As seen in Figure 6.9, the initial Hookean region lies between 0%-3.4% strain for both control and crosslinked fibers. This region exhibits a linear relationship between stress and strain. Wool protein, in relaxed state, is called α-keratin wherein the keratin molecules are unstressed and in their natural helical shape. At low level of strain (~3.5%) the distortion involves extension of weaker bonds such as hydrogen bonding within the amino acids (seen in Figure 6.4), Van der Waals forces, and coulombic interactions.[44]. The folded α-helix structure of the fiber, hydrogen bonds between the helices, coulombic interactions due to side chains and some $-COO^-$ and $-NH_3^+$ groups oppose the distortion or strain. It was observed that the tensile stress of the fibers, at the end of the Hookean region, increased from 88 MPa to about 116 MPa, an increase of about 32%, after crosslinking with OSFS while the tensile strain reduced from 3.4% to 3.1%. Also, the Young's modulus of the fibers in the Hookean region increased from 2.5 GPa to 3.9 GPa, an increase of 56%, after crosslinking. Increases in tensile stress and Young's modulus values after crosslinking in the initial Hookean region were found to be statistically significant using an unpaired t-test at a significance level of 0.05. The increase in the tensile stress and Young's modulus is clearly a result of the crosslinks formed within the microfibrils, macrofibrils and in the matrix region of the cortical cells of the wool fibers, that oppose the deformation. The microfibrils embedded within the matrix in the cortical cells are responsible for the strength of the

fibers.[45] The Maillard reaction between aldehyde groups from OSFS and amine groups of the keratin molecules creates intermolecular covalent bonding between the fibrils. This leads to an increase in tensile stress and modulus in the initial Hookean region after crosslinking.

Beyond initial 3% strain, the strain increases rapidly for a small increase in the stress. This region is called the 'yield region'. The overall stress in the yield region increased from 88 MPa for control fibers to over 119 MPa, over 35% increase, for crosslinked fibers. At the same time the yield region which extended from 3.4% to 25.3% for control fibers changed to 3.1% to 21.7% for crosslinked fibers and the stress at the yield point increased from 117 MPa to 146 MPa. The reduction in the tensile strain, from 25.3% for control to 21.7% for crosslinked fibers confirms the formation of crosslinks between the peptide chains that restrict the molecular movement. The modulus in the yield region was also found to increase from 0.18 GPa to 0.27 GPa after crosslinking (50% improvement in the modulus).

Beyond the yield region, the wool fibers stiffen rapidly. This region is called the post-yield region and the stiffening phenomenon is called strain hardening. The post-yield region terminates on the rupture of the fiber. As seen in Figure 6.9, the strain hardening phenomenon in the post yield region is more prominent in the crosslinked fibers as compared to the control fibers. The tensile fracture stress of the fibers increased from 203 MPa to 276 MPa after crosslinking, a 36% increase. The tensile strain was found to reduce from 47.4% to 41.8% after crosslinking. The secant modulus for the strain hardening region increased from 0.35 GPa to 0.53 GPa (51.4 % increase) after crosslinking. Unpaired t-test showed that the increase in the moduli for

all the three regions after crosslinking of the fibers were statistically significant at the significance level of 0.05. As mentioned earlier, OSFS contains a mixture of different sugars having aldehyde groups. The major sugars present in OSFS, sucrose and stachyose, form tetra-aldehyde and octa-aldehyde, respectively, with different molecular lengths. This makes it easy to form various crosslinks with the protein side chains and allows forming a better 3-dimensional network within the fiber leading to an increase in the tensile stress and modulus in all regions of the fiber stress-strain plots. Hassan et al. crosslinked wool fibers using four different crosslinkers and found that the tensile strength increased from 103 MPa to 111.7 MPa, 115.2 MPa, 116.2 MPa, and 122 MPa for the glyoxal, itaconic anhydride, naphthalene disulfonic acid and succinic anhydride crosslinked wool fibers, respectively.[46] They observed a maximum of 18.5% increase in the strength of the wool fibers after crosslinking with succinic anhydride.[46] As seen earlier, crosslinking of fibers with OSFS showed an increase of about 36% in the tensile strength (from 203 MPa to 276 MPa). This shows that the natural soy flour sugar based green crosslinker is more effective in improving tensile properties of wool fibers than all other toxic bifunctional aldehyde-based crosslinkers currently used.

Keratin fibers have a tendency to absorb moisture which plasticizes them and causes a decrease in Young's modulus.[45] The moisture content of the conditioned fibers reduced from 9.14% in control fibers to 6.6%, a decrease of about 28%, after crosslinking. As expected, the 3-dimensional network obtained by crosslinking creates a more compact structure that acts as a moisture barrier. Reduced moisture absorption is beneficial since it can reduce the effect of moisture on fiber tensile properties. The

cortex of the wool fiber is composed of ortho and para cortical cells. The para cortical cells contain disulfide (S-S) crosslinks resulting from cystine amino acid whereas the ortho cortical cells do not have S-S covalent crosslinks allowing them to absorb more moisture as compared to para cortical cells. This results in ortho cortical cells swelling and elongating more than para cortical cells which causes the crimp in the fiber. Absorbing less water could automatically reduce the undesired issues related to crimp.

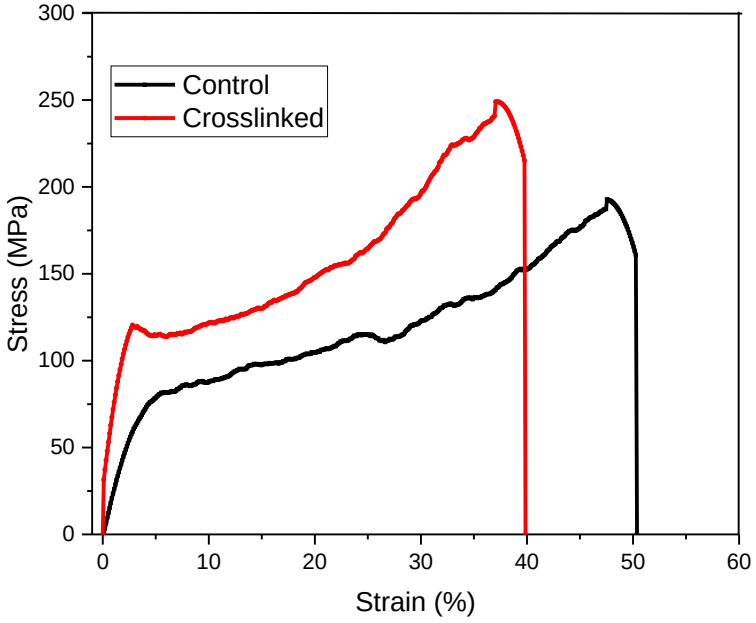

Figure 6.9 Typical stress-strain plots for control and crosslinked fibers.

Table 6.3 Tensile properties of the control and crosslinked fibers.

		Initial Hookean region			Yield region			Post Yield region		
Specimen	Diameter (μm)	Stress (MPa)	Strain (%)	Modulus (GPa)	Stress (MPa)	Strain (%)	Modulus (GPa)	Stress (MPa)	Strain (%)	Modulus (GPa)
Control	19.5 ± 1.8	88.2 ± 30.4	3.4 ± 1.4	2.5 ± 0.8	119.8 ± 32.9	25.3 ± 5.1	0.18 ± 0.06	203.0 ± 40.8	47.4 ± 7.6	0.35 ± 0.12
Crosslinked	19.0 ± 1.3	116.8 ± 37.3	3.1 ± 1.3	3.9 ± 1.2	145.5 ± 50.3	21.7 ± 3.5	0.27 ± 0.12	276.0 ± 54.5	41.8 ± 5.9	0.53 ± 0.13

6.4.4 Surface Characteristics of Control and Crosslinked Wool Fibers.

Figure 6.10 shows SEM images of the surfaces of the control and crosslinked wool fibers taken at different magnifications. Figures 6.10(a) and 6.10(b) show control wool fibers with scales on the surface. These scales form the cuticle layer on the fiber surface.[47] Figure 6.10(c) and 6.10(d) show the surfaces of crosslinked fibers. When compared, the crosslinked fibers do not show any effect on the scalar structure of the fiber cuticle. No visible change or damage of scales can be observed after crosslinking the fibers with OSFS. Oxidized sugar molecules from OSFS are small molecules that can penetrate inside the cortex of the fiber and crosslink them internally, enhancing the tensile properties, while leaving the surface unchanged.

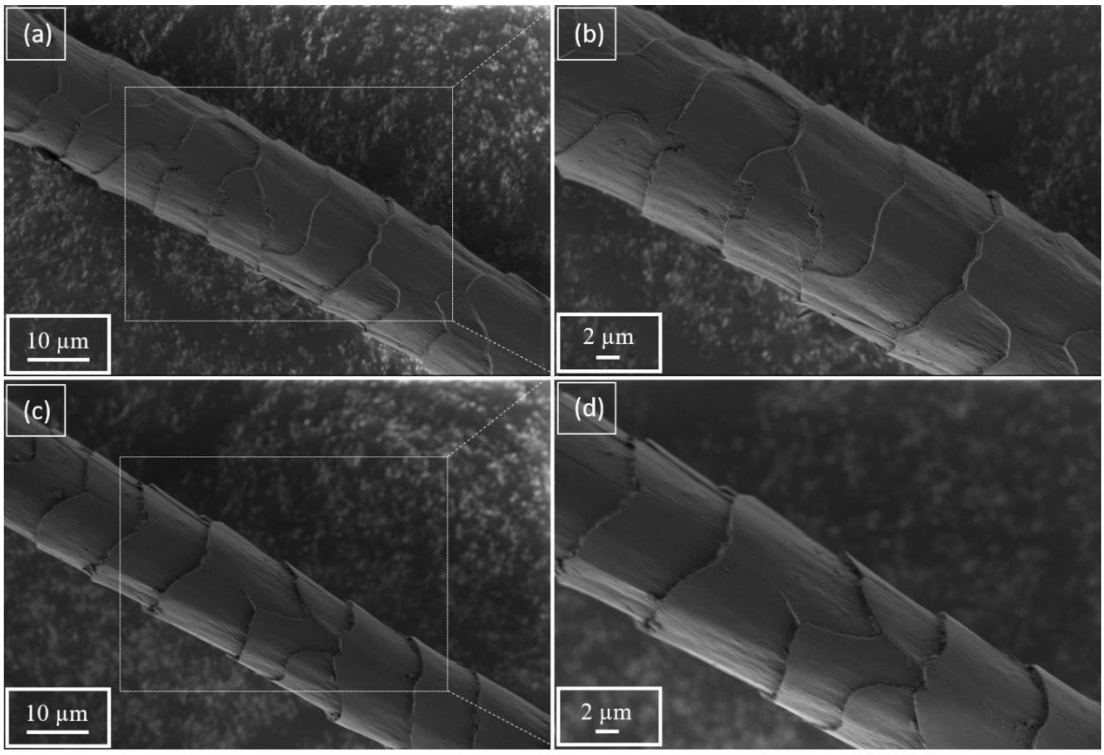

Figure 6.10 SEM of surface of (a, b) control and (c, d) crosslinked wool fibers.

Figure 6.11 shows SEM images of the fractured ends of control and crosslinked fibers taken at different magnifications. As seen in Figure 6.11, the fracture surfaces of both control and crosslinked fibers show similar fracture characteristics. It can also be seen from the tensile plots of the fibers (Figure 6.9) that the fibers do not fracture in stepwise fashion but undergo catastrophic failure after the strain hardening.

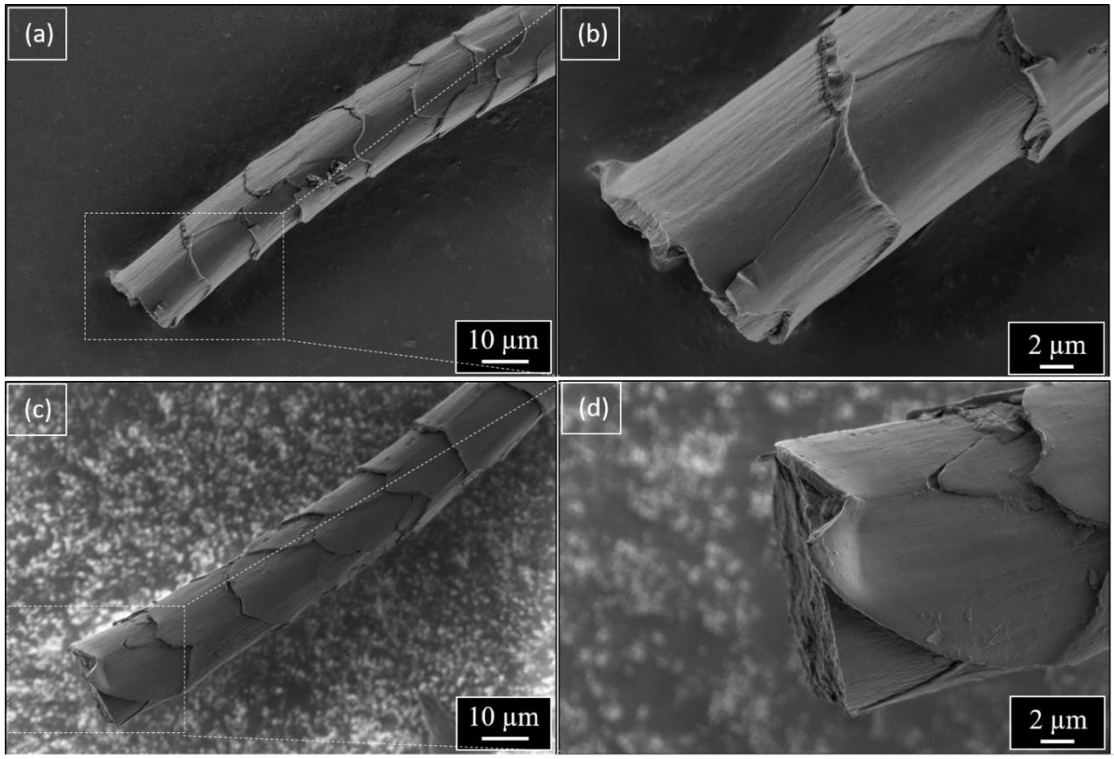

Figure 6.11 SEM images of fractured ends of (a, b) control and (c. d) crosslinked wool fibers.

6.5 Conclusions

The present study has successfully demonstrated that the tensile performance of the wool fibers can be enhanced significantly using a 'green' bio-based crosslinker. The utilization of SFS, a by-product with no potential application, showed promising results after oxidizing it to a polyaldehyde. This valorizes the by-product from soy processing industry and reduces the waste. The presence of different sugars in SFS was found to be beneficial by not only providing multiple aldehyde groups but also different molecular lengths, increasing crosslinking efficiency. The higher crosslink density within the wool fiber improves its strength and modulus significantly. The room temperature extraction and oxidization process used in this study is also an

energy efficient way of making a natural, bio-based crosslinker for protein-based polymers. The availability of SFS at very low cost and ease of oxidation reaction makes it scalable at the commercial level. The method presented here can be easily extended for crosslinking other protein-based materials. The OSFS prepared in this study can easily replace currently used toxic crosslinkers such as glyoxal and glutaraldehyde. Enhanced tensile properties of wool fibers can not only increase the efficiencies of wool fiber spinning and weaving by reducing breakages but can also reduce yarn and fabric defects. More importantly, stronger wool can allow spinning finer yarns from the same fibers, increasing their value significantly.

Acknowledgments

This research was partially supported New York Corn & Soybean Growers Association (NYCSGA). The use of Cornell Center for Materials Research (CCMR) shared facilities supported through the NSF MRSEC program (DMR-1719875) and of the Department of Fiber Science & Apparel Design facilities are also acknowledged.

6.6 References

(1) Chen, D.; Tan, L.; Liu, H.; Tang, F.; Hu, J.; Li, Y. Fabrication of Fast-Absorbing and Quick-Drying Wool Fabrics with Good Washing Durability. *ChemSusChem* **2010,** *3* (9), 1031-1035.

(2) Chen, D.; Tan, L.; Liu, H.; Hu, J.; Li, Y.; Tang, F. Fabricating superhydrophilic wool fabrics. *Langmuir* **2009,** *26* (7), 4675-4679.

(3) Johnson, N. A.; Russell, I. In *Advances in wool technology*. Elsevier: Woodhead publishing: England, 2008.

(4) Prins, M. Advances in wool spinning technology. In *Advances in Wool Technology*, Elsevier: Woodhead publishing, 2009; pp 86-105.

(5) Barani, H.; Calvimontes, A. Effects of oxygen plasma treatment on the physical and chemical properties of wool fiber surface. *Plasma Chem.Plasma P.* **2014,** *34* (6), 1291-1302.

(6) Rahman, M. M.; Netravali, A. N. Green resin from forestry waste residue "Karanja (Pongamia pinnata) seed cake" for biobased composite structures. *ACS Sustain. Chem. Eng.* **2014,** *2* (10), 2318-2328.

(7) Corfield, M.; Robson, A. The amino acid composition of wool. *Biochem. J.* **1955,** *59* (1), 62.

(8) Di Modica, G.; Marzona, M. Cross-linking of wool keratin by bifunctional aldehydes. *Text. Res. J.* **1971,** *41* (8), 701-705.

(9) Song, K.; Xu, H.; Mu, B.; Xie, K.; Yang, Y. Non-toxic and clean crosslinking system for protein materials: Effect of extenders on crosslinking performance. *J. Clean. Prod.* **2017,** *150*, 214-223.

(10) Xu, H.; Song, K.; Mu, B.; Yang, Y. Green and Sustainable Technology for High-Efficiency and Low-Damage Manipulation of Densely Crosslinked Proteins. *ACS Omega* **2017,** *2* (5), 1760-1768.

(11) Reddie, R.; Nicholls, C. Some reactions between wool and formaldehyde. *Text. Res. J.* **1971,** *41* (10), 841-852.

(12) Mohsin, M.; Farooq, U.; Raza, Z. A.; Ahsan, M.; Afzal, A.; Nazir, A. Performance enhancement of wool fabric with environmentally-friendly bio-cross-linker. *J. Clean. Prod.* **2014,** *68*, 130-134.

(13) Milazzo, M.; Spina, F.; Cavallaro, S.; Bart, J. Sustainable soy biodiesel. *Renew. Sust. Energ. Rev.* **2013,** *27*, 806-852.

(14) Qiu, K.; Netravali, A. N. " Green" composites based on bacterial cellulose produced using novel low cost carbon source and soy protein resin. In *Recent Advances in Adhesion Science and Technology in Honor of Dr. Kash Mittal*, CRC Press: 2014.

(15) Ghosh Dastidar, T.; Netravali, A. N. A soy flour based thermoset resin without the use of any external crosslinker. *Green Chem.* **2013,** *15* (11), 3243-3251.

(16) Duus, J. Ø.; Gotfredsen, C. H.; Bock, K. Carbohydrate structural determination by NMR spectroscopy: modern methods and limitations. *Chem. Rev.* **2000,** *100* (12), 4589-4614.

(17) Fort, D. A.; Swatloski, R. P.; Moyna, P.; Rogers, R. D.; Moyna, G. Use of ionic liquids in the study of fruit ripening by high-resolution ^{13}C NMR spectroscopy:'green'solvents meet green bananas. *Chem. Commun.* **2006,** (7), 714-716.

(18) Kazalaki, A.; Misiak, M.; Spyros, A.; Dais, P. Identification and quantitative determination of carbohydrate molecules in Greek honey by employing 13 C NMR spectroscopy. *Anal. Methods* **2015,** *7* (14), 5962-5972.

(19) Bubb, W. A. NMR spectroscopy in the study of carbohydrates: Characterizing the structural complexity. *Concept. Mag. Reson. A* **2003,** *19* (1), 1-19.

(20) Barclay, T.; Ginic-Markovic, M.; Johnston, M. R.; Cooper, P.; Petrovsky, N. Observation of the keto tautomer of D-fructose in D2O using 1H NMR spectroscopy. *Carbohyd. Res.* **2012,** *347* (1), 136-141.

(21) Jarrell, H. C.; Conway, T. F.; Moyna, P.; Smith, I. C. Manifestation of anomeric form, ring structure, and linkage in the ^{13}C-NMR spectra of oligomers and polymers containing D-fructose: maltulose, isomaltulose, sucrose, leucrose, 1-kestose, nystose, inulin, and grass levan. *Carbohydrate Research* **1979,** *76* (1), 45-57.

(22) Obendorf, R. L.; Sensenig, E. M.; Wu, J.; Ohashi, M.; O'Sullivan, T. E.; Kosina, S. M.; Schnebly, S. R. Soluble carbohydrates in mature soybean seed after feeding D-chiro-inositol, myo-inositol, or D-pinitol to stem-leaf-pod explants of low-raffinose, low-stachyose lines. *Plant Sci.* **2008,** *175* (5), 650-655.

(23) Anjos, O.; Campos, M. G.; Ruiz, P. C.; Antunes, P. Application of FTIR-ATR spectroscopy to the quantification of sugar in honey. *Food Chem.* **2015,** *169*, 218-223.

(24) Lin, C.-A.; Ayvaz, H.; Rodriguez-Saona, L. E. Application of portable and handheld infrared spectrometers for determination of sucrose levels in infant cereals. *Food Anal. Methods* **2014,** *7* (7), 1407-1414.

(25) Bureau, S.; Ruiz, D.; Reich, M.; Gouble, B.; Bertrand, D.; Audergon, J.-M.; Renard, C. M. Application of ATR-FTIR for a rapid and simultaneous determination of sugars and organic acids in apricot fruit. *Food Chem.* **2009,** *115* (3), 1133-1140.

(26) Xu, H.; Canisag, H.; Mu, B.; Yang, Y. Robust and flexible films from 100% starch cross-linked by biobased disaccharide derivative. *ACS Sustain. Chem. Eng.* **2015,** *3* (11), 2631-2639.

(27) Jalaja, K.; James, N. R. Electrospun gelatin nanofibers: a facile cross-linking approach using oxidized sucrose. *Int. J. Biol. Macromol.* **2015,** *73*, 270-278.

(28) Ghosh, B.; Jones, A. D. Profiling, characterization, and analysis of natural and synthetic acylsugars (sugar esters). *Anal. Methods* **2017,** *9* (6), 892-905.

(29) Liu, P.; Xu, H.; Mi, X.; Xu, L.; Yang, Y. Oxidized Sucrose: A Potent and Biocompatible Crosslinker for Three-Dimensional Fibrous Protein Scaffolds. *Macromol. Mater. Eng.* **2015,** *300* (4), 414-422.

(30) Xu, W.; Ke, G.; Wu, J.; Wang, X. Modification of wool fiber using steam explosion. *Eur. Polym. J.* **2006,** *42* (9), 2168-2173.

(31) Yao, J.; Liu, Y.; Yang, S.; Liu, J. Characterization of Secondary Structure Transformation of Stretched and Slenderized Wool Fibers with FTIR Spectra. *J. Eng. Fiber. Fabr. (JEFF)* **2008,** *3* (2).

(32) Rahman, M. M.; Netravali, A. N. Micro-fibrillated cellulose reinforced eco-friendly polymeric resin from non-edible 'Jatropha curcas' seed waste after biodiesel production. *RSC Adv.* **2016,** *6* (52), 47101-47111.

(33) Lodha, P.; Netravali, A. N. Thermal and mechanical properties of environment-friendly 'green'plastics from stearic acid modified-soy protein isolate. *Ind. Crop. Prod.* **2005,** *21* (1), 49-64.

(34) Chabba, S.; Matthews, G.; Netravali, A.N. 'Green'composites using cross-linked soy flour and flax yarns. *Green Chem.* **2005,** *7* (8), 576-581.

35. Li, R.; Wang, D., Preparation of regenerated wool keratin films from wool keratin–ionic liquid solutions. *J. Appl. Polym. Sci.* **2013,** *127* (4), 2648-2653.

(36) Nguyen, T.-H.; Lee, B.-T., Fabrication and characterization of cross-linked gelatin electro-spun nano-fibers. *J. Biomed. Sci. Eng.* **2010,** *3* (12), 1117.

(37) Park, S.; Bae, D.; Rhee, K. Soy protein biopolymers cross-linked with glutaraldehyde. *J. Am. Oil Chem.' Soc.* **2000,** *77* (8), 879-884.

(38) Rhim, J.-W.; Gennadios, A.; Weller, C. L.; Cezeirat, C.; Hanna, M. A. Soy protein isolate–dialdehyde starch films. *Ind. Crop. Prod.* **1998,** *8* (3), 195-203.

(39) Happich, W.; Windus, W.; Naghski, J. Stabilization of wool by glutaraldehyde. *Text. Res. J.* **1965,** *35* (9), 850-852.

(40) Song, F.; Tang, D.-L.; Wang, X.-L.; Wang, Y.-Z. Biodegradable soy protein isolate-based materials: a review. *Biomacromolecules* **2011,** *12* (10), 3369-3380.

(41) Wang, L.-F.; Rhim, J.-W. Preparation and application of agar/alginate/collagen ternary blend functional food packaging films. *International journal of biological macromolecules* **2015,** *80*, 460-468.

(42) Bhat, R.; Karim, A. Towards producing novel fish gelatin films by combination treatments of ultraviolet radiation and sugars (ribose and lactose) as cross-linking agents. *J. Food Sci. Tech.* **2014,** *51* (7), 1326-1333.

(43) Jiang, B.; Liu, Y.; Bhandari, B.; Zhou, W. Impact of caramelization on the glass transition temperature of several caramelized sugars. Part I: chemical analyses. *J. Agr. Food Chem.* **2008,** *56* (13), 5138-5147.

(44) Feughelman, M. *Mechanical properties and structure of alpha-keratin fibres: wool, human hair and related fibres*. UNSW press: 1997.

(45) Popescu, C.; Wortmann, F.-J. Wool–structure, mechanical properties and technical products based on animal fibres. *Industrial Applications of Natural Fibres:*

Structure, Properties and Technical Applications,; John Wiley & Sons, **2010**, 255-266.

(46) Hassan, M. M.; Schiermeister, L.; Staiger, M. P. Sustainable Production of Carbon Fiber: Effect of Cross-Linking in Wool Fiber on Carbon Yields and Morphologies of Derived Carbon Fiber. *ACS Sustain. Chem. Eng.* **2015,** *3* (11), 2660-2668.

(47) Hossain, K. M. G.; González, M. D.; Juan, A. R.; Tzanov, T. Enzyme-mediated coupling of a bi-functional phenolic compound onto wool to enhance its physical, mechanical and functional properties. *Enzyme Microb. Tech.* **2010,** *46* (3-4), 326-330.

(48) Mayo Jr, J.; Wetzel, E. Cut resistance and failure of high-performance single fibers. *Text. Res. J.* **2014,** *84* (12), 1233-1246.

Chapter 7 Natural 'Green' Sugar-based Treatment for Hair Styling

Namrata V. Patil and Anil N. Netravali
Department of Fiber Science & Apparel Design,
Cornell University, 37 Forest Home Dr., Ithaca, NY 14853, USA

Graphical abstract:

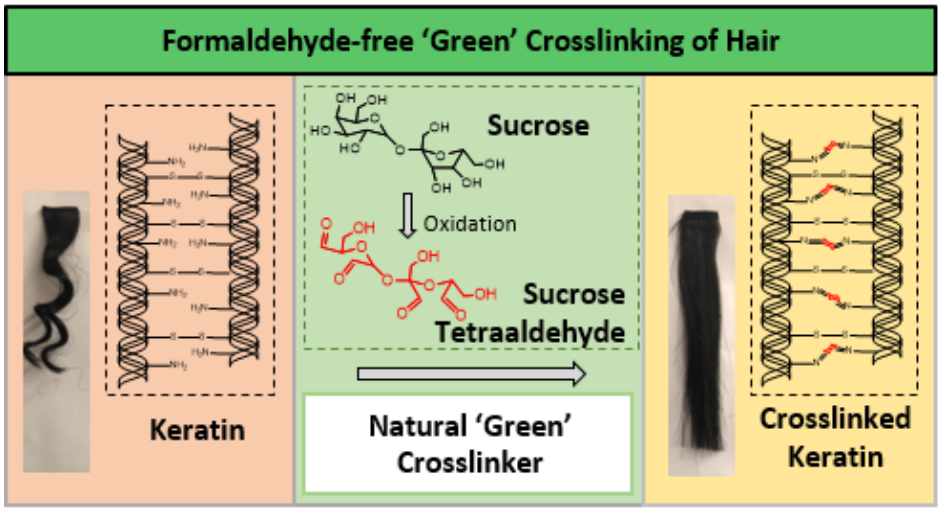

Submitted to:

ACS Omega

7.1 Abstract

A major drawback of current hair styling treatments is that it involves the use of toxic carcinogens such as thioglycolates, sulfites, formaldehyde and others. Constant exposure to such chemicals is harmful for the person getting the hair treatment and certainly to the hairstylists performing the treatment. A new 'green' sugar-based hair styling treatment was developed in this research. Chemical composition of the sugar-based crosslinker, studied using ATR-FTIR and ^{1}H-NMR showed the presence of multiple aldehyde groups on sugar, which were then used to react with amine groups present in keratin protein in hair. Chemical crosslinking of keratin molecules was carried out using a flat iron which can be readily adopted for practical applications in hair styling treatments. Crosslinked hair swatches were hung at high humidity condition (65%) as well as repeatedly washed with shampoo to characterize the permanency of treatment. The hair straightening treatment was found to be durable to high humidity and several shampoo washings. In addition, tensile characteristics of hair such tensile stress, strain and Young's modulus showed that the properties remained unaffected after treatment. SEM images showed no surface damage to the scales. Natural sugar-based 'green' crosslinker may also be used to create curls on straight hair.

7.2 Introduction

The haircare industry has been constantly growing and so have the number of products associated with haircare in the past couple of dacades.[1] Hair styling is a major part of haircare which involves grooming the hair to achieve more manageable,

frizz-free hair.[2] Hair straightening treatments are in vogue and require both chemical and heat treatments to achieve temporary to permanent hair straightening to achieve hair styling versatility.[2] Human hair is made up of keratin-based protein.[3] Keratin consists of amino acids linked by polypeptide bonds.[4-5] Polypeptide chains form an alpha helix structure which are twisted together to form microfibrils.[4] Many microfibrils together form a macrofibril. The inner layer of hair known as cortex is made-up cortical cells of macrofibrils and contributes to the strength, color and texture of the hair.[4] The cortex forms about 75% of the hair volume.[6] The outer layer of hair, cuticle, consists of scales which act as a preventive barrier for the cortex and, thus, protects the hair.[4-5]

There are a variety of treatments for hair straightening offered at present. Alteration of the cortex is important for straightening of hair.[5, 7-8] The most common method used for hair straightening is by using a flat iron.[6] Flat ironing process involves alterations of hydrogen bonds and salt linkages through heat and mechanical stress.[6] However, flat ironing manages to straighten the hair only temporarily as it can return back to its original state when exposed to high humidity or washing. Hair rebonding or chemical straightening are some of the other methods used to obtain more permanent straightening. In these processes strong chemical relaxers or reducing agents are used to break the disulfide bonds in the hair structure and then neutralizers or oxidizing agents are used to rebond the structure again. Permanent straightening is achieved through the modification of covalent bonds. The relaxers used for breaking the bond are generally strong and alkaline in nature and can be hydroxide based (pH 13) or thio-based (pH 10).[9] 3.5% Sodium hydroxide (lye-based) or guanidine

hydroxide activated with 4-7% calcium hydroxide, potassium hydroxide or lithium hydroxide (non-lye based) alkaline straighteners are commonly used by which the sulfur atom from a disulfide bond is removed and converted into a lanthionine bond creating a permanent non-reversible straightness.[6] Thio-based chemicals such as ammonium or ethanolamine thioglycolate and sulfites are commonly used reducing agents for hair which convert the disulfide bonds to sulfhydryl groups (chemical reduction) and further oxidized to reform the disulfide bonds at desired (straighter) conformation.[10-11] Both, hydroxide based lanthionization and thio-based reduction and oxidation techniques weaken and damage the hair permanently as it alters the cystine content or the disulfide bonds in the cortex and hydrolysis the peptide bonds.[6, 9] It also requires great amount of after-hair-care measures and results in hair thinning and dullness in the long run. These chemicals have a strong odor and can be irritating to skull skin or eyes during application. Thioglycolate and ammonium thioglycolate which are toxic and carcinogenic can be harmful if they get in contact with the skin.[9-10] Besides the hydroxide and thio-based straighteners, formaldehyde and glutaraldehyde have been actively used for hair straightening, despite of being banned due to their toxicity, simply because they are inexpensive and result in shiny, straight hair by crosslinking the amine groups in the keratin peptide.[6] Formaldehyde is more dangerous as compared to glutaraldehyde as it causes serious damage to tissues and respiratory tracts of the users as well as the hairdressers working in salons and has been classified as a carcinogen.[6, 9, 12]

There have been some attempts to use non-toxic reducing agents to break the disulfide bond in the keratin and reform them to attain straightness. The use of

cysteine as a ‘green’ reducing agent and use of polycarboxylic acids such as citric acid, butane tetra carboxylic acid (BTCA), malic acid and others to crosslink the hair have been studied.[2, 13-15] However, all these are two-step processes that still involve the reduction step (breaking of the disulfide bonds) which affects the strength of the hair permanently.

This paper reports the development of a novel sucrose-based nontoxic keratin crosslinker used to straighten the hair. Sucrose was oxidized using sodium periodate to form sucrose tetraaldehyde (ST) as shown in the Figure 7.1. The four aldehyde groups generated on sucrose after oxidation can react with the amine groups present on the protein (keratin) molecules in the hair forming covalent crosslinks within the keratin. Crosslinking stabilizes the hair forming a 3D network and when straightened using a flat iron, the crosslinking can be completed which retains its straightness. The effect of ST treatment on durability of the straightness after exposure to high humid conditions and repeated shampoo washing was studied. While Brazilian natural curly hair was used in this straightening study, any other hair can be expected to perform similarly. Alternatively, this innovative green natural hair styling crosslinker could also be used to create curls on straight hair.

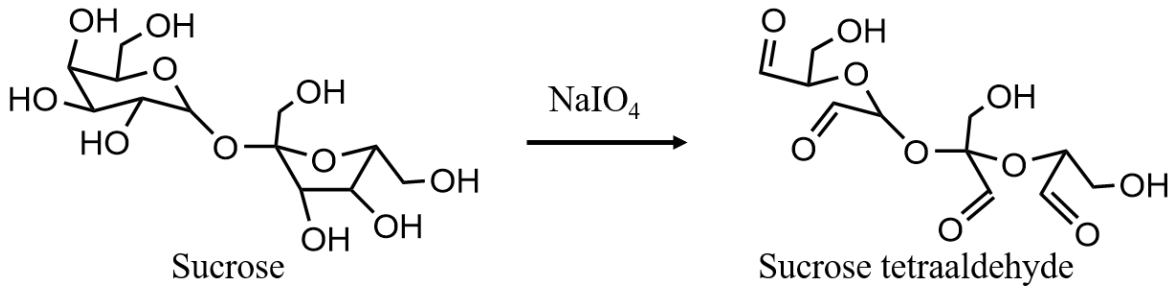

Figure 7.1 Oxidation reaction of sucrose forming sucrose tetraaldehyde.

7.3 Materials and methods

7.3.1 Materials.

100% virgin Brazilian natural curly human hair (7.5" curly length; 12" stretched length) sample was obtained from Amazon. Remington© flat iron with settings from 10 to 30 and Pantene© shampoo were purchased from local Target Store. Sodium periodate ($NaIO_4$) ≥ 99% was bought from Acros Organics, Bound Brook, NJ. Barium dichloride ($BaCl_2$) was purchased from VWR, Rochester, NY. Sucrose powder and sodium hydroxide (NaOH) pellets were purchased from Sigma-Aldrich Chemical Co., Allentown, PA.

7.3.2 Preparation of Sucrose Tetraaldehyde (ST) Solution for Hair Treatment.

Five g of sucrose was dissolved in 100 ml of DI water. Six g of $NaIO_4$ was added to the sucrose solution. Oxidation was carried out in complete dark at room temperature (RT) for 16 h with gentle stirring at 200 rpm. At the end of 16 h, 4 g of $BaCl_2$ was added to the solution to stop further oxidation. $BaCl_2$ reacts with $NaIO_3$ to form $Ba(IO_3)_2$ which is insoluble in water at lower temperatures. After addition of $BaCl_2$, the solution was stirred for 5 min and placed in a refrigerator for 1 h to allow precipitation of $Ba(IO_3)_2$. After 1 h, the solution was filtered to separate the

insolubilized $Ba(IO_3)_2$ from the ST. At this time the pH of ST solution was observed to be around 3.5. The pH of the ST solution was adjusted to 7 using NaOH before the hair treatment.

7.3.3 Characterizations of ST Solution.

The prepared ST solution for hair straightening was characterized using ATR-FTIR and ^{1}H-NMR to analyze the functional chemical groups. The ATR-FTIR spectra were collected using Thermo Nicolet Magna-IR 560 spectrometer (Madison, WI) having a split pea accessory. Each scan was an average of 300 scans from 4000 cm^{-1} to 500 cm^{-1} wavenumbers. ^{1}H NMR spectra were recorded on INOVA 400 spectrometer (Varian Inc., Palo Alto, CA) using D_2O as a solvent.

7.3.4 Hair Straightening Treatment.

A swatch of hair (7.5” in curly length and weighing 1.2 g) was washed with shampoo and air dried before the treatment. The washed swatch of hair was clamped onto an aluminum foil using a clip and the prepared ST solution was applied onto the curls of the hair using a hair dye brush. The hair dye brush was dipped in the prepared ST solution and smaller sections of hair were individually coated with the ST solution from top to bottom, using 3-4 strokes of brush of about 2 inches length. The brush was dipped in the ST solution multiple times to ensure that all the hair in the swatch were well coated or wetted with ST solution from all sides. The hair swatch was then allowed to dry for about 8 min and flat ironed for about 8 passes at the flat iron setting 25 which corresponded to 180°C (the flat iron had 30 settings with highest temperature at 30 of 215°C). ST solution was applied to the hair again and dried and flat ironed, as mentioned above. The straightened hair swatch was set aside for 10 min

at room temperature (RT) before washing it off with tap water at RT and flat ironed again for another 4-5 passes, if the hair curls after washing. This ST solution treated hair was termed as STA. Another swatch of hair was washed with shampoo, air dried and flat ironed at iron setting 25 for 25-30 passes until straight without using ST solution. This swatch was termed at FI.

7.3.5 Characterizations of Hair.

Since humidity affects the straightness and curliness of the hair, most of the hair characterizations were performed in a conditioning room maintained at standard conditions of 21°C and 65% relative humidity (RH). The untreated control (C), FI and STA hair were hung in the same conditioning room (21°C and 65% RH) for upto 45 days and pictures were taken at regular intervals to observe the effect of humidity on the hair.

One set of hair swatches (C, FI and STA) was washed with shampoo every two days and hung in the conditioning room and pictures were taken after washing, drying and two day after washing to mimic the real-life application. Straightening efficiencies (SE) for FI and STA hair specimens were calculated after measuring their lengths before and after treatments using a ruler and the number of curls (twists) and using the formula given in equation 1.[9]

$$Straightening\ efficiency\ (\%) = 100 - \left(\frac{\frac{number\ of\ twists_{\ after\ treatment}}{length\ of\ hair_{\ after\ treatment}}}{\frac{number\ of\ twists_{\ before\ treatment}}{length\ of\ hair_{\ before\ treatment}}} \right) \times 100$$

……. (1)

SE values were calculated for C, FI and STA treated hair as a function of days of exposure in conditioning room at 21°C and 65% RH as well as shampoo washings.

Tensile properties of hair were characterized using an Instron universal testing machine, model 5566 (Instron Corp., Canton, MA). Individual hair specimens from various C, FI and STA swatches were mounted on rectangular paper tabs by securing the two ends with a self-adhesive tape. The diameter of every hair was measured using a calibrated optical microscope, Olympus, model BX51 (Melville, NY), at three **different locations, and the average was used to calculate the tensile properties of** individual hair. The hair specimens were conditioned at 21°C and 65% prior to testing. The tests were also conducted at 65 ± 3% RH and 21 ± 1°C using a gauge length of 30 mm and a strain rate of 0.6 min^{-1}. Thirty single hair specimens were randomly chosen from top, middle and bottom parts of the swatches of each type (C, FI and STA) for testing and statistical analysis. For the FI and STA hair, 10 specimens were chosen from each of the three different swatches treated at different times using ST solutions prepared at different times to ensure reproducibility of the results.

The surface characterization of the C, FI and STA hair was performed using Zeiss Gemini 500 scanning electron microscope (Germany), and at 1 kV.

7.4 Results and discussion

7.4.1 Characterization of ST Solution.

Figure 7.2 shows the ATR-FTIR and ^{1}H-NMR spectra of sucrose and the prepared ST solution. As seen in Figure 7.1(a), the spectrum of sucrose shows unique peaks associated with sucrose in the fingerprint region between 1500 cm^{-1} to 700 cm^{-1} wavenumbers. The peak at 907 cm^{-1} corresponds to the C-H bending in sucrose. The peaks at 1049 cm^{-1} and 1237 cm^{-1} corresponds to the C-O stretch as well as C-C stretch

in sucrose from C-OH groups while the peak at 1003 cm^{-1} corresponds to the stretching if C-O band of the C-O-C linkage.[16] The peaks at 1322 cm^{-1} and 1411 cm^{-1} are due to O-H bending of C-OH groups in sucrose. The ATR-FTIR spectra of the ST shows an additional peak at 1712 cm^{-1}. This peak corresponds to carbonyl groups formed as a result of oxidation of sucrose.[16-17] Similar peak at 1718 cm^{-1} was seen by Jalaja and James after oxidizing sucrose using $NaIO_4$.[18] As seen in the spectrum of ST in Figure 7.2(a), the peak 1237 cm^{-1} disappeared and the peak intensity of the one at 1411 cm^{-1} reduced. Both of these peaks correspond to the C-OH bending in sucrose and the reduction in the peak intensity is the result of oxidation of hydroxyls to aldehyde groups. In both spectra (sucrose and ST), a peak around 3360 cm^{-1} corresponds the hydroxyl groups in the sucrose and the peaks between 2900 and 2700 cm^{-1} correspond to the C-H stretch. The additional peak at 1630 cm^{-1} in the ST is from the hydroxyl groups from water.

Figure 7.2(b) shows the ^{1}H-NMR spectra for sucrose and ST. The protons associated with sucrose are seen at 5.4 ppm and between 4.2 ppm and 3.2 ppm. The proton shift seen at 4.7 ppm in both spectra is a result of the D_2O used as solvent. The proton shifts at 4 ppm and 4.2 ppm in sucrose are due to the protons from secondary hydroxyl groups present on the fructose ring in the sucrose. The three proton shifts associated with the three secondary hydroxyl groups on the glucose are seen between 3.5 and 3.75 ppm in sucrose. Fructose and glucose have two and three vicinal hydroxyl groups or secondary hydroxyl groups, respectively, which are cleaved due by $NaIO_4$ and oxidized to form two aldehyde groups on each fructose and glucose (as seen from the reaction in Scheme 1). The aldehyde group formation can be seen from

the ^{1}H-NMR of ST where an additional proton shift is clearly observed at 8.3 ppm due to the protons associated with the aldehyde groups created by oxidation.[17] The additional proton shifts between 4.8 and 5.5 ppm indicate the intermolecular acetal protons due to the hemiacetal formation.[17-20]

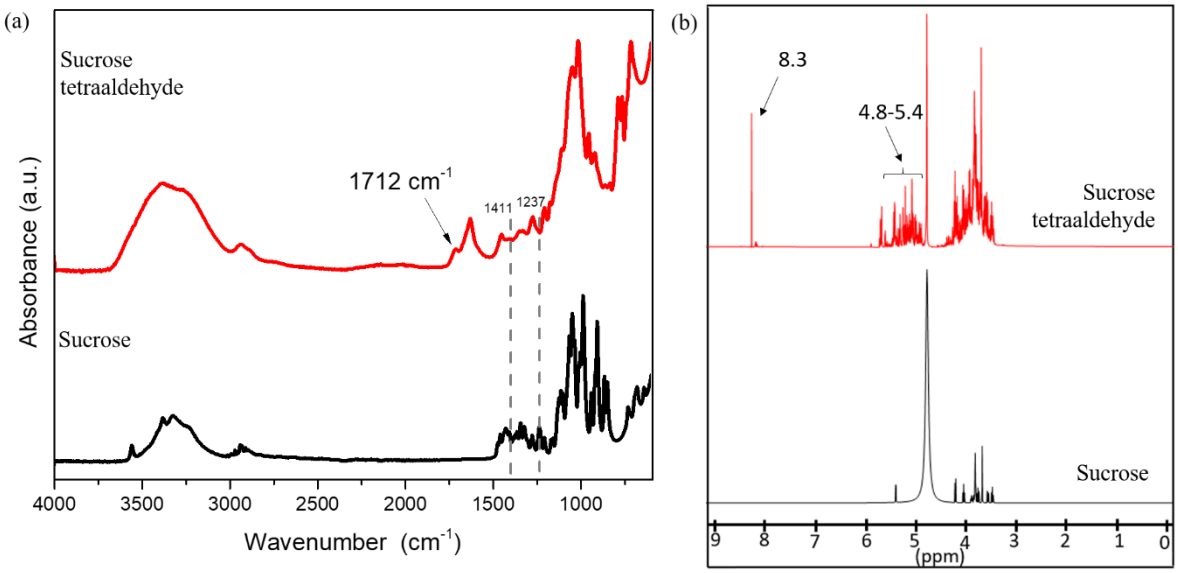

Figure 7.2 (a) ATR-FTIR and (b) 1H-NMR of sucrose and ST.

7.4.2 Characterization of Hair.

Figure 7.3 shows pictures of C, FI and STA hair swatches, from left to right, respectively, taken from day 0 to day 15 exposure in conditioning room, after the treatments. As seen in Figure 7.3(a), the control hair swatch showed 5 curls (each curl is counted as a z from top to bottom). Flat iron helps to straighten the curls as seen in Figure 7.3(a) (0 day) and so does the STA treatment. As seen in Figure 7.3(b), the FI hair showed at least 1 curl at the bottom of the swatch after 1 day in the conditioning room at 21°C and 65% RH while the STA hair maintained its straightness. Figure

7.3(c) shows pictures of hair after 2 days in the conditioning room. It is clear that for the curl formed after 1 day on the FI hair got enhanced and is now accompanied by 2 additional distinct curls. The STA hair, however, retained most of its straightness except for the bottom tip of the swatch after 2 days in conditioning room. The hair near the bottom of the swatch are fewer in number because of their unequal lengths and probably slip through the flat iron gap. As a result, it is possible that the fibers at the bottom of the swatch do not get adequate treatment as in the top and middle of the swatch. Figure 7.3(d), 7.3(e) and 7.3(f) show the pictures of hair swatches after 3, 5 and 7 days, respectively. It was observed that the FI hair got fluffed-up showing at least 3 distinct curls while only the bottom tip of STA hair showed signs of curling. Most of the top hair of the STA hair showed perfect straightness. Similar effect was observed at the end of 15 days in the conditioning room (Figure 7.3(h)). It was observed that the STA hair maintains its straightness for up to 45 days at 21°C and 65% RH while the FI has the tendency to curl and frizz after just 2 days in the conditioning room. As mentioned earlier, the STA hair is well crosslinked due to the reaction of aldehyde groups from the ST solution and the amine groups from the keratin in hair. The amine groups from hair and aldehyde groups from sugar react to form a covalent bond via imine (Schiff base) formation.[17] Since the crosslinked molecules are unable to move, this provides the hair significant stabilization against the humidity. The FI hair on the other hand is just straightened due to the mechanical force and the heat applied due to flat ironing which involves rearrangement of hydrogen bonds. However, the newly formed hydrogen bonds from using a flat iron (heat and mechanical treatment) are susceptible to humid conditions and the hair

reverts back to its original state over time.[21] Moisture from the conditioning room tends to easily plasticize the FI hair causing them to curl and fluff-up.[22] As four aldehyde groups are present on ST, it increases the potential crosslinking opportunities with the amine groups present in the keratin as compared to formaldehyde or glutaraldehyde which consists of one and two aldehyde groups respectively. Multiple intra and interfibrillar crosslinks can be formed with and within the cortex after ST treatment forming a dense 3D network which stabilizes the hair and helps retain its desired shape.

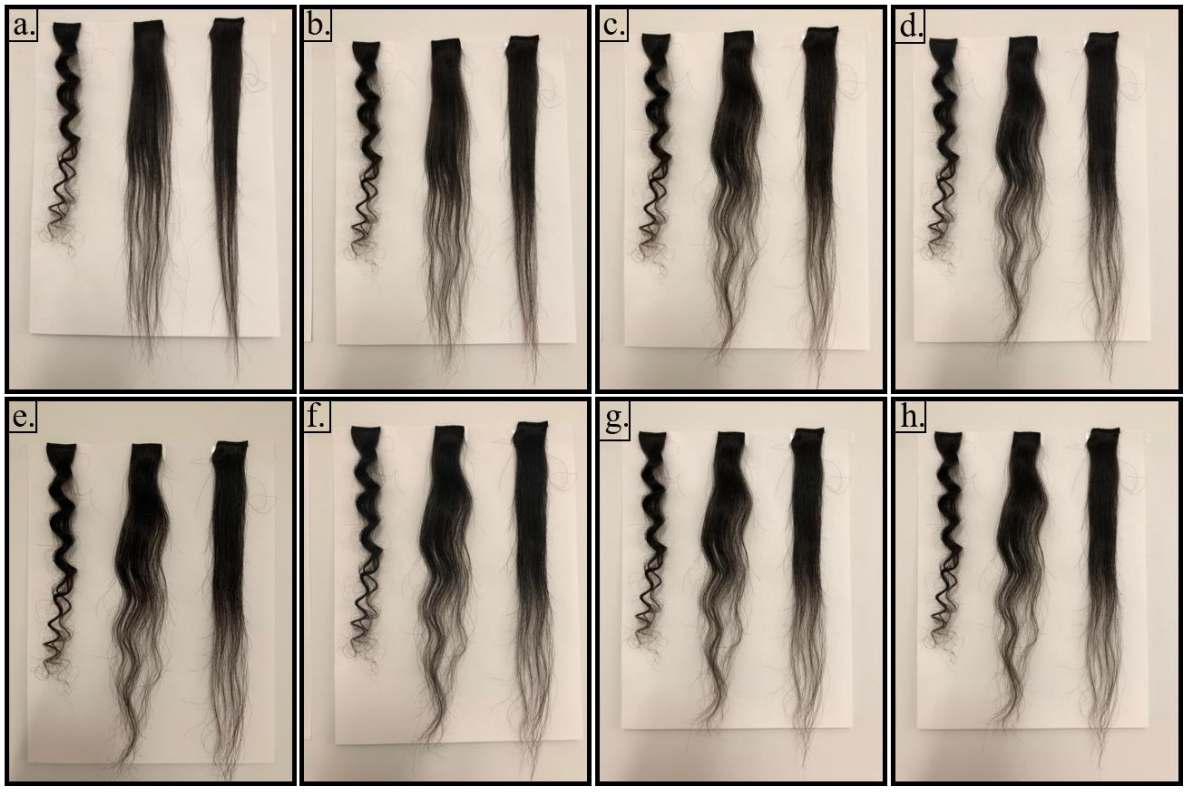

Figure 7.3 C, FI and STA hair swatches from left to right in each picture at (a) day 0, (b) day 1, (c) day 2, (d) day 3 (e) day 5, (f) day 7, (g) day 10, (h) day 15.

The C, FI and STA hair swatches were repeatedly washed using a warm 2% shampoo solution for 5 min and rinsed thoroughly under running water at RT until the

lather was gone. The wet hair swatches were placed on a paper and hung on a wall in the conditioning room for 2 days before washing again. Figure 7.4 shows the pictures of C, FI and STA hair swatches after 4 shampoo washes. Pictures of wet hair were taken immediately after washing. The second set of pictures in all of the shampoo washes were taken after 2 hours of drying in the conditioning room and the third one after 2 days in the conditioning room. As seen in Figure 7.4, the control wet hair show 5 distinct curls when washed with shampoo. Upon drying for 2 hours in the conditioning room, the hair fluffs-up causing reduction in the length of the hair swatch and enhancing the curvature of the curls. The FI hair also immediately curled-up during the first shampoo wash while the STA hair remained straight after the first shampoo wash. Upon drying in the conditioning room after shampoo wash, the wet FI hair fluffed-up and the curvature of the curls increased. As a result, the length of the FI swatch reduced. The FI hair looked similar to the C hair as it regains all its original curls after the 1st shampoo wash. As mentioned earlier, flat ironing only straightens the hair temporarily as it only involves alterations of hydrogen bonds and salt linkages.[21] The FI hair regained most of its original curl and the length decreased close to control hair. It was, however, observed that the STA hair maintained its straightness for 2 shampoo washes because of the covalent crosslinks formed which are more durable. As mentioned earlier, the 3D network formed within the cortex after crosslinking restricts the molecular movement or slippage and helps retain its shape. The STA hair was straight even after the third shampoo wash. It, however, started to curl around the bottom of the swatch while drying in the conditioning room. As mentioned earlier, the bottom part of the swatch is sparse and probably does not come in complete contact

with the plates of the flat iron causing inadequate treatment. Because of the insufficient crosslinking, the moisture in the conditioning room causes the STA hair to begin to curl. At least 1 curl, with low curvature, was observed after the third and fourth shampoo wash while drying with negligible reduction in the overall length of hair swatch.

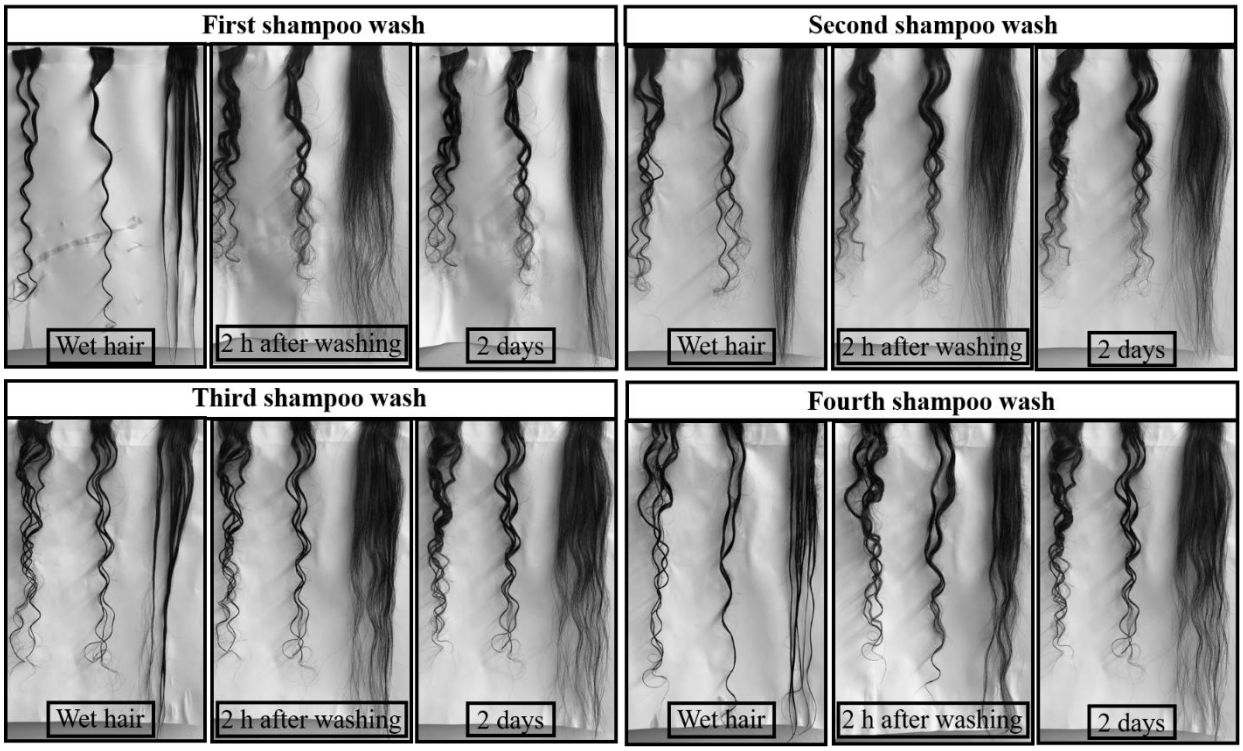

Figure 7.4 C, FI and STA hair swatches from left to right in each picture after 4 shampoo washes.

The straightening efficiency (SE) values were calculated for FI and STA hair swatches for up to 45 days of exposure to 65% RH and for C, FI and STA hair swatches after repeated shampoo washings for up to 4 washes, using equation 1. Figure 7.5(a) shows SE of FI and STA hair as a function of days the hair swatches were hung on a wall in conditioning room at 65% RH for up to 45 days. As seen in Figure 7.5(a), SE of FI and STA hair was 100% on day 0. After 1 day in the

conditioning room, SE of the FI hair reduced to 66.7% while SE of STA hair was still 100%. At least 1 curl was observed in the FI hair after 1 day at 65% RH while the STA hair was fully straight (SE 100%). This can be clearly seen in Figure 7.3(b). SE of FI hair further reduced to 60.3% after 2 days at 65% RH when 3 curls developed on FI swatch while a slight curl in the bottom part of the STA hair was observed bringing down the efficiency of the STA hair to 86.8% after 2 days in the conditioning room. SE of the FI hair further reduced to 58.3% and 57.6% as the intensity of the curvature of the curls and the number of curls increased after 3 and 5 days in the conditioning room respectively. No additional curls were observed on the STA hair and its SE remained constant at 86.8% for up to 5 days in the conditioning room. SE of the FI hair further reduced to 56.9% after 7 days in the conditioning room and remained constant at 56.9% over time for up to 45 days. SE of STA hair was found to be 86.6% after 7 days in the conditioning room after which it remained unchanged for up to 45 days. Overall, SE of the STA hair was found to be much higher and more permanent compared to the FI hair.

Figure 7.5(b) shows the SE values of C, FI and STA hair as a function of number of shampoo washes. It should be noted that each shampoo wash is accompanied by 2-day exposure to 65% RH at 21°C. As seen from Figure 7.5(b), the SE of FI hair reduced to 22.44% after the very 1st shampoo wash. This implies that the FI hair regains most of it curls upon washing with shampoo. Again, this is because flat ironing is only a temporary way of hair straightening. Hair straightening using a flat iron only involves breaking and reforming of few hydrogen bonds in the keratin. These hydrogen bonds are weak and easily disrupted by water and, as a result, the FI

hair reverts back to its original curly state after washing.[6] SE of the FI hair was found to decrease to 12.8% after 2nd and 3rd shampoo washes and down to just 8% after 4th shampoo wash. This implies that the FI hair is as close to the original state or C hair after shampoo wash. It was also found that shampoo washing of the C hair introduces slight additional curls onto the swatch. Thus, SE of the C hair was negative. It was found to be -4.2% after 2 shampoo washes after which it remained constant at -13.6% after 3rd and 4th shampoo washes. The SE of STA hair was maintained at 100% for up to 2 shampoo washes after which it reduced to 86.6% after the 3rd and 4th shampoo washing. Overall, Figure 7.5(b) shows that the SE of FI hair reduces significantly (as close to control) as the hair regains most of its curls after washing, while the SE of STA only reduces to 86.56% after 4 shampoo washes. This shows that the STA treatment is more durable than FI hair and can be used to attain permanent hair styling.

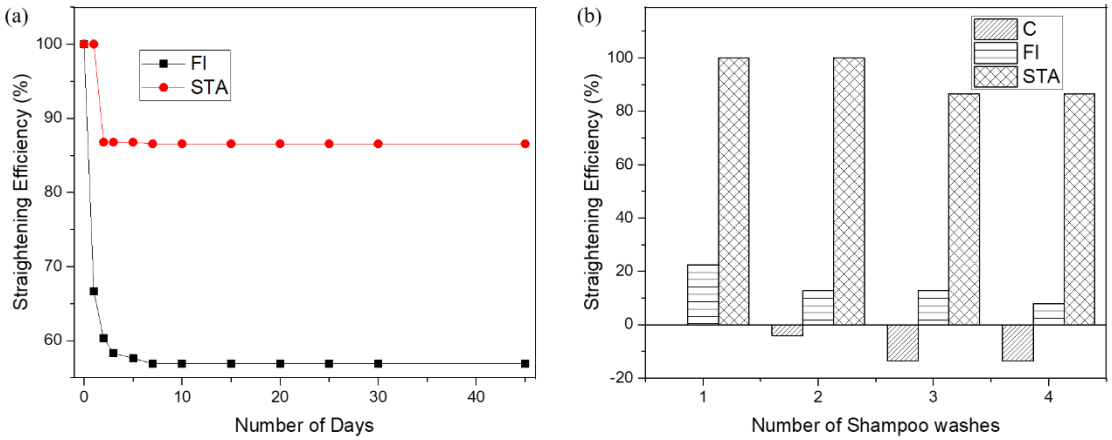

Figure 7.5 Straightening efficiency of the FI and STA hair hung at 21°C and 65% as a function of (a) number of days and (b) number of shampoo washes.

Figure 7.6 shows the typical stress-strain plots for C, FI and STA hair specimens. As seen from Figure 7.6, the typical stress-strain plots of the all hair show

three distinct regions: initial Hookean region, yield region and post yield region.[23] The tensile properties of the C, FI and STA hair are summarized in Table 7.1. As can be seen from Figure 7.6, the Hookean region lies between 0% - 5% tensile strain. The average tensile stress value of the C hair specimen at the end of the Hookean region was 103 MPa. In comparison, the average tensile stress value of the FI and STA hair specimens were observed to be 99.8 MPa and 99.7 MPa, respectively, indicating that the tensile stress of the FI and STA hair specimens in the Hookean region remained unchanged after treatments. The tensile strain of C, FI and STA hair specimens in the Hookean region was found to be 4.1%, 4.7%, 4.3%, respectively, which suggests that the properties of the FI and STA hair remained unchanged compared to C hair. The strain in the Hookean region comes from extension of weaker bonds such as hydrogen bonding within the amino acids, Van der Waals forces and coulombic interactions.[17] Immediately following the Hookean region the hair shows yielding behavior where large amount of strain is accompanied by very small rise in stress signifying very low modulus or high compliance. This yield region extends from 5% to 30% strain for all the hair specimens. It involves unfolding of the α-keratin into β-keratin configuration allowing larger deformation in the hair before breaking.[17, 23] Strain-hardening phenomenon was observed beyond the yield region for all fibers.[17, 23] Strain-hardening region extends from 30% - 50% strain and ends upon the rupture of the hair. The breaking or ultimate fracture stress values for C, FI and STA hair specimens were found to be 164 MPa, 171 MPa, 166 MPa, respectively. These fracture stress values were found to be statistically insignificant, using an unpaired t-test, at a significance level of 0.05. This implies that the tensile stress of the hair strands was unaffected

after flat ironing and the ST treatment. It is known that the keratin-based peptide in the hair is susceptible to thermal degradation after flat ironing which results in weakening the hair strands.[6] Continual heat treatments especially flat ironing in wet conditions increases the hair damage.[24] In the present study, flat ironing in the wet state was intentionally avoided, and the ST solution was allowed to dry before flat ironing the hair. While the pH of most commercial hair straightening products is highly alkaline (above 10), the pH of ST solution was adjusted to 7 to avoid alkaline denaturation of keratin peptides and retain tensile properties. Overall, the tensile results suggest that the tensile properties of the hair remained unchanged after the ST treatment and hence, could be a viable healthy alternative to currently used toxic hair crosslinkers. It is also clear from Table 7.1 that the FI treatment reduces the initial modulus (Young's modulus) to 2.3 GPa compared to 2.6 GPa for C hair. However, after the STA treatment the modulus recovers back to 2.6 GPa as a result of the crosslinking.

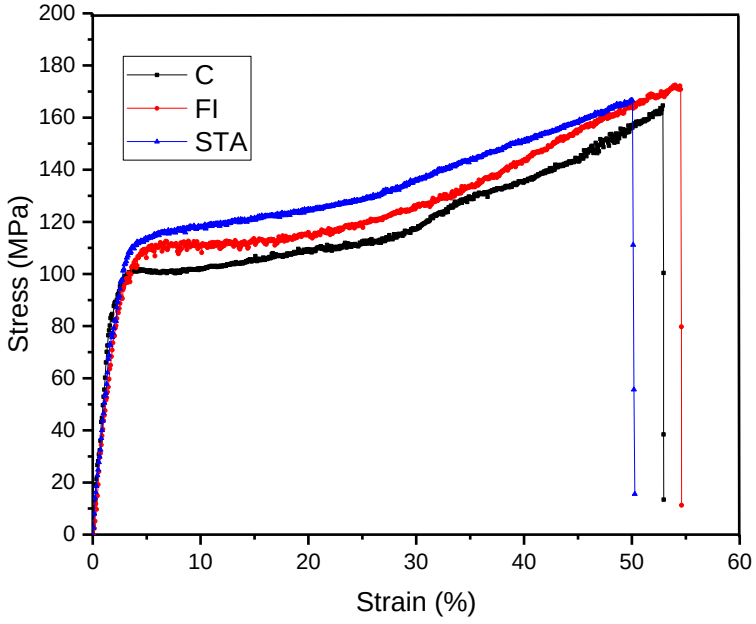

Figure 7.6 Typical stress-strain plots for C, FI and STA hair strands.

Table 7.1. Tensile properties of the C, FI and STA hair strands.

		Initial Hookean Region			Post Yield Region	
	Diameter (μm)	Stress (MPa)	Strain (%)	Young's Modulus (GPa)	Stress (MPa)	Strain (%)
C	68.2 ± 11.9	103 ± 36.9	4.1 ± 0.6	2.6 ± 1.1	163.8 ± 54.8	49.3 ± 7.5
FI	73.3 ± 07.9	99.8 ± 34.3	4.7 ± 1.1	2.3 ± 1.0	171.0 ± 35.6	51.8 ± 8.6
STA	74.0 ± 16.0	99.7 ± 28.1	4.3 ± 1.4	2.6 ± 1.2	166.1 ± 44.0	49.7 ± 5.8

Figure 7.7 shows SEM images of C, FI and STA hair. As seen in Figure 7.7(a), the control hair shows scales on the surface. No visible change or damage to the scales can be observed after FI or STA treatments on the hair. Since excess heat from the flat iron can damage the hair, especially the scales, if done in the wet condition, care was taken to ensure that the hair was dry enough after treating with STA (by leaving them to air dry at RT for 10 min) before flat ironing. Most of the keratin crosslinking by ST solution occurs inside the hair as the ST molecule is small enough to penetrate the hair, leaving the surface of the hair undamaged after STA treatment.

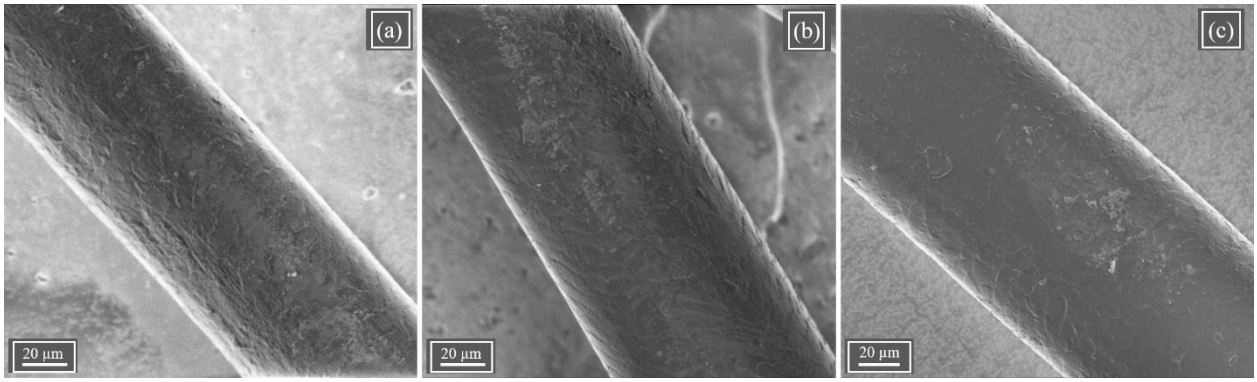

Figure 7.7 SEM images of (a) C, (b) FI and (c) STA hair.

7.5 Conclusions

The present study has successfully demonstrated that hair can be crosslinked using a 'green' sugar-based crosslinker. Sucrose was oxidized using $NaIO_4$ to convert the secondary hydroxyl groups to the aldehyde groups leading to a product with four aldehyde groups on sucrose (sucrose tetraaldehyde). Crosslinking of hair was carried out using chemical and mechanical treatment which involved diffusion of sucrose tetraaldehyde into the hair cortex along with flat ironing. The chemical crosslinking via covalent bond formation (imine) from the reaction of amine groups from keratin and aldehyde groups from sucrose resulted in a stable crosslinked 3D network within the hair cortex. The hair straightening process was optimized to achieve maximum straightening efficiency with the least damage to the tensile properties or the surface scales of the hair. The straightening was found to be stable up to 4 shampoo washings. These promising results open up a new 'green' innovative alternative of chemical treatment for hair styling without being exposed to currently used toxic, carcinogenic chemicals.

7.6 References

1. Williams, T. N.; Kuenemann, M. A.; Van Den Driessche, G. A.; Williams, A. J.; Fourches, D.; Freeman, H. S. Toward the Rational Design of Sustainable Hair Dyes Using Cheminformatics Approaches: Step 1. Database Development and Analysis. *ACS Sustain. Chem. Eng.* **2018,** *6* (2), 2344-2352.

2. Dixon, F.; Pistorio, B.; Ellington, A.; Yee, M. Process for Relaxing or Straightening hair, Using Weak Dicarboxylic Acids with Heat. WO2010049434A2, 2013.

3. Deb Barma, S.; Banerjee, B.; Chatterjee, K.; Paria, S. Natural Surfactants-Based Ag nanofluids for Enhanced Wettability on Hair Surface. *ACS Sustain. Chem. Eng.* **2018,** *6* (3), 3615-3623.

4. Pienpinijtham, P.; Thammacharoen, C.; Naranitad, S.; Ekgasit, S. Analysis of Cosmetic Residues on a Single Human Hair by ATR FT-IR Microspectroscopy. *Spectrochim. Acta A* **2018,** *197*, 230-236.

5. Esfahani, J. M.; Luu, A.; Kluft, C. Keratin Delivery Process by Reactive Chemical Composition for Improved Methods of Strengthening and Smoothing Hair. US10022311, 2018.

6. Miranda-Vilela, A.; Botelho, A.; Muehlmann, L. An Overview of Chemical Straightening of Human Hair: Technical Aspects, Potential Risks to Hair Fibre and Health and Legal Issues. *Int. J. Cosmetic Sci.* **2014,** *36* (1), 2-11.

7. Bryant, H.; Dixon, F.; Ellington, A.; Porter, C. Hair Straightening. In *Cosmetic Dermatology*, pp 262-269.

8. Fondin, T.; Sabbagh, A. Method for Treating Hair Fibers. US9675822, 2017.

9. Cruz, C. F.; Martins, M.; Egipto, J.; Osorio, H.; Ribeiro, A.; Cavaco-Paulo, A. Changing the Shape of Hair with Keratin Peptides. *RSC Adv.* **2017,** *7* (81), 51581-51592.

10. Song, K.; Xu, H.; Xie, K.; Yang, Y. Effects of Chemical Structures of Polycarboxylic Acids on Molecular and Performance Manipulation of Hair Keratin. *RSC Adv.* **2016,** *6* (63), 58594-58603.

11. de Sá Dias, T. C.; Baby, A. R.; Kaneko, T. M.; Robles Velasco, M. V. Relaxing/Straightening of Afro-Ethnic Hair: Historical Overview. *J. Cosmet. Dermatol.* **2007,** *6* (1), 2-5.

12. Oiye, E. N.; Ribeiro, M. F. M.; Okumura, L. L.; Saczk, A. A.; Ciancaglini, P.; de Oliveira, M. F. Forensic Investigation of Formaldehyde in Illicit Products for Hair Treatment by DAD-HPLC: A Case Study. *J. Forensic Sci.* **2016,** *61* (4), 1122-1125.

13. Song, K.; Xu, H.; Mu, B.; Xie, K.; Yang, Y. Non-toxic and Clean Crosslinking System for Protein Materials: Effect of Extenders on Crosslinking Performance. *J. Clean. Prod.* **2017,** *150*, 214-223.

14. Xu, H.; Song, K.; Mu, B.; Yang, Y., Green and Sustainable Technology for High-Efficiency and Low-Damage Manipulation of Densely Crosslinked Proteins. *ACS Omega* **2017,** *2* (5), 1760-1768.

15. Malle, G.; Barbarat, P.; Pasini, I. Method for Straightening Keratinous Fibers using Heating Means and Malic Acid. US9743736B2. 2017.

16. Dastidar, T. G.; Netravali, A. N. A Soy Flour Based Thermoset Resin without the use of any External Crosslinker. *Green Chem.* **2013,** *15* (11), 3243-3251.

17. Patil, N. V.; Netravali, A. N. Enhancing Strength of Wool Fiber Using a Soy Flour Sugar-Based "Green" Cross-linker. *ACS Omega* **2019,** *4* (3), 5392-5401.

18. Jalaja, K.; James, N. R. Electrospun Gelatin Nanofibers: A Facile Cross-Linking Approach using Oxidized Sucrose. *Int. J. Biol. Macromol.* **2015,** *73*, 270-278.

19. Xu, H.; Liu, P.; Mi, X.; Xu, L.; Yang, Y. Potent and Regularizable Crosslinking of Ultrafine Fibrous Protein Scaffolds for Tissue Engineering using a Cytocompatible Disaccharide Derivative. *J. Mater. Chem. B* **2015,** *3* (17), 3609-3616.

20. Xu, H.; Canisag, H.; Mu, B.; Yang, Y. Robust and Flexible Films from 100% Starch Cross-Linked by Biobased Disaccharide Derivative. *ACS Sustain. Chem. Eng.* **2015,** *3* (11), 2631-2639.

21. Krause, T.; Rust, R. C. Hair Styling: Technology and Formulations. *Cosmetic Dermatology: Products and Procedures* **2016,** *3*, 270-279.

22. Pye, S.; Paul, P., Trehalose in Hair Care: Heat Styling Benefits at High Humidity. *J. Cosmet. Sci.* **2012,** *63* (4), 233-241.

23. Feughelman, M. In *Mechanical Properties and Structure of Alpha-Keratin Fibres: Wool, Human Hair and Related Fibres*. UNSW press: 1997.

24. Wang, N.; Barfoot, R.; Butler, M.; Durkan, C. Effect of Surface Treatments on the Nanomechanical Properties of Human Hair. *ACS Biomater. Sci. Eng.* **2018,** *4* (8), 3063-3071.

Chapter 8 Conclusions and suggestions for future research

Namrata V. Patil and Anil N. Netravali
Department of Fiber Science & Apparel Design,
Cornell University, 37 Forest Home Dr., Ithaca, NY 14853, USA

The present research has clearly demonstrated that naturally occurring or plant-based raw materials such as sucrose, cyclodextrin (CD), halloysite nanotubes (HNT), fatty acids, soy-flour sugars, etc., can be chemically modified to create desired functional groups and further react them with cotton, human hair or wool fibers. Treating cotton and wool fibers or their fabrics with such benign raw materials can easily impart desired characteristics such as hydrophobicity, superhydrophobicity, and wrinkle-resistance to cotton fabrics, higher strength to wool fibers and stabilization of human hair.

Sucrose and CD were oxidized using hydrogen peroxide and further carboxylated using malic acid to form multiple carboxylic acid groups. The carboxylic acid groups were used to react with the hydroxyl groups from cotton via esterification to form crosslinks and improve the wrinkle recovery angle.

Silica particles with various shapes, e.g., spheres, cones and needles, were synthesized and chemically bonded onto the surface of the cotton fabrics. These fabrics were then grafted with fatty acid to reduce the surface energy. Surface roughness combined with reduced surface energy resulted in superhydrophobic cotton fabrics.

Wool fibers were crosslinked in the sliver form using oxidized sugars of various lengths obtained from soy flour as a byproduct. The crosslinking resulted in improved strength of the wool fibers.

Oxidized sucrose containing 4 aldehyde groups (sucrose tetraaldehyde) was used to treat human hair. This treatment resulted in chemically crosslinked keratin structure which can be effectively used in hair styling to straighten naturally curly hair.

The sustainable chemistry solutions developed in this research can be easily scalable, as they use facile synthesis techniques. The chemicals created should be inexpensive as well because of the inexpensive raw materials used. Importantly, these processes replace the current practices/processes that use toxic or even carcinogenic chemicals such as formaldehyde. The use of such 'green' materials and chemicals will reduce the adverse effects of the textile processing and finishing on the environment as well as humans working in these industries.

The wrinkle-free finishing and superhydrophobic finishing developed for cotton fabrics can be extended to other cellulosic fabrics such as viscose rayon, lyocell and all natural cellulosic fibers. The crosslinking of hair with the 'green' crosslinker developed in this research can be used to curl the straight hair and retain the curls for several days or weeks.

Based on the present research, the following suggestions can be made for future directions in various chapters:

1. Chapter 3: Cyclodextrin can be hydrolyzed enzymatically to break-down the structure, oxidized and carboxylated further using similar methods described in

chapter 3. The hydrolysis might facilitate breaking down of CD into smaller molecules which will allow easier penetration and, hence, superior crosslinking ability resulting in higher wrinkle recovery angle or improve the laundry durability of the fabrics. Glycosyl hydrolase family no. 13, containing α-amylases and the cyclodextrin producing cyclodextrin-glycosyltransferases have known to break down the CD.[1]

2. Chapter 4 and 5: Silica (SiO_2) particles were synthesized using TEOS as described in Chapters 4 and 5. However, SiO_2 particles can also be synthesized from rice husk instead of TEOS making it a greener and even cheaper process.[2]
3. Chapter 5: The pentanol used as an oil phase in the emulsion to create anisotropic SiO_2 particles in chapter 5 could be reused after centrifuging to make SiO_2 particles, making it a greener process with recycling and reusing the solvent. However, as it might contain PVP and other reactants and if used without purifying could result in different shapes of SiO_2 particles. Different shapes of SiO_2 particles can be beneficial to create desired surface roughness on the fabrics.
4. Chapter 5: Different oil phase solvents such as hexanol, heptanol or octanol may be used to study the effect of oil phase on the shape and size of the SiO_2 particles. In addition, variation of temperature and sonication of the emulsion could result in different shapes of SiO_2 particles.[3]
5. Chapter 4 and 5: The fatty acid treatment of the fabrics described in chapters 4 and 5 could be carried out on the carboxylated CD (C-CD) treated fabrics described in chapter 3. The C-CD treatment would impart wrinkle-resistance while the fatty acid would make the fabrics hydrophobic. Since the fatty acid treatment grafts a

long chain hydrocarbon on to cellulose, it acts as a lubricant and would be beneficial to counter-act the harsh effect of crosslinking seen in tensile and tear strength reduction after C-CD treatment.

6. Chapter 4 and 5: Cotton fabrics are known for its comfort and breathability as it absorbs moisture. The superhydrophobic treatment in Chapter 4 and 5 does not affect the feel and handle of the fabrics. However, the moisture and water vapor permeability of the fabrics was not determined. It would be ideal to have the superhydrophobic coating on one side leaving the other side of the fabric hydrophilic. Attempts were made to spray the nanoparticles and fatty anhydride on one side (rather than dipping the fabrics in) and then cured for grafting reactions. However, both and nanoparticles and fatty anhydride were readily wicked to the other side making both sides of the fabrics superhydrophobic. Strategy to make one side hydrophobic while leaving the other side hydrophilic is required.

References

1. Buedenbender, S.; Schulz, G. E., Structural base for enzymatic cyclodextrin hydrolysis. *Journal of molecular biology* **2009,** *385* (2), 606-617.

2. Shen, Y., Rice husk silica derived nanomaterials for sustainable applications. *Renewable and Sustainable Energy Reviews* **2017,** *80*, 453-466.

3. Yu, Q.; Wang, K.; Zhang, J.; Liu, M.; Liu, Y.; Cheng, C., Synthesis of anisotropic silica colloids. *RSC Advances* **2017,** *7* (60), 37542-37548.